Comparative transcriptomics within *Arabidopsis thaliana* accessions and across Brassicaceae species reveal evolutionary conserved and lineage-speficic expression signatures in pattern triggered immunity

Thomas Maximilian Winkelmüller

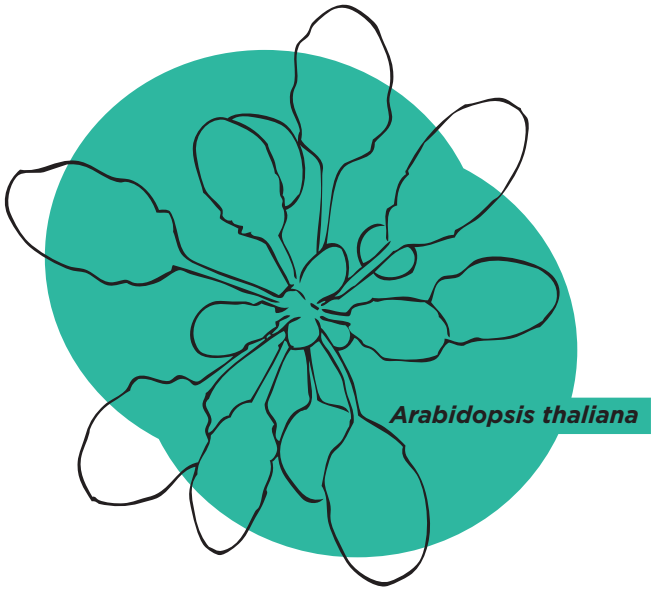

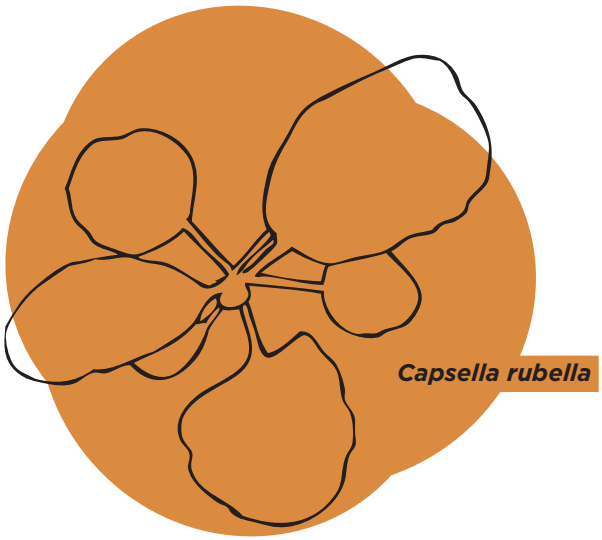

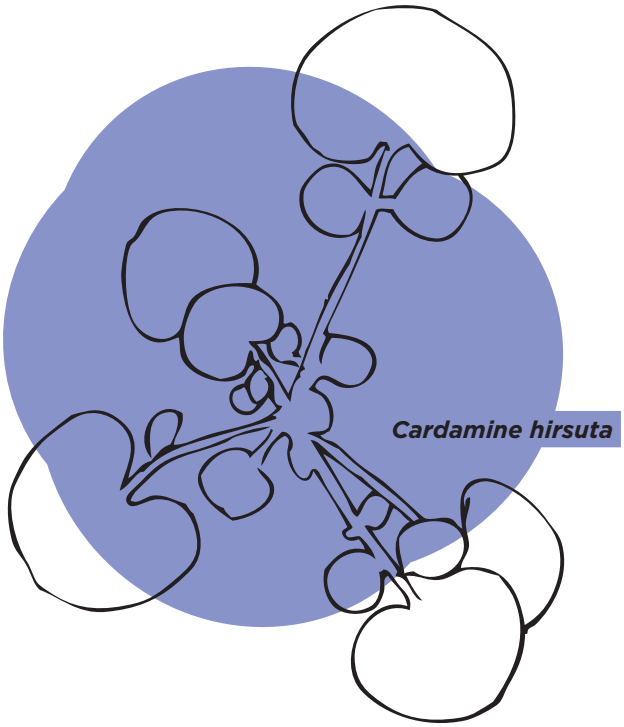

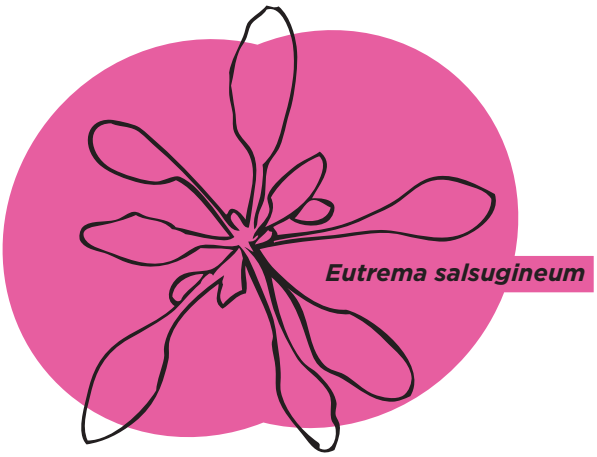

Comparative transcriptomics within *Arabidopsis thaliana* accessions and across Brassicaceae species reveal evolutionary conserved and lineage-specific expression signatures in pattern-triggered immunity

I n a u g u r a l - D i s s e r t a t i o n

zur
Erlangung des Doktorgrades
der Mathematisch-Naturwissenschaftlichen Fakultät
der Universität zu Köln

vorgelegt von
Thomas Maximilian Winkelmüller
aus Leverkusen

Köln, Februar 2018

Die vorliegende Arbeit wurde am Max-Planck-Institut für Pflanzenzüchtungsforschung in Köln in der Abteilung für Pflanze-Mikroben Interaktionen (Direktor: Prof. Dr. Paul Schulze-Lefert), in der Arbeitsgruppe von Dr. Kenichi Tsuda angefertigt.

Berichterstatter:	Prof. Dr. Paul Schulze-Lefert
	Prof. Dr. Stanislav Kopriva
Prüfungsvorsitzender:	Prof. Dr. Gunther Döhlemann
Tag der Disputation:	11.04.2018

Publications

Mine, A., Nobori, T., Salazar-Rondon, M.C., **Winkelmüller, T.M.**, Anver, S., Becker, D., and Tsuda, K. (2017). An incoherent feed-forward loop mediates robustness and tunability in a plant immune network. EMBO Rep. 18: 464–476.

Mine, A., Berens, M.L., Nobori T., Anver, S., Fukumoto, K., **Winkelmüller, T.M.**, Takeda, A., Becker, d., and Tsuda, K. (2017). Pathogen exploitation of an abscisic acid- and jasmonate-inducible MAPK phosphatase and its interception by *Arabidopsis* immunity. Proc. Natl. Acad. Sci.114: 7456-7461.

Winkelmüller, T.M., Anver, S., Garrido-Oter, R., Dahms, E., Song, B., Gao., X., Schulze-Lefert, P., Bednarek, P., and Kenichi Tsuda. Comparative transcriptomics within and between Brassicacea species reveal evolutionary conserved and lineage-specific expression signatures in pattern-triggered immunity. *In preperation*

Table of Contents

List of figures

List of tables

List of Abbreviations

AA	Amino acid
Aar	*Aethionema arabicum*
ABA	Abscisic acid
Aly	*Arabidopsis lyrata*
Ath	*Arabidopsis thaliana*
BrC	*Brassica rapa chifu*
BrF	*Brassica rapa fast plant*
cfu	colony forming unit
Cgr	*Capsella grandiflora*
Chi	*Cardamine hirsuta*
Cru	*Capsella rubella*
DAMP	damage-associated molecular pattern
DEG	differentially expressed genes
dpi	days post inoculation
Esa	*Eutrema salsugineum*
ETI	effector triggered immunity
FLS2	*FLAGELLIN-SENSITIVE 2*
FW	fresh weight
GO	Gene Ontology
Hpa	*Hyaloperonospora arabidopsidis*
hpi	hours post inoculation
hpt	hours post treatment

JA	jasmonic acid
LRR	leucine-rich-repeat
MAMP	microbe-associated molecular pattern
MAPK	mitogen-activated protein kinase
MeJA	Methyl Jasmonate
MS	Murashige and Skoog
NLR	nucleotide-binding domain leucine rich repeat proteins
OD	optical density
PRR	pattern recognition receptor
PTI	pattern-triggered immunity
Pto	*Pseudomonas syringae* pv. *tomato*
RLK	receptor-like kinase
RLP	receptor-like protein
ROS	reactive oxygen species
RT-qPCR	reverse transcriptase quantitative polymerase chain reaction
SAR	systemic acquired resistance
SD	standard deviation
SE	standard error
SID2	*SALICYLIC ACID INDUCTION DEFICIENT 2*
Spa	*Shrenkiella parvula*
T3SS	type 3 secretion system
TF	transcription factor
wt	wild type

Abstract

In nature plants are surrounded by a diverse set of beneficial and harmful microbes. Plants can recognize these microbes by sensing conserved microbe-associated molecular patterns (MAMPs) via cell surface-localized receptors, leading to the activation of pattern-triggered immunity (PTI). PTI protects plants from potential microbial pathogens through induction of a myriad of defence responses including massive transcriptional reprogramming in *Arabidopsis thaliana*. Despite the significance of PTI responses for the plant adaptation to diverse microbes, we currently do not understand the importance of this massive transcriptional reprogramming, whether PTI responses are conserved, and how they evolved. Here I used comparative transcriptomics to analyse the responses of six *A. thaliana* accessions and three additional Brassicaceae species to the bacterial MAMP flg22. This analysis revealed that large parts of the transcriptional response to flg22 are conserved among Brassicaceae species, suggesting that these are under purifying selection over the Brassicaceae evolution and that flg22-triggered transcriptional reprogramming during PTI is important. At the same time, I found that a considerable fraction of flg22-responsive genes showed species-specific expression signatures. Moreover, variation in flg22-triggered transcriptional reprogramming was incongruent with the Brassicaceae phylogeny, suggesting that adaptive evolution acts on subsets of flg22-responsive genes. In contrast, flg22-triggered transcriptional responses among genetically and geographically diverse *A. thaliana* accessions were extremely conserved. Thus, inter-species clearly exceeds intra-species transcriptome variation in response to flg22. This further suggests the adaptive nature of gene expression evolution and points to a small contribution of neutral transcriptome evolution during PTI within Brassicaceae. Regulatory regions of conserved flg22-inducible genes were highly enriched for WRKY transcription factor (TF)-binding motifs throughout all tested species. Interestingly, regulatory regions of genes specifically induced in *A. thaliana* or *Capsella rubella* were enriched for WRKY-binding motifs only in *A. thaliana* or *C. rubella*, respectively. This indicates that WRKY TFs play an important role in flg22-triggered gene induction and that the gain of WRKY-binding motifs in regulatory regions accounts for some species-specific expression changes. Taken together, this study advances the field of comparative transcriptomics by providing empirical analysis for the evolution of stress-induced transcriptome changes within and across plant species with a defined phylogenetic framework.

Zusammenfassung

In der Natur sind Pflanzen von einer Vielzahl verschiedenartiger Mikroorganismen umgeben. Pflanzen können diese Mikroorganismen anhand von konservierten Mikroben-Molekülen sogenannten „microbe associated molecular patterns“ (MAMPs) wahrnehmen, welche von Pflanzenrezeptoren auf der Zelloberfläche erkannt werden. Dies aktiviert das Pflanzen-Immunsystem, eine sogenannte „pattern triggered immunity“ (PTI) wird in der Pflanze ausgelöst. PTI schützt die Pflanze vor einer Vielzahl schädlicher Mikroben und löst zahlreiche Abwehrreaktionen, unter anderem eine heftige Transkriptions-Antwort, aus. Obwohl PTI ein wichtiger Prozess für die Adaptierung von Pflanzen auf unterschiedliche Mikroorganismen darstellt, ist unklar wie bedeutend diese massive Transkriptionsantwort ist, in wieweit diese Reaktion in anderen Pflanzenarten konserviert ist und wie PTI evolviert. Um diese offenen Fragen zu klären, habe ich die Transkriptionsantworten zwischen drei *A. thaliana* verwandten Brassicaceae Spezies sowie von fünf *A. thaliana* Ökotypen auf das bakterielle MAMP flg22 untersucht und miteinander vergleichen.

Diese Analyse ergab das große Teile der Transkriptionsantwort auf flg22-indizierte PTI zwischen den getesteten Brassicaceae Arten, durch stabilisierende Selektion während der Brassicaceae Evolution, konserviert wurden. Dies verdeutlicht die Bedeutung dieser massiven Transkriptionsantwort während PTI. Gleichzeitig weisen Arten-spezifische Transkriptionsmuster, welche inkongruent mit der Brassicaceae Phylogenese sind, darauf hin, dass adaptive Evolution einige Diversifizierungen der flg22-induzierten Transkriptionsantworten beeinflusst hat. Im Gegensatz dazu waren flg22-induzierte Transkriptionsantworten zwischen verschiedenen *A. thaliana* Ökotypen hoch konserviert. Die inter-Spezies Variation der Transkriptionsantwort, welche die intra-Spezies Variation weit übersteigt, zeigt zum einen, dass die die kurze evolutive Zeit innerhalb einer Art nicht ausreichend ist, um solch eine Diversifizierung zu erzeugen, und andererseits das neutrale Evolution vermutlich einen geringen Einfluss auf die beobachteten Diversifizierungen zwischen den Arten gehabt hat. Regulatorische Sequenzen konservierter flg22-induzierter Gene waren in allen getesteten Arten mit WRKY Transkriptiosfaktor(TF)-Motiven angereichert. Interessanterweise waren *A. thaliana* und *C. rubella* spezifisch induzierten Gene nur in *A. thaliana* und *C. rubella* regulatorischen Sequenzen für WRKY TF Motive angereichert. Dies deutet darauf hin, dass WRKY TFs eine wichtige Rolle bei der flg22-induzierten Geninduktion spielen und dass der Gewinn von WRKY-Bindungsmotiven in den regulatorischen Sequenzen für einige artspezifische Expressionsänderungen verantwortlich ist. Insgesamt treibt diese Studie das Feld der komparativen Transkriptionsanalyse voran, da hier zum ersten Mal Stress-

induzierte Transkriptionsantworten mehrere Ökotypen innerhalb einer Pflanzenart mit denen zwischen mehreren Pflanzenarten, in einem phylogenetisch definierten Rahmen, verglichen wurden. Dabei untermauerten evolutiv konservierte Transkriptionsantworten ihre Bedeutung für das Pflanzenimmunsystem, wohingegen Arten-spezifische Transkriptionsmuster potenziell adaptive Merkmale hervorhoben.

1. Introduction

1.1. The plant immune system

In nature, plants are surrounded by a myriad of diverse microbes which can be beneficial or harmful for the plant (Bulgarelli et al., 2013; Agler et al., 2016). In order to stay healthy and grow, plants must recognize non-self or altered-self and mount the appropriate responses when sensing microbes in their surroundings (Jones and Dangl, 2006; Couto and Zipfel, 2016). Since plants lack an adaptive immune system, they rely on an innate immune system enabling plant cells to recognize pathogens via different types of receptors (Spoel and Dong, 2012). Plants detect pathogens via cell surface localized pattern recognition receptors (PRRs) by utilizing the presence of conserved structures, called pathogen- or microbe-associated molecular patterns (PAMPs or MAMPs) (Jones and Dangl, 2006; Spoel and Dong, 2012; Ranf, 2017). Since MAMPs are often relevant for the microbial fitness, plants exploit that MAMPs cannot be easily changed by the microbes (Martin and Kamoun, 2012). MAMP recognition results in pattern-triggered immunity (PTI), which is effective against the vast majority of potential pathogens (Zhang and Zhou, 2010; Macho and Zipfel, 2014; Bigeard et al., 2015). Moreover, plants can activate PTI by sensing plant-derived molecules called damage-associated molecular patterns (DAMPs) via PRRs (Gust et al., 2017).

To increase virulence, microbes evolved virulence factors called effectors, which are delivered inside the plant cell to modify the plant's behaviour to the microbe's benefit; often by perturbing plant immune responses (Toruño et al., 2016; Varden et al., 2017). As a countermeasure, plants evolved a second layer of immunity to not only directly recognize virulence effectors, but also perturbation caused by them via intracellular receptors called nucleotide-binding domain leucine-rich repeat proteins (NLRs) (Jones and Dangl, 2006; Cui et al., 2015). In addition, some NLR receptors even present so-called decoy domains which mimic plant immune components such as WRKY transcription factors that are targeted by effectors and thus trick the pathogen as it activates the NLR receptor rather than perturbing its intended target (Le Roux et al., 2015; Sarris et al., 2015). Successful detection of effector actions activates effector-triggered immunity (ETI), which shares many overlapping features with PTI but is considered stronger and more robust as compared to PTI (Katagiri and Tsuda, 2010). In plant cells surrounding the infection site, ETI often leads to a programmed cell death called

hypersensitive response (HR) to limit further pathogen spread. Taken together, PTI and ETI represent two distinct layers of immunity which help plants to fight against pathogens.

1.1.1. Pattern triggered Immunity (PTI)

In the past three decades, various MAMPs and their cognate PRRs have been identified (Tang et al., 2017). PRRs belong to either of two large protein families called receptor-like kinases (RLKs) or receptor-like proteins (RLPs) (Couto and Zipfel, 2016). RLKs are composed of an ectodomain responsible for specific ligand binding, a transmembrane domain, and an intracellular kinase domain transducing the signal inside the cell (Ranf, 2017). The kinase domain is absent in RLPs (Wang et al., 2008). PRRs can be further classified by the nature of their extracellular ligand-binding domain which can consists of leucine-rich repeat domains (LRR), lysin motifs (LysM), or lectin-like motifs (Ranf, 2017). These different ectodomain structures mostly bind to specific ligand classes; peptides, carbohydrates, and lipids are often recognized by LRR, LysM and lectin-containing PRRs, respectively (Couto and Zipfel, 2016).

The MAMPs recognized by PRRs are conserved structures that are often important for the microbial fitness. The two best described MAMPs to date are the bacterial oligo-peptides flg22 and elf18. Flg22 is derived from the bacterial flagellin, hence it is important for motility, whereas elf18 originates from the bacterial elongation factor Tu, one of the most abundant bacterial proteins with a major function in protein biosynthesis (Felix et al., 1999; Kunze et al., 2004). Flg22 and elf18 are detected by the two corresponding LRR-type PRRs FLAGELLIN SENSING 2 (FLS2) and EF-TU RECEPTOR (EFR), respectively (Gómez-Gómez and Boller, 2000; Kunze et al., 2004; Chinchilla, 2006; Zipfel et al., 2006). Other PTI-triggering structures sensed by plants include peptidoglycans, forming bacterial cell walls and chitin, the main component of fungal cell walls (Kaku et al., 2006; Gust et al., 2007). Both MAMPs are perceived by LysM-PRRs. In *A. thaliana*, chitin is perceived by a heterodimer consisting of CHITIN ELICITOR RECEPTOR KINASE 1 (CERK1) and LysM-CONTAINING RECEPTOR KINASE 5 (Lyk5) (Cao et al., 2014). CERK1 is also associated with the two redundant RLPs LysM DOMAIN-CONTAINING GPI-ANCHORED PROTEIN 1 (LYM1) and LYM3, which sense peptidoglycan (PGN), although CERK1 itself does not directly bind to PGN (Gimenez-Ibanez et al., 2009b; Willmann et al., 2011). Recently an S-lectin-domain receptor called LIPOOLIGOSACCHARIDE-SPECIFIC REDUCED ELICITATION (LORE) was found to contribute to immunity in Brassicaceae plants by sensing the lipid A moiety of bacterial Lipopolysaccharides (LPS) (Ranf et al., 2015). The previously mentioned examples described PRRs and MAMPs identified in *A. thaliana*, but several other PRR/MAMP pairs

have been described for other plants species for example: an epitope from bacterial cold-shock protein (csp22) sensed by the PRRs RECEPTOR-LIKE PROTEIN REQUIRED FOR CSP22 RESPONSIVENESS (NbCSPR) (Saur et al., 2016) and COLD SHOCK PROTEIN RECEPTOR (CORE) in *Nicotiana benthamiana* and tomato (Wang et al., 2016), respectively; a *Xanthomonas oryzae* protein called RaxX which is perceived by the rice PRR XA21 (Song et al., 1995; Pruitt et al., 2015); or the fungal MAMP ethylene-inducing xylanase 1 (EIX1) which is sensed by the tomato PRRs LeEix1 and LeEix2 (Ron and Adi, 2004; Bar et al., 2010). Taken together, different PRRs can detect a broad spectrum of microbe-derived molecules.

In addition to MAMPs, some PRRs evolved to detect DAMPs. DAMPs are host-derived molecules originating from presumably damaged plant cells or can be produced by plants after pathogen recognition (Gust et al., 2017). For example, the two RLKs PEP 1 RECEPTOR 1 (PEPR1) and PEPR2 redundantly perceive a group of small peptides called AtPep1-AtPep6 produced by *A. thaliana*, to boost PTI (Yamaguchi et al., 2006; Huffaker et al., 2006; Huffaker and Ryan, 2007; Yamaguchi et al., 2010).

PRRs often form sophisticated heteromeric receptor complexes, through interaction with co-receptors or signal transducers. For example, BRI1-ASSOCIATED RECEPTOR KINASE 1 (BAK1), as well as several related SOMATIC EMBRYOGENESIS RECEPTOR KINASES (SERK) family members, interact with multiple PRRs including FLS2, EFR and PEPR1, in a ligand-dependent manner and in case of FLS2, BAK1 acts as a co-receptor (Heese et al., 2007; Chinchilla et al., 2007; Schulze et al., 2010; Roux et al., 2011). Moreover, many known RLPs lacking an intracellular signalling domain interact with SUPPRESSOR OF BIR1-1 (SOBIR1) to transduce the signal inside the cell (Zhang et al., 2013a; Liebrand et al., 2014; Albert et al., 2015). Thus, MAMPs are perceived by receptor complexes rather than by single PRRs.

After MAMPs are successfully sensed, multiple PTI responses are triggered in a temporally coordinated manner (Yu et al., 2017). Within minutes after MAMP perception, Ca^{2+} influx, reactive oxygen species (ROS) burst, and mitogen-activated protein kinase (MAPK) phosphorylation are triggered (Blume et al., 2000; Asai et al., 2002; Sagi et al., 2006; Jeworutzki et al., 2010; Yu et al., 2017). These responses are often mediated and coordinated by receptor-like cytoplasmic kinases (RLCKs) associating with PRR receptor complexes (Tang et al., 2017). For example, BOTRYTIS-INDUCED KINASE 1 (BIK1) is a RLCK interacting with multiple PRRs including FLS2, BAK1, EFR, PEPR1, and CERK1 (Tang et al., 2017) and directly connects MAMP perception with the ROS burst by activating the plasma membrane-resident NADPH oxidase RESPIRATORY BURST OXIDASE HOMOLOGUE PROTEIN D

(RBOHD) after MAMP perception (Nühse et al., 2007; Li et al., 2014b; Kadota et al., 2014; Tang et al., 2017).

These early responses are followed by intermediate responses including a massive transcriptional reprogramming (Li et al., 2016) and increased accumulation of different phytohormones. Multiple phytohormones such as ethylene, salicylic acid (SA), or jasmonate (JA) modulate a complex downstream signalling network after MAMP perception (Tsuda et al., 2008; Pieterse et al., 2012; Anver and Tsuda, 2015). This enables plants to integrate other processes like growth, development, and abiotic stresses to optimize their responses (Vos et al., 2013; Berens et al., 2017). Depending on the type of invading microbes, phytohormones accumulate to different levels and synergistic as well as antagonistic interactions between them enable plants to fine tune the appropriate defence responses (Pieterse et al., 2012; Berens et al., 2017). For example, SA-mediated signalling is classically believed to be active against biotroph or hemibiotroph pathogens whereas JA signalling is important to fight against necrotrophic pathogens or insect pests (Glazebrook, 2005). Many studies reported an antagonistic crosstalk between SA and JA responses (Van der Does et al., 2013; Robert-Seilaniantz et al., 2011), but recent studies also demonstrated positive contributions of either pathway to the other (Liu et al., 2016; Mine et al., 2017). For instance, we recently demonstrated a positive effect of JA on SA signalling if *PAD4*, an important component for SA accumulation, is mutated (Mine et al., 2017). Importantly, a positive effect of JA on SA is also observed when the PAD4 function is disturbed by high temperatures reflecting a condition often faced by plants in nature. Thus, positive interactions of otherwise antagonistically acting phytohormones in perturbed immune networks illustrate an important mechanism to ensure robust signalling protected from pathogens or environmental perturbations. Taken together, the SA-JA crosstalk exemplifies how positive and negative interactions between phytohormone pathways can fine tune and ensure robust PTI signalling, enabling the plant to integrate multiple information to mount the appropriate defence responses.

The signalling cascades triggered by MAMPs finally lead to physiological responses including stomatal closure, callose deposition, plant growth inhibition, and production of secondary metabolites which function together to limit infections of non-adapted pathogens (Yu et al., 2017). Although these responses help plants to fight against attackers, they are costly; hence they need to be tightly controlled to prevent unnecessary resource loss (Belkhadir et al., 2014; Lozano-Durán and Zipfel, 2015; Couto and Zipfel, 2016). Below, further detailed mechanisms are described in the context of flg22 perception by FLS2 as an example.

1.1.2. Flg22 perception, signalling and control via FLS2

Nearly 20 years ago, flg22 and its cognate receptor FLS2 were the first discovered MAMP and PRR pair (Felix et al., 1999; Gómez-Gómez et al., 1999). Today this pair is still under investigation and likely the best-described PRR/MAMP pair in plants. The flg22 epitope of the bacterial flagellin can be sensed by many plant species including Brassicaceae species, tomato, and rice (Gómez-Gómez et al., 1999; Dunning et al., 2007; Robatzek et al., 2007; Takai et al., 2008). Interestingly, some pathogens managed to evade recognition by FLS2 through sequence variation in their flagellin (Cai et al., 2011). Vice versa some plants are able to sense additional flagellin epitopes, for example, tomato sensing flgII-28 by an additional receptor named FLS3 (Clarke et al., 2013; Hind et al., 2016). These examples demonstrate that MAMP recognition is influenced by the co-evolution of microbes and plants.

A. thaliana FLS2 is essential to sense flg22 (Gómez-Gómez and Boller, 2000), but the effective perception of flg22 requires many more components. Upon flg22 binding, FLS2 associates with BAK1 and the crystal structure of this complex revealed that flg22 acts like a molecular glue to stabilize the FLS2/BAK1 heterodimer (Chinchilla et al., 2007; Sun et al., 2013). BAK1 serves as a co-receptor, consequently, *bak1* mutants are impaired in flg22-mediated responses and resistance to *Pseudomonas syringae* (Roux et al., 2011). Upon heterodimerization, FLS2 and BAK1 rapidly phosphorylate each other (Schulze et al., 2010), which is required for early flg22 responses (Schwessinger et al., 2011; Cao et al., 2013).

Besides BAK1, recent publications identified other plasma membrane-localized RLKs interacting with FLS2 to regulate MAMP perception. The LRR-RLK IMPAIRED OOMYCETE SUSCEPTIBILITY1 (IOS1) not only constitutively interacts with both FLS2 and BAK1 but also positively regulates their complex formation upon MAMP perception (Yeh et al., 2016). Furthermore, mutation in *IOS1* decreased *P. syringae* resistance and impaired multiple PTI responses including MAPK phosphorylation and callose deposition (Yeh et al., 2016). The second recently identified interactor of FLS2, which is required for effective immunity, is LORELEI-LIKE GPI-ANCHORED PROTEIN 1 (LLG1). LLG1 interacts with both FLS2 and EFR and forms complexes with BAK1 in a ligand-dependent manner (Shen et al., 2017). Interestingly, *llg1* mutants compromise the flg22-induced ROS burst but do not affect other PTI responses such as MAPK phosphorylation or defence marker gene expression. LLG1 likely mediates ROS burst by regulating flg22-induced phosphorylation of BIK1 (Shen et al., 2017). Moreover, LLG1 influences accumulation as well as ligand-dependent degradation of FLS2. The third recently discovered interactor of FLS2 is the malectin-like receptor kinase FERONIA (FER). FER seems to act as a scaffold to modulate receptor complex

formation by weakly interacting with FLS2 and EFR and by facilitating their ligand induced-complex formation with BAK1 (Stegmann et al., 2017). Interestingly, overexpression of the FER ligand RAPID ALKALINIZATION FACTOR 23 (RALF23) reduced not only flg22-induced BAK1/FLS2 but also elf18-induced BAK1/EFR complex formation, providing a possible negative regulatory mechanism for PRR complex formation. Together these recent publications demonstrate that the flg22 perception by FLS2 involves a multicomponent receptor complex.

Despite aforementioned plasma-membrane localized interactors of FLS2, there are several intracellular proteins interacting with the FLS2 receptor complex to mediate downstream signalling. These are often RLCKs like BIK1, which is phosphorylated upon flg22 binding and thereby released from its constitutive interaction with FLS2 to phosphorylate RBOHD, connecting flg22 perception with the ROS burst (Lu et al., 2010a; Zhang et al., 2010; Kadota et al., 2014; Li et al., 2014b). BIK1 is the first example of a direct connection between PRRs and downstream responses, and early PTI signalling converges on BIK1 as a multitude of PRR complexes described until today interact with BIK1 including FLS2/BAK1, EFR, PEPR1, CERK1 (Tang et al., 2017). The only other example of a direct connection between PRRs and downstream signalling is PBS1-LIKE KINASE 27 (PBL27) which connects CERK1 with a downstream MAPK cascade (Shinya et al., 2014; Yamada et al., 2016). However, PBL27 does not interact with FLS2. Hence, the connection between FLS2 and the MAPK cascade remains elusive. Two other RLCKs interacting with FLS2 and positively regulating PTI are PTI-COMPROMISED RLCK 1 (PCRK1) and PCRK2 (Sreekanta et al., 2015; Kong et al., 2016). *pcrk1 prck2* double mutants exhibit reduced SA accumulation and increased susceptibility against bacterial pathogens (Kong et al., 2016). However, mechanistic insights concerning the connection of these RLCKs to downstream signalling are still obscure. BR-SIGNALING KINASE 1 (BSK1) is another RLCK interacting with FLS2 (Shi et al., 2013). *BSK1* knock out mutants increase susceptibility to a variety of pathogens and similar to LLG1, BSK1 is genetically required for ROS burst but not for flg22-induced MAPK phosphorylation (Shi et al., 2013). Taken together, RLCKs are major components of PRR complexes and play important roles in signal transduction from the plasma membrane to the cytoplasm after MAMP perception.

FLS2 complex formation and signalling are tightly controlled in order to mount the appropriate strength of defence and to save resources from unwanted immune elicitation (Belkhadir et al., 2014; Lozano-Durán and Zipfel, 2015; Couto and Zipfel, 2016). Recently several regulatory mechanisms affecting MAMP perception were discovered. Two redundant

ubiquitin E3 ligases of the Plant U-box (PUB) family, PUB12, and PUB13, are phosphorylated by BAK1 upon flg22 perception and subsequently ubiquitinate FLS2 for proteasomal degradation (Lu et al., 2011). In contrast to PUB12/13, the alpha-subunit EXTRA- LARGE GUANINE NUCLEOTIDE-BINDING PROTEIN 2 (XLG2) of a heteromeric G-proteins complex formed by GUANINE NUCLEOTIDE-BINDING PROTEIN SUBUNIT-β (AGB1) and GUANINE NUCLEOTIDE-BINDING PROTEIN SUBUNIT-γ1/2 (AGG1/2) interact with FLS2 and BIK1 to prevent the proteasomal degradation of BIK1, thereby positively affecting PTI (Liang et al., 2016).

Apart from proteasomal degradation, not only FLS2 but also EFR and PEPR1/2 undergo BAK1-dependent endocytosis in a ligand-specific manner (Robatzek et al., 2006; Mbengue et al., 2016). However, it is not yet clear whether this promotes or attenuates flg22 responses (Khaled et al., 2015).

The phosphorylation status of the FLS2 receptor complex is an important signalling component and consequently presents a major control mechanism of flg22 perception and signalling. For instance, the *A. thaliana* Ser/Thr PHOSPHATASE TYPE 2A (PP2A) negatively regulates flg22-triggered PTI by controlling BAK1 phosphorylation levels (Segonzac et al., 2014). Similarly, the Ca^{2+}-dependent protein kinase CPK28 attenuates flg22-activated immune responses by controlling BIK1 turnover via phosphorylation in both the presence and absence of flg22 (Monaghan et al., 2014). In contrast, the protein phosphatase PP2C38 negatively regulates BIK1-mediated signalling by controlling the BIK1 phosphorylation status only in the absence of flg22 (Couto et al., 2016). This likely prevents auto-activation of FLS2 signalling in the basal state while allowing effective PTI signalling upon pathogen attack. These recent publications describing the regulation of BIK1 by heteromeric G protein, CPK28, and PP2C38 indicate a key role of BIK1 in the regulation of FLS2-mediated immune signalling. Taken together FLS2 activation is tightly controlled by multiple proteasomal degradation and phosphorylation mechanisms to prevent PTI misfire.

Interestingly, many above described regulatory mechanisms are also targeted by pathogens. For example, the *P. syringae* effector AvrPtoB has a dual mode of action acting as a kinase inhibitor to inactivate BAK1 (Cheng et al., 2011) and encoding a ubiquitin E3 ligase which promotes proteasome-mediated degradation of targeted PRRs including FLS2, EFR, and CERK1 (Abramovitch et al., 2006; Göhre et al., 2008; Gimenez-Ibanez et al., 2009a). In addition, it was recently reported that this effector also targets NPR1, a key signalling component of SA and systemic acquired resistance, providing evidence that the same effector can target a multitude of sequence-unrelated immune signalling components at the same time

(Chen et al., 2017). In contrast to ubiquitination-mediated degradation, other effectors directly cleave its target such as the AvrPphB effector targeting BIK1 (Zhang et al., 2010). Both BAK1 and BIK1 present PTI-hubs targeted by virulence effectors, exemplifying the previous finding that hubs in immune networks are frequently targeted by pathogen effectors (Mukhtar et al., 2011). These and many other effectors enable pathogens to circumvent PTI responses and render the plant susceptible.

1.1.3. Transcriptional reprogramming during PTI

Transcriptional reprogramming is one of the hallmarks of PTI activation and thousands of genes rapidly change their expression upon MAMP perception within an hour (Zipfel et al., 2004, 2006; Denoux et al., 2008; Frei dit Frey et al., 2014; Lewis et al., 2015; Li et al., 2016). Large parts of the transcriptional responses triggered by different MAMPs or DAMPs overlap with each other. For example, expression changes in response to flg22 or elf-26 in *A. thaliana* seedlings are highly similar to each other (Zipfel et al., 2006). Similar overlaps of differentially expressed genes were observed in comparisons of flg22 with peptidoglycan (PGN)(Gust et al., 2007), chitin (Wan et al., 2008) or oligogalacturonide (OG) (Denoux et al., 2008) treatments, indicating a large overlap in transcriptional responses between different MAMPs and DAMPs. Typical for this early MAMP responsive transcriptomes are overrepresentations of genes connected to signal perception (many RLK), signal transduction (kinase-activity/phosphorylation), posttranslational modification (ubiquitination), and transcriptional regulation (WRKY transcription factors) (Denoux et al., 2008; Navarro et al., 2004; Frei dit Frey et al., 2014).

Although most previous studies reported no obvious sets, Wan et al. detected some MAMP specific expression changes. However, they compared transcriptome data from different studies, potentially introducing experimental biases and distinguished MAMP-specific DEGs only by Venn-diagrams, which were dependent on subjective significance cut-offs and thus did not indicate qualitative expression similarity between different treatments. In contrast, a recent study identified many genes with flg22-specific expression changes compared to elf18-induced expression changes (Briggs et al., 2017). These results indicate that subsets of genes could be MAMP-specific regulated at specific time points although the authors noted a strong correlation between the flg22 and elf18 transcriptome responses.

In contrast to Briggs et al, all previously mentioned studies used microarray technology and only a few recent studies used RNAseq to capture transcriptional responses upon MAMP treatment. A recent study compared transcriptional responses induced by short trimer-OGs and

longer OGs. Long OGs altered the expression of approximately 3500 genes 1 h after treatment, whereas shorter OGs only regulated approximately 650 genes (Davidsson et al., 2017). Two other recent studies also investigated flg22-triggered transcriptional responses and showed the importance of a CAMTA TFs (Jacob et al., 2017) and the complex interactions between different phytohormone signalling sectors on the regulation of flg22-triggered transcriptional responses (Hillmer et al., 2017).

Transcriptional responses to MAMPs in other species than *A. thaliana* have not received much attention yet. In tomato, flgII-28 treatment triggers a massive transcriptional reprogramming altering expression of over 3500 genes (Rosli et al., 2013). nterestingly, flagellin-derived MAMPs had the greatest impact on tomato gene expression since most of the transcriptional responses induced by *Pseudomonas syringae* pv. *tomato* DC3000 (*Pto* DC3000) was absent in a *Pto ΔfliC* mutant, lacking flagellin. To my knowledge, no other studies investigated transcriptional responses after MAMP treatments in plants other than *A. thaliana*, thus a comprehensive knowledge about the conservation of MAMP induced transcriptional responses is lacking.

The transcriptional regulation after MAMP perception is partly connected to the rapid Ca^{2+} signalling and MAPK cascades activated after MAMP perception (Boudsocq et al., 2010; Frei dit Frey et al., 2014; Li et al., 2016). For example, individual *mpk3*, *mpk4*, and *mpk6* knock out mutants affect the expression of about 36% induced and 68% repressed flg22-responsive genes, despite functional redundancy described for these MAPKs (Frei dit Frey et al., 2014). Similarly to MAPKs, calcium dependent protein kinases (CPKs) are rapidly activated after flg22 treatment and *cpk5 cpk6 cpk11* triple mutants abolish transcriptional induction of several flg22-responsive marker genes (Boudsocq et al., 2010). Thus, both MAPKs and CPKs have important functions in PTI-activated transcriptional responses.

Co-expressed genes often share common cis-regulatory motifs within their 5'-regulatory regions, connecting specific expression patterns with certain transcriptional regulators. Different analysis for enriched sequence-motifs within regulatory regions of early MAMP responsive genes consistently revealed an enrichment for WRKY transcription factor (TF) binding sites (Navarro et al., 2004; Lewis et al., 2015; Jacob et al., 2017). This is in line with the fact that expression of many WRKY TFs is upregulated by MAMP treatments (Navarro et al., 2004; Gust et al., 2007; Wan et al., 2008; Birkenbihl et al., 2017). MPK3 and MPK6 directly target WRKY33, a key TF regulating many downstream targets during immunity, suggesting a direct link between MAPK dependent flg22-responsive transcriptional changes and WRKY mediated transcriptional reprogramming during PTI (Mao et al., 2011; Liu

et al., 2015; Tsuda and Somssich, 2015). Another recent publication identified a large subset of early responsive PTI genes with overrepresented calmodulin-binding transcriptional activator (CAMTA) motifs within their cis-regulatory regions (Jacob et al., 2017). Consequently, a dominant negative camta3-D mutation altered flg22-triggered transcriptional responses. This provides additional evidence for the importance of Ca^{2+} signalling during MAMP induced transcriptional reprogramming.

Besides activation of specific TFs, the general transcriptional machinery itself is modulated after MAMP perception. A recent study demonstrated targeted phosphorylation of specific residues in the carboxyl-terminal domain of RNA polymerase II which positively regulated immune gene induction (Li et al., 2014a). Moreover, multiple mediator subunits, regulators of transcription interacting with RNA polymerase II, are involved in immune gene regulation (Zhang et al., 2013b; Lai et al., 2014; Li et al., 2016). Although many studies investigated the massive transcriptional reprogramming after MAMP perception, there is no direct evidence that these transcriptional responses are required for an effective PTI. To solve this question remains a challenging endeavour since transcriptional responses can hardly be cancelled if they can be blocked at all.

1.1.4. Conservation and Evolution of PTI

Most immunity research has been performed with the model plant *A. thaliana* as well as in crop species such as tomato and rice and comparative studies on the evolution of plant immunity remain scarce. In a recent study addressing the conservation of ETI-mediating NLR receptors, only 5 out of 528 tested NLR genes were conserved across five tested Brassicaceae species (Peele et al., 2014), indicating strong variation in the NLR repertoire even within the Brassicaceae family. In contrast, the perception of MAMPs by PRRs and some early signalling events seem to be conserved in closely related species and some are conserved among land plants (Zipfel et al., 2006; Lacombe et al., 2010). For example, the FLS2 receptor is highly conserved in many plant species including rice, tomato or potato (Boller and Felix, 2009). Despite its conservation, a recent study indicated that FLS2 orthologs from *A. thaliana* accessions and Brassicaceae vary in their flg22 binding capacity (Vetter et al., 2012). Some Brassicaceae FLS2 orthologs e.g. the *C. hirsuta* one did not bind flg22 in their assay. Thus, it appears that sensitivity to specific MAMPs cannot necessarily be inferred from conservation of their cognate PRR receptors. The perception of elf18 by EFR is restricted to the Brassicaceae family, although several homologs of EFR with very similar architecture exist in rice or poplar, suggesting that these might function in MAMP perception as well (Boller and Felix, 2009).

Thus, even highly similar PRRs possibly sense different MAMPs. Interestingly, stable expression of the *A. thaliana* EFR receptor in tomato confers elf18 sensitivity and increased bacterial resistance to tomato, indicating some conservation of downstream signalling between Brassicaceae and tomato after elf18 perception (Lacombe et al., 2010). Similarly, stable expression of the *A. thaliana* RLP23 receptor in potato (*Solanum tuberosum*) confers sensitivity to nlp20 and increased resistance to *Phytophthora infestans* (Albert et al., 2015). Furthermore, swapping of kinase domains from *A. thaliana* EFR with the related rice PRR XA21 does not affect their functions, providing evidence that downstream components directly interacting with PRRs to transduce the signal are likely conserved, even between dicots and monocots (Holton et al., 2015). This is coherent with the extraordinarily high conservation of the PTI signalling hub BAK1 which even has a homolog in the moss *Physcomitrella* (Boller and Felix, 2009). Taken together, PTI evolution was mainly addressed on the receptor levels and PRR swapping experiments indicate some degree of conservation of immediate downstream signalling components.

However, PTI responses can be affected by many other physiological processes such as growth and especially by the environment including abiotic stresses (Pieterse et al., 2009; Vos et al., 2013; Berens et al., 2017). Therefore, it is conceivable that different plants evolved different PTI responses, which are adaptive to specific environments. For example, long-term adaptation to specific abiotic stresses or specific pathogen pressures in a given environment can act as a strong selective force leading to adaptive evolution of the immune system in different plant species. Nevertheless, we actually don't know to what extent PTI responses are conserved in Brassicaceae or any other plant family. Moreover, it is unknown how PTI evolved within a plant family such as Brassicaceae.

1.2. Comparative transcriptomics and evolution of gene expression

Evolution are the genetic changes over time within heritable traits that lead to the adaptation of species to certain environments over multiple generations and ultimately determines the species we face today on our planet. In eukaryotes, the major basis of genome evolution is genetic variation within populations, which can arise from genetic changes such as mutations or changes in the genepool of a population; that is changes in the number and frequencies of alleles for a specific locus within the population.

Mutations can create new alleles whereas different mechanisms such as gene flow and genetic drift change the frequencies of alleles within a population. The concept of natural selection describes the forces that act on this genetic variation to create new phenotypes.

Favourable traits arising from natural selection are also called adaptations. Selection of genetic variation can be positive, selecting for beneficial traits, or purifying (sometimes called negative selection), selecting against deleterious changes. In contrast to adaptive evolution mediated by positive or purifying selection, some mutations result in alleles that do not affect fitness, called selectively neutral alleles, leading to genetic variability within and between species described as neutral evolution (Kimura, 1983). Over time natural selection can change or stabilize traits within a population by directional or stabilizing selection. Stabilizing selection generally reduces genetic variation within a population.

Molecular evolution studies the mechanisms of evolution on macromolecules. By comparing genomic sequences between closely related species, the mechanisms of evolution acting on DNA can be determined; hence neutral and adaptive evolution can be distinguished. If a genomic sequence evolves neutrally, the number of mutations leading to synonymous (without an effect on amino acid sequence) or non-synonymous (with amino acid changes) should be approximately equal at a given protein-coding locus; hence their ratio is close to one. A sequence under positive selection is expected to harbour more non-synonymous than synonymous mutations, whereas in a sequence under purifying selection the rate of synonymous exceeds the rate of non-synonymous mutations (Miyata and Yasunaga, 1980; Yang and Bielawski, 2000; Delport et al., 2009). These analyses help to understand gene functions as they can identify genomic regions important for the species adaptation, thereby potentially connecting genetic variation with phenotypic variation.

For many organisms sharing almost identical genetic information, genetic differences such as mutations in protein-coding genes cannot fully explain phenotypic variation (Haygood et al., 2010; Harrison et al., 2012). It has been demonstrated that transcriptome variation can be a key to understand phenotypic variation. The melanisation in *Drosophila* (Rebeiz et al., 2009) and camouflage in beach mice (Manceau et al., 2011) are classical examples of phenotypes that are the result of gene expression changes rather than protein structure changes. However, in contrast to the latter examples, many complex or condition-dependent phenotypes are influenced by a myriad of genes and can therefore not be explained by single quantitative trait loci (QTLs) (Harrison et al., 2012). Here comparative transcriptomics provides great advantages compared to comparative genomics to identify sets of genes controlling phenotypes or influencing adaptation. Consequently, comparative transcriptomics have been applied to many newly established model systems to gain new insights into the respective process under investigation (Taji et al., 2004; Slotte et al., 2013; Gan et al., 2016). Furthermore, understanding existing variation in gene expression is important since it may transfer into phenotypic variation

allowing organisms to respond to novel stresses and adapt to a new environment (Alvarez et al., 2015; Whitehead, 2012).

Already 15 years ago with the rise of the microarray technique, first comparative transcriptomic studies were conducted. For example, human and closely related ape transcriptomes were compared revealing species-specific expression patterns especially pronounced in the brain, suggesting that cognitive differences between these species might be connected to diversified gene expression in the brain (Enard et al., 2002). In plants, an early comparative microarray study compared *A. thaliana* with its metal tolerant relative *A. halleri* and found elevated expression of multiple genes associated with metal homeostasis in *A. halleri* compared to *A. thaliana* (Weber et al., 2004).

Together with these first studies comparing transcriptomes from multiple species, a theory of neutral evolution was proposed to explain gene expression variation. This hypothesis expected that most expression variation between species arises from selectively neutral evolution combined with genetic drift rather than from positive selection reflecting adaptive evolution (Yanai et al., 2004; Khaitovich et al., 2004, 2005). Following this hypothesis, expression variation should increase with phylogenetic distances between species. However, this hypothesis is under debate and was criticized for several constraints in sampling as well as quantifying and normalizing polymorphic genome sequences (Gilad et al., 2006). Moreover, other studies in the animal field proposed that transcriptional regulation between species is largely affected by natural selection and that large subsets of gene expression evolved under stabilizing/purifying selection (Rifkin et al., 2003; Lemos et al., 2005; Whitehead and Crawford, 2006; Romero et al., 2012). Regarding plants, Broadley and his colleagues found evidence for a general neutral transcriptome evolution (Broadley et al., 2008). Thus, there is evidence for and against a theory of neutral evolution of gene expression changes between species.

In comparison to the existence of powerful evolutionary models to predict adaptive footprints in DNA sequences (Yang, 2007; Delport et al., 2009), similar models describing gene expression evolution are still premature (Harrison et al., 2012). Although a neutral evolutionary model for gene expression evolution was already proposed over ten years ago, the nature of comparative transcriptomic data makes it challenging to create an appropriate null hypothesis for neutral evolution; yet there is no consensus on a null model allowing statistical tests for adaptive signatures of expression changes (Brawand et al., 2011; Harrison et al., 2012). However, since transcriptional variation arising from a neutral evolutionary process should increase with phylogenetic distance between species, large transcriptional variation that is

incongruent with phylogenetic relationships can be understood as a sign of adaptive evolution (Whitehead, 2012). Thus, including multiple species with different phylogenetic relationships is prerequisite for distinguishing neutral from adaptive variation (Whitehead, 2012).

One problem which complicates these analyses is to distinguish transcriptional variation resulting from environmental differences from variation with a genetic basis (Romero et al., 2012). This is especially a problem in the animal field when dead individuals which did not live under controlled environmental conditions are sampled. Consequently, expression variation may arise from different diets, disease status, or environmental influences which cannot be controlled (Harrison et al., 2012; Romero et al., 2012; Voelckel et al., 2017). Here plant science offers a great advantage as it is considerably easier to minimize variation in environmental conditions between compared species.

Up to now multiple studies have compared transcriptomes of different plant species, initially using heterologous microarray hybridisation technology. This technique was successfully applied to compare *A. thaliana* with *E. salsugineum* transcriptomes suggesting elevated gene expression of abiotic stress-related genes as a potential mechanism of salt stress adaptation in *E. salsugineum* (Taji et al., 2004; Gong et al., 2005). ATH1 microarrays, designed for the *A. thaliana* accession Col-0, were even used to compare the metal hyperaccumulator *Thlaspi caerulescens* with the metal sensitive *Thlaspi arvense* species revealing candidate genes involved in Zn hyper-accumulation (Hammond et al., 2006). Despite opening the world for comparative transcriptomics, microarray-based studies have the disadvantage of using the same probes for multiple strains or even species which can bias the measured expression levels due to sequence or splice variation between species (Whittle et al., 2014; Buckley, 2007).

The development of more and more powerful sequencing and omics methods in combination with decreasing prices facilitates multi species transcriptome comparisons (Whitehead, 2012; Alvarez et al., 2015). Furthermore, RNAseq eliminates multiple drawbacks like hybridisation biases immanent to microarray studies. Up to now a variety of studies compared transcriptomes from multiple plant species with each other investigating diversification of gene expression in C3 versus C4 photosynthesis (Brautigam et al., 2011), Poaceae gene expression evolution (Davidson et al., 2012), tomato domestication (Koenig et al., 2013) or transcriptome conservation among *Lolium*/*Festuca* species (Czaban et al., 2015). Despite these and other studies, RNAseq is still under-utilized for comparative transcriptomic studies in plants (Voelckel et al., 2017).

Several aspects of comparative transcriptomics have not received much attention up to now. For example, most studies compared strains rather than different species with a defined

phylogenetic framework. Even fewer studies not only compared inter-species but also included intra-species expression variation alongside to gain insights into how transcriptional regulation evolved within and between species. This is important because it can help to distinguish evolutionary forces acting on expression changes. If expression is highly conserved within and between species, it likely evolved under purifying selection, whereas conserved expression within species and large expression variation between species point to adaptive evolution. Neutral evolution can be indicated by expression variations within as well as between species (Harrison et al., 2012; Romero et al., 2012). In addition, this comparison helps to assess how short-term adaptation versus long-term adaptation to different environments affects gene expression responses. Furthermore, recent studies concentrated predominantly on basal expression changes between species. Consequently, we lack a comprehensive understanding of transcriptome responses to environmental perturbations within and between related species and how these responses might have evolved.

1.3. Brassicaceae as a model family for comparative genomics and transcriptomics

As discussed in the previous section comparative genomics and transcriptomics are powerful tools to study the evolution of complex traits by identifying common but also diversified genes and their regulations, providing a basis for adaptation of species (Touchman, 2010). To compare genomic features and their regulation, orthologous relationships need to be defined as an underlying framework for comparison (Emms and Kelly, 2015; Tekaia, 2016; Nichio et al., 2017). Related species facilitate the identification of valuable orthologous relationships. As indicated previously, including closely as well as more distantly related species with rich genomic resources facilitates the discovery of evolutionary transitions in the investigated processes and hold the potential to discriminate neutral from adaptive expression variation (Evans, 2015; Whitehead, 2012). For these reasons, the Brassicaceae family provides an excellent framework for comparative studies.

Brassicaceae, alternatively called mustards or Cruciferae based on their cross-like flower architecture, is a diverse plant family harbouring over 3700 species, which can be found throughout all temperate zones (Koenig and Weigel, 2015; Franzke et al., 2016). Different publications date the origin of Brassicaceae between 30 to 100 million years ago but a generally accepted hypothesis for a temporal framework of the family is still debated (Franzke et al., 2016). Most recent publications estimated the Brassicaceae origin between 32 and 38 million

years ago (Hohmann et al., 2015; Edger et al., 2015; Huang et al., 2016). Brassicaceae not only include important crops such as cabbage (*Brassica oleracea*), canola (*Brassica napus, Brassica rapa*), and mustard (*Sinapis alba, Brassica nigra)* but also the most prominent plant model *A. thaliana*. Its superior genome annotation, a multitude of genomic tools, and a large mutant collection for reverse genetic screens helped to reveal numerous concepts and mechanisms in nearly every aspect of plant science (Somerville and Koornneef, 2002; Koornneef and Meinke, 2010; Koenig and Weigel, 2015). However, investigations of a single model species cannot reflect the whole diversity of a plant family not to mention a genus (Koenig and Weigel, 2015). Moreover, comparative analysis is required to understand evolutionary processes. Consequently, many other *A. thaliana*-related Brassicaceae species were recently introduced as model systems for a variety of traits ranging from development to stress responses.

Model species within the Brassicaceae include the selfing species *Capsella rubella* and its outcrossing sister species *Capsella grandiflora* both used to investigate the transition from outcrossing to selfing (Slotte et al., 2013). *Cardamine hirsuta* is another recently established model species that is analysed for its developmental programs affecting the leaf shape and pot shattering (Hay et al., 2014) and whose genome was recently sequenced (Gan et al., 2016). Comparative genomics and transcriptomics with *A. thaliana* revealed important key genes whose duplication, loss, changed transcriptional regulation, and neofunctionalisation led to the complex leaf forms in *C. hirsuta* (Vlad et al., 2014). Besides developmental processes, abiotic stress responses have been investigated using multiple salt and drought adapted Brassicaceae species like *Eutrema salsugineum* (former *Thellungiella halophila* or *Thellungiella salsuginea*; for more information on pervious names see Koch and German, 2013) or *Schrenkiella parvula* (former *Thellungiella parvula*) to understand adaptation to extreme abiotic stress environments (Inan et al., 2004; Gong et al., 2005; Dassanayake et al., 2011; Wu et al., 2012). Along with the development of these model systems, genomes of new model species were sequenced in recent years, facilitating comparative genomics and transcriptomics (Koenig and Weigel, 2015). Taken together, rich genomic resources, many model species, and a clear phylogenetic framework are key advantages of the Brassicaceae family to conduct comparative genomic and transcriptomic studies.

1.4. Thesis aims

Numerous studies have investigated the molecular mechanisms of MAMP perception, downstream signalling, and the MAMP-triggered defence responses that increase the pathogen resistance in *A. thaliana*. Moreover, *A. thaliana* PRRs can be transformed to distantly related

crops like tomato or rice to confer increased resistance. Although this indicates that crucial components for MAMP perception identified in *A. thaliana* also function in distantly related species, we still lack a comprehensive understanding to what extent downstream PTI responses are conserved or diversified and how they evolved. Therefore, the general aim of my PhD thesis was to use comparative approaches between *A. thaliana* and related Brassicaceae species to address the evolution of PTI responses.

Although flg22 perception is generally conserved in angiosperm, recent studies indicate major variation in flg22 binding and responses within *A. thaliana* accessions and among closely related Brassicaceae species (Vetter et al., 2012, 2016). Therefore, the first aim of my thesis was to establish a system to robustly trigger PTI in Brassicaceae species and compare typical PTI responses among Brassicaceae species. I used comparative genomics to reveal sequence conservation of important MAMP perception complexes and compared PTI responses including MAPK phosphorylation, marker gene expression, phytohormone accumulation, and seedling growth inhibition in different Brassicaceae species. In addition, I investigated the effect of flg22 on resistance against the bacterial pathogen *P. syringae*.

Comparative transcriptomics were often utilized to reveal effects of environmental perturbation on gene expression only within one species or to investigate gene expression variation across species in a static environment (Whitehead, 2012). Thus, comparisons of gene expression across species after environmental perturbation have not received much attention. Several studies investigated transcriptional reprogramming after MAMP perception in *A. thaliana* and tomato, but we still do not know how transcriptional reprogramming during PTI is conserved in other species. Therefore, the second goal of my thesis was to generate a comparative transcriptome dataset to compare dynamic transcriptome responses to flg22 among multiple Brassicaceae species.

The importance of massive transcriptional reprogramming during PTI is obscure since MAMP-induced transcriptional reprogramming cannot be specifically blocked. Moreover, it is unknown to what extent other species evolved specific transcriptome responses during PTI. Consequently, my third aim was to investigate the importance of flg22-triggered transcriptional reprogramming during Brassicaceae evolution by determining the degree of conservation. At the same time, I aimed at identifying diversified transcriptome responses to flg22 across Brassicaceae and within *A. thaliana*. This allowed me to tackle my fourth aim: to create new insights into the evolutionary mechanisms affecting PTI responses. On one hand, comparing intra- with inter-species expression variation in response to flg22 indicated how long-term compared to short-term evolution drives diversification of flg22-transcriptome responses. On

the other hand, it facilitated to distinguish whether diversifications in the flg22-triggered transcriptome response evolved under neutral or adaptive evolution.

In summary, this PhD thesis provides new insights into the gene expression evolution during environmental perturbation by comparative transcriptomics within a species and between species with a defined phylogenetic framework.

.

2. Results

To understand the conservation and evolution of PTI responses, I employed Brassicaceae species including *A. thaliana* (Ath), *Arabidopsis lyrata* (Aly), *Capsella rubella* (Cru), *Cardamine hirsuta* (Chi), *Eutrema salsugineum* (Esa) and *Aethionema arabicum* (Aar). These Brassicaceae species offer a defined phylogenetic framework that can be utilized for comparative analyses; *C. rubella* represents a close *A. thaliana* relative, splitting about 9 Mio years ago from *A. thaliana*, while the more distantly related *E. salsugineum* has been evolving for about 26 Mio years independently from *A. thaliana* (Figure 2A). Importantly, compared for instance to the distance between *A. thaliana* and tomato (approximately 118 Mio years) or rice (approximately 160 Mio years), these are relatively close phylogenetic relationships. Together with the rich genomic resources for these Brassicaceae species, this close relationship facilitates comparative approaches (Koenig and Weigel, 2015). Therefore, the Brassicaceae family provides an excellent platform to study conservation and diversification of PTI in an evolutionary framework. A prerequisite for comparative genomics and transcriptomics is solid orthologous relationships of genes between species. Therefore, I determined 1 to 1 orthologous genes for each Brassicaceae using best reciprocal blast between *A. thaliana* and corresponding Brassicaceae species, building the basis for my subsequent analysis.

2.1. MAMP perception and initial signalling components are generally conserved among Brassicaceae species

To reveal the sequence conservation of different PRRs as well as interacting components, I compared Brassicaceae amino acid sequences to their corresponding *A. thaliana* sequences. I extracted genes coding for PRRs, co-receptors, and proteins directly interacting with those receptors from the current literature and extracted corresponding ortholog sequences from *A. lyrata*, *C. rubella*, *C. grandiflora*, *C. hirsuta*, *Brassica rapa* fastplant, *Brassica rapa chifu,* and *E. salsugineum*. The function and mean sequence identity across all analysed Brassicaceae species compared to *A. thaliana* is represented by a schematic overview (Figure 1A) and an additional heatmap indicates pairwise conservation of the proteins for each tested Brassicaceae species compared to *A. thaliana* (Figure 1B). Overall, most PTI components exhibited a high sequence identity to their *A. thaliana* orthologs and their sequence conservation

was generally congruent with the Brassicaceae phylogeny (Figure 1A, B). The mean amino acid sequence identities ranged from 68% to nearly 97%.

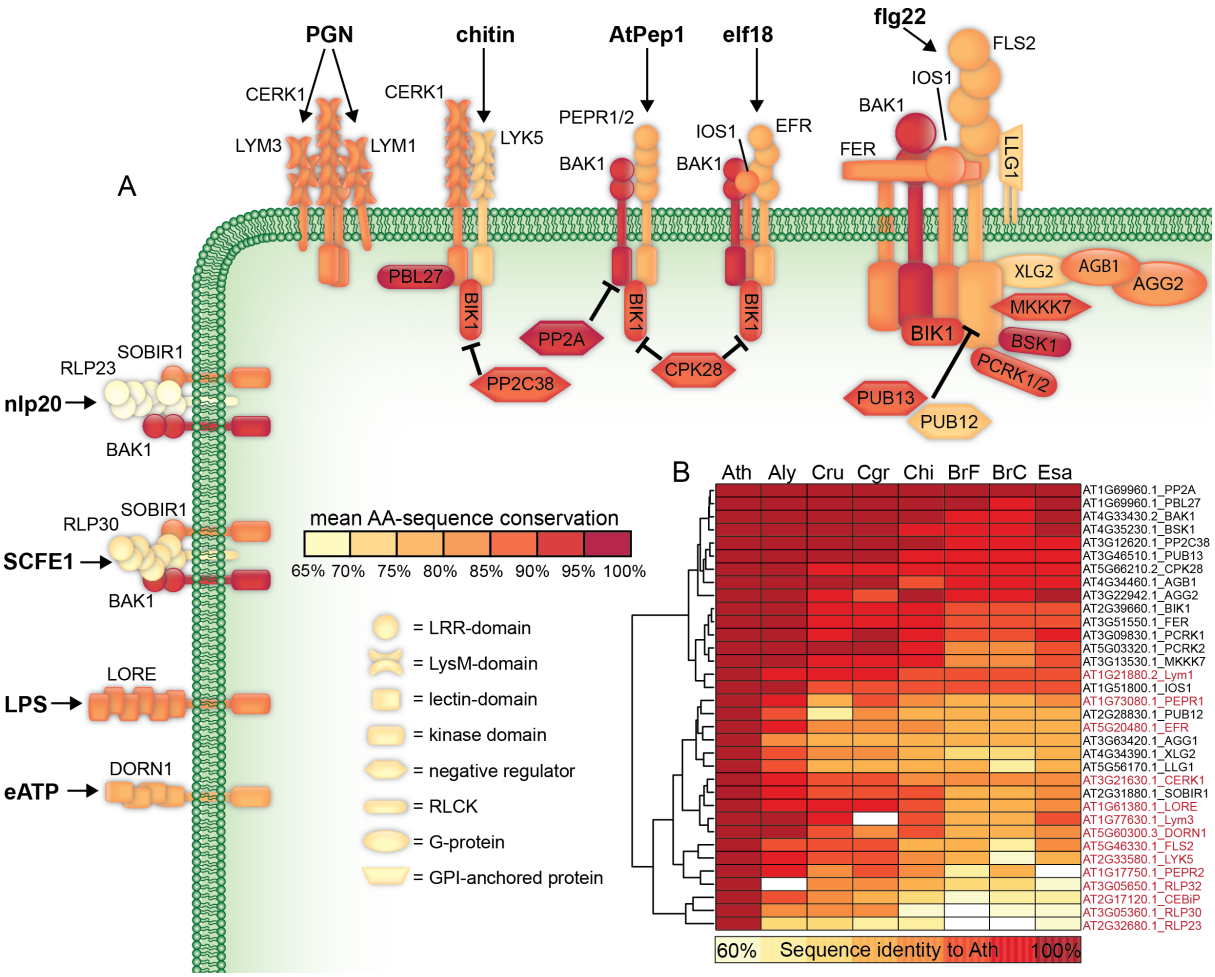

Figure 1: Conservation of MAMP perception components across Brassicaceae species. A: Schematic representation of known components in PRR complexes. The colour-code of the components indicates the mean amino acid-sequence conservation of *A. lyrata*, *C. rubella*, *C. grandiflora*, *C. hirsuta*, *B. rapa* fastplant, *B. rapa chifu*, and *E. salsugineum* compared with *A. thaliana*. **B:** Heatmap showing conservation of the individual proteins depicted in A in each Brassicaceae species compared to *A. thaliana*. Names of PRRs are highlighted in red. White colour in the heatmap indicates genes without a clear 1to1 ortholog match in the species compared to *A. thaliana*. For full names of genes included in this overview please refer to Table 5.

Interestingly, hierarchical clustering of pairwise amino acid sequence identities as well as the mean sequence identities indicated a generally lower sequence conservation of MAMP receptors compared to their co-receptors and interacting partners that connecting receptors and downstream signalling (Figure 1 A, B). Especially RLPs, lacking an intracellular kinase domain, exhibited a relatively low amino acid sequence identity compared to other proteins. Thus, in particular PRRs which confer ligand specificity to MAMPs are more diversified than intracellular signalling components. In line with this, most RLCKs including BIK1, BSK1, PBL27, and PCRK1/2 are highly conserved with on average over 90% amino acid sequence identity to *A. thaliana* orthologs across tested Brassicaceae. Especially, PBL27, which directly connects chitin perception with a MAPK cascade, was extremely conserved with an average

conservation of 97%. Although less conserved compared to other tested components PRRs were still relatively well conserved between Brassicaceae. Altogether, many known MAMP perception and PTI signalling components of *A. thaliana* are conserved in Brassicaceae species, suggesting that tested Brassicaceae species likely respond to MAMPs identified with *A. thaliana*. At the same time, the data suggests different selective pressures on sequence variation of PRRs interacting with microbial ligands and intracellular signalling components connecting MAMP perception to downstream responses.

2.2. Brassicaceae species respond to flg22 in a conserved manner

Flg22 perception is conserved in many plant species and its receptor, FLS2, is one of the best studied PRRs to date (Boller and Felix, 2009). To ensure a robust activation of PTI in the selected Brassicaceae species, I investigated whether flg22 treatment induces phosphorylation of MPK3 and MPK6, reflecting an early signalling event during PTI (Asai et al., 2002). Treatment of 12-day-old seedlings with 1 μM flg22 induced a rapid (15 min) phosphorylation of MPK3 and MPK6 in all tested Brassicaceae species, which was absent in the *A. thaliana fls2* mutant, lacking the flg22 receptor (Figure 2B). To elucidate whether transcriptional responses are triggered similarly, I analysed expression of a flg22-responsive transcription factor *WRKY29* (Asai et al., 2002), at early (1 h), intermediate (9 h), and late stages (24 h) of the PTI response. At all time-points, flg22 treatment significantly induced *WRKY29* expression in all tested Brassicaceae species except the *fls2* mutant (Figure 2C). Thus, flg22 is sensed to trigger typical PTI responses in all tested Brassicaceae.

Next, I tested whether flg22 treatment results in physiological alterations after initial signalling events. A typical feature of PTI is the prioritization of defence over growth resulting in a reduced growth rate (Gómez-Gómez et al., 1999; Huot et al., 2014). Indeed, growing Brassicaceae seedlings for 12 days in flg22 solution significantly reduced fresh weights of each species compared to corresponding control samples (Figure 2D). Yet, the flg22-triggered growth reduction varied among Brassicaceae with a significantly lower impact on *E. salsugineum.* This observation might be influenced by lower growth rates of *E. salsugineum* compared to the other Brassicaceae, potentially lowering the capacity for flg22-mediated growth reduction, or reflects a lower impact of flg22 on seedling growth in *E. salsugineum*. Taken together these results reveal that all tested Brassicaceae seedlings robustly respond to flg22 with certain differences. Therefore, treatment of Brassicaceae seedlings with flg22 is a robust test system for a deeper analysis of PTI responses among the tested Brassicaceae species.

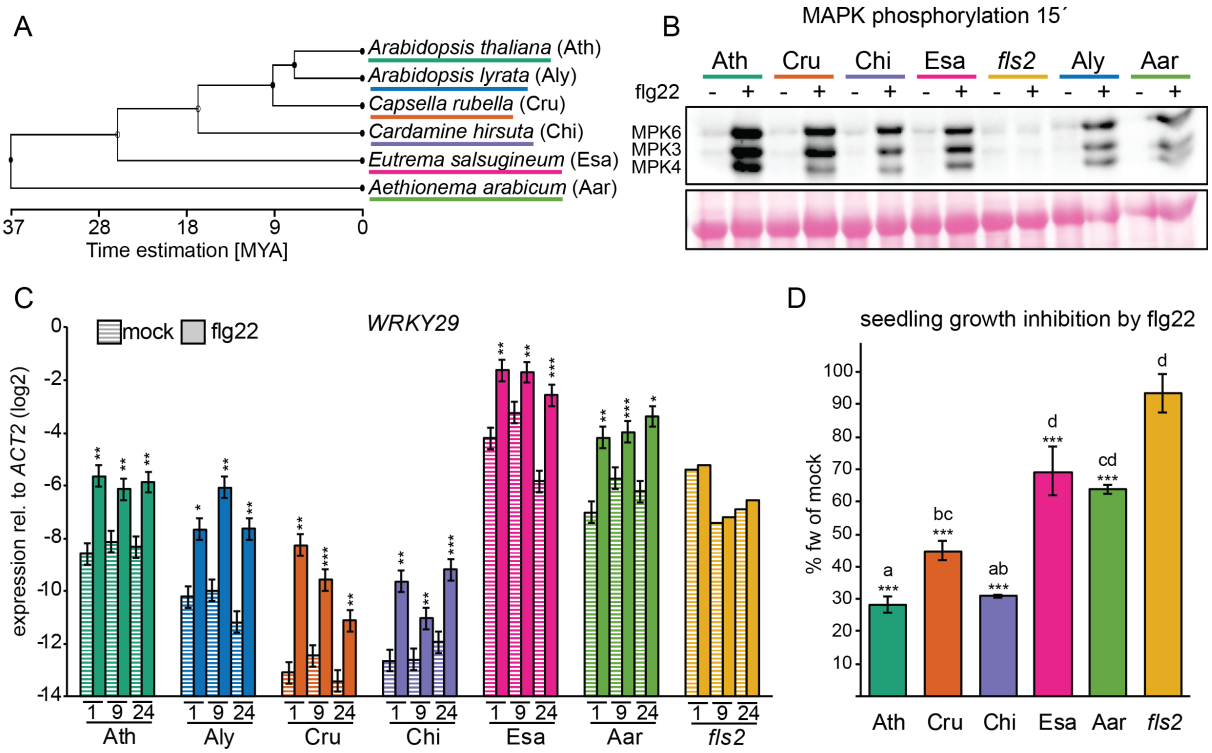

Figure 2: All tested Brassicaceae species respond to flg22. A: Phylogenetic tree generated with Treeview.org indicating the evolutionary distance between the Brassicaceae species used in this study. **B:** Phosphorylation of MPK6/3/4 15 min after the treatment of 12-day-old seedlings with mock or 1 µM flg22 was detected by immunoblotting using an anti-p42/44 antibody. Ponceau staining is shown as a loading control. The experiment was repeated 3 times with similar results. **C:** Expression of *WRKY29* was analysed by RT-qPCR at 1, 9, and 24 h after mock or 1 µM flg22 treatment of 12-day-old seedlings. Bars represent the means ±SE from 3 independent experiments (for *fls2* bars represent one independent experiment). Asterisks indicate significant differences to the respective mock sample (mixed linear model followed by Student´s t-test *, $p < 0.05$; **, $p < 0.01$; ***, $p < 0.001$). **D:** 7-day-old seedlings were grown in liquid medium containing mock or 1 µM flg22 for additional 12 days. The fresh weight (fw) of 12 pooled seedlings was measured. The bars represent the mean percentage of fw ±SE from flg22-treated seedlings compared to mock seedlings from 3 independent experiments. Statistical analysis was performed with log_2-transformed raw fw. Asterisks indicate significant flg22 effects in each genotype (mixed linear model followed by Student´s t-test, **, $p<0.01$; ***, $p<0.001$). Different letters indicate significant differences of flg22 effects between different genotypes (mixed linear model followed by Student´s t-test, adjusted $p < 0.01$).

2.3. Phytohormone levels and their responses to flg22 drastically differ between Brassicaceae species

The crosstalk of different phytohormones such as salicylic acid (SA), jasmonic acid (JA), and abscisic acid (ABA) is one of the key regulatory mechanisms to fine-tune immunity by integrating information from environment and the characteristics of intruders to mount the appropriate level of immunity with minimized resource losses (Vos et al., 2015; Berens et al., 2017). Therefore, phytohormone levels might reflect certain adaptations of different Brassicaceae species with potential impact on PTI outcomes. To capture dynamic changes of phytohormone-levels in different Brassicaceae species, we determined SA, JA, and ABA levels at an early (1 h), intermediate (9 h), and late (24 h) time-point after PTI activation by flg22. SA

has a major influence on immunity and SA levels increase around 6 hours after flg22 treatment of *A. thaliana* (Tsuda et al., 2008). In line with the previous literature, SA accumulation slightly increased in *A. thaliana* 9 h after flg22 treatment and was significantly induced after 24 hpt (Figure 3A). A similar trend was observed for *C. hirsuta*. However, in *C. rubella*, SA levels were significantly increased 1 h after flg22 treatment, but slightly decreased after 9 and 24 h. (Figure 3). This decreased trend of SA accumulation at 9 and 24 hpt was also observed in *E. salsugineum* although SA levels were not affected 1 hpt (Figure 3A).

There was a general trend that flg22 treatment decreased ABA levels of all Brassicaceae, except *C. hirsuta,* at all time-points, especially at 1 hpt (Figure 3B). Interestingly, the basal ABA level of *E. salsugineum* was significantly elevated at the 9 and 24 hpt compared to other Brassicaceae. This might be connected to its adaptation to saline environments (Inan et al., 2004; Gong et al., 2005) and is consistent with the notion that its adaptation might be mediated by enhanced ABA responses (Taji et al., 2004; Wu et al., 2012).

JA levels significantly increased in *C. rubella* and *E. salsugineum* 1 h after flg22 treatment but not later time-points (Figure 3C). In contrast, flg22 treatment did not alter JA-levels in *A. thaliana* or *C. hirsuta* (Figure 3C). Strikingly, basal JA levels were more than a 100-fold higher in *A. thaliana* compared to other species. In summary, phytohormone levels can greatly vary between Brassicaceae not only on a basal level, but also in their responsiveness to flg22. Thus, different hormone levels may affect PTI responses in Brassicaceae species and may reflect evolutionary adaptation to different environments.

2.4. Reduction of *Pto* growth by flg22 varies between species

Although flg22 elicited typical PTI responses in all tested Brassicaceae species, the variable effect on seedling growth-inhibition and phytohormone levels queries whether flg22 treatment can effectively protect different Brassicaceae species against bacterial infection. In *A. thaliana*, flg22-triggered PTI significantly reduces growth of the bacterial pathogen *Pseudomonas syringae* pv. *tomato* DC3000 (*Pto* DC3000) (Tsuda et al., 2009). Therefore, I tested whether flg22-pretreatment similarly reduces *Pto* DC3000 growth in other Brassicaceae species. Flg22-pretreatment of 5-week-old plants greatly reduced *Pto* DC3000 titres in *A. thaliana*, *A. lyrata*, *C. rubella,* and *A. arabicum* compared to mock treated samples (Figure 4A). In contrast, *Pto* DC3000 titres were only slightly reduced in *C. hirsuta* and not altered in *E. salsugineum* and *A. thaliana fls2* mutants. Thus, the robust induction of early PTI responses by flg22 observed in all tested Brassicaceae (Figure 2B, C, D) does not necessarily lead to inhibition of *Pto* DC3000 growth.

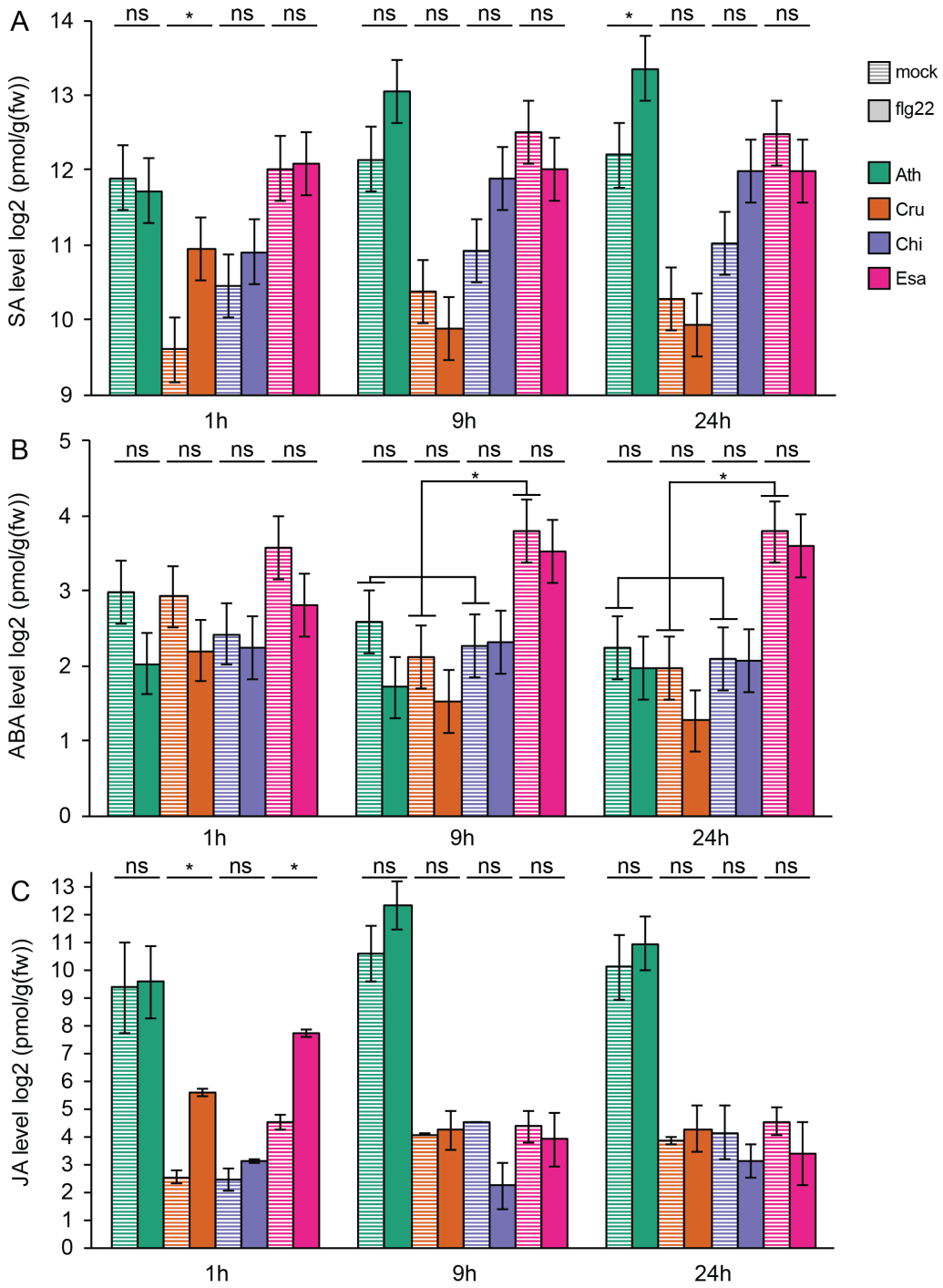

Figure 3: Distinct accumulation and flg22-responsiveness of phytohormone in Brassicaceae species. Phytohormone levels of 12-day-old seedlings were determined via HPLC-MS at the indicated time-points after mock or 1 µM flg22 treatment. **A:** Free salicylic acid (SA) **B:** Abscisic acid (ABA) **C:** Jasmonic acid (JA). Bars represent the means ±SE from 3 independent experiments. **A** and **B** Asterisks indicate significant difference to mock (mixed linear model followed by Student´s t-test; *, $p<0.05$). C The data violated the assumptions to apply a mixed linear model. Therefore, the data was analysed by pairwise Student t-test (flg22 compared to mock treated samples; *, $p<0.05$).

In mock conditions, *Pto* DC3000 titres were significantly lower in *E. salsugineum* compared to other species (Figure 4A). This suggests an incompatible interaction between *Pto* DC3000 and *E. salsugineum* possibly mediated by effector recognition in *E. salsugineum*, leading to ETI activation. Alternatively, *Pto* DC3000 effectors might be less adapted to *E.*

salsugineum targets causing reduced virulence. In any case, this incompatibility might have masked the flg22 effect on *Pto* DC3000 growth in *E. salsugineum*. To test this hypothesis, I conducted a second experiment using a type-3-secretion system (T3SS) deficient *Pto hrcC* mutant. In mock samples, *Pto hrcC* grew to a similar level in *A. thaliana* and *E. salsugineum,* whereas flg22-pretreatment reduced bacterial titres in *A. thaliana* but not in *E. salsugineum* (Figure 4B). Similar to the *Pto* DC3000 assays, flg22-pretreatment of *C. hirsuta* did not affect *Pto hrcC* titres. Interestingly, *Pto hrcC* did not grow in *C. rubella*, both in mock and flg22 treated leaves. Together these results indicate that flg22-triggered PTI responses in *E. salsugineum* were insufficient to lower *Pto* DC3000 or *hrcC* titres and that flg22-induced PTI in *C. hirsuta* only marginally affected *Pto* DC3000 growth, which was not confounded by variation in the effector recognition of these two species.

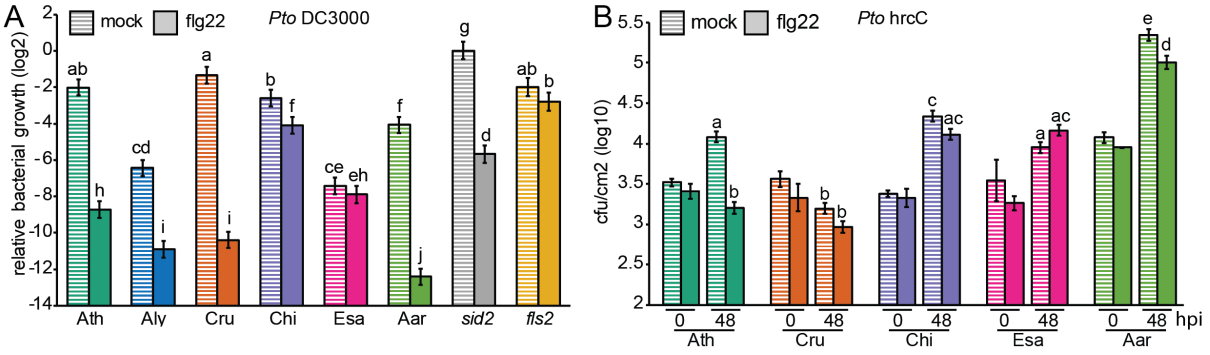

Figure 4: flg22-triggered bacterial growth inhibition in Brassicaceae species. 5-week-old Brassicaceae plants were syringe-infiltrated with 1 µM flg22 or mock 24 h prior to infiltration with *Pto* DC3000 (OD_{600} = 0.0002) (**A**) or *Pto hrcC* (OD_{600} = 0.001) (**B**). **A:** The bacterial titer was determined 48 hours after bacterial infiltration by measuring the DNA amount of the *Pseudomonas syringae* specific *OprF* gene relative to the plant *ACT2* gene by qPCR. Bars represent the means ±SE from 3 independent experiments with each 3 biological replicates (n = 9). **B:** Bacterial titre was determined 0 and 48 hours after bacterial infiltration by serial dilution and counting colony forming unit on plates. Bars represent the means ±SE from 2 independent experiments with each 12 replicates (n = 24). Different letters indicate statistically significant differences (mixed linear model followed by Student´s t-test; adjusted $p < 0.01$).

2.5. Flg22 triggers a massive transcriptional reprogramming in tested Brassicaceae

Phenotypic variation between species is often achieved by diversification of transcriptional regulation and flg22 is known to activate massive transcriptional reprogramming in *A. thaliana* (Navarro et al., 2004; Zipfel et al., 2004; Briggs et al., 2017). However, the evolutionary conservation of flg22-triggered transcriptional responses is not understood. In addition, the importance of the massive PTI-induced transcriptional reprogramming remains obscure because specifically blocking the entire transcriptional reprogramming is challenging if not unfeasible. Alternatively, the importance of a biological process can be inferred by its

evolutionary conservation. Therefore, if flg22-triggered transcriptional reprogramming is conserved, evolutionary theory predicts that it is important.

To investigate temporal dynamics of transcriptional responses, I captured early (1 h), intermediate (9 h), and late (24 h) transcriptome responses of Brassicaceae seedlings to flg22 using RNA-seq (Figure 5A). Mapping the RNA-seq reads to individual Brassicaceae genomes resulted in high mapping efficiencies (Supplement Table 1). To further check the quality of the data, I performed a principle component analysis (PCA) with normalized gene expression values. In all species, except *A. lyrata*, mock and flg22-treated samples were clearly separated and independent replicates were clustered together, indicating the high quality of the dataset (Supplement Figure 1). I removed *A. lyrata* transcriptome data from further analysis, due to its poor reproducibility among biological replicates (Supplement Figure 1F).

For each species and time-point, I determined differentially expressed genes (DEGs) with a q-value < 0.01 and a minimum fold-change of 2 in response to flg22. Flg22 treatment triggered a massive transcriptional reprogramming in each species, significantly changing the expression of 4964 (Ath), 4398 (Cru), 4038 (Chi) and 2861 (Esa) DEGs, suggesting the importance of flg22-triggered transcriptional responses for Brassicaceae plants (Figure 5B). The number of upregulated genes at 1 h was similar among species (2000 to 3000), whereas numbers of downregulated genes varied more drastically; *C. rubella* downregulated approximately three times more genes than *E. salsugineum*. Further, the number of DEGs at later time-points was different: *A. thaliana* and *C. rubella* showed expression changes of about 2000 genes at 24 h, whereas in *C. hirsuta* and *E. salsugineum,* only 300 to 500 genes were affected 24 h after flg22 treatment (Figure 5B).

To compare expression changes between Brassicaceae species, I used a set of 17,857 orthologous genes showing a clear 1 to 1 relationship between *A. thaliana* and each of the three Brassicaceae. From a total of 6106 DEGs, 868 DEGs (14.2 %) were shared among all four Brassicaceae species (Figure 5C). The number of shared DEGs was the highest at 1 hpt, suggesting that late transcriptome responses diverged among Brassicaceae compared to early ones (Supplement Figure 2). This was consistent with the variable number of DEGs at later time-points (Figure 5B) and the stronger conservation of early flg22 responses like MAPK phosphorylation compared to more variable late responses such as seedling growth inhibition or *Pto* growth reduction (Figure 2). Approximately one third of flg22-induced transcriptional changes (34.6% with Cru, 35.9% with Chi and 31.3% with Esa) were shared between *A. thaliana* and each of the other species (Figure 5D).

Despite this core fraction of shared expression changes, many genes were differentially expressed in just one of the species. The specific regulation of 460 (minimum) and 1102 (maximum) DEGs, in *C. rubella* and *E. salsugineum,* respectively, suggests that substantial parts of the transcriptomic response might have diversified (Figure 5C). Together, these findings suggest that a large number of genes might be conserved for their response to flg22, whereas, at the same time, each species has evolved a specific set of genes that are not significantly affected in other species.

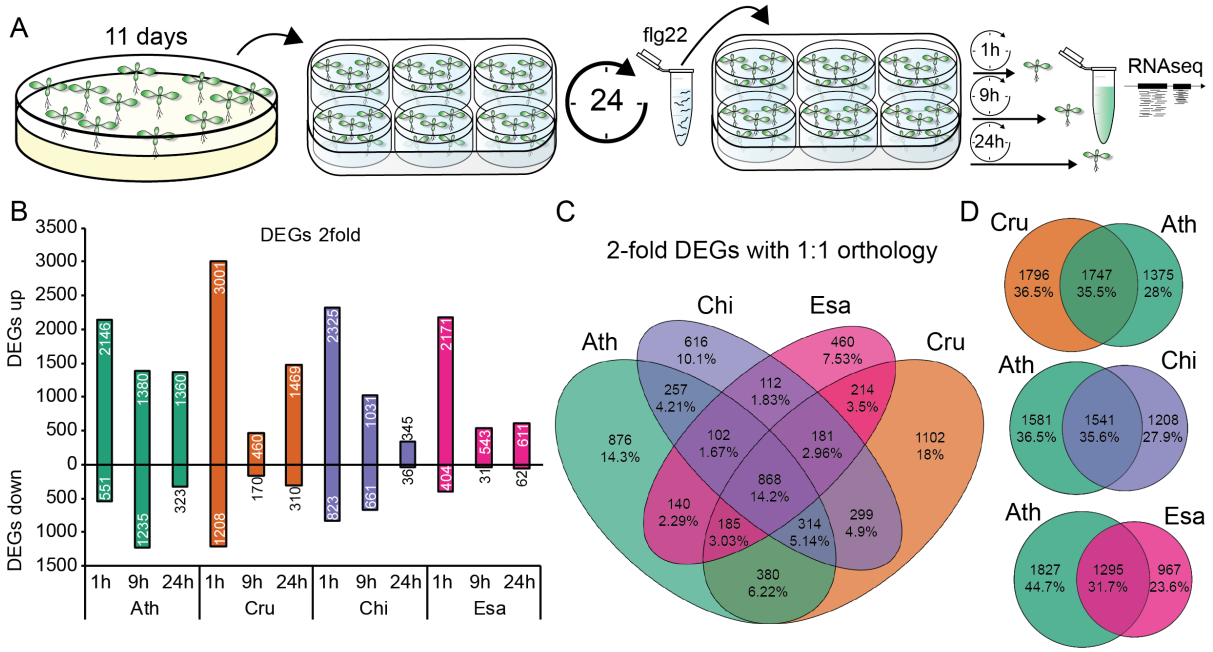

Figure 5: All tested Brassicaceae species induce massive transcriptional reprogramming upon flg22 perception. A: Schematic representation of the experimental design. **B:** Differentially expressed genes (DEGs) were determined using following criteria: q-value < 0.01 and $|\log_2$ fold change$| > 1$. The bars represent the number of up- or down-regulated DEGs at the indicated time points for each species. **C:** A Venn-diagram showing shared DEGs between species. All DEGs which are at least differentially expressed at 1 time point in 1 species were used. **D:** Venn diagrams showing shared DEGs between Ath and the indicated species.

2.6. A core set of genes is conserved for its flg22-responsivness

The Venn-diagram indicated a high overlap of 868 shared DEGs between all four Brassicaceae (Figure 5C). However, the overlap in a Venn-diagram does not necessarily indicate whether the overlapping genes are similarly regulated between species; for instance, shared DEGs might change their expression in opposite directions. To investigate the expression conservation and possible functions of shared DEGs, I extracted the 868 overlapping DEGs (Figure 5C) and clustered them (Figure 6A). Overall these genes behaved similar between species: genes induced in one species were also induced in other species (Figure 6A). Most shared DEGs were strongly upregulated 1 h after flg22 treatment, suggesting an important function of gene induction shortly after flg22 perception. In contrast, only a small number of

DEGs were commonly downregulated, indicating a minor role of transcript reduction during PTI.

To get additional insights into possible functions of shared DEGs, I visualized their expression in *A. thaliana* under a variety of stresses using publicly available datasets from Genevestigator. The shared DEGs were similarly expressed in MAMP (flg22, elf18, and OGs) or DAMP (Pep2) treated *A. thaliana* plants, suggesting that the conserved flg22-responsive genes in Brassicaceae are involved in various MAMP or DAMPs responses (Figure 6A, right heatmap). Likewise, many genes were induced after pathogen attack by *Pto* DC3000 or *Botrytis cinerea* and, to a lesser extent, by SA treatment. In contrast, expression of these genes was barely affected by ABA or MeJA treatment or abiotic stresses, including drought, hypoxia or heat.

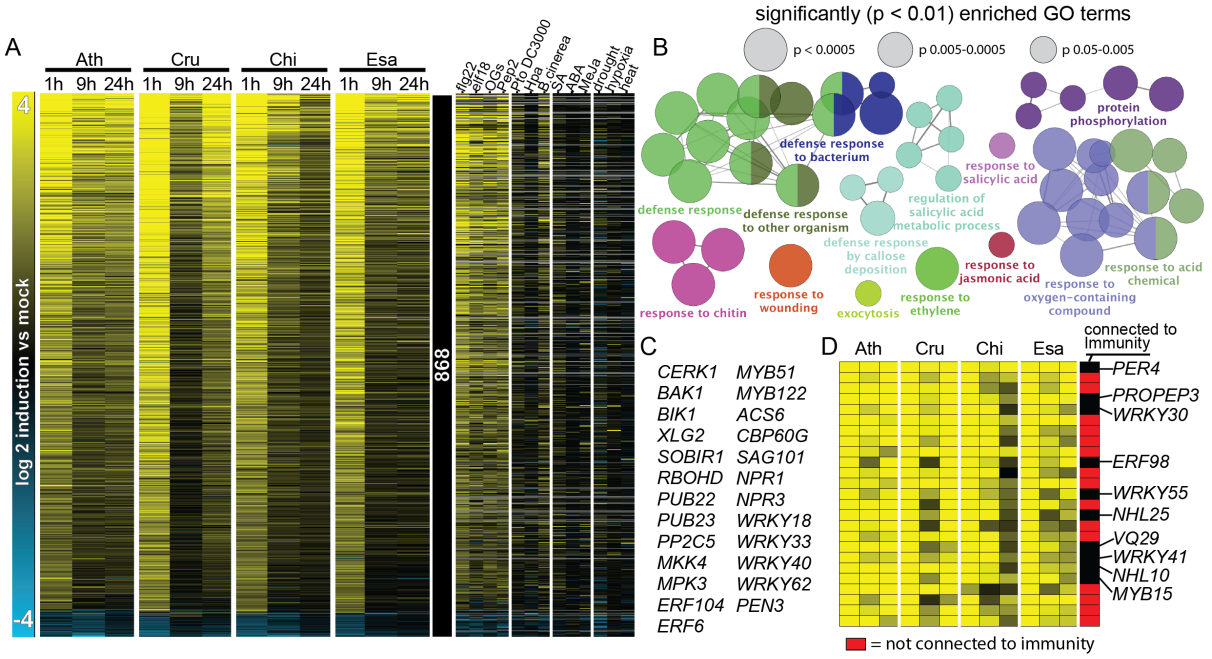

Figure 6: Conserved flg22-responsive genes are associated with immune responses. A: Heatmap of 868 DEGs shared among all tested Brassicaceae species (see Figure 5C). The right heatmap displays expression changes of the 868 DEGs under the indicated stress conditions in publicly available *A. thaliana* datasets (Genevestigator). **B:** The most enriched GO terms of 868 genes grouped using ClueGO Cytoscape plugin. The circle sizes represent significance levels. **C:** Arbitrary selected genes known to be associated with plant immunity. **D:** Heatmap of top 25 induced genes after flg22 treatment based on the mean induction over all samples. Red indicates DEGs that previously have not been implicated in immune responses.

In line with the highly similar expression changes induced by MAMPs, DAMPs and pathogen treatments in publicly available datasets, many highly enriched GO terms within shared DEGs were associated to immune responses or signalling mechanisms, including "defense response to bacterium", "defense response by callose deposition", "response to chitin" and "protein phosphorylation" (Figure 6B). Moreover, genes connected to SA, JA, and ethylene responses were significantly enriched. Consistently, many well-known genes responsible for key processes during immunity including MAMP perception (*CERK1, BAK1, BIK1, SOBIR1*),

ROS burst (*RBOHD*), signal transduction (*MKK4, MPK3*), SA accumulation and responses (*CBP60G, NPR1, NPR3*), and transcriptional reprogramming (*WRKY13/33/40/62, ERF6/104, MYB51/122*) are among these conserved flg22-responsive genes (Figure 6C). These results indicate that the shared DEGs represent a core set of evolutionary conserved PTI components within Brassicaceae.

Despite the large number of known immunity genes among flg22-responsive conserved genes, many shared DEGs among Brassicaceae had no annotation or were not previously described in relation to immunity. For example, half of the top 25 common upregulated genes were previously not connected to immunity (Figure 6D, red boxes), suggesting that a substantial number of genes likely playing roles in plant immunity have yet to be characterized.

2.7. Transcriptomic responses to flg22 differ in their temporal dynamics between species

In contrast to the similar number of genes affected 1 h after flg22 treatment in all Brassicaceae species, there was a substantial diversification at later time points. The total number of DEGs substantially drops at 9 hpt in all Brassicaceae except *A. thaliana* (Figure 7A). In *C. rubella,* the sharp drop at 9 hpt is followed by an increase in the number of DEGs, whereas the number of DEGs in *E. salsugineum* remained around 500 DEGs at 24 hpt. Similar, to *E. salsugineum*, few *C. hirsuta* genes responded to flg22 at 24 hpt. Thus, *C. hirsuta* and *E. salsugineum* showed a rather transient transcriptional response, in contrast to a sustained response in *A. thaliana* and *C. rubella*. Strikingly, the latter observation was correlated with the higher efficacy of flg22 treatment to reduce *Pto* DC3000 growth in *A. thaliana* and *C. rubella* (Figure 4). Notably the total number of expressed genes was very similar among all four species and thus does not explain variation in expression dynamics between species (Figure 7B).

Likewise to the lower number of DEGs in *C. hirsuta* and *E. salsugineum*, the induction level of many shared DEGs was also lower at later time points (Figure 6A). To understand the species-specific kinetics of gene expression, I extracted genes initially induced in *A. thaliana* and *E. salsugineum* ($\log_2$ induction > 0.6), with sustained induction in *A. thaliana* ($\log_2$ induction > 0.6), but transient induction in *E. salsugineum* ($\log_2$ induction < 0.5), resulting in 187 genes (Figure 7C). To reveal possible functions of this gene set, I determined overrepresented GO-terms and found an enrichment for SA-responsive genes (Figure 7D). In line with this, nearly all of these genes are responsive to SA treatment in *A. thaliana* according to publicly available data (Figure 7E). This encouraged me to further extract known immune

genes following the same expression dynamics. I found many genes coding for key genes involved in SA inducting (*SARD1, CBP60G*), biosynthesis (*SID2*), transport (*EDS5*) and signalling (*NPR1,3,4*) (Figure 7F). Importantly, other flg22 responsive genes like the PTI marker gene *FRK1* were expressed at all time-points even in *E. salsugineum* (the bottom row Figure 7F), suggesting that 24 h flg22 treatment is still capable of inducing immunity genes in *E. salsugineum.* Together, these results present accumulating evidence that the distinct temporal dynamics may be explained by distinct activities of SA signalling in different Brassicaceae species.

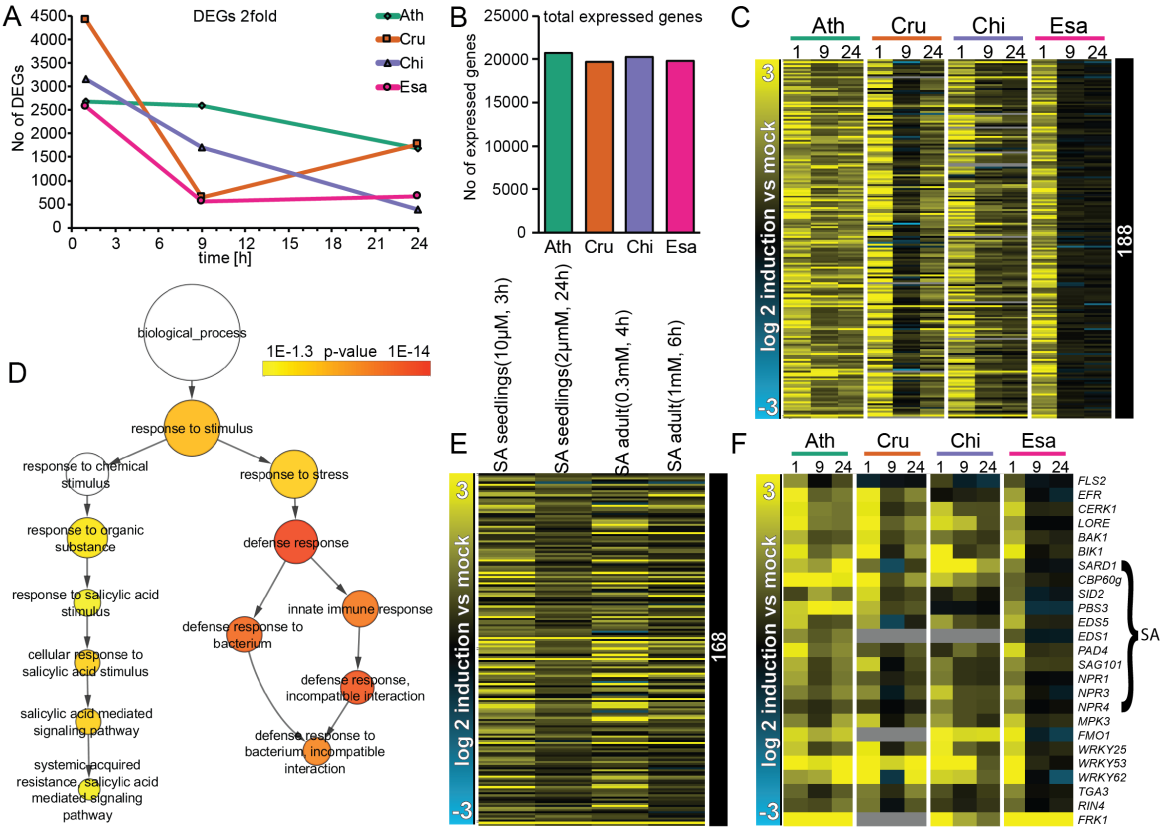

Figure 7: Distinct sustainability of transcriptional response to flg22 in Brassicaceae species is associated with SA-responsive genes. A: Temporal dynamics of transcriptional response to flg22 differs in Brassicaceae species**.** The numbers of DEGs (q-value < 0.01; $|\log_2$ fold change$| > 1$) at each time point in each species are plotted. **B:** Bars indicate the numbers of expressed genes analysed with RNAseq. **C:** Heatmap visualizing 188 genes induced at 1 hpt in Ath and Esa ($\log_2$ induction > 0.6) with sustained induction in Ath ($\log_2$ induction > 0.6 at 9 and 24 hpt) but transient induction in Esa ($\log_2$ induction < 0.5 at 9 and 24 hpt). **D:** GO-terms connected to SA and defence are overrepresented among the 188 genes in **C**. GO enrichment analysis with BinGO plugin for Cytoscape. **E:** Most of the 188 genes (missing genes are caused by missing probes on microarrays of public datasets) are responsive to SA in publically available expression data of *A. thaliana* (Genevestigator). **F:** Heatmap visualizing selected immune genes known as PRRs or SA-related genes of the 188 genes in **C**.

2.8. SA levels do not explain distinct temporal transcriptome dynamics

The significant induction of SA levels at 24 hpt in *A. thaliana* which was absent in *E. salsugineum,* is in line with the hypothesis that different temporal transcriptome dynamics may be connected to SA signalling (Figure 3A). However, the missing induction in *C. rubella* at 24 hpt, together with a slight SA induction in *C. hirsuta,* suggests that SA accumulation at 24 h after flg22 treatment does not fully explain dynamic transcription patterns in these two species (Figure 3A). To further test the hypothesis that SA signalling dictates distinct temporal transcriptional dynamics, I selected three maker genes (*SARD1*, *CBP60G,* and *PBS3)* exhibiting sustained induction in *A. thaliana* but transient induction in *E. salsugineum* and tested their expression in the *sid2* mutant of *A. thaliana*, which lacks the SA-biosynthesis enzyme (isochorismate synthase 1) responsible for immunity induced SA-biosynthesis (Wildermuth et al., 2001). In line with our RNA-seq results, expression of *SARD1*, *CBP60G* and *PBS3* was induced at 9 and 24 h after flg22 treatment of wild-type *A. thaliana* and was absent in the *fls2* mutant (Figure 8A, B, C). All three genes were similarly induced in the *sid2* mutant at 9 and 24 hpt, suggesting that SID2-mediated SA accumulation is dispensable for the sustained induction of these genes by flg22.

In addition, I checked the induction of 185 out of 187 extracted genes in Figure 7C, in a previously published RNAseq dataset which quantified flg22-responsive expression in the *sid2* mutant at different time-points (Hillmer et al., 2017). In agreement with the previous RT-qPCR results, flg22 induced most of the genes shown in Figure 7C in the *sid2* mutant after 9 or 18 hpt (Figure 8D). Nevertheless, the induction level in the *sid2* mutant was slightly lower at 9 and 18 h after flg22 treatment compared to wildtype; hence, I cannot exclude a minor role of SA in later transcriptional responses. However, despite the clear link between SA responsive genes and observed transcriptional patterns, these results indicate that the sustained transcriptional response in *A. thaliana* cannot be fully explained by SA accumulation. In line with these results, flg22 treatment efficiently reduced *Pto* DC3000 growth in the *sid2* mutant of *A. thaliana*, but not in the wildtype of *C. hirsuta* and *E. salsugineum* (Figure 4A).

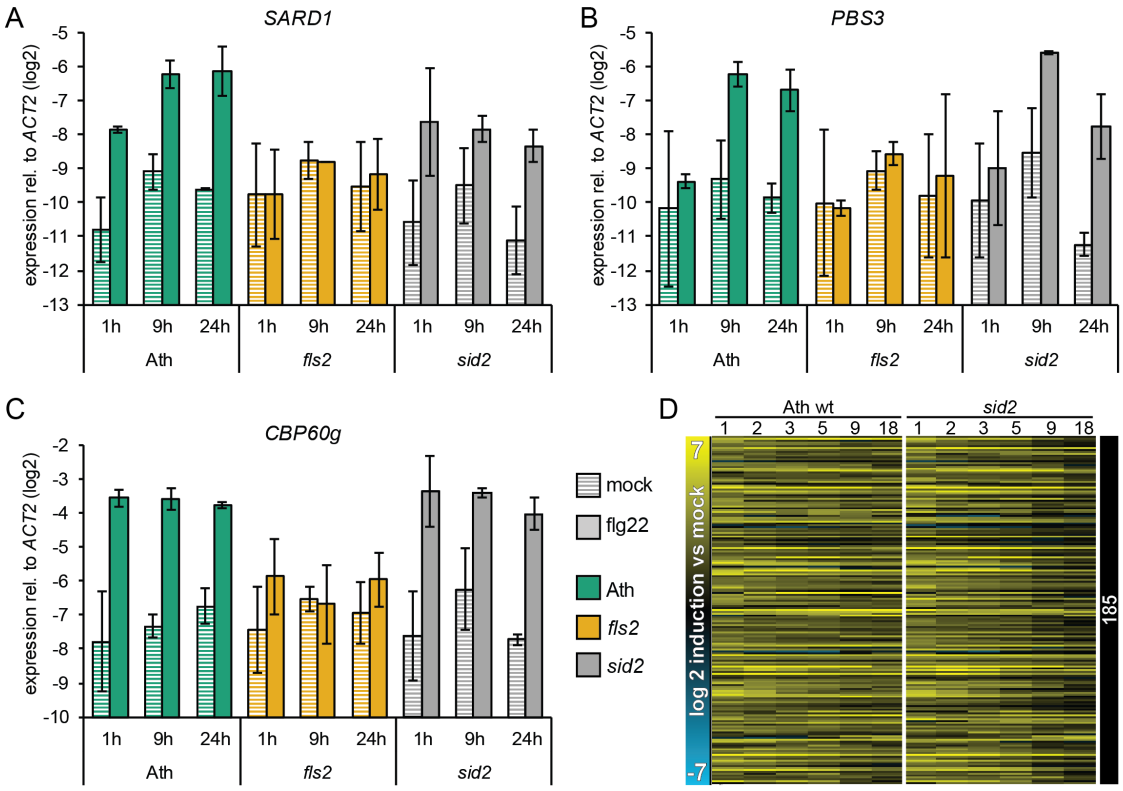

Figure 8: SID2-mediated SA production is not required for sustained flg22-triggered transcriptional response in *A. thaliana*. 12-day-old seedlings of *A. thaliana* wt (Ath), *fls2*, and *sid2* were treated with mock or 1µM flg22 for 1, 9, or 24 h. Expression of three marker-genes extracted from the heatmap in Figure 6C namely *SARD1* **A**, *PBS3* **B**, and *CBP60g* **C** was quantified via RT-qPCR. Bars represent the means ±SD from 2 independent experiments. **D:** 185 genes showing transient induction in Esa (Figure 7C) were analysed for their expression induction in 31 to 32 day-old Col-0 and *sid2* leaves at the indicated time points compared to 0 h after 1 µM flg22 treatment (Hillmer et al., 2017).

2.9. Analysis of Brassicaceae accessions and sister species revealed no correlation between sustained gene activation and the flg22 capacity to reduce *Pto* growth

Sustained transcriptional induction of flg22-responsive genes correlated well with a significant growth reduction of *Pto* DC3000 in flg22-preatreated *A. thaliana* and *C. rubella* plants. In contrast, flg22 had a weak or no effect on *Pto* DC3000 growth in *C. hirsuta* and *E. salsugineum* which exhibited transient gene induction after flg22 (Figure 4). Interestingly, a previous study uncovered a mutant with intact early elf18-induced PTI responses but transient immune-gene expression which was more susceptible to *Pto* DC3000 compared to the wildtype, suggesting that early responses were insufficient, whereas late responses might be crucial for plant-bacterial interaction (Lu et al., 2009). To clarify whether these observations resulted from coincidence or whether sustained transcriptional responses are correlated to effective flg22-triggered immunity to *Pto* DC3000, I performed bacterial growth assays in combination with

marker gene expression analysis in a set of available Brassicaceae accessions and sister species of tested Brassicaceae. I included *Capsella grandiflora*, two additional *C. hirsuta* accessions OLI and GR2 (Chi_OLI; Chi_GR2), another *E. salsugineum* accession YT (Esa_YT), a sister species of *E. salsugineum Thellungiella halophyla* (Tha) and *Schrenkiella parvula* (Spa) another Brassicaceae closely related to *E. salsugineum*. Flg22 pre-treatment significantly reduced *Pto* DC3000 titres only in *A. thaliana*, *C. hirsuta* GR2, and *Thellungiella halophyla* (Supplement Figure 3A). However, marker gene expression at 24 hpt was only induced in *A. thaliana* and *S. parvula*, but not in *C. hirsuta* GR2 or *Thellungiella halophyla* (Supplement Figure 1 B, C, D). Consequently, effective flg22-induced growth reduction of *Pto* DC3000 and sustained marker gene expression were not correlated, suggesting that sustained flg22-induced transcriptome responses are insufficient and unnecessary for effective flg22-induced resistance.

2.10. Early flg22 transcriptomic responses diversified qualitatively between Brassicaceae

A substantial number of DEGs was differentially expressed only in one of the species (Figure 5C). To determine whether the large number of species-specific DEGs is the consequence of the stringent cut-off criteria applied or reflects qualitative differences in flg22 responses among these species, I clustered and visualized expression changes of all 6106 DEGs (Supplement Figure 4). Most DEGs showed qualitatively similar expression changes between species, particularly for early induced genes, indicating that a large proportion of species-specific DEGs resulted from quantitative differences. This also suggests that many early flg22-triggered expression changes evolved under purifying selection, pointing to their importance for PTI.

However, I also found that four out of 15 clusters exhibited species-specific expression signatures (Figure 9A). These four clusters contained 1086 genes, representing about 18% of all DEGs (Figure 9A). To understand their potential functions, I investigated publicly available expression data and analysed GO term overrepresentation in these clusters. Publicly available gene expression data of *A. thaliana* in a variety of conditions did not infer specific functions associated with these species-specific genes (Figure 9B). Analysis of enriched GO terms among species-specific expression patterns revealed a weak but significant enrichment of “phenylpropanoid metablic process” and “lignin metabolic process” in the *A. thaliana* specific pattern and “coumarin metabolic process” in the *C. hirsuta* specific pattern, indicating an enrichment of genes associated with secondary metabolites, which are known to be involved in

plant-microbe interactions (Piasecka et al., 2015) (Figure 9C, D). The distinct expression changes of these genes might affect the production of certain secondary metabolites. I found no enriched GO term for *C. rubella* and *E. salsugineum* specific expression signatures. This may be due to the fact that GO-term annotations strongly depend on *A. thaliana* research and other Brassicaceae species have previously barely been studied in the context of plant immunity. Hence, poorer GO-term annotation of species-specific flg22-responsive genes might impede GO-term analysis of these expression clusters. In summary, large parts of the flg22 transcriptional responses are conserved, but some expression changes diversified during the Brassicaceae evolution, which may be associated to potential adaptations of PTI in different Brassicaceae species.

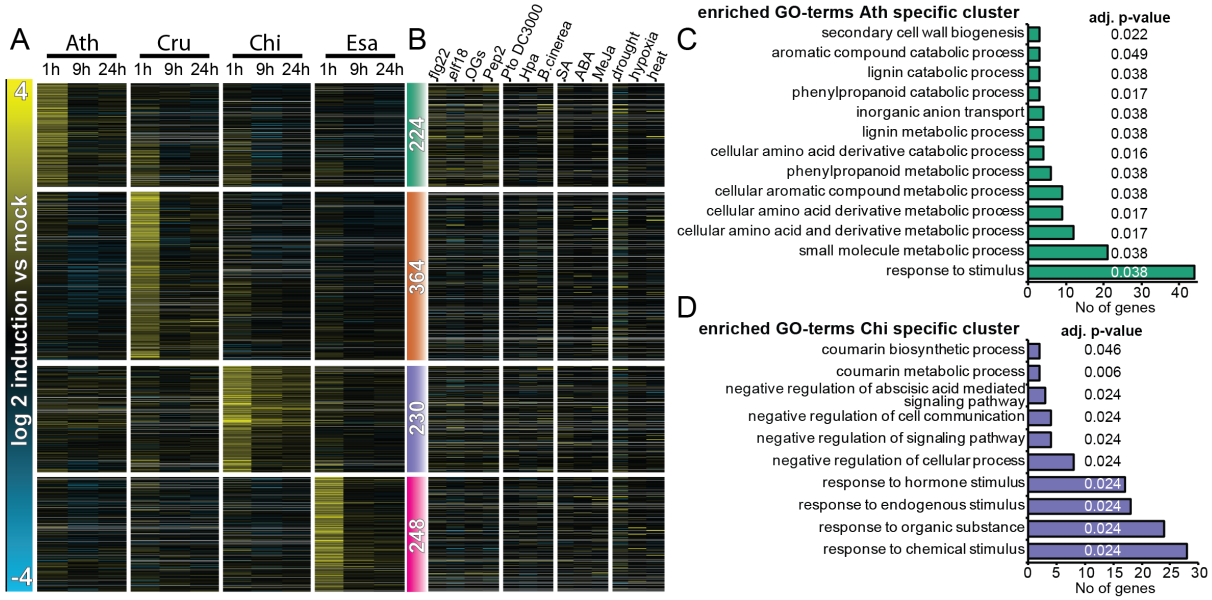

Figure 9: A large fraction of DEGs exhibited species specific expression signatures. A: All 6025 DEGs were clustered by k-means and 4 clusters exhibiting species-specific expression signatures are shown (see also supplemental Figure 3). Colored bars with the number of genes indicate Ath (green), Cru (orange), Chi (purple) and Esa (magenta) specific flg22-responsive genes. **B:** The heatmap displays expression changes of genes within species-specific clusters under indicated stress conditions in publicly available *A. thaliana* datasets (Geneinvestigator). **C** and **D:** Significantly enriched GO terms for Ath specific (**C**) and Chi specific (**D**) clusters determined with BinGO plugin of Cytoscape. For Cru and Esa specific clusters no significantly enriched GO-terms could be determined.

2.11. Flg22 transcriptome responses are highly conserved between genetically and geographically distinct *A. thaliana* accessions

To understand expression evolution and distinguish neutral from adaptive evolutionary processes, it is important to also analyse within species variation of gene expression (Harrison et al., 2012; Romero et al., 2012). Expression under purifying selection is similar within and between species, whereas selectively neutral expression changes are predicted to show a high variation both within and between species. In contrast, evolutionary adaptive expression

changes should vary specifically between species but not within species (Harrison et al., 2012; Romero et al., 2012). Moreover, regarding the large impact of environmental variation on immunity, it is unclear whether inter-species transcriptome variation needs long-term evolution over several Mio years associated with species diversification or whether short-term evolution within a species can lead to similar degree of variation. To disentangle these possibilities, I analysed flg22-induced transcriptome responses in a set of genetically and geographically diverse *A. thaliana* accessions.

First, I tested the responsiveness of 24 *A. thaliana* accessions to flg22 using a MAPK phosphorylation assay. Flg22 treatment induced MAPK phosphorylation in all accessions except CVI-0, which lacks a functional FLS2 receptor (Dunning et al., 2007), and therefore serves as a natural negative control (Figure 10A). To avoid underestimation of diversity in flg22 responses within *A. thaliana*, I further picked 12 accessions that belong to distinct genetic groups (based on admixture groups from 1001genomes.org) and are geographically distributed over the USA, Europe and Asia (Figure 10B). To test whether flg22 triggers transcriptional responses in these accessions, I determined the *PROPEP3* expression 1 h after flg22 treatment. All 12 accessions significantly induced *PROPEP3* expression to similar levels (Figure 10C). I selected five of these accessions to capture their transcriptome 1 h after flg22 treatment using RNAseq. This included Can-0, Gy-0, Kn-0, Kon and No-0 *A. thaliana* accessions. Importantly, these five accessions were collected from geographically distant regions (Figure 10B), are genetically diverse, and present variable growth phenotypes (Figure 10D).

The transcriptional response of *A. thaliana* accessions to flg22 treatment was similar in magnitude compared to the Brassicaceae response, ranging from 2443 (Kn0) to 4372 (Kon) DEGs (compared to 2861 to 4964 for Brassicaceae) (Figure 10E). However, the overlap of DEGs between *A. thaliana* accessions exceeded the overlap between Brassicaceae, as 1232 DEGs, 26% of all DEGs, were shared by all the accessions as compared to 15.7% overlap between Brassicaceae species at 1 hpt (Figure 10F and Supplement Figure 2A). To detect accession specific expression signatures, I applied K-mean clustering, with the same parameters used to analyse Brassicaceae DEGs. Consistent with the high overlap of DEGs between accessions, expression changes of all 4733 DEGs (being differentially expressed in at least one accessions) were highly conserved between *A. thaliana* accessions without obvious accession-specific expression signatures (Figure 10G). Thus, in contrast to Brassicaceae, diverse *A. thaliana* accessions, adapted to different environments, exhibited little variation in their early transcriptional response to flg22, indicating that short-term adaptation within a species barely influences diversification of flg22 induced transcriptional reprogramming. In addition, the little

expression variation within *A. thaliana* accessions suggests a low number of neutral evolving expression changes, suggesting that species-specific expression changes may resulted from adaptive evolution.

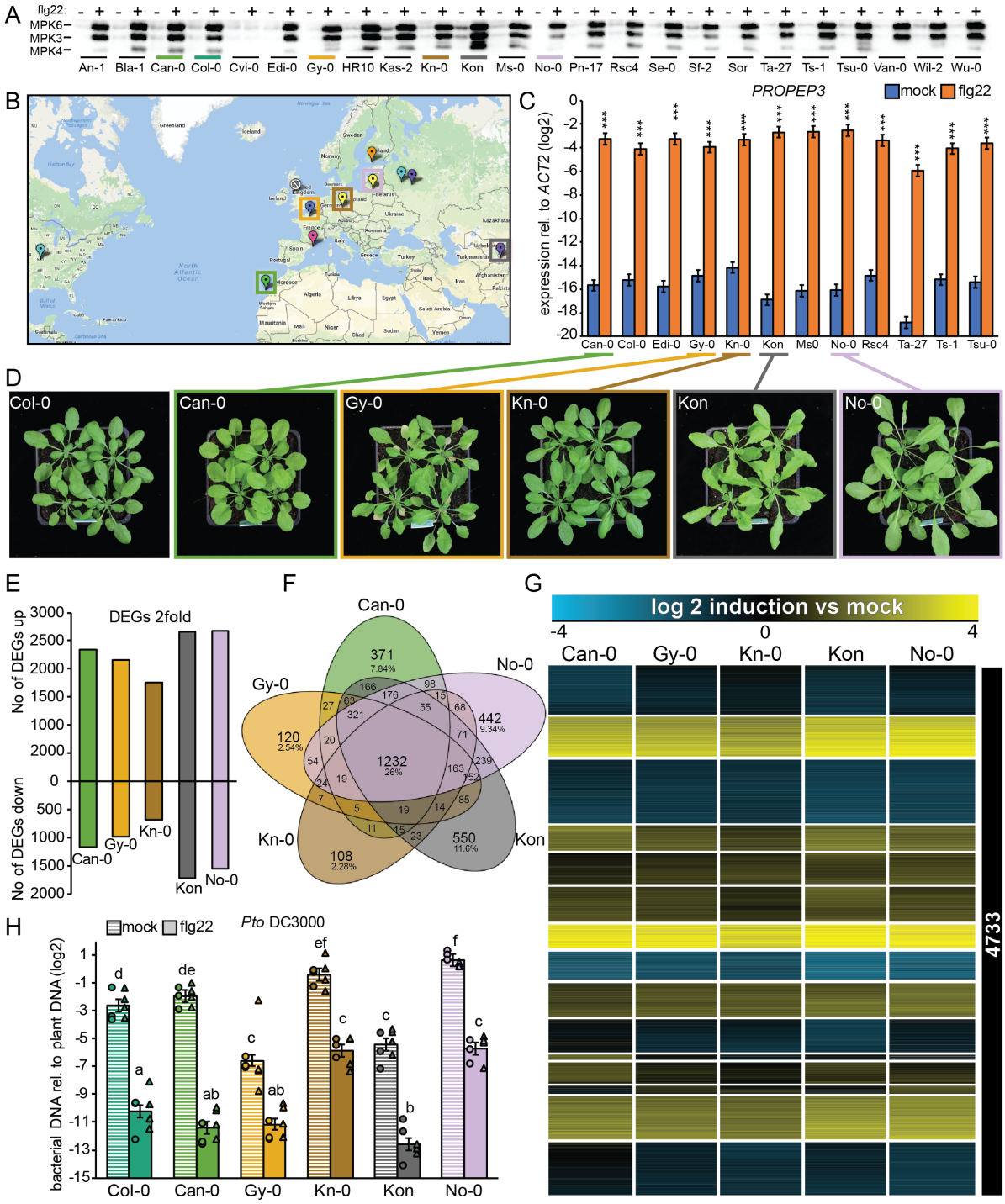

Figure 10: flg22 triggered transcriptional responses are highly conserved among *A. thaliana* accessions with diverse genetic backgrounds. A: Phosphorylation of MPK3/6/4 was detected 15 min after treatment of 12-day-old seedlings with mock or 1 µM flg22 in the indicated *A. thaliana* accessions by immunoblotting using an anti-p42/44 antibody. **B:** Geographic origins of the 5 accessions chosen for RNAseq analysis are shown on the map created from 1001genomes.org. Colours of the markers indicate different genetic groups determined in The 1001 Genome Consortium (2016) Cell. **C:** Expression of the PTI marker *PROPEP3* 1 h after treatment of 12-day-old *A. thaliana* accessions with mock or 1 µM flg22. The accessions highlighted in colour were used for RNAseq experiments. Bars represent the means ± SE from 3 independent experiments and asterisks indicate significant differences between flg22 and mock samples (mixed linear model followed by Student´s t-test; ***, p <0.001). **D:**

Representative pictures of the 4-week-old *A. thaliana* accessions, chosen for RNAseq. **E, F, G:** 12-day-old *A. thaliana* seedlings were treated with mock or 1 µM flg22 for 1 h and extracted RNA was subjected to RNAseq. The analysis was limited to the list of 17,856 genes showing 1 to 1 orthologs in all tested Brassicaceae species to directly compare inter- and intra-species variation in transcriptome responses. DEGs were defined using following criteria: q-value < 0.01 and $|\log_2$ fold change$| > 1$. **E:** Bars represent the number of up- or down-regulated DEGs. **F:** A Venn diagram showing shared DEGs between accessions. **G:** Heatmap of DEGs in at least 1 accession clustered by k-means. Expression changes are shown. **H:** 5-week-old plants were syringe-infiltrated with mock or 1 µM flg22 24 h prior to infiltration with *Pto* DC3000 (OD_{600} = 0.0002). The bacterial titer was determined 48 h after bacterial infiltration by measuring the DNA amount of the *Pseudomonas syringae* specific *OprF* gene relative to the plant *ACT2* gene using qPCR. Bars represent the means ±SE from 2 independent experiments with each 3 biological replicates (n = 6). Different letters indicate significant differences (mixed linear model followed by Student´s t-test; adjusted p < 0.01).

Initially, I mapped the RNAseq reads of the five different *A. thaliana* accessions to the Col-0 reference (TAIR10) genome. To exclude that less flg22-induced expression variation between the *A. thaliana* accessions was biased by this mapping approach, I re-mapped the RNAseq reads to SNP corrected accession-specific genome sequences. Analysis of the data mapped to individual accession genomes revealed comparable results (Supplement Figure 5), indicating that the same conclusion can be drawn regardless of the reference genome used, and thus I further used the initial mapping result with the Col-0 reference.

In Brassicaceae, flg22 differentially affected *in vivo Pto* DC3000 growth, which might be connected to diversification of transcriptional responses during flg22-triggered PTI. Therefore, I speculated that flg22 pre-treatment of *A. thaliana* accessions, sharing very similar transcriptional reprogramming after flg22, might more robustly reduce bacterial titres. Indeed, flg22 significantly reduced *Pto* DC3000 titres in all accessions, although the basal growth of bacteria in mock conditions was variable, with reduced growth in Gy-0 and Kon and enhanced growth in No-0 compared to the Col-0 reference accession (Figure 10H). The variation of bacterial growth in mock-treated *A. thaliana* accessions might be influenced by constitutively activated immune signalling in Gy-0 (Todesco et al., 2010) and reduced defence gene expression in No-0, which were previously reported (Gangappa et al., 2017). However, this did not affect the capability of flg22-pretreatment to reduce *Pto* DC3000 growth. This data demonstrates that together with the highly conserved flg22-triggered transcriptome responses, the capacity of flg22 to reduce *Pto* D3000 growth was highly conserved between genetically and geographically distinct *A. thaliana* accessions.

2.12. Inter-species transcriptome variation exceeds intra-species variation in response to flg22

Species-specific flg22-responsive genes might reflect neutral evolution driven by genetic drift or adaptive evolution by natural selection. Generally, selectively neutral variation

of expression changes should follow the phylogeny, whereas adaptively evolving expression changes can be incongruent with the phylogeny and can show less variation within a species (Romero et al., 2012; Harrison et al., 2012). To disentangle these possibilities, I normalized and analysed the 1 h transcriptome-data of Brassicaceae species together with the *A. thaliana* accession data. A principal component analysis (PCA) including all DEGs across Brassicaceae and *A. thaliana* accessions, clustered *A. thaliana* accessions closely together, whereas other Brassicaceae were clearly separated, mirroring the conserved transcriptional response to flg22 between *A. thaliana* accessions contrary to the diversified response across Brassicaceae (Figure 11A). This is supported by high Pearson correlation coefficients of flg22-induced fold changes between *A. thaliana* accession, ranging from 0.86 to 0.94, which dropped to 0.73 to 0.77 between Brassicaceae and all other samples (Figure 11B). Although the *A. thaliana* Col-0 accession was handled in the same experimental trials with the other Brassicaceae species, and the other *A. thaliana* accessions were handled in independent experimental trials, Col-0 still clustered together with the other *A. thaliana* accession. Together, these analyses demonstrate that inter-species transcriptome variation exceeds intra-species transcriptome variation of flg22-triggered PTI.

To define and analyse diversified transcriptome responses, I recovered species-specific expression signatures similar to the clusters obtained from the individual analyses of Brassicaceae, using K-mean clustering of all DEGs (Figure 11C). In contrast to specific expression signatures present in each Brassicaceae species, I was unable to identify *A. thaliana* accession-specific expression clusters (Supplement Figure 6A). Around 20% of all DEGs across Brassicaceae and *A. thaliana* accessions (1295 of 5961 DEGs) exhibited species-specific expression signatures among Brassicaceae. *C. rubella* specific DEGs represented the largest cluster (451 DEGs). Moreover, some genes were less flg22-responsive in *A. thaliana* compared to all of the other Brassicaceae species (black cluster Figure 11C).

These species-specific flg22-responsive expression clusters could be potentially biased by ambiguously selected orthologous relationships. Determining orthologous genes is especially challenging for genes belonging to a large gene family with many homologs. Therefore, if misassignments of orthologous genes explain species-specific expression patterns, species-specific expression clusters should be enriched for genes belonging to larger gene families compared to other clusters. To test this possibility, I compared gene family sizes in each cluster. Importantly, the species-specific expression clusters were not enriched for large gene families, making it unlikely that species-specific expression patterns resulted from misassignments of orthologous genes (Supplement Figure 7A). Further, the basal expression

pattern of these genes does not explain their selective induction signature in different Brassicaceae species (Supplement Figure 7B). Together, these results demonstrate that the expression variation between Brassicaceae species is not biased by gene-family sizes or basal expression and clearly exceeds the variation within *A. thaliana* accessions.

If the transcriptome variation between Brassicaceae arises from neutral evolution, transcriptome variation should correlate with phylogenetic distance between the species (Broadley et al., 2008). However, *C. rubella*, representing the closest relative to *A. thaliana* within the tested species, clustered most distantly from *A. thaliana* compared to the other Brassicaceae species in the PCA using DEGs (Figure 11A) and presented a much larger number of specifically regulated genes compared to other Brassicaceae (Figure 11C). Moreover, the flg22-induced transcriptional changes did not clearly separate *C. hirsuta* and *E. salsugineum* although their ancestor split approximately 25 Mio years ago (Figure 2A). Thus, the transcriptional variation among Brassicaceae species is incongruent with their phylogeny, suggesting that differences in transcriptome responses to flg22 may be adaptive traits arisen from selective pressures during the Brassicaceae evolution.

Clustering flg22-induced expression changes revealed inter-species expression variation exceeded intra-species expression variation. To further strengthen this observation by statistics, I fitted a mixed linear model to the expression changes after flg22 treatment to determine the number of genes that significantly diversified their flg22-response between *A. thaliana* accessions or between Brassicaceae species. About 2000 genes responded significantly differently to flg22 across the Brassicaceae species (Figure 11D). In stark contrast and in line with the results obtained by clustering, only 131 genes were statistically diversified in response to flg22 among *A. thaliana* accessions. Thus, the number of genes with diversified flg22 responses is more than 15 times higher among Brassicaceae compared to *A. thaliana* accessions.

In addition, I determined the number of genes whose expression change by flg22 is significantly different from all other tested Brassicaceae species or all other *A. thaliana* accessions. Only the Can0 accession harbours one gene that was differentially affected compared to all other accessions. Among Brassicaceae, many genes were specifically regulated in only one of the species and, in accordance with the large size of the *C. rubella* specific cluster, flg22 specifically regulated 262 *C. rubella* genes compared with all other Brassicaceae (Figure 11E).

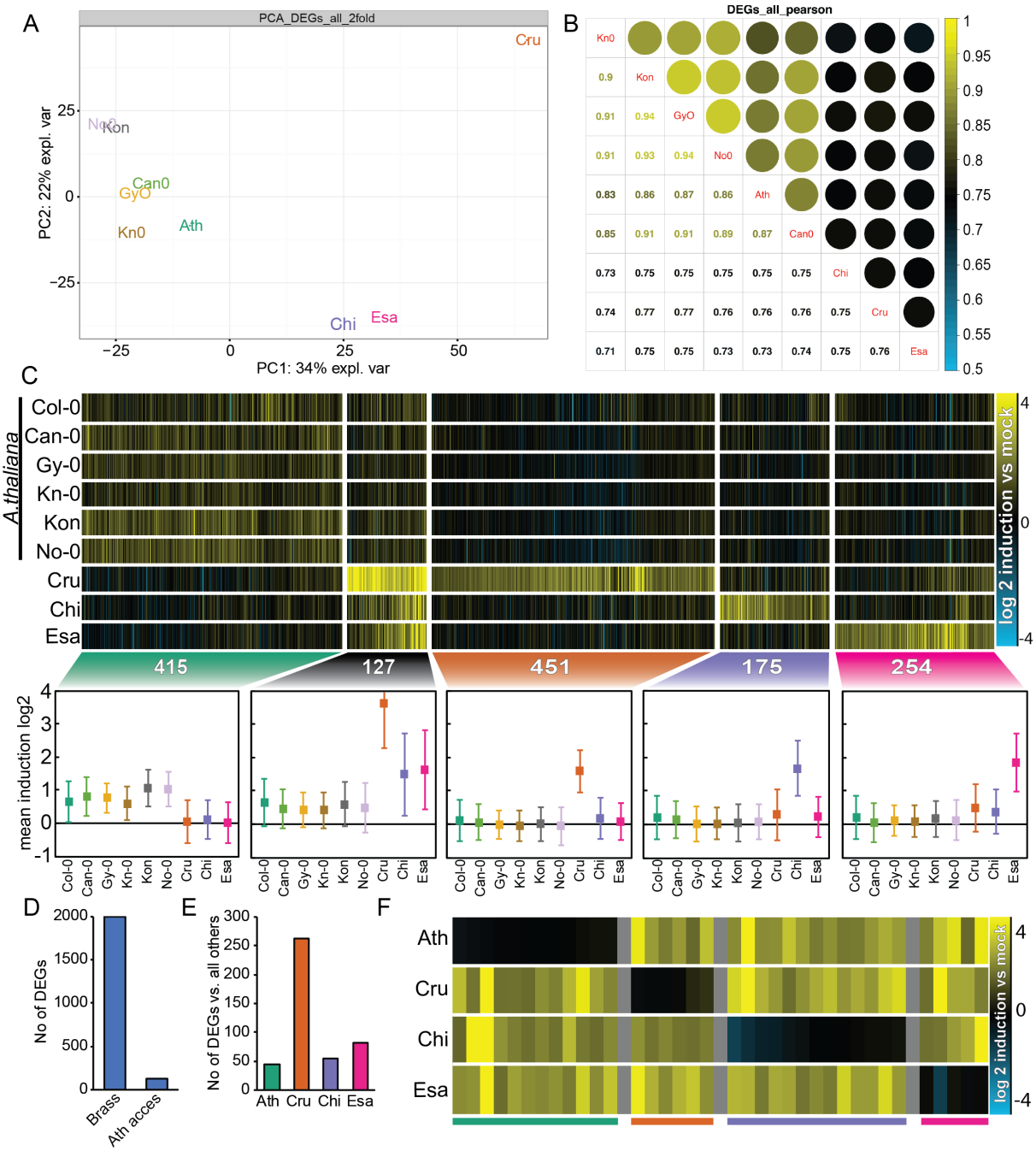

Figure 11: Inter-species variation exceeds intra-species variation in transcriptome response to flg22 and is incongruent with phylogenetic relationships. A to F: Only 1 hour samples were analysed. **A:** Principal component analysis of 1 to 1 orthologous genes that are differentially expressed (q-value < 0.01; $|\log_2$ fold change$|$ > 1) in at least 1 species or accession. **B:** Correlation plot displaying the Pearson correlation between samples based on the gene-expression of differentially induced genes. **C:** All 5961 DEGs were clustered using k-means and 5 selected clusters exhibiting lineage-specific expression signatures [Ath (green), non-Ath (black), Cru (orange) Chi (purple), Esa (magenta)] 1 h after 1 µM flg22 treatment are shown. The number of genes within each cluster is represented by colored bars below the clusters. The mean expression changes ±SD of each cluster in **C** (Visualized with Genesis) are also shown. **D:** The number of DEGs in flg22 response between Brassicaceae species (Brass) and between *A. thaliana* accessions (Ath access) in at least one comparison. **E:** The number of genes responding to flg22 differently in each Brassicaceae species compared to all of the other 3 Brassicaceae species. **F:** Heatmap showing genes which are significantly induced in 3 species but not in the other. Coloured bars indicate specificity for Ath (green), Cru (orange), Cru (purple) and Esa (magenta).

Inspection of these specifically affected genes between Brassicaceae additionally revealed some genes whose expression is significantly less affected by flg22 compared to other Brassicaceae (Figure 11F). These genes were previously not captured by the clustering and might as well play a role for diversified outcomes of plan-microbe interactions. The number of genes which have specifically lost their flg22 responsiveness was much lower compared to specifically induced genes. This further strengthens that the majority of species-specific flg22-induced genes are no artefact since this should result in comparable numbers of specifically induction gain and loss. These specific losses of gene induction in individual Brassicaceae species provide another example how different Brassicaceae adapted their flg22-triggered PTI responses.

2.13. Species-specific flg22-responsive genes are connected to potential diversification of secondary metabolism

If the large amounts of species-specific expressed genes confer an adaptive advantage during evolution, certain biological processes within species-specific genes might be enriched. Unfortunately, I could not detect significant enrichment of specific GO terms within the clusters presented in Figure 11 (Supplement Table 3). Thus, it is likely that the potential adaptive advantage conferred by the species-specific expression signatures is not relying on few important functions but is rather mediated by smaller distinct functions that might additively help adaptation to certain environments.

Despite the absence of significantly enriched biological processes, certain GO-terms were slightly enriched. Some of these GO-terms were associated with secondary metabolism once more, including: “secondary metabolic process” and “glucosinolate biosyntethis process”, “phenylpropanoid metabolic process” and “phenylpropanoid biosynthetic process” enriched within *A. thaliana*, *C. rubella* and *E. salsugineum* specific expression clusters, respectively (Supplement Table 3). As secondary metabolites can have direct influence on the interactions of plants with pathogens, these genes are potentially interesting candidates that might influence the outcome of plant-pathogen interactions. Therefore, I focussed my analysis on genes known to be involved in the secondary metabolism.

Interestingly, a number of genes connected to tryptophan and indole glucosinolate metabolism showed significantly larger induction upon flg22 treatment in *C. rubella* compared with other Brassicaceae. These genes include *ASB1, TSA1, TSB1, CYP79B2/B3, MYB51, PEN3, and IGMT5* (For full names refer to Table 5). This is surprising giving the finding that *C. rubella*

does likely not produce indole glucosinolates at detectable amounts (Bednarek et al., 2011). I hypothesized that these genes might be significantly higher induced in *C. rubella* since they are lowly expressed in the basal state. Indeed, extraction of the normalized basal expression levels of corresponding genes revealed that most of these genes, except of the tryptophan biosynthetic genes, exhibited extremely low basal expression levels compared to their orthologous genes in other Brassicaceae (Supplement Figure 8). For example, the expression level of *IGMT5* in control samples was at least 250 times lower in *C. rubella* compared to the other Brassicaceae (Supplement Figure 8). This reduced basal expression might explain the undetectable indole glucosinolates in *C. rubella* and might reflect potential adaptations of *C. rubella* to certain microbial interactions. Furthermore, the conserved high flg22-responsivness of these genes may suggest additional functions during immunity.

2.14. Species-specific expression signatures are conserved in Brassicaceae accessions and sister species and can be partially triggered by elf18.

To investigate whether the species-specific expression signatures present novel innovations just within one species or accession, or whether they are conserved in accessions or sister species, I tested selected marker genes via RT-qPCR for species-specific expression signatures in *Capsella grandiflora* (Cgr, sister species of Cru), two additional *C. hirsuta* accessions (OLI and GR2), one additional *E. salsugineum* accession (YT) and *Thellungiella halophyla* (Tha, Esa sister species). I selected *PR4*, *CYP79B2* and *NAC32* as *C. rubella*-specific markers. All three genes were significantly induced in *C. rubella* and as well in its sister species *C. grandiflora* (Figure 12). *PR4* and *NAC32* were specifically induced in these two species whereas *CYP79B2* was significantly induced in *A. thaliana* as well (Figure 12). The two *C. hirsuta*-specific marker genes *RAC7* and "*AT3G60966"* (as there is no common name for "*AT3G60966"* I used the AGI code of this gene to designate its orthologs in other Brassicaceae which refer to *Carubv10018513m*; *Cagra.0239s0006*; *Thhalv10006444m*; *CARHR170490.1*) were specifically induced in all three *C. hirsuta* accessions, with exception of a specific "*AT3G60966"* induction in *C. grandiflora*. Finally, all three *E. salsugineum* specific marker genes (*APK4; bZipTF* an unknown bZip domain transcription factor*; CYP77A4*) were specifically induced in the Shandong and Yukon accessions as well as in its sister species *T. halophyla* (Figure 12). Together, these findings confirm our RNAseq results and indicate that the genes specifically regulated in the tested Brassicaceae are also responsive to flg22 in sister

species and other accessions, strengthening their potential role in an adaptation of these species during evolution.

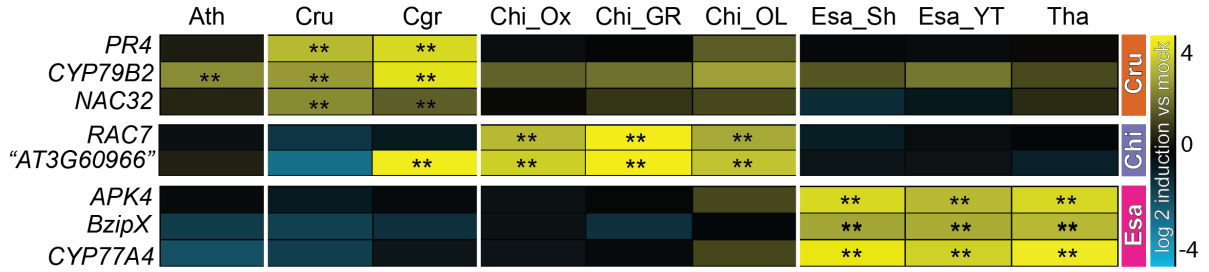

Figure 12: Species-specific expression signatures are preserved in sister species and Brassicaceae accessions. Expression of selected genes, showing species-specific expression signatures depicted in Figure 6C, was determined in available sister species or accessions by RT-qPCR. The colored bars to the right indicate genes showing Cru (orange)-, Chi (purple)-, or Esa (magenta)-specific expression signatures. The heatmap represents the mean $\log_2$ changes upon flg22 compared to mock treatment from 3 independent experiments with each 2 biological replicates (n = 6). Asterisks indicate significant flg22 effects (mixed linear model followed by Student's t-test; $p < 0.01$). Ath, *Arabidopsis thaliana* Col-0; Cru, *Capsella rubella*; Cgr, *Capsella grandiflora*; Chi_Ox, Chi_GR, Chi_Ol, different *Cardamine hirsuta* accessions; Esa_Sh, *Eutrema salsugineum* Shandong; Esa_YT, Esa Yukon; Tha, *Thellungiella halophyla.*

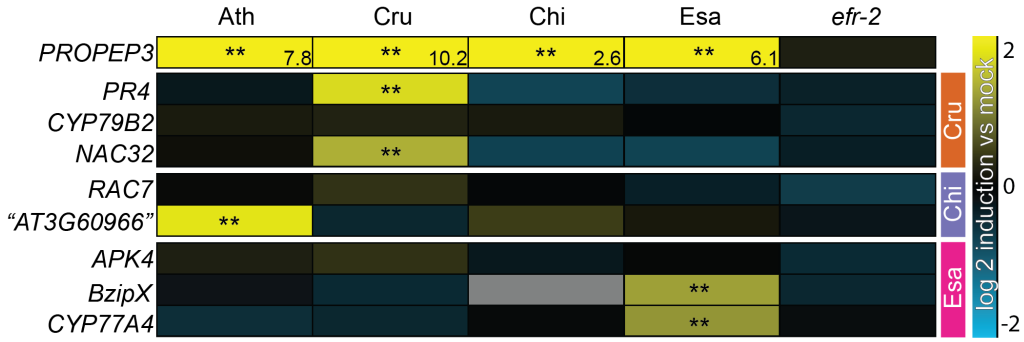

Figure 13: A subset of the species-specific expression changes triggered by flg22 is conserved after elf-18 treatment. Expression changes of selected genes showing species-specific expression signatures depicted in Figure 6C, after elf18 compared to mock treatment in 12-day-old seedlings determined by RT-qPCR. *PROPEP3* expression indicates responsiveness to elf18, with induction levels indicated by small numbers within the heatmap. The colored bars to the right indicate genes showing Cru (orange), Chi (purple) or Esa (magenta) specific expression signatures. The heatmap shows the mean $\log_2$ changes upon elf18 compared to mock from 3 independent experiments with each 2 biological replicates (n = 6). Asterisks indicate significant elf18 effects (mixed linear model followed by Student's t-test; $p < 0.01$).

Although flg22 and elf18 are perceived by a similar perception machinery (Figure 1) and trigger similar responses such as MAPK phosphorylation, ROS burst, and callose deposition, transcriptional reprogramming, exhibits distinct features between these two MAMPs (Briggs et al., 2017). To reveal whether the species-specific expression signatures are a general PTI feature or might be specific to flg22-PTI, I tested the expression of previously identified marker genes after elf18 treatment. The *C. hirsuta* specific marker genes did not show their *C. hirsuta*-specific induction, whereas some of the *C. rubella* and *E. salsugineum* specific genes exhibited a species-specific induction after elf18 treatment (*PR4, NAC32, BzipX, CYP77A4*) (Figure 13). Noteworthy, all species responded to elf18 as *PROPEP3* expression was significantly induced in each Brassicaceae (Figure 13). However, induction of *PROPEP3*

was lower in *C. hirsuta* (2.6 log_2-fold change) compared to other Brassicaceae (6.1 to 10.2 log_2-fold change). This suggests a lower sensitivity of *C. hirsuta* towards elf18 which might explain why *C. hirsuta* specific marker genes were not induced by elf18. Taken together, these findings suggest that parts of the species-specific expression signatures are a general feature of PTI, while some may be specific for flg22-triggered PTI.

2.15. WRKY TF motifs are highly enriched in commonly induced clusters and present in some species-specific expression signatures.

Transcriptional regulation is often mediated by TF binding to specific motifs in the 5´-regulatory regions, near the transcriptional start site (also called cis-regulatory region), to activate or repress transcription. Consequently, similar expression patterns of flg22-responsive genes might be associated with the conservation of similar cis-regulatory motifs controlling the transcription of these genes. Vice versa, species-specific expression signatures might be achieved by gaining or losing specific cis-regulatory motifs. To test this hypothesis, I screened the 5´regulatory regions of genes within each expression cluster for enrichment of known TF-motifs. Regulatory regions of commonly flg22-induced genes were highly enriched for WRKY TF motifs in all four Brassicaceae species (Figure 14A, Supplement Table 4-7). The WRKY TF-family is one of the largest with over 70 members in *A. thaliana* plants and WRKYs are key players during plant immune responses (Pandey and Somssich, 2009; Tsuda and Somssich, 2015; Birkenbihl et al., 2017). Especially, clusters 4, 13 and 14 are strongly enriched for many WRKY TF motifs in all four Brassicaceae species (Figure 14A, Supplement Figure 6, Supplement Table 4-7), suggesting that regulation by WRKY TFs is a conserved feature of transcriptional induction during Brassicaceae PTI.

In addition, *A. thaliana*, *C. rubella* and *C. hirsuta* regulatory sequences were also significantly enriched for several CAMTA TFs in clusters 13, 6, 14, respectively (Supplement Table 4-7). A recent study suggested an important role of CAMTA motifs during the early transcriptional immune response and showed that genetic perturbation of CAMTA3 influences ETI and PTI transcriptome responses (Jacob et al., 2017). Only in clusters 6 and 12, no significantly enriched WRKY motif was detected within *E. salsugineum* and *C. rubella* regulatory sequences. This might be connected to the only moderate expression induction of genes within these two clusters. Overall most flg22-responsive expression changes conserved within *A. thaliana* and across Brassicaceae are connected to WRKY TF regulation.

Regulatory regions of flg22-downregulated genes were enriched for different ATHB TF motifs in each Brassicaceae and AHL TF (AT-hook motif nuclear-localized proteins) in *A. thaliana* and *C. hirsuta* (Figure 14B). In particular, cluster 8 with moderately downregulated genes exhibited multiple enriched TF binding motifs in each Brassicaceae. In contrast, the largest cluster 15 was not enriched for any known TF-motif in neither of the species. Although ATHB TF motifs were commonly found in each of the Brassicaceae, much less common motifs were detected for downregulated genes, suggesting less conservation in transcriptional regulatory mechanisms of flg22-downregulated compared to flg22-upregulated genes.

Interestingly, 5´regulatory regions of some species-specific expression signatures were specifically enriched for certain TF-binding motifs only in the species showing species-specific expression. Whereas *C. hirsuta* specific expression signatures were not enriched for TF-motifs, 5´-regulatory regions of *A. thaliana* and *E. salsugineum* specific flg22-responsive genes were significantly enriched for WRKY TF-motifs (Figure 14C). This was especially pronounced in *E. salsugineum* specific expression signatures (Supplemental table 5, cluster 10). In addition, 5´-regulatory regions of genes with a lower induction in all *A. thaliana* accessions compared to the other three Brassicaceae species were enriched for WRKY3 and WRKY33 motifs in *C. rubella*. This is in line with higher induction of these genes in *C. rubella* compared to other species. The *C. rubella* specific expression signatures were linked to enrichment of AHL12 and AHL25 TF-motifs (Figure 14C). Taken together, WRKY TFs were not only associated with conserved flg22-responsive expression signatures, but also with some of the species-specific flg22-responsive expression signatures, highlighting the importance of WRKYs TF for PTI and suggesting that gain of WRKY TF might be associated with the gain of species-specific flg22-responsive expression changes.

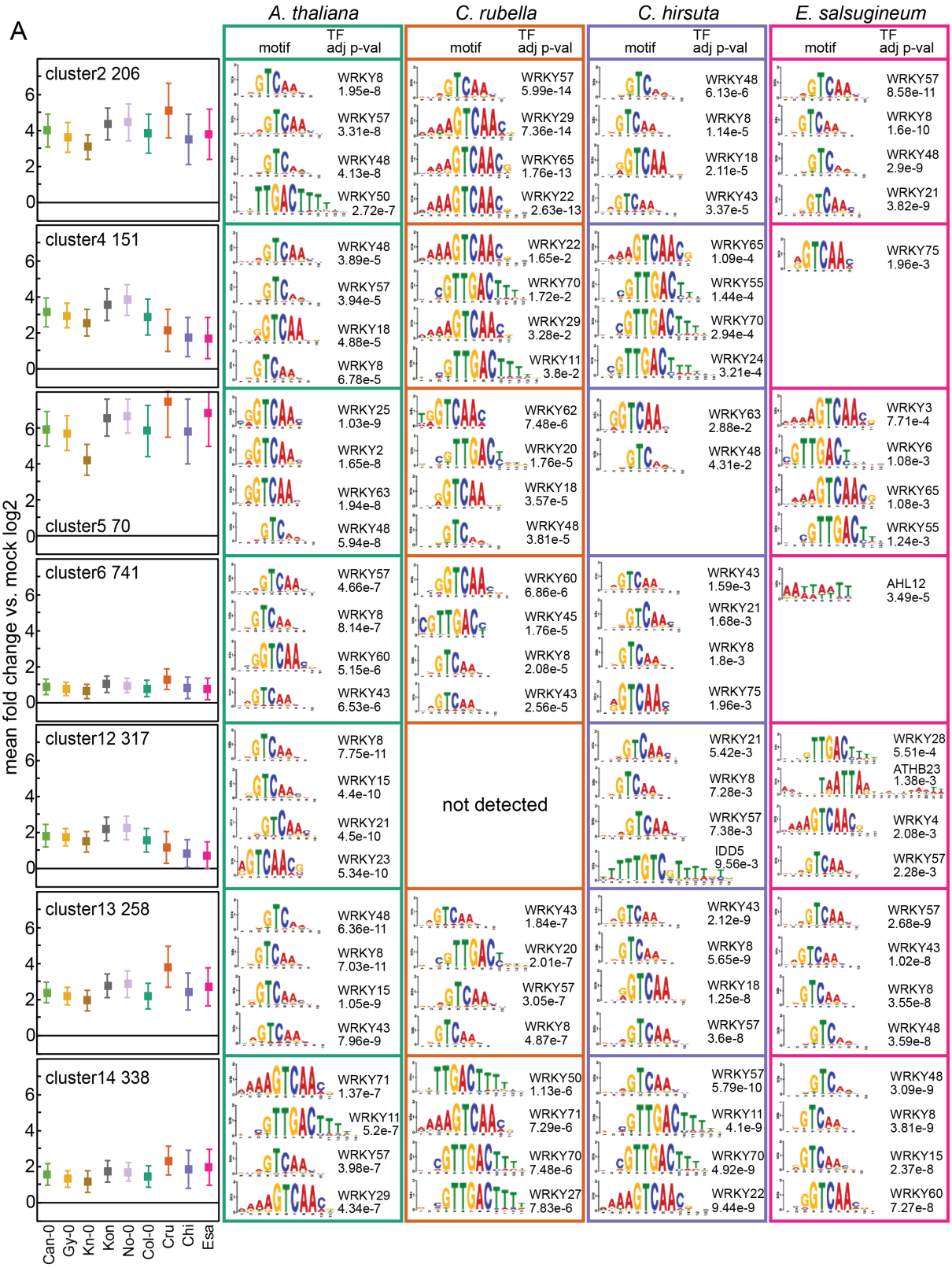
A
A. thaliana
C. rubella
C. hirsuta
E. salsugineum
motif
TF
adj p-val
cluster2 206
cluster4 151
cluster5 70
cluster6 741
cluster12 317
cluster13 258
cluster14 338
mean fold change vs. mock log2
Can-0
Gy-0
Kn-0
Kon
No-0
Col-0
Cru
Chi
Esa
not detected

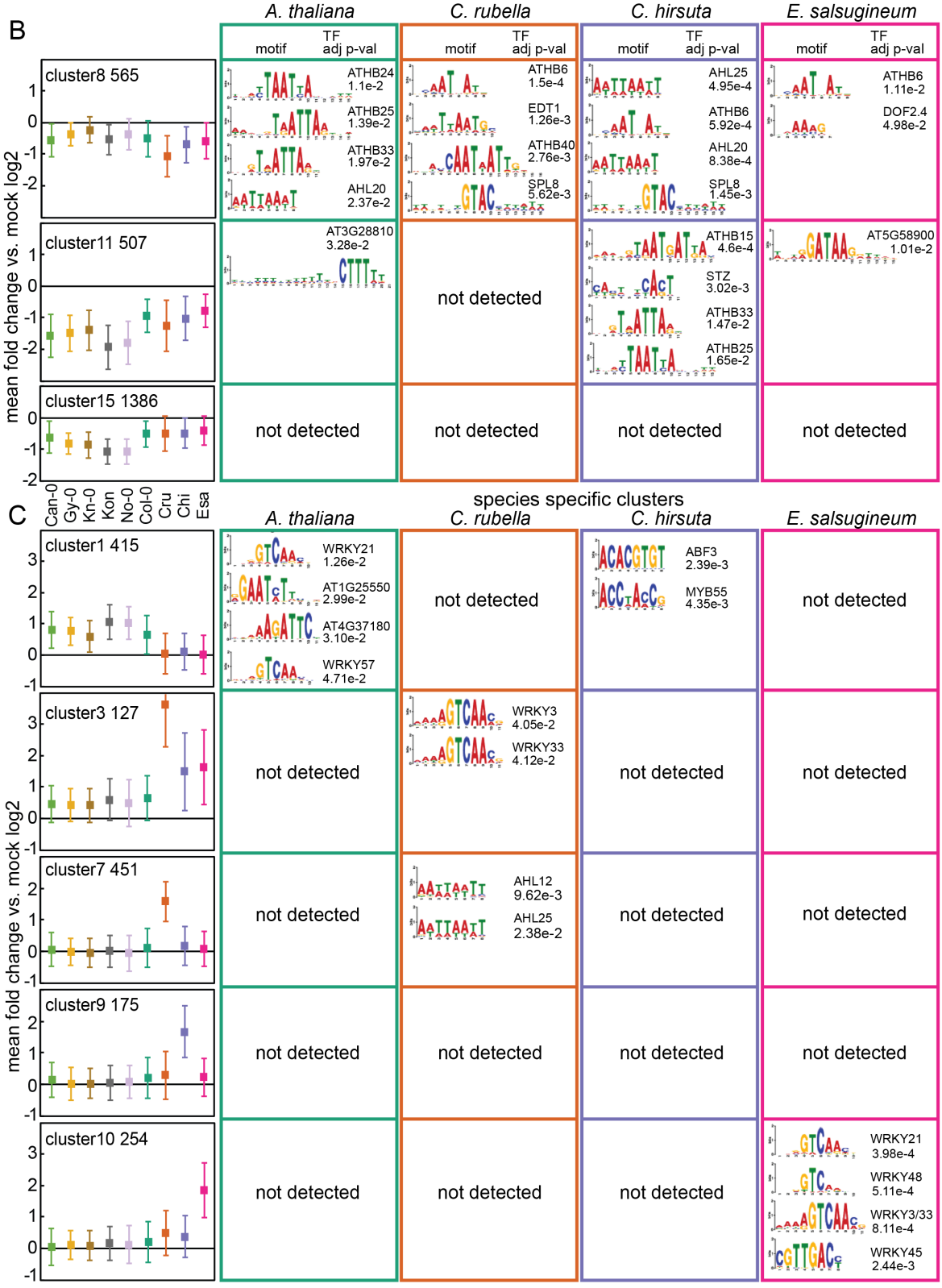

Figure 14: Enrichment of TF-motifs within the 5´regulatory regions of DEG clusters. Enrichment of known TF-binding motifs in DEGs clusters (see Supplemental Figure 4) was determined using the -500 bp region upstream of the transcriptional start site separately for each Brassicaceae. Cluster name, DEG numbers and mean flg22-induced expression changes vs. mock ±SD are shown on the left site. Logos, TF and adjusted p-values for up to the 4 most significantly enriched motifs are shown for each Brassicaceae species. **A:** clusters with commonly induced DEGs. **B:** Clusters with commonly downregulated genes. **C:** clusters with species-specific expression signatures. For a complete list of all enriched TF-binding motifs, please see Supplement Table 4-7.

2.16. Coding sequence and promoter variation does not correlate with expression variation

Some previous comparative transcriptome studies connected transcriptome variation to amino acid sequence variation between species (Hunt et al., 2013; Whittle et al., 2014; Necsulea and Kaessmann, 2014). Since these studies focussed on basal expression levels, the relationship of stress-responsive expression changes and sequence conservation between species has not been investigated. Therefore, I tested whether the amino acid sequence-identity correlates with variation of flg22-induced expression changes between Brassicaceae species. I divided the SD of basal expression values by their means across the four Brassicaceae species as a measure of expression variation. The SD/mean of basal gene expression did not correlated with the sequence variation, suggesting that amino acid sequence diversification is not connected to the diversification of expression changes between the tested Brassicaceae species (Figure 15A). Thus, the results obtained here are not in line with a previous publication reporting a correlation between basal expression variation and amino acid sequence conservation (Broadley et al., 2008).

Similarly, plotting the SD/mean of flg22-induced expression changes against mean amino acid sequence identities did not result in a clear correlation (Figure 15B) and limiting the analysis to DEGs (all DEGs in the combined analysis of Brassicaceae and *A. thaliana* accession) resulted in a similar result (Figure 15C). This suggests that diversification of flg22-induced expression changes is not correlated to coding sequence evolution.

Furthermore, I tested whether pairwise differences of flg22-induced expression between *A. thaliana* and individual Brassicaceae were linked to AA sequences diversification. Separate analysis including all expressed genes or only DEGs both indicated that flg22-induced expression changes were not coupled to sequence divergence in any of the pairwise comparisons (Figure 15D-I). Together, this data indicates that the basal expression variation as well as the flg22-responsive expression variation between Brassicaceae species did not correlate with coding-sequence variation.

Moreover, I was interested whether species-specific or core flg22-responsive genes show altered sequence variation compared to other genes. I plotted percentages of amino acid identities from pairwise comparisons of each Brassicaceae with *A. thaliana* next to the k-mean expression clusters determined previously (Supplement Figure 6). Neither species-specific expression clusters nor the core flg22-responsive genes exhibited a clear pattern of sequence variation diverging from other expression clusters, except of cluster 5 which exhibited a lower

amino-acid sequence conservation in each Brassicaceae compared to other clusters. Cluster 5 contained 70 highly induced and conserved DEGs. This may indicate that highly induced genes faced a stronger selective pressure to diversify their sequence compared to other flg22-responsive genes.

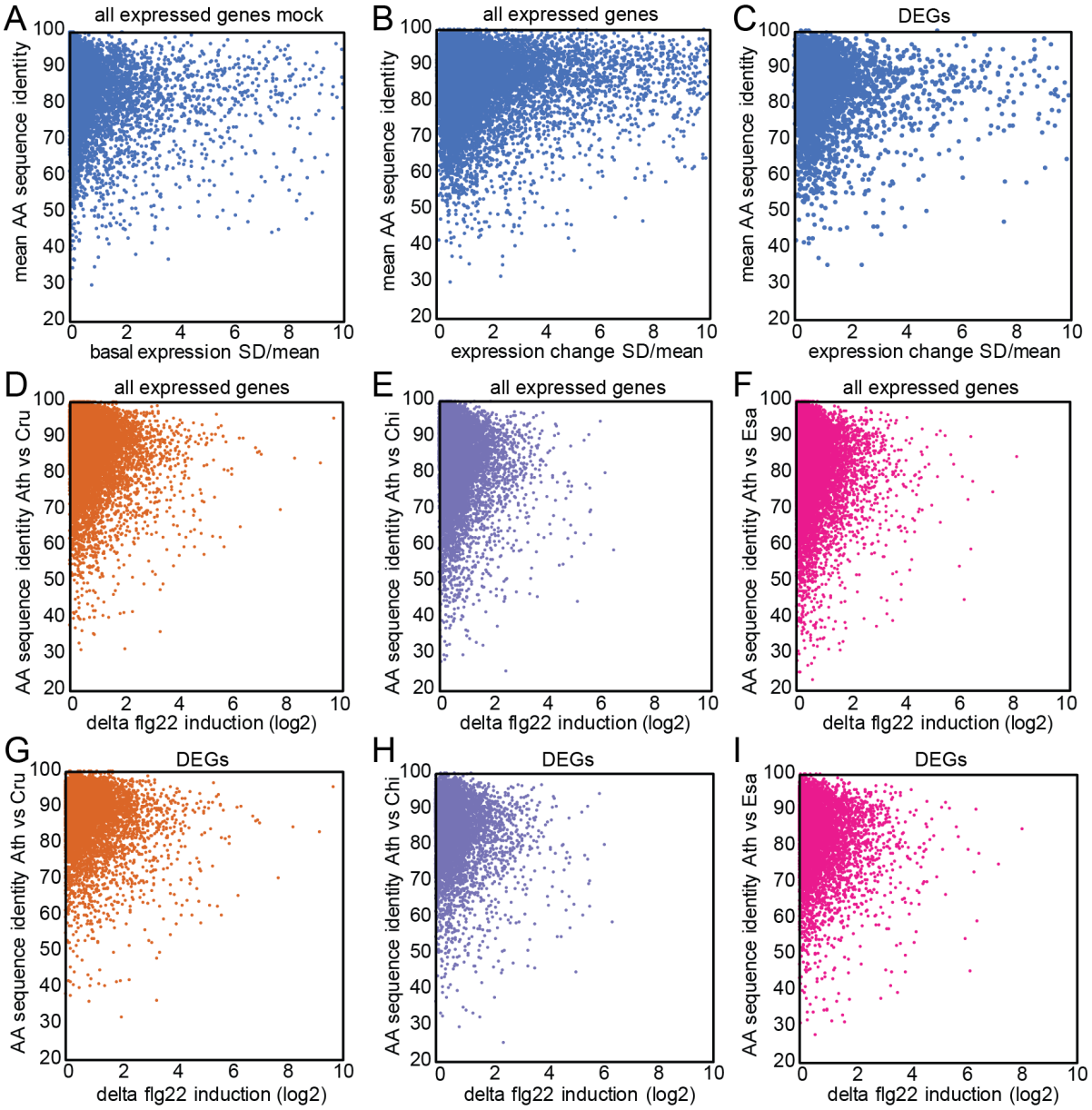

Figure 15: Gene expression variation does not correlate with coding sequence variation. A: mean amino acid (AA) sequence identities of *C. rubella*, *C. hirsuta* and *E. salsugineum* to *A. thaliana* (y axis) was plotted against the SD/mean of the expression values in mock samples of all four Brassicaceae plants for all expressed genes (x axis). **B, C:** mean AA identities of *C. rubella*, *C. hirsute*, and *E. salsugineum* to *A. thaliana* were plotted against the SD/mean of flg22-induced expression changes in all four Brassicaceae plants for all expressed genes with 1to1 orthologs (16100 genes) (A) or 5961 DEGs (B). **D - I:** Pairwise AA sequence identity of *C. rubella* (D, G), *C. hirsuta* (E, H) and *E. salsugineum* (F, I) to *A. thaliana* was plotted against the flg22-induced expression changes between the compared species for all expressed genes (D-F) or DEGs (G-I).

Diversified expression changes between species may be mediated by changes in cis-regulatory sequences which can influence gene expression levels. To test a potential influence of cis-regulatory variation on species-specific expression signatures, I extracted -500 bp 5´-

regulatory sequences and plotted their identities next to the K-mean clusters of all DEGs between Brassicaceae and *A. thaliana* accessions (Supplement Figure 6C). In line with previous observation of amino acid sequence variation, there was no clear correlation between expression variation and promoter sequence variation, except for cluster 5. Interestingly and in contrast to the amino acid sequence identity, the promoter sequence identity was higher in cluster 5 compared to that of the other clusters. Thus the 70 conserved and highly flg22-responsive genes seem to have a more conserved 5´regulatory region compared to other flg22-responsive genes but a lower coding sequence conservation. Expression variation between species within other clusters might be either mediated by trans-acting regulatory sequences or by small differences in TF binding sites that are masked by the high sequence variation in 5´-regulatory regions. For example, the gain of WRKY TF in some of the species-specific flg22-responsive genes might have affected their expression without a strong impact on the overall variation of the 5´-regulatory regions. Taken together coding and promoter sequence conservation were not clearly correlated with conservation of flg22-responsive expression signatures.

2.17. Heat stress-induced transcriptome responses vary among Brassicaceae similarly as flg22-triggered responses

The considerable variation of flg22-responsive expression changes between Brassicaceae species might be a unique feature of PTI or alternatively a more general phenomenon which similarly applies to other stress-induced transcriptome responses. To resolve this question, I captured the transcriptomic changes after a strong heat stress, since a similar comparative-transcriptomic study with a defined input stress is lacking. I placed 12-day-old seedlings for 1 h at 22°C or 38°C. This stress significantly induced the heat-stress marker genes HEAT STRESS PROTEINs 70 and 90.1 (*HSP70* and *HSP90.1*) in all tested Brassicaceae species (Supplement Figure 9). The subsequent RNAseq analysis revealed a high, but slightly lower number of heat-stress affected DEGs compared to the flg22-induced transcriptional response, with 3249, 3889, 2271 and 4563 DEGs in *A. thaliana, C. rubella*, *C. hirsuta* and *E. salsugineum,* respectively (Figure 16A). In stark contrast to the flg22-induced transcriptome, heat-stress downregulated a much higher number of genes in each species. These results demonstrate, that despite generally similar extent of expression changes, transcript reduction seems to play a more important role in heat- compared to flg22-triggered transcriptional reprogramming.

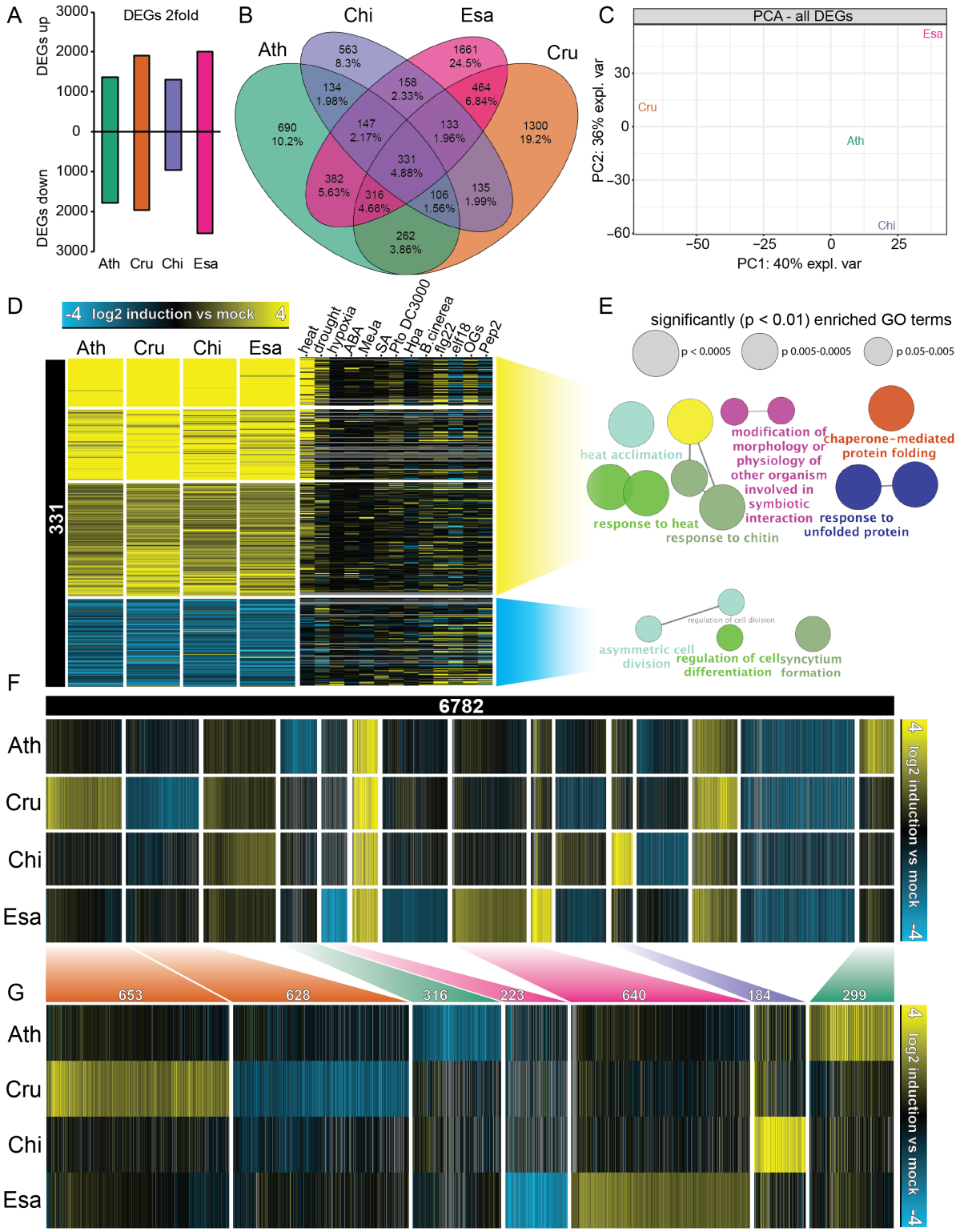

Figure 16: The transcriptome response to heat stress is diversified across Brassicaceae. 12-day-old Brassicaceae seedlings were transferred for 1 h to 22°C (control) or 38°C (heat-stress) and extracted RNA was subjected to RNAseq. Differentially expressed genes (DEGs) were determined using the following criteria: q-value < 0.01 and $|\log_2$ fold change$| > 1$. **A:** Bars represent the number of up- or down-regulated DEGs for each species. **B:** A Venn diagram showing shared DEGs between species. All DEGs which are at least differentially expressed in 1 species were used. **C:** Principal component analysis of 1to1 orthologous genes that are differentially expressed (q-value < 0.01; $|\log_2$ fold change$| > 1$) in at least 1 species. **D:** Heatmap of 331 shared DEGs among all Brassicaceae species generated by k-means clustering. The right heatmap displays expression changes of the 331 DEGs under indicated stress conditions in publicly available *A. thaliana* datasets (Geneinvestigator). **E:** GO term enrichment for heat-induced and heat-repressed genes, showing the most enriched GO terms grouped using

ClueGO Cytoscape plugin. The circle sizes represent significance levels. **F:** Heatmap showing expression changes of all 6782 DEGs, generated using k-means clustering. **G:** Enlarged clusters showing species-specific expression signatures observed in **F**.

Only 331 DEGs were overlapped in all Brassicaceae species, which is a small fraction of 4.88% compared to 15.7% overlap of DEGs after flg22 treatment (Figure 16B, Supplement Figure 2A). A PCA based on all DEGs that were expressed in each species (5256) clearly separated the four species from each other. The transcriptional response of *C. rubella* was most diversified from the other Brassicaceae (Figure 16C), which was in agreement with previous observations for the flg22-induced transcriptome changes. Thus, as observed for flg22-induced expression changes, the variation in heat-stress induced transcriptional responses is incongruent with the phylogenetic relationship between the tested Brassicaceae species.

The 331 shared DEGs between the Brassicaceae species were similarly regulated not only in each species, but also in two previous heat- or drought-stress studies conducted in *A. thaliana* (Figure 16D). Moreover, upregulated genes were significantly enriched for the GO terms “heat acclimation”, “response to heat” and “chaperone-mediated protein folding”, whereas downregulated genes were enriched for “regulation of cell differentiation”, presenting typical processes connected to heat-stress (Figure 16E). The GO-term “response to chitin” was as well among the overrepresented GO terms of upregulated genes. This was in line with the observation that many of these genes were similarly upregulated in publically available flg22 and oligogalacturonides (OG) induced *A. thaliana* transcriptomes and suggests that certain heat-stress responsive expression changes overlap with MAMP induced expression changes (Figure 16D, E). In summary, the DEGs conserved for their responsiveness to heat-stress overlap to a certain degree with MAMP responsive genes but present typical genes previously associated to heat-stress.

To resolve whether the large diversification of transcriptional responses to heat-stress, indicated by the small overlap DEGs among Brassicaceae and the large variance visualized in the PCA of DEGs (Figure 16B, C), results in species-specific expression signatures I clustered all DEGs using K-mean clustering. Indeed, large parts of the species-specific DEGs translate to expression clusters with species-specific expression signatures (Figure 16 F). Extracting only the most obvious of these clusters results in nearly 3000 genes exhibiting species-specific expression changes after heat-stress (Figure 16 G). *C. rubella,* closely followed by *E. salsugineum,* specifically regulated the largest number of DEGs. To exclude that the substantial amount of species-specific expressed genes was biased by not or lowly expressed genes in individual species, I re-analysed the data, based on the 17,857 1 to 1 orthologous genes and excluded lowly expressed genes. This analysis revealed a comparable amount of species-

specific expression signatures, suggesting that the considerable number of species-specific regulated genes was not explained by lowly expressed genes (Supplement Figure 10). Taken together, compared to the species-specific responses induced by flg22, heat-stress transcriptional responses diversified even more drastically between Brassicaceae species and were incongruent with phylogeny. This suggests that major diversifications of transcriptional responses during both biotic and abiotic stresses may play an important role during adaptation.

3. Discussion

3.1. Flg22 perception machinery and flg22-triggered early responses are conserved in Brassicaceae

3.1.1. Sequence conservation of PTI perception machinery

PTI is activated after the perception of MAMPs by plasma membrane-localized PRRs. Comparing amino acid sequences of PRRs as well as interacting proteins revealed in general a high conservation of these components among tested Brassicaceae species. The high sequence conservation emphasises the importance of these components across the Brassicaceae family. This is in general congruent with the literature describing conservation of elf18 or nlp20 perception across Brassicaceae and flg22 perception in multiple other plant families (Zipfel et al., 2006; Takai et al., 2008; Boller and Felix, 2009; Böhm et al., 2014). However, even within a species, individual receptors can lose their function as observed for the *A. thaliana* accessions WS-0 and CVI-0, which harbour premature stop codons in their *FLS2* sequences (Gómez-Gómez et al., 1999; Dunning et al., 2007; Vetter et al., 2016). Interestingly, for some *A. thaliana* accessions, the loss of flg22-responsiveness was associated with lower protein abundance or changes in catalytic sites rather than the complete loss of the *FLS2* gene (Vetter et al., 2016). This opens up the question why these accessions do not lose the *FLS2* receptor completely. One possible explanation is that those receptors, impaired in flg22 perception, might recognize other flagellin epitopes than flg22. Alternatively, even catalytically impaired PRRs might conserve their interaction with other RLKs which might be important to control and fine-tune various other functions mediated by RLKs. In recent years, it was noticed that many RLKs work in bigger complexes at the plasma membrane (Macho and Zipfel, 2014; Ranf, 2017). For example, BAK1 not only interacts with FLS2 but also many other RLKs involved in immunity and brassinosteroid signalling (Nam and Li, 2002; Li et al., 2002; Yasuda et al., 2017; Lozano-Durán and Zipfel, 2015). Thus, the interaction of FLS2 with BAK1 could potentially influence other processes as well for example by modulating available BAK1 levels.

Interestingly, protein sequences of PRRs seem to be less conserved than those of intracellular components connecting ligand perception to subsequent signalling cascades. This lower sequence conservation of PRRs among Brassicaceae species might reflect a functional diversification in ligand recognition specificities of the PRRs. Different plant species or

accessions evolving in diverse environments were conceivably exposed to distinct microbes possessing different MAMPs. Thus, changes in receptor recognition specificities may provide evolutionary advantages to plants. For example, it is known that *Agrobacterium tumefaciens* has an altered FliC sequence thereby escaping from flg22 and flgII-28 perception by *A. thaliana* and tomato plants, respectively (Felix et al., 1999; Rosli et al., 2013). Hence, it would be beneficial for plants to evolve flagellin receptors with different ligand specificities. Alternatively, plants may evolve additional PRRs to sense different epitopes of the same microbial molecule like tomato which senses multiple flagellin epitopes by an additional PRR called FLS3 sensing flgII-28 (Hind et al., 2016). It is conceivable that sequence variation among PRRs, especially in the extracellular domain, might help the plant to adapt to invading pathogens. In line with this idea, the RLP23 and RLP30 which lack an intracellular kinase domain, exhibit the lowest conservation of all tested PRRs over Brassicaceae (Figure 1A). Interestingly, for the intracellular NLR receptors, multiple studies indicated that the NB-ARC domain, important for ATP binding, is generally more conserved by purifying selection among NLR genes within and between species, whereas positive diversifying selection acts in regions encoding LRR domains responsible for effector binding (Mondragón-Palomino et al., 2002; Ashfield et al., 2012; Jacob et al., 2013). Further studies comparing sequence conservation of different PRR domains will help to understand whether different RLK domains evolve under different selection pressures similarly to NLRs.

Apart from keeping up with pathogenic microbes, changing ligand perception specificity might also help plants differentiate between pathogenic and beneficial microbes. Additional investigations concerning the relationship of sequence variation to ligand recognition specificity in PRRs among different species would advance our understanding of co-evolution between plants and microbes. The natural diversity in extracellular PRR domains might enable plants to recognize additional MAMPs, which paves the ways to broadening pathogen resistance and fine-tuning microbiota assembly of crop species. This could provide substantial advantages as it might allow tailoring PRRs by combining desired extracellular and intracellular PRR domains which have increased recognition specificity and are resilient to pathogen perturbation, respectively.

In contrast to PRRs, cofactors like BAK1 which interact with various different PRRs were highly conserved among Brassicaceae species. BAK1 is even conserved in the moss *Physcomitrella patens* (Boller and Felix, 2009). A possible explanation for this might be that BAK1 is not only a key player in immunity but also crucial for developmental processes by modulating brassinosteroid signalling (Nam and Li, 2002; Li et al., 2002; Chinchilla et al.,

2009; Yasuda et al., 2017). However, PBL27 is not known to be involved in other processes besides chitin-induced PTI responses but is still highly conserved. Hence, components interacting with PRRs downstream of MAMP perception might be more conserved as they do not confer ligand specificity and might be consequently less affected by selection pressure arising from MAMP evolution on the microbial side. Moreover, the general conservation of components acting directly downstream of MAMP perception is in line with recent findings that the transfer of PRRs such as EFR or RLP23 to plants lacking these receptors is functional and confers additional resistance (Lacombe et al., 2010; Albert et al., 2015).

3.1.2. All Brassicaceae tested in this study sensed flg22

Previously it was shown that FLS2 orthologs from different *C. hirsuta* accessions, including the Oxford, GR2 and OLI accessions that were used in this study, did not bind flg22 (Vetter et al., 2012). However, in my hands, all tested Brassicaceae species sensed flg22 and induced early PTI responses like MPK3/6 phosphorylation or marker gene expression after flg22 treatment (Figure 2, Figure 12), which was in line with the generally high sequence conservation of FLS2 and its interacting partners (Figure 1). Vetter and colleges used in vitro assays in which the competitive binding of radioactively labelled flg22 epitopes was recorded (Vetter et al., 2012). Flg22 binding to *C. hirsuta* FLS2 orthologs was not detected by this method, but no further downstream responses were analysed in this study. In contrast, I specifically investigated flg22-induced responses. One possibility is that the *C. hirsuta* FLS2 ortholog senses flg22 but the method used by Vetter et al. was not sensitive enough to detect this binding. For example, *C. hirsuta* might sense flg22 by a more transient flg22 binding. Another possibility is that indeed the *C. hirsuta* FLS2 ortholog does not sense flg22, but another *C. hirsuta* receptor is capable of sensing flg22 and triggering downstream responses. A way to distinguish these two possibilities is to create a *fls2* knock-out mutant in *C. hirsuta* for example by using CRISPR-Cas9 and subsequently test its flg22-responsiveness. If a *C. hirsuta fls2* mutant still responds to flg22, it would be very interesting to investigate which PRR might have taken over this function. The data presented here clearly demonstrate that all three *C. hirsuta* accessions sense flg22. Whether this is indeed mediated by their FLS2 orthologs remains to be addressed.

3.2. Variation in flg22-mediated responses among Brassicaceae

3.2.1. Variable effect of flg22 on growth reduction

All tested Brassicaceae responded to flg22 treatment, demonstrated by MPK3/6 phosphorylation, marker gene expression, and seedling growth inhibition (Figure 2). However, the effect of flg22 on seedling growth varied between Brassicaceae species. These differences might be in part influenced by diversified growth rates between these species; e. g. *E. salsugineum* grows relatively slow compared to *C. hirsuta*. Thus, the relative fresh weight differences between mock- and flg22-treated seedlings of fast-growing Brassicaceae species might be larger if flg22 treatment leads to a nearly complete stop of seedling growth.

Differences might be as well explained by other factors influencing growth defence crosstalk. The growth-immunity trade-off might be beneficial for the plant as it can prioritize between growth and defence in order to regulate its resource allocation accordingly (Yang et al., 2012; Meldau et al., 2012; Belkhadir et al., 2014). It is known that even within *A. thaliana* there can be substantial variation in flg22-induced seedling growth inhibition between accessions (Vetter et al., 2016). This might be mediated by variations in flg22-sensitivity but could be also explained by diversifications of the growth-immunity trade-off across accessions. For example, BAK1 not only acts as a co-receptor for FLS2 but also for the brassinosteroid receptor BRASSINOSTEROID INSENSITIVE 1 (BRI1) (Nam and Li, 2002; Li et al., 2002). Brassinosteroids are phytohormones involved in many developmental processes including cell expansion (Kim and Wang, 2010). Thus, it has been suggested that BAK1 might play an important role in integrating growth signals with immunity by preferentially interacting with BRI1 or FLS2 to induce growth or immunity (Belkhadir et al., 2012; Wang, 2012). Environmental factors may have a strong impact on this crosstalk as species that face high pathogen pressure might adapt this crosstalk in favour of defence, whereas species whose fitness relies on high growth rates might favour growth instead. Consequently, alterations in the growth-defence trade-off might differentially affect flg22-mediated seedling growth inhibition in different Brassicaceae.

3.2.2. Variation in hormone levels

SA, JA, and ABA levels not only responded differently after flg22 treatment but also differed in mock-treated samples among tested Brassicaceae (Figure 3). Phytohormones are involved in the regulation of various processes such as growth, development, abiotic and biotic

stress responses and build up a complex network with synergistic as well as antagonistic relationships (Pieterse et al., 2009). Hence, phytohormone levels can be affected by multiple signals and might need to be adjusted according to the lifestyle of an individual species or even accession. Indeed, basal phytohormone levels were recently measured in 17 *A. thaliana* accessions and substantial variation in gibberellin and SA levels were detected in some of the accessions (Nam et al., 2017). For example, the SA levels in the C24 accession were approximately ten times higher compared to Col-0 SA-levels. Another study investigated variation in phytohormone levels in roots of 13 *A. thaliana* accessions and noted high variation in some cytokinins and gibberellin levels across the tested accessions (Lee et al., 2018). Yet, to my knowledge, there are no studies comparing phytohormone levels between species in a controlled environment. However, the two previously mentioned studies demonstrated considerable variation in basal phytohormone levels even within a species. Thus, it is conceivable, that the substantial variation in basal phytohormone levels between Brassicaceae species observed here, might be a more general phenomenon between plant species, which may reflect adaptations to different environments.

Interestingly, *E. salsugineum* accumulated ABA at higher levels compared to other Brassicaceae species (Figure 3B). Plants increase ABA levels in response to abiotic stresses like drought or salt stress and ABA is important for the tolerance to these stresses (Qin et al., 2011). *E. salsugineum* was isolated from saline environments and is extremely tolerant to drought and salt stress (Zhu, 2001; Taji et al., 2004; Inan et al., 2004; Gong et al., 2005). Indeed, it was suggested that the high salt stress tolerance of *E. salsugineum* might be achieved by a gene number expansion within gene families involved in ABA biosynthesis pathways, combined with a higher sensitisation for abiotic stresses (Taji et al., 2004; Wu et al., 2012). However, despite pointing out the potential role of ABA in the stress adaptation of *E. salsugineum*, this hypothesis has not been tested up to now and ABA levels in *E. salsugineum* in comparison to other plant species have not been reported. The higher ABA levels in *E. salsugineum* compared to other Brassicaceae species observed here indeed point to an important role of ABA in the extreme abiotic stress tolerance of *E. salsugineum*. However, to clarify the role of ABA in this process genetic perturbation of ABA biosynthesis or ABA signalling is needed to create causal links between salt stress adaptation and ABA. In *A. thaliana ABA2* encodes a key enzyme in the ABA biosynthesis pathway and *aba2* knockout mutants have reduced ABA levels (Koornneef et al., 1998; Gonzalez-Guzman et al., 2002; Adie et al., 2007; Finkelstein, 2013). Therefore, I currently use CRISPR-Cas9 targeted genome editing to create *aba2* mutants in *E. salsugineum*. If *aba2* mutations in *E. salsugineum* lead to reduced ABA

levels, these mutants will be an important future resource to test the involvement of ABA on abiotic stress tolerance of *E. salsugineum*.

SA and ABA have been shown to act antagonistically with each other (Robert-Seilaniantz et al., 2011). Numerous studies demonstrated that abiotic stress or ABA application negatively affects resistance against pathogens which are sensitive to SA-mediated immunity (Yasuda et al., 2008; Fan et al., 2009; De Torres Zabala et al., 2009; Pye et al., 2013; Ueno et al., 2015; Liu et al., 2015). For example, ABA application not only reduces SA accumulation by inhibiting expression of the SA biosynthesis gene *ISOCHORISMATE SYNTHASE 1* (*ICS1*; also named *SID2*) (De Torres Zabala et al., 2009), but also blocks SA signalling by initiating proteasome degradation of the key SA regulator NONEXPRESSER OF PR GENES 1 (NPR1) (Ding et al., 2016). This crosstalk might be beneficial under individual stress situations by prioritizing the appropriate stress response (Asselbergh et al., 2008; Vos et al., 2015; Ueno et al., 2015). Consequently, *E. salsugineum* might prioritize abiotic stress responses by higher ABA levels which may negatively affect PTI responses. This assumption is consistent with the relatively transient flg22-induced transcriptome responses in *E. salsugineum* compared to the other Brassicaceae species (Figure 7C) and with the inability of flg22 to trigger growth reduction of *Pto* DC3000 and *Pto hrcC* in *E. salsugineum* compared to *A. thaliana* (Figure 4). However, until we can gain a genetic proof, e.g. by mutation of ABA synthesis, it remains speculation whether elevated ABA levels are connected to an inefficient flg22-triggered PTI in *E. salsugineum*. Thus, the previously mentioned *aba2* mutants created by CRISPR-Cas9 might help to clarify the role of ABA not only for abiotic stress tolerance of *E. salsugineum* but also for its impact on PTI responses. Since *E. salsugineum* responds to flg22, can be infected with *Pto* and has a sequenced genome it is an excellent model to study the evolutionary trade-off between abiotic and biotic stress responses.

Phytohormone measurements further revealed strongly elevated JA levels in *A. thaliana* that were up to 100-fold higher compared to other Brassicaceae species. These high JA levels seem to be generally conserved in *A. thaliana* accession as a recent study measured comparable JA levels in various *A. thaliana* accessions (Nam et al., 2017). This suggests that the exceptionally high JA levels in *A. thaliana* compared to other Brassicaceae species are stabilized over evolution and thus presumably present an important adaptive trait of *A. thaliana*. Moreover, JA levels strongly increased 1 h after flg22 treatment in *C. rubella* and in *E. salsugineum* but not in *A. thaliana* and *C. hirsuta* (Figure 3C). Contrasting this observation, a recent publication detected elevated JA levels in *A. thaliana* 1 h after flg22 treatment (Hillmer et al., 2017). Major differences in the experimental setup might account for this discrepancy.

Hillmer et al. infiltrated flg22-solution in leaves of four-week-old plants. Water-infiltration into leaves can trigger wound responses in *A. thaliana,* for example MPK3 activation (Kohler et al., 2002; Beckers et al., 2009). JA normally accumulates after wounding and during interactions with necrotrophic pathogens as well as upon herbivore attack (De Vos et al., 2005; Glauser et al., 2008; Koo et al., 2009; Campos et al., 2014). Since Hillmer et al. compared the JA levels to a 0 h time-point rather than to mock infiltrated leaves, the early increase in JA levels might be confounded by an infiltration elicited wound-response. Usually, JA signalling antagonizes SA signalling (Robert-Seilaniantz et al., 2011; Thaler et al., 2012; Van der Does et al., 2013). This crosstalk is often exploited by pathogens like *Pto* DC3000 producing the JA-isoleucine mimic coronatine, which can bind to the JA-receptor COI1 and activate JA-signalling (Katsir et al., 2008). This JA-signalling activation suppresses SA signalling which is effective against hemibiotroph pathogens (Glazebrook, 2005; Brooks et al., 2005; Zheng et al., 2012). Hence it seems counterintuitive that plants increase JA levels upon treatment with flg22, a MAMP present in hemibiotroph *Pto* DC3000. However, JA is important for the immune responses against necrotrophic pathogens and it is conceivable that certain necrotrophic pathogens as well have flg22 epitopes (Mengiste, 2012). Thus, different plant species might modulate the phytohormone accumulation downstream of MAMP perception based on the pathogen pressure in their native environments.

3.2.3. Variation in bacterial growth

Flg22 treatment reduced *Pto* DC3000 growth in all tested Brassicaceae except *E. salsugineum*. Moreover, in *C. hirsuta* the reduction was much lower compared to other Brassicaceae (Figure 4). This might be explained by a better adaptation of *Pto* DC3000 to *C. hirsuta* and *E. salsugineum* enabling a more efficient inhibition of PTI responses. It was previously proposed that the failure of effectors to find their appropriate host targets might be positively associated with non-host resistance (Schulze-Lefert and Panstruga, 2011). Indeed, it was recently shown that *Phytophthora infestans* effectors targeting proteases in potato are specifically tailored to potato proteases and fail to target orthologous proteases of the potato relative *Mirabilis jalapa,* rendering *P. infestans* non-virulent on *Mirabilis jalapa* (Dong et al., 2014). Hence, a more efficient inhibition of flg22-triggered PTI responses in specific Brassicaceae is in principle possible. However, in *E. salsugineum* and *C. hirsuta,* flg22 treatment did not inhibit growth of *Pto hrcC*, lacking the functional delivery of pathogen effectors (Figure 4 B). Thus, the inability of flg22 to reduce *Pto* DC3000 growth in *E.*

salsugineum and *C. hirsuta* is not explained by the possibility that *Pto* DC3000 effectors can effectively suppress pre-activated PTI in *E. salsugineum* and *C. hirsuta.*

Pto DC3000 titres were also lower in *E. salsugineum* compared to the other Brassicaceae species (Figure 4A). The repertoire of NLR genes to detect pathogen effectors varies greatly across Brassicaceae species with only a few conserved NLRs among *A. thaliana*, *A. lyrata*, *C. rubella* and *E. salsugineum* (Peele et al., 2014). In contrast to *A. thaliana*, *Pto* DC3000 triggers ETI in several tomato strains which can recognize the *Pto* DC3000 effector AvrPto by a receptor complex comprised of the protein kinase Pto and the NLR Prf (Salmeron et al., 1996; Tang et al., 1996; Gutierrez et al., 2010). Thus, the lower *Pto* DC3000 growth in *E. salsugineum* may result from recognition of *Pto* DC3000 effectors which are not recognized by the other Brassicaceae. An effective ETI response in *E. salsugineum* might preclude further reduction of bacterial titres by flg22 treatment. However, this is very unlikely since flg22-treatment did not reduce *Pto hrcC* which grew to comparative levels in untreated *A. thaliana* and *E. salsugineum*. Furthermore, bacterial titres in flg22 treated *A. lyrata* and *A. arabicum* were much lower compared to *E. salsugineum* (Figure 4A), indicating that further reduction of bacterial titres is in principle possible. A previous publication reported lower *Pto* DC3000 growth in *E. salsugineum* compared to *A. thaliana* and bacterial titres were further reduced in ETI triggering *Pto* AvrRpt2 and AvrRps4 strains (Yeo et al., 2015). However, inoculation levels between different *Pto* strains were already significantly different at 0 hpi and consequently later differences in the bacterial titres may arise from different starting inocula. Thus, it is unclear whether the bacterial titres in *E. salsugineum* can be further reduced by additional ETI responses.

The most obvious explanation for the observed inefficiency of flg22 to reduce *Pto* titres in *C. hirsuta* and *E. salsugineum* might be that flg22 induced a less potent PTI in these species. This is in line with the lower amplitude of transcriptional regulation at 24 h observed in *C. hirsuta* and *E. salsugineum* compared to the other species (Figure 7A). However, marker gene expression combined with *Pto* DC3000 growth assays in several Brassicaceae accessions and sister species indicated that the latter correlation is not generally applicable and was likely observed by chance (Supplement Figure 3). Moreover, SA was ruled out as a regulator of sustained transcriptional responses in *A. thaliana* compared to *E. salsugineum*, since the *sid2* mutant exhibits nearly unaltered transcriptional responses 18 h after flg22 treatment (Figure 8). However, it cannot be ruled out that the lower transcriptional induction of many SA-responsive genes observed in *E salsugineum* (Figure 7F) might influence the efficacy flg22-mediated bacterial growth reduction.

In *C. rubella Pto hrcC* was not able to grow, whereas *Pto* DC3000 grew normally in mock condition. This might be explained by DC3000 effectors that modulate the apoplastic space to make it habitable for the bacteria, e.g. by modifying the water status of the apoplast or releasing nutrients from the plant, whereas *Pto hrcC* which lacks these functions might face an unfavourable environment in the *C. rubella* apoplast that impedes its growth. For example, the apoplastic water status is critical for *Pto* DC3000 proliferation and is actively modulated by the two *Pto* DC3000 effectors HopM1 and AvrE1 which cause water soaking (Xin et al., 2016). Thus, a lower water content in the *C. rubella* apoplast compared to the other Brassicaceae species might be one possibility why *Pto* hrcC did not grow in *C. rubella*. In addition, multiple results indicated that *C. rubella* might trigger a very strong PTI response since it induced SA accumulation and exhibited the largest transcriptome changes early after flg22 treatment. Moreover *C. rubella* might recognize additional MAMPs from *Pto hrcC*. Consequently, *C. rubella* might trigger strong PTI responses upon *Pto hrcC* infection, that are sufficient to inhibit *Pto hrcC* growth, in the absence flg22 pre-treatment.

3.3. Comparative transcriptomics after a defined stress – a dataset advancing the field of comparative transcriptomics

In this thesis, I compared transcriptome responses of four Brassicaceae species during flg22-triggered PTI. This enabled me to identify not only core genes, which conserved their flg22-responsiveness during Brassicaceae evolution, but also species-specific expression patterns. Since the rise of microarray technology, comparative transcriptomics between species have been commonly used to reveal candidate genes regulating important traits or investigate the correlation of expression changes to phenotypic differences, by defining conserved and diversified gene regulations (Whitehead, 2012; Romero et al., 2012). Yet, this study extends previous studies in various aspects.

Many studies compared gene expression levels in different species at the “basal” state (Weber et al., 2004; Hammond et al., 2006; Davidson et al., 2012; Perry et al., 2012; Koenig et al., 2013; Hunt et al., 2013; Whittle et al., 2014; Czaban et al., 2015; Morandin et al., 2016). Some comparative transcriptome studies noted that biotic and abiotic stresses are main drivers of expression variation between and within species (Koenig et al., 2013; Kawakatsu et al., 2016). However, a comprehensive understanding how stress-induced transcriptomes differ between species is lacking. The comparison of flg22-triggered transcriptional responses among four Brassicaceae species addresses this previously unanswered question.

Moreover, my experimental approach overcomes multiple concerns which complicate interpretation of many previous comparative transcriptomic studies. Especially in animal studies, multiple problems may introduce noise to gene expression variation which cannot be distinguished from heritable variation (Romero et al., 2012). Usually, samples need to be taken from dead organisms which did not live in the same controlled environments. It is conceivable that a variety of uncontrollable factors including diet, disease and other environmental influences, will introduce gene expression variation between species (Romero et al., 2012; Breschi et al., 2017). I excluded these biases by growing the Brassicaceae species under the same controlled environments, minimizing potential noise in gene-expression introduced by environmental factors. Furthermore, by sampling all species at the same time of the day, I excluded biases arising from circadian and diurnal gene regulations. These controlled environmental conditions are important to measure gene expression differences with a genetic basis (Voelckel et al., 2017). Thus, the substantial inter-species variation in gene induction that I observed likely reflects genetically encoded variation across species.

Only a few studies compared transcriptional responses towards a stress between different strains, ecotypes or species. For instance, transcriptome responses of different *E. salsugineum* accessions during salt stress were characterized to find candidates genes mediating salt-stress tolerance (Taji et al., 2004). Another study compared transcriptome responses of different tomato varieties towards salt stress (Sun et al., 2010). However, in contrast to the four-species comparison I used, the previous mentioned and many other studies used binary systems comparing only two species or compared strains within a species (Mangelsen et al., 2011; Lenka et al., 2011; Schroder et al., 2012; Zhang et al., 2014; Lindlöf et al., 2015; Yang et al., 2015; Amrine et al., 2015; Clauw et al., 2015; Gleason and Burton, 2015; Van Veen et al., 2016; Zhang et al., 2016; Mondragón-Palomino et al., 2017). Two species comparisons are valuable to identify candidate genes mediating increased stress resistance, but cannot distinguish neutral from adaptive expression evolution (Evans, 2015). In other words, it cannot be interpreted whether expression changes are selectively neutral or of adaptive advantage for these species. I compared stress-responsive transcriptome responses between four Brassicaceae with a defined phylogenetic framework to fill this previously neglected knowledge gap in the field of comparative transcriptomics.

A handful of studies compared stress-responsive expression changes in more than two species. For example, cold-stress induced transcriptome responses of two *Solanum* species with variable cold stress tolerance were compared to *A. thaliana,* identifying conserved cold stress responses (Carvallo et al., 2011). Another study compared salt stress-responsive gene

expression changes of six *Lotus* species differing in their salt tolerance and found only very few conserved transcriptional responses, indicating a highly variable *Lotus* response to salt stress (Sanchez et al., 2011). The conservation of low-oxygen stress induced transcriptomes was even compared across four different kingdoms including plant, fungi, animal and bacterial expression datasets (Mustroph et al., 2010). However, the first two studies both lack a clear phylogenetic framework comparing either very distantly related species such as *A. thaliana* and tomato or only very closely related species, whereas the third study compared only publicly available datasets impeding comparability between different samples due to differences in experimental conditions between samples. Thus, up to now there is no study comparing stress-responsive transcriptomes across multiple species that include both closely- and distantly-related species in the same experimental setup. Therefore, this dataset opens up the door for more in-depth analysis regarding gene expression evolution among related species during stress responses. For example, the data produced here can be further used to build up co-expression networks and interfere ancestral gene regulatory networks of PTI.

3.3.1. Massive transcriptional reprogramming shows importance of flg22 induced transcriptional reprogramming

Despite variation in hormone levels and flg22-triggered *Pto* DC3000 growth reduction, flg22 treatment induced a massive early transcriptional reprogramming in all tested Brassicaceae changing the expression of 2575 to 4209 DEGs (Figure 5). Most previous publications investigating flg22-triggered transcriptional changes detected a smaller, but still substantial number of DEGs ranging from approximately 1000 to 2500 DEGs at a single time-point within the first hour after flg22 treatment (Zipfel et al., 2004; Denoux et al., 2008; Frei dit Frey et al., 2014). In contrast, two more recent studies detected approximately 8500 or 7000 DEGs one or two hours after flg22 treatment and over 5800 DEGs one hour after elf18 treatment of *A. thaliana* seedlings (Briggs et al., 2017; Birkenbihl et al., 2017). The large quantitative differences between these studies are likely explained by a combination of different statistical methods to determine DEGs and newer microarray or RNAseq technologies with higher detection sensitivity. Similarly, the higher number of flg22-responsive genes here compared to older microarray-based studies is likely explained by a higher detection sensitivity of the RNAseq approach combined with the powerful statistical framework used in my analysis.

Previous flg22 transcriptome studies exclusively investigated transcriptional responses within the first hours after treatment; hence a comparative dataset investigating later time-points is lacking. However, RT-qPCR analysis in another study indicated that marker gene expression

returns to basal expression levels about 24 h after flg22 treatment (Denoux et al., 2008). In contrast, I still detected not only marker gene expression (Figure 8A, B, C) but also many DEGs 24 h after flg22 treatment (Figure 5B). A recent study investigated transcriptional responses to elf18 or pep2 treatment 10 hpt and detected around 1100 DEGs or 400 DEGs, respectively (Ross et al., 2014) This is within the same range as transcriptional responses detected at 9 h after flg22 treatment here (Figure 5B). In contrast to previous studies I could show here that especially in *A. thaliana* and *C. rubella,* there are still many genes differentially expressed at 9 and 24 h after flg22 treatment (Figure 5B). Importantly the number of DEGs as well as their induction levels varied between different Brassicaceae suggesting that different temporal dynamics in different species might play an important role in the adaptation of PTI responses in different species. Although transcriptomic data for later time-points are missing for most MAMPs, transcriptional responses of *A. thaliana* to *Pto hrpA* infection have been investigated over an extensive time course (Lewis et al., 2015). Since *Pto hrpA* lacks functional effector delivery, it resembles a PTI transcriptional response. This study revealed that some transcriptional responses towards *Pto hrpa* are still sustained 17.5 h after inoculation but on the other hand stated that from 11 h on no novel transcripts are regulated anymore. However, it is difficult to compare this data with MAMP triggered transcriptome studies since we do not know which MAMPs at which concentrations are present in the bacteria.

Interestingly, *E. salsugineum* induced a massive transcriptional reprogramming in response to flg22, although flg22 did not trigger effective resistance against *Pto* DC3000 and *Pto hrcC*. This opens up the question what selective pressures forced *E. salsugineum* to keep this massive transcriptional response if it does not result in increased resistance against pathogens. One possibility is that flg22-triggered transcriptional reprogramming does not lead to inhibition of *Pto* growth but effectively limits the growth of other bacterial species. *E. salsugineum* colonizes saline environments (Zhu, 2001; Inan et al., 2004; Wu et al., 2012). It is conceivable that different types of microbial pathogens colonize these extreme environmental conditions and consequently *E. salsugineum* adapted its defence responses downstream of transcriptional reprogramming to these specific environments. For example, it was shown that different sets of defence secondary metabolites are produced in *E. salsugineum* compared to *A. thaliana* (Pedras and Adio, 2008; Pedras et al., 2010; Pedras and Zheng, 2010; Bednarek et al., 2011), which might differentially affect interactions with bacterial pathogens.

Alternatively, pathogen pressure may be low in these extreme environments and therefore *E. salsugineum* can afford a weaker defence against pathogens. The soil microbiome composition varies with salinity and salt-stress was associated to shifts in the microbial

communities of plants (Canfora et al., 2014; Yaish et al., 2016; Yang et al., 2016). Moreover, it has been hypothesized that the plant microbiome plays important role in the salt-stress adaptation of plants growing in saline environments (Ruppel et al., 2013; Qin et al., 2016). Thus, conserved flg22 transcriptional responses in *E. salsugineum* might be required for recruiting specific microbiota members. Consistently, several studies implicated a role of the plant immune system to coordinate the establishment of microbiota (Hacquard et al., 2017). For example, production of tryptophan-derived secondary metabolites in *A. thaliana* affects the colonisation by beneficial fungal microbiota (Kei Hiruma et al., 2016). However, the role of MAMP perception and PTI responses in the microbiota establishment is not well understood. Future research will be required to understand the link between MAMP-triggered massive transcriptional reprogramming and the establishment of functional microbiota.

3.3.2. Purifying selection conserved flg22-responsiveness of a core set of genes during Brassicaceae evolution

Many studies investigated the massive transcriptional reprogramming triggered during PTI (Navarro et al., 2004; Zipfel et al., 2004, 2006; Gust et al., 2007; Denoux et al., 2008; Rosli et al., 2013; Lewis et al., 2015; Jacob et al., 2017; Briggs et al., 2017; Birkenbihl et al., 2017). Nevertheless, we do not understand how essential and important these massive transcriptional responses are for PTI. Genetically removing flg22-induced transcriptional reprogramming would be desirable to test its relevance for plant-microbe interactions. However, flg22-induced transcriptional reprogramming cannot be easily cancelled without severe side effects. Yet, another way to test the importance of transcriptional responses during PTI is to investigate whether they are precious enough to be conserved during evolution.

Indeed, over 800 genes conserved their flg22-responsiveness across the four tested Brassicaceae indicating that a large part of the flg22-responsive transcriptome evolved under purifying selection. In addition to the 868 genes which are differentially expressed after flg22 treatment in all species, many genes show qualitatively similar expression patterns between species (Supplement Figure 4). The species-specific appearance of these genes in the Venn-diagram (Figure 5C) is likely caused by the stringed cut-off criteria I applied. This strong conservation of transcriptional responses over approximately 30 Mio years of Brassicaceae evolution suggests that these transcriptional responses are essential for their fitness.

Many previous publications stated that large parts of expression patterns between species are conserved by purifying selection (Rifkin et al., 2003; Lemos et al., 2005; Gilad et al., 2006; Whitehead and Crawford, 2006; Romero et al., 2012). However, these publications

compared expression variation between unstressed organisms. Thus, information about the number of genes that are likely under purifying selection for their regulation during particular stress responses is so far unknown. Unfortunately, many studies comparing stress responsive transcriptomes between multiple species only used Venn-diagrams to compare the overlap of DEGs and determine species-specific gene regulations (Carvallo et al., 2011; Sanchez et al., 2011; Zhang et al., 2014). However, as it largely depends on significance cut-offs this approach excludes important information on the similarity of gene expression changes between species. Thus, in my view, it is not sufficient to solely rely on Venn-diagrams as justification to define conserved or distinct gene expression across species. Therefore, this study provides the first evidence that the regulation of many genes between related Brassicaceae during a complex stress-response like PTI is stabilized by evolution and therefore likely crucial during their evolution.

3.3.3. Regulatory mechanisms controlling conserved flg22-responsive transcriptional reprogramming

Co-expressed genes are often regulated by similar mechanisms. Indeed, 5´regulatory regions of conserved flg22-responsive genes were highly enriched for WRKY TF motifs (Figure 14A, Supplement Table 4-7). Multiple previous publications found WRKY TF motifs enriched in the 5´regulatory regions of MAMP responsive genes (Navarro et al., 2004; Zipfel et al., 2004; Lewis et al., 2015; Jacob et al., 2017) and it is known that WRKY TF are key regulators of plant immune transcriptional reprogramming (Pandey and Somssich, 2009; Tsuda and Somssich, 2015; Li et al., 2016; Birkenbihl et al., 2017).

A recent study suggested that the fast and massive transcriptional response during PTI might be partly mediated by de-repression (Jacob et al., 2017). Since treatment with the protein synthesis inhibitor cycloheximide trigger very similar transcriptional changes as MAMP treatments, the authors speculated that a block in the continuous protein synthesis of short-lived transcriptional repressors might cause these similar cycloheximide and MAMP induced transcription responses. Yet it is unclear what TFs or motifs might be connected to this potential de-repression. A recent study investigating genome-wide binding sites of WKRY18, WRKY33 and WRKY40 by Chip-Seq experiments noted that WKRY33 and WRKY40 binding is dependent on flg22 treatment, whereas WRKY18 binding was also detected in untreated *A. thaliana* seedlings (Birkenbihl et al., 2017). However, the authors noted that this was likely mediated by higher protein levels in their complementation lines and that flg22 treatment increased binding of WRKY18 at previously bound sites. This suggests that these induced

WRKY TFs are not bound to targets in the resting state but mainly bind upon MAMP elicitation. However, the authors as well found several constitutively expressed WRKY TF that are bound to target genes in untreated samples (personal communication with Imre Somssich). These constitutively bound WRKYs seem to be replaced by induced WRKYs upon flg22 treatment. Therefore, WRKY TFs might regulate PTI transcriptional responses by de-repression coupled with activation, mediated by distinct WRKYs.

Just recently a calmodulin-binding transcriptional activator called CAMTA3 was proposed to be involved in the early transcriptional reprogramming during PTI and ETI (Jacob et al., 2017). However, although CAMTA motifs were overrepresented within the promoters of immediate response genes not all of these genes exhibited this motif. Here, CAMTA TF-motifs were as well slightly enriched in the regulatory regions of *A. thaliana*, *C. rubella* and *C. hirsuta* in certain flg22-induced expression clusters (Supplement Table 4, 5, 6). Thus, CAMTA TF-motifs seem to participate in the early transcriptional regulation of multiple Brassicaceae. In *A. thaliana,* this was genetically proven by alterations of the flg22-induced transcriptional responses in a dominant *camta3-D* mutant (Jacob et al., 2017). However, many flg22-responsive genes lack a CAMTA motif and the enrichment of CAMTA motifs compared to WRKY-motifs was comparably weak. Therefore, the exact role of CAMTA TFs in PTI needs further experimentation.

Other regulatory mechanisms that mediate flg22-triggered transcriptional reprogramming await their discoveries. The evolutionary conserved core set of flg22-responsive genes provide an excellent resource to mine regulatory regions to discover additional regulatory mechanisms. For instance, phylogenetic shadowing might help to identify evolutionary conserved non-coding DNA regions in conserved flg22-responsive genes. When non-coding gene regulatory DNA sequences, often in the proximity of transcriptional start sites, show signs of purifying selection, they are likely important for gene regulation (Schranz et al., 2007; Davies et al., 2015; Van de Velde et al., 2016). Identifying these conserved non-coding DNA sequences will allow me to test whether they are required and/or sufficient for gene regulation by, for instance, transient reporter assays or genetic manipulation analysis. These analyses should provide new mechanistic insights how gene expression is regulated during PTI and how gene regulatory mechanisms evolved in plants.

3.3.4. Factors that might influence detection of species-specific expression signatures

In contrast to the majority of DEGs whose flg22-responsive expression changes were conserved by purifying selection across Brassicaceae, many genes exhibited species or lineage-specific expression patterns (Figure 9, Figure 11). As described in previous sections, my approach overcame several problematic issues faced by previous studies comparing multiple species. However, there are still factors which can influence the results of comparative transcriptomics and which should be considered when interpreting the data.

To compare transcriptomic responses generated by RNAseq between species, orthologous genes need to be defined, which is not trivial (Li et al., 2003; Emms and Kelly, 2015; Tekaia, 2016; Nichio et al., 2017). In this study, we used the best reciprocal blast to define 1to1 orthologous genes among the Brassicaceae species. Although we carefully assigned 1to1 orthologs, we cannot fully exclude the possibility that some orthologous relationships were misassigned. Especially for large gene families in which many genes share similar sequences, wrong assignment of 1to1 orthologs could have been introduced. For instance, gene A and B have similar sequences, yet only gene A is flg22-responsive. If gene A of species 1 and gene B of species 2 are assigned as an orthologous pair, these genes show species-specific expression patterns. However, my analysis showed that the size of gene families does not explain species-specific expression patterns. I compared the size of gene families for each gene within each of the 15 k-mean clusters determined for all DEGs (Supplement Figure 7). This analysis suggested that the gene-family sizes of species-specific clusters did not differ from those clusters exhibiting conserved flg22-responsive expression pattern and from all DEGs. Furthermore, much less species-specific loss of gene regulation compared to the species-specific gain of gene regulation suggests that the large numbers of species-specific gene regulation that I observed are very unlikely artefacts. Thus, although individual misassignments cannot be fully excluded, the majority of species-specific gene regulations is a true feature of the flg22 transcriptional response among Brassicaceae species.

Another factor potentially affecting gene expression patterns in different species is distinct developmental stages. Comparing species at the same age, one cannot fully exclude that different developmental stages between species influence variation in gene expression among those species. Hence, I used seedlings to minimize the effects of developmental variation on transcriptome responses as proposed by another comparative transcriptome study in plants (Koenig et al., 2013). Moreover, I focussed my analysis on relative expression changes

between mock- and flg22-treated samples which further minimizes biases introduced by variation in developmental stages. In addition, the comparison between *A. thaliana* accessions revealed almost no accession-specific regulated genes although developmental differences between these accessions are macroscopically visible (Figure 10D). Together these findings make it unlikely that the substantial number of species-specific flg22-responsive genes is based on developmental differences between seedlings. However, to fully exclude this possibility additional experiments are needed to compare transcriptome responses at different developmental stages e.g. on different days after germination and investigate whether similar species-specific regulated genes can be detected independently of the developmental stage.

Species-specific expression signatures might reflect qualitative differences in the transcriptome response to flg22 across Brassicaceae species. However, since I only took a snapshot of the transcriptional response at 1 hpt I cannot exclude that diversified temporal dynamics between the Brassicaceae species led to the detection of species-specific expression changes at 1 hpt. To exclude this possibility a more stringent time-course experiment would be needed, detecting transcriptome responses at multiple time-points around 1 hpt. However not only qualitative differences in the transcriptional response, but also differences in the transcriptional dynamics between Brassicaceae species might reflect adaptive processes during Brassicaceae evolution.

3.3.5. Lineage-specific gene expression as a sign of adaptive evolution

Variation in gene expression between species might have arisen from two different evolutionary processes. On one hand, gene expression changes between species might be selectively neutral and accumulate with genetic drift over evolution. On the other hand, gene expression changes might be adaptive. Indeed, expression changes between species have previously been associated to adaptive advantages (López-maury et al., 2008; De Nadal et al., 2011). Concerning sequence evolution, robust null models for neutral evolution exist to adequately identify sequences affected by adaptive evolution (Yang and Bielawski, 2000; Delport et al., 2009). However, there is still no consensus for an appropriate null hypothesis of neutral gene expression evolution (Harrison et al., 2012; DeBiasse and Kelly, 2016).

The nature of current transcriptome data introduces multiple problems that complicate the design of appropriate models. For example, expression data is largely affected by environmental conditions (Romero et al., 2012). Therefore, especially when samples are taken from different environments in nature, observed gene expression variation between species may simply result from different environmental factors but not genetic differences (Romero et al.,

2012; Voelckel et al., 2017). If this is not properly accounted for, gene expression variation that is classed as heritable would be overestimated (Harrison et al., 2012). Thus, minimizing environmental variation is crucial to model gene expression evolution. In this study, I performed the experiments in the same experimental setup. Hence my dataset, as opposed to ecological studies, provides a basis to analyse heritable gene expression variation between species.

However, a major remaining problem for modelling gene expression evolution is the relationship between genetic changes and expression changes. Whereas for coding sequence evolution, it can be predicted which DNA mutations lead to altered protein sequences, which is an important assumption for modelling coding sequence evolution (Gilad et al., 2006), it is challenging to link genetic changes with gene expression (Harrison et al., 2012; Hodgins-Davis et al., 2015). For example, changes in regulatory regions, alternative splicing, RNA stability, or DNA methylation can have substantial influences on gene expression (De Nadal et al., 2011; Romero et al., 2012; Voss and Hager, 2014). Consequently, these mechanisms would need to be considered in appropriate models. Given these problems, it is not surprising that different modelling approaches lead to a contrasting interpretation of gene expression evolution. For example, Khaitovich et al. interpreted most expression changes between human and primates as selectively neutral, whereas Gilad et al. proposed that most expression changes between human and primates evolved under purifying selection (Khaitovich et al., 2004; Gilad et al., 2006). For these reasons, I decided not to model gene expression evolution since these modelling approaches are premature to robustly conclude gene expression evolution.

One alternative way to understand gene expression evolution is to assume that the degree of expression variation should correlate with phylogenetic distance if expression changes are neutral (Gilad et al., 2006; Romero et al., 2012; Harrison et al., 2012). When the variation in expression changes is larger than expected from the phylogenetic distance, this implies that some of these expression changes evolved under positive selection and are adaptive (Romero et al., 2012; Harrison et al., 2012). Based on phylogeny, *C. rubella* is the closest relative of *A. thaliana* among the Brassicaceae species included in this study. Therefore, we would expect less variation in flg22-induced expression changes between *C. rubella* and *A. thaliana* than those between *A. thaliana* and the other two Brassicaceae species if most expression changes are neutral. However, flg22-induced expression changes in *C. rubella* are most different from *A. thaliana* compared to the other Brassicaceae species (Figure 11A); hence flg22-triggered expression changes in these species is incongruent with phylogeny. This suggests that a large part of variation in flg22-triggered transcriptional reprogramming of

Brassicaceae does not reflect neutral but adaptive evolution. Consequently, the lineage-specific expression signatures observed in this study likely arose from directional selection and possibly reflect adaptive evolutionary processes. These presumably adaptive gene expression changes might be important for the individual Brassicaceae species to effectively deal with the diverse microbial environments that they faced over million years of evolution.

3.3.6. Regulatory mechanisms affecting lineage-specific gene expression

To elucidate potential mechanisms regulating the lineage-specific expression changes, I searched within the -500 bp 5´-regulatory regions of lineage-specific expression patterns for an enrichment of known TF-motifs. Interestingly, *A. thaliana* specific expression signatures were specifically enriched for WRKY TF binding motifs in *A. thaliana* regulatory regions but not in regulatory regions of other Brassicaceae (Figure 14C). Similarly, genes specifically induced by flg22 in *E. salsugineum* were highly enriched for WRKY TF motifs only in *E. salsugineum* regulatory regions but not in other Brassicaceae species. In addition, *C. rubella* regulatory regions were enriched for WRKY TF motifs only in genes which were specifically highly induced in *C. rubella* (Figure 14C). Considering that WRKY TF motifs are commonly enriched in the regulatory regions of all species (cluster 2,4,5) for evolutionary conserved flg22-inducible genes, it is conceivable that at least some of the species-specific expression patterns are mediated by the gain of WRKY TF-binding motif(s) within 500 bp 5'-regulatory regions of these genes. Similarly, for the *C. rubella*-specific expression gene cluster, AHL12 and AHL25 binding sites were enriched only in *C. rubella* promoters but not in the other Brassicaceae promoters. AHL TFs are conserved in land plants and have been mostly linked to plant development (Zhao et al., 2013; Lou et al., 2014; Zhao et al., 2014). However, some AHL TFs were shown to inhibit MAMP-induced gene expression. For instance, overexpression of *AHL20* negatively regulated defence responses in *A. thaliana* (Lu et al., 2010b). In addition, our group has recently found that multiple AHL TF-motifs are enriched in the promoters of immune-upregulated genes and that expression of multiple *AHL* genes was repressed during immunity. Together, these data suggest that repression of *AHL* TF might be coupled to upregulation of MAMP responsive genes. This mechanism may explain *C. rubella*-specific regulation of flg22-responsive genes.

However, by far not all species-specific expression changes can be explained by these motifs. For example, for *C. hirsuta* specific expression changes, no enriched cis-regulatory motifs were identified. This might have been caused by various reasons. My analysis was based on enrichment of known motifs and therefore would not identify cis-regulatory motifs with low

frequency in a set of regulatory sequences (multiple different mechanisms account for individual gene expression) or novel regulatory motifs. In addition, I focussed my analysis on regulatory regions, 500 bp upstream of transcriptional start sites, since previous studies indicated that this region is generally conserved across related species and that functional cis-regulatory motifs are often found within this region (Baxter et al., 2012; Korkuc et al., 2014; Van de Velde et al., 2016; Yu et al., 2016). For example, many WRKY binding sites are found within the first -400 bp from the transcriptional start site (Birkenbihl et al., 2017). Nevertheless, this does not exclude that additional motifs, important for the species-specific flg22-responsive expression regulation, are located outside this – 500 bp region. A more precise definition of regions enriched for potential TF motifs might be advantageous to search for additional TF motifs. This could be achieved by determining conserved non-coding regions in regulatory sequences of DEGs among Brassicaceae species. Determination of conserved non-coding regions in individual genes (sometimes called phylogenetic shadowing) has proven helpful to elucidate regulatory motifs controlling gene expression (Herrero et al., 2012; Baxter et al., 2012; Van de Velde et al., 2016). Unfortunately, the tools to determine conserved non-coding regulatory regions have been designed to determine these regions in individual genes across multiple species and are not yet designed to be applied to analysis of expression clusters containing hundreds of DEGs.

Besides cis-regulatory motifs, other transcriptional regulatory mechanisms might affect the species-specific expression patterns observed. Trans-regulatory mechanisms such as distant enhancers or chromatin structure and modifications can have strong impacts on gene expression (Tirosh et al., 2009; Field et al., 2009; Tsankov et al., 2010; Shi et al., 2012). Moreover, differential RNA stability might affect species-specific expression patterns (Dori-Bachash et al., 2011; Staiger et al., 2013). Taken together species-specific expression signatures are probably regulated by a combination of different expression regulatory mechanisms and it is conceivable that individual genes are not regulated by the same mechanisms. Nevertheless, the gain of WRKY TF motifs in some of the species-specific flg22-responsive genes likely contributes to their specific expression regulation.

3.3.7. Potential functions of species-specific expression signatures

My results indicated that at least some of the species-specific expression changes in response to flg22 are a consequence of adaptive evolution. Therefore, some of these specific gene inductions should provide fitness advantages in the specific environments where these Brassicaceae species evolved. The functions of species-specific flg22-responsive genes might

point to potential processes involved in this adaptation. However, in stark contrast to the conserved flg22-responsive genes, only a few weakly overrepresented GO-terms could be determined for *A. thaliana* and *C. hirsuta* specific expression signatures (when Brassicaceae were analysed separately, Figure 9C, D) and no GO-terms were significantly enriched within the species-specific expression signatures determined in the combined analysis of Brassicaceae with *A. thaliana* accessions (Supplement Table 3). This suggests that potential adaptation resulting from expression changes is not explained by a small number of dominant biological processes but rather by a multitude of diverse biological processes. Alternatively, biological functions of genes important for the adaptation of other Brassicaceae species might be still unknown. Thus GO-terms of species-specific flg22-responsive genes might be poorly annotated, since GO-term annotations heavily rely on *A. thaliana* research.

Identifying causal relationships between gene expression and phenotypes is a major problem of comparative transcriptomics (Evans, 2015; Voelckel et al., 2017). One difficulty is that complex and conditional phenotypes like PTI are often regulated by multitudes of genes, each of which often fulfils a small contribution to the investigated phenotype (Feder and Walser, 2005; MacKay et al., 2009), a phenomenon described "marginal benefit" hypothesis (Thatcher et al., 1998). This may be one reason why I did not observe enrichment of a particular biological process within the species-specific expression signatures. In addition, these contributions might be detected only under certain circumstances e.g. when pathogens perturb other components or in certain environmental conditions, known as the "contingent function" hypothesis (Feder and Walser, 2005; Thatcher et al., 1998). Consequently, the function of these genes for the investigated phenotype may not be uncovered in laboratory conditions. Thus, functions for some of the species-specific flg22-responsive genes may be difficult to reveal with genetic perturbation. For example, in yeast, it is known that perturbation of genes upregulated by a certain stress often do not change the response to this stress (López-maury et al., 2008; Giaever et al., 2014). Yet, the observation that some of the tested species-specific expression responses are conserved within species or in sister species (Figure 12) suggests that these are unlikely random observations but truly adaptive in nature.

Despite the absence of significantly enriched GO-terms, some genes in *A. thaliana*, *C. rubella* and *E. salsugineum* specific expression clusters were connected to defence secondary metabolism (Supplement Table 3). It is known that Brassicaceae plants are capable of synthesizing a diverse set of often antimicrobial secondary metabolites that can function as phytoanticipins or phytoalexins to protect plants from pathogen infection (Bednarek et al., 2011; Piasecka et al., 2015). For example, 4-methoxy indol-3-ylmethylglucosinolate (4MI3G)

or camalexin are two tryptophan-derived secondary metabolites which are important for *A. thaliana* immunity (Thomma et al., 1999; Bednarek et al., 2009; Clay et al., 2009). 4MI3G belongs to the group of tryptophan-derived indole-glucosinolates, which have been well described in different Brassicaceae and whose pathway genes are activated by flg22 treatment (Clay et al., 2009; Bednarek et al., 2011). Although indole-glucosinolates can be detected in many Brassicaceae, a recent study did not detect any indole-glucosinolates in *C. rubella* (Bednarek et al., 2011). Interestingly, several genes involved in indole-glucosinolate metabolism are significantly stronger induced in *C. rubella* upon flg22 treatment but they are very lowly expressed compared to the other Brassicaceae species in mock samples (Supplement Figure 8). This is exemplified by the expression profile of *MYB51* which encodes a major transcriptional regulator of camalexin and indole-glucosinolate pathway genes (Gigolashvili et al., 2007; Frerigmann et al., 2016). The low basal expression is in line with the previously undetected indole glucosinolates, but why are these genes still induced by flg22 in *C. rubella*? One explanation might be that the level of indole glucosinolates that are still produced by these components in *C. rubella* are below the detection limit and that these components were previously not detected does not allow the conclusion that these are not produced at all in *C. rubella*. Another explanation is that some of these components might have diversified their function to participate in the biosynthesis of new, potentially unknown, secondary metabolites. It is known that these secondary metabolites can have a strong impact not only on defence against pathogenic microbes (Bednarek et al., 2009; Rajniak et al., 2015; Piasecka et al., 2015) but also on the recruitment of beneficial microbes potentially influencing the microbiome composition (Kei Hiruma et al., 2016; Hacquard et al., 2017). Thus, gene expression evolution for secondary metabolite genes suggests new innovations in secondary metabolite metabolisms that might directly affect plant-microbe interactions thereby providing adaptive advantages.

3.3.8. Conservation of flg22-triggered transcriptional responses between *A. thaliana* accessions was robust to a diverse geographic distribution and diversified basal immune levels in certain accessions.

Despite variation in geographical distribution, genetic background and morphological phenotype, the transcriptional responses 1 h after flg22 treatment are extremely conserved among the five *A. thaliana* accessions (Figure 10F, G; Figure 11A, B). As discussed earlier environment can have a strong impact on immunity e.g. abiotic stresses can sometimes supress immune responses. However, my results indicate that adaptations of these *A. thaliana* accessions, to the different environments, did not strongly associate with changes in the early

transcriptional responses upon flg22 treatment. This is not obvious since some of the chosen accessions exhibit very specific variation in immunity-related traits. For example, not only expression of defence marker genes, but also resistance against *Pto* DC3000 is significantly reduced in the No-0 accession compared to Col-0 (Gangappa et al., 2017). Moreover, transcriptome profiling revealed that downregulated genes in No-0 compared to Col-0 are enriched for defence-related GO terms. This is in agreement with the significantly increased *Pto* DC3000 growth in No-0 compared to most other accessions (Figure 10H). Gy-0 constitutes another accession with altered basal immunity since it carries a hyperactive *ACD6* allele, originally identified in the Est-1 accession. In Est-1, this allele leads to increased basal immunity with the cost of negatively influencing growth and producing spontaneous necrosis on fully developed leaves (Todesco et al., 2010). Consistently, I observed that adult Gy-0 plants developed similar lesions and were significantly more resistant against *Pto* DC3000 compared to Col-0 plants. Interestingly, these differences among *A. thaliana* accessions seem to be uncoupled from flg22-induced inhibition of *Pto* DC3000 growth and early transcriptional responses.

The high conservation of flg22-induced transcriptional responses among diverse *A. thaliana* accessions might be specific for PTI or common for stress-induced transcriptome responses. Two recent studies comparing transcriptomic responses after flooding stress or mild-drought stress showed a similar degree of conservation to my study (Van Veen et al., 2016; Clauw et al., 2015). Van Veen et al. investigated transcriptional responses to flooding stress between eight *A. thaliana* accessions from diverse geographic regions. The magnitude of transcriptome response to flg22 and to flooding stress was similar (2443 to 4372 DEGs affected by flg22 and 2356 to 3102 DEGs affected by flooding, depending on accession). Although the authors noted that the transcriptional response to flooding and darkness was very similar between the eight *A. thaliana* accessions, 562 genes exhibited significant variation in their response among the accessions. In comparison, I found 131 DEGs across the five tested *A. thaliana* accessions in response to flg22 (Figure 11D). However, it is conceivable that the more stringed significance cut-off applied in this study (padj < 0.01 compared to padj < 0.05) and the different numbers of accessions included (five compared with eight) presumably explain the different numbers of DEGs detected in these two studies. Thus, the degree of variation between stress-induced transcriptomes compared across different *A. thaliana* accessions seems to be moderate as well for flooding and darkness stress. Similarly, a recent study investigated transcriptional variation in response to mild drought stress among six *A. thaliana* accessions (Clauw et al., 2015). The authors detected 60 accession specific DEGs out of 439 DEGs in

response to mild drought-stress. However, the authors noted that in pairwise tests between accessions, none of the 60 accession-specific genes responded significantly different from all other five accessions. This is in agreement to my analysis that identified only one gene in the Can-0 accession with significantly different response to flg22 compared to all other four accessions. These results indicate that the stress-responsive transcriptional reprogramming is highly conserved between *A. thaliana* accessions.

3.3.9. Within and between species variation in gene expression – Interspecies variation exceeds intra species variation

An important observation of this work was that inter-species transcriptome variation exceeds intra-species variation in response to flg22. This suggests that short-term adaptation to diverse environments within a species is not sufficient to diversify early transcriptional responses during PTI and that longer evolutionary times between species led to increased flg22-responsive transcriptome variation which reflects adaptive processes during Brassicaceae evolution.

Research investigating transcriptome conservations within and between species is currently scarce. Early studies in the animal field investigated transcriptome conservation within and between species to identify genes evolving under neutral, purifying or positive (adaptive) evolution (Oleksiak et al., 2002; Rifkin et al., 2003). Genes with little variation within and between species are likely under purifying selection, whereas genes with little variation within species but large variation between species evolved presumably under positive selection. Genes with variable expression within and across species are probably affected by neutral evolution and genetic drift (Harrison et al., 2012; Romero et al., 2012). Using this assumption, a study on Drosophila noted that the majority of expression changes likely evolved under purifying selection, while at the same time substantial number of expression changes showed signs of positive evolution and a smaller subset was associated with neutral evolution (Rifkin et al., 2003). In contrast, a study on killifish determined much more expression variation within compared to between species suggesting that these expression changes evolved under neutral evolution (Oleksiak et al., 2002). These opposing conclusions might be affected by the effect of environment on gene expression noise discussed earlier. Alternatively, different modes of gene expression evolution may exist in different species.

More recent studies found less expression variation between species in the same organ than expression variation in different organs within species (Brawand et al., 2011; Gilad and Mizrahi-Man, 2015; Uebbing et al., 2016). However, these studies investigated basal

expression levels and it is not clear whether stress-induced expression changes show a high organ specificity. Unfortunately, there are yet no transcriptome studies investigating expression changes within and between plant species. Therefore, future studies will be required to understand whether inter-species transcriptional variation exceeding intra-species transcriptional variation is a general phenomenon for other species and whether it is restricted to certain plant tissues or stress responses.

3.3.10. Specificity of lineage-specific flg22-responsive transcriptional signatures

Expression profiles of selected genes showing species-specific expression signatures in available accessions and sister species of the four tested Brassicaceae revealed that species-specific expression signatures are mostly conserved among tested accessions and sister species (Figure 12). These results strengthened my RNAseq analysis of species-specific innovations and extended them to closely-related species in the case of *C. rubella* and *E. salsugineum*. This suggests that some specific flg22-resposnsice expression changes might be lineage-specific rather than species-specific. However, the *C. hirsuta* specific marker gene, orthologous to AT3G60966, was also significantly induced in *C. grandiflora*. This suggests that a species-specific innovation might occur independently in multiple species. Investigating transcriptome responses of a larger set of sister species and accessions would certainly define the range of conservation of species-specific innovations. Nevertheless, my study clearly showed that species-specific expression signatures detected in the RNAseq are not peculiar phenotypes of the accession that I picked but conserved features within species or related species. This is in line with the high conservation of flg22-responsive transcriptome changes among *A. thaliana* accessions.

Elf18 specifically triggered two out of three marker genes tested for *C. rubella* and *E. salsugineum*, whereas the two *C. hirsuta* specific marker genes did not respond to elf18 treatment. This indicates that parts of the lineage-specific expression changes triggered by flg22 are common for elf18-induced PTI. A recent study indicated that despite strong correlation of flg22 and elf18 activated transcriptome responses, a large number of genes exhibit a flg22-specific response which was absent in elf18-treated seedlings (Briggs et al., 2017). Vice versa much fewer genes were specifically responsive to elf18. Given these recent insights, it is not surprising that only a subset of lineage-specific flg22-responsive genes was activated by elf18 in *C. rubella* and *E. salsugineum*. In the perspective of plant adaptation, diversified responses to different MAMPs might be used by plants to fine tune their immunity depending on different

ratios of MAMPs in microbial communities. It was recently hypothesized that the repertoire of PRRs that can sense different MAMPs might be a driving factor of local adaptation to specific microbial communities (Hacquard et al., 2017). Moreover, flg22 and elf18 have presumably different accessibility for the host plant as flagellin is on the outside of bacterial cells, whereas Ef-Tu is one of the most abundant proteins inside bacterial cells. Hence in a natural infection context, it is likely that such MAMPs might be perceived in temporally distinct manner and consequently trigger some specific responses that help the plant to distinguish the current state of infection. These are potential reasons why species-specific flg22-specific transcriptome responses might only be partly conserved for other MAMP triggered transcriptional responses. It would be interesting to see whether similar species-specific responses can be also detected in PTI triggered by different for example fungal-derived MAMPs like chitin.

Furthermore, an additional transcriptome analysis after heat-stress suggested that the large transcriptome variation in flg22-response among Brassicaceae species is not specific for PTI but can be rather a general phenomenon in early stress responsive transcriptomes. Compared to the variation of flg22-induced transcriptome changes among Brassicaceae, the heat-induced transcriptional changes were even more variable among the tested species with large numbers of species-specific heat-responsive genes (Figure 16F, G). However, these heat-stress RNAseq results must be analysed with caution since the mapping quality in some samples was inferior compared to the flg22 dataset, potentially affected by lower RNA integrity (Supplement Table 2). This probably lowered the number of reliably expressed genes, which might have inflated the number species-specific expressed genes. Consequently, I re-analysed the heat-stress data, normalizing expression data of all species together and excluding lowly expressed genes. Excluding lowly expressed genes still resulted in a substantial number species-specific heat stress-responsive expression changes (Supplement Figure 10). Thus, it is unlikely that variation solely arose from RNA quality issues and therefore indicates that large variations in early stress-responsive transcriptomes between different species are a more general phenomenon. Since both biotic, as well as abiotic stress responses, are heavily affected by each other and environmental conditions it is conceivable that these variations reflect genetically encoded long-term adaptations to different environments which are still visible under controlled growth conditions.

3.4. Connection of sequence and expression variation.

Several previous studies connected the variation at the expression level with the diversification of DNA sequences (Hunt et al., 2013; Whittle et al., 2014; Necsulea and

Kaessmann, 2014). In this study, we did not detect a clear correlation between them (Figure 16), suggesting that gene expression variation is uncoupled with protein coding sequence divergence. In contrast, protein sequence evolution was associated with gene expression variation between and within different fire ant species (Hunt et al., 2013). Another study compared expression variation of sexual and vegetative tissues between the model fungal species *Neurospora crassa* and *Neurospora tetrasperma* (Whittle et al., 2014). Comparison of sexual tissues revealed a correlation between transcriptome and genome evolution, whereas in vegetative tissues, expression variation was not connected with sequence variation between the Neurospora species. This suggests that the positive relationship between expression and sequence evolution is tissue dependent in some cases. Therefore, sampling whole seedlings including different organs might have precluded the detection of a clear correlation between expression variation and protein sequence variation. Separating different tissues like root and shoot tissue might help future studies investigating this phenomenon in plants. Nevertheless, several studies in the animal field did not detect a correlation of gene expression variation with sequence variation (Renaut et al., 2012; Uebbing et al., 2016). Thus, it is still under debate whether protein coding sequence evolution is correlated with gene expression evolution.

Another possible explanation why expression and coding sequence divergence did not correlate might be that adaptive changes in sequences or expression present alternative routes in response to selection pressure since expression changes might prevent negative pleiotropic effects when sequences are constraint and vice versa (Shapiro et al., 2004; Harrison et al., 2012). Consequently, expression evolution would allow plasticity for genes that are constraint for sequence evolution. If this would be the case expression evolution and sequence evolution would likely not be correlated with each other. Further studies investigating the relationship of sequence evolution and expression evolution, on one hand, should incorporate more species along a phylogenetic relationship and resolve the sampling for different organs and on the other hand specifically investigate how expression behaves in genes with a constraint sequence evolution.

3.5. Concluding remarks and future perspectives

Although PTI is crucial for plants to deal with pathogens surrounding them, the conservation and evolution of PTI responses between species is poorly understood. In this thesis, I investigated flg22-induced responses within *A. thaliana* and across multiple Brassicaceae species with a defined phylogenetic framework.

I found that all tested Brassicaceae species sensed flg22 and activated typical PTI responses including MPK3/6 activation and seedling growth inhibition. Comparisons of phytohormone levels between the Brassicaceae species showed substantial variation not only on the basal level but also in their flg22-responsivness. Moreover, the flg22-induced reduction of *Pto* growth was variable among Brassicaceae species. Investigating how flg22-treatment affects interactions of Brassicaceae species with other pathogens, such as necrotrophic pathogens, might clarify whether flg22 pre-treatment of *E. salsugineum* and *C. hirsuta* effectively reduces pathogen growth or whether flg22 treatment elicits a weaker PTI response in these species compared to the other Brassicaceae species. Moreover, elevated ABA levels in *E. salsugineum* compared to other species might be connected to its extreme salt stress tolerance and could affect PTI responses. Future experiments with *aba2* mutants of *E. salsugineum*, generated by CRISPR-Cas9 technology, will help to understand the role of ABA in the abiotic stress tolerance as well as the potential influence on PTI responses in *E. salsugineum*.

It was previously unknown to what extent MAMP-responsive and more generally stress-responsive transcriptional changes are conserved within and between species and how gene expression evolved. Here I showed that most flg22-induced expression changes are advantageous enough to be conserved over approximately 30 Mio years of evolution, since speciation between the tested Brassicaceae occurred. This conservation indicates the importance of this massive transcriptional reprogramming during PTI and suggests a pivotal role of purifying selection on flg22-triggered transcriptomic responses. In addition, a substantial number of genes exhibited a species/lineage-specific expression signature in the early response to flg22. These specific expression patterns were absent in geographically and genetically distinct *A. thaliana* accessions. Thus, inter-species exceeded intra-species expression variation. Importantly, the expression variation between Brassicaceae was incongruent with their phylogeny. In addition to the extremely conserved transcriptome responses within *A. thaliana* this indicates that parts of the species-specific expression signatures evolved adaptively. Moreover, heat stress also induced considerable expression variation between species, suggesting that substantial inter-species variation might be a common phenomenon of stress-induced transcriptomic responses. This thesis revealed unprecedented insights into the evolution of flg22-triggered transcriptomic reprogramming and provides the first dataset comparing stress-induced transcriptomes within and between species with a defined phylogenetic framework in plants. This dataset can be utilized for subsequent analyses such as the implementation of co-expression networks to infer ancestral expression networks of PTI.

The complex and conditional nature of PTI probably precluded the determination of specific processes which might mediate the adaptive advantage of these specific expression signatures, but diversification of secondary metabolism might be a possibility. An in-depth analysis of secondary metabolites produced during PTI in different Brassicaceae might help to connect expression changes with diversification in secondary metabolite synthesis.

Analysis of 5´regulatory regions indicated an important role of WRKY TF motifs, not only in the regulation of conserved flg22-induced genes, but also in the gain of certain species-specific expression changes. Determining conserved non-coding regions across Brassicaceae species in regulatory sequences of conserved as well as species-specific flg22-responsive genes will help to reveal additional regulatory mechanisms associated with conserved and species-specific flg22-responsive genes.

To reach a comprehensive understanding of how plants interact with microbes in their environment, we need to understand which of the plant responses to microbial invasion are evolutionary conserved and how diversification of responses enables plants to adapt their immune system to new environments. If we understand how plant responses are modified in order to adapt and which responses are essential, we can apply this knowledge to tackle upcoming challenges like climate change and improvement of crop production. However, we are just beginning to understand how transcriptome responses evolve within and between plant species and what impact diversifications might have on complex phenotypes such as PTI. This study paves the way for future studies investigating consequences and molecular mechanisms for gene expression evolution in the interaction of plants with microbes.

4. Material and Methods

4.1. Materials

4.1.1. Plant Material

Table 1: Brassicaceae species and accessions used in this study
Bold entries indicate species used for RNAseq.

Species	Accession	Abbreviation	Source
Arabidopsis thaliana	Col-0	Ath	Kenichi Tsuda lab
Arabidopsis lyrata	MN47	Aly	Hu et al., 2011
Capsella rubella	N22697	Cru	Slotte et al., 2013
Capsella grandiflora	unknown	Cgr	Slotte et al., 2014
Cardamine hirsuta	Oxford	Chi	Tsiantis/Janne Lempe
Cardamine hirsuta	OLI	OLI	Tsiantis/Janne Lempe
Cardamine hirsuta	GR2	GR2	Tsiantis/Janne Lempe
Eutrema salsugineum	Shandong	Esa	Tsiantis/Janne Lempe
Eutrema salsugineum	Yukon	Eyt	Tsiantis/Janne Lempe
Thellungiella halophyla	unknown	Tha	
Shrenkiella parvula	unknown	Spa	Dassanayake et al., 2011
Aethionema arabicum	unknown	Aar	Haudry et al., 2013

Table 2: *A. thaliana* accessions used in this study
Bold entries indicate accessions used for RNAseq.

Accession	Cs number	Country	Admixture group[1]	Source
An-1	CS76435	BEL	admixed	Jane Parker lab (MPIPZ)
Bla-1	CS76451	ESP	spain	Jane Parker lab (MPIPZ)
Can-0	CS76740	ESP	relict	Eric Kemen lab (MPIPZ)
Col-0	CS76778	USA	germany	Eric Kemen lab (MPIPZ)
CVI-0	CS76789	CPV	relict	Eric Kemen lab (MPIPZ)
Edi-0	CS76831	UK	admixed	Eric Kemen lab (MPIPZ)
Gy-0	CS78901	FRA	western europe	Jane Parker lab (MPIPZ)
HR10	CS76940	UK	western_europe	Eric Kemen lab (MPIPZ)
Kas-2	CS78905	IND	asia	Jane Parker lab (MPIPZ)
Kn-0	CS76969	LTU	central_europe	Jane Parker lab (MPIPZ)
Kondara	CS76532	TJK	asia	Jane Parker lab (MPIPZ)
Ms-0	CS76555	RUS	asia	Jane Parker lab (MPIPZ)
No-0	CS77128	GER	central_europe	Eric Kemen lab (MPIPZ)
Pna-17	CS76575	USA	germany	Eric Kemen lab (MPIPZ)
Rsch4	CS77222	RUS	germany	Eric Kemen lab (MPIPZ)
Se-0	CS76597	ESP	spain	Eric Kemen lab (MPIPZ)
Sf-2	CS77247	ESP	spain	Eric Kemen lab (MPIPZ)

[1] Admixture group based on 1001 genomes consortium Cell, 2016

Accession	Cs number	Country	Admixture group[1]	Source
Sorbo	CS78917	TJK	asia	Jane Parker lab (MPIPZ)
Tamm-27	CS77341	FIN	north_sweden	Jane Parker lab (MPIPZ)
Ts-1	CS76615	ESP	spain	Eric Kemen lab (MPIPZ)
Tsu-0	CS77389	JPN	admixed	Eric Kemen lab (MPIPZ)
Van-0	CS76623	CAN	western_europe	Eric Kemen lab (MPIPZ)
Wil-2	CS78856	LTU	central_europe	Eric Kemen lab (MPIPZ)
Wu-0	CS78858	GER	germany	Eric Kemen lab (MPIPZ)

Table 3: *A. thaliana* mutants used in this study

Species	Mutant allele	Locus	Source
Arabidopsis thaliana	*sid2-2*	AT1G74710	Tsuda et al., 2008
Arabidopsis thaliana	*fls2* (SAIL_691C4)	AT5G46330	Zipfel et al., 2004

4.1.2. Bacterial Material

Pseudomonas syringae pv. *tomato* DC3000 (*Pto* DC3000) and a *Pto* DC3000 mutant lacking *hrcC* gene (*Pto hrcC*) were grown on NYGA agar plates for three days at 28°C. For infection, the bacteria were transferred to liquid NYGA medium and incubated overnight at 28°C and 200 rpm until they reached an OD600 between 0.8 and 1.

4.1.3. Primer

All nucleotides in the table below were ordered from Sigma-Aldrich (Steinheim, Germany)

Table 4: Primers used in this study

Name	Locus	Sequence (5'-3')
qP_Br_ACT2_fw	AT3G18780; Carubv10013961m; CARHR094190.1; Thhalv10020949	TAAGGTCGTTGCACCACCTG
qP_Br_ACT2_rv	AT3G18780; Carubv10013961m; CARHR094190.1; Thhalv10020949	GCTGGAATGTGCTGAGGGAA
qP_Br_WRKY29_fw	AT4G23550, Carubv1000515, CARHR230930, Thhalv10025799	TCAAGAGCTGATCATATCCGAAT
qP_Br_WRKY29_rv	AT4G23550, Carubv1000515, CARHR230930, Thhalv10025799	GCGTCCGACAACAGATTCTC
qP_At_PROPEP3_fw	AT5G64905	CTTGCGATCTTTCGTCATCA
qP_At_PROPEP3_rv	AT5G64905	GTTCTTCCCTCTCGCTTTGA
qP_Cr_PROPEP3_fw	Carubv10027429	TCTTCATCTCACAGCGAGGA
qP_Cr_PROPEP3_rv	Carubv10027429	TGGGCCTACTCTTCTGCAAC
qP_Es_PROPEP3_fw	Thhalv10005182	CGACCGTTGAAATCACAGAG
qP_Es_PROPEP3_rv	Thhalv10005182	TTTTGCCTCCTTTTCCTGAG
qP_Ch_PROPEP3_fw	CARHR278940.1	TGAGGAAGATGAGGGTATGGTT
qP_Ch_PROPEP3_rv	CARHR278940.1	GTTTTCCTGTGCTTGGTGGT
qP_AtCg_PR4_fw	AT3G04720.1; Cagra.9490s0001.1	TAGTGGACCAATGCAGCAAC
qP_AtCg_PR4_rv	AT3G04720.1; Cagra.9490s0001.1	AGATGGCCTTGTTGATAGCC

Name	Locus	Sequence (5'-3')
qP_Cr_PR4_fw	Carubv10014707	AAGTGCTTGAGGGTGAGGAA
qP_Cr_PR4_rv	Carubv10014707	ATTGAACATCGCAACATCCA
qP_EsCh_PR4_fw	Thhalv10021503; CARHR078970.1	TCCTCGTGGTCAAGCTTCTT
qP_EsCh_PR4_rv	Thhalv10021503; CARHR078970.1	AATCCAATCCTCCATTGCTG
qP_AtEs_CYP79B2_fw	AT4G39950; Thhalv10024861	CCGCCGATGAAATCAAACCC
qP_AtEs_CYP79B2_rv	AT4G39950; Thhalv10024861	TTTGTTCACCATCTCCGCCA
qP_CrCg_CYP79B2_fw	Carubv10004524; Cagra.5414s0021.1	CAAGGACGAACAAGGCAACC
qP_CrCg_CYP79B2_rv	Carubv10004524; Cagra.5414s0021.1	TTTGATGGATTGTCTGGCGC
qP_Ch_CYP79B2_fw	CARHR246750.1	GCGCCAGACAATCCATCAAA
qP_Ch_CYP79B2_rv	CARHR246750.1	TCTTCCATTGCTTTCCGGAGA
qP_AtCrCg_NAC32_fw	AT1G77450; Carubv10020834; Cagra.0096s0087.1	ATGCACGAATACCGGCTAGC
qP_AtCrCg_NAC32_rv	AT1G77450; Carubv10020834; Cagra.0096s0087.1	CGACACAATACCCAATCGTCC
qP_Es_NAC32_fw	Thhalv10018998	CGGTCGGTTCGCATGAAAAA
qP_Es_NAC32_rv	Thhalv10018998	CGGTCATAGGCTTCACGTCA
qP_Ch_NAC32_fw	CARHR070970.1	TATCGAGAAGCAACGGAGCG
qP_Ch_NAC32_rv	CARHR070970.1	TAATCCCGCCACAGATACCG
qP_AtEs_RAC7_fw	AT4G28950.1; Thhalv10026246	GGGAGAGGAATTGAGGAAGC
qP_AtEs_RAC7_rv	AT4G28950.1; Thhalv10026246	CTTGGAGGCTGAAGAACCAC
qP_CrCg_RAC7_fw	Carubv10005734; Cagra.5133s0005.1	TCAGGGAGAGGAGTTGAGGA
qP_CrCg_RAC7_rv	Carubv10005734; Cagra.5133s0005.1	TTTTCCGTGTGACCTCCTTC
qP_Ch_RAC7_fw	CARHR236700	GTGGTTCTTCAGCCTCCAAG
qP_Ch_RAC7_rv	CARHR236700	ATACTCGCAATGGAGCAACC
qP_AT3G60966fw	AT3G60966.1	GATGAGGCGATTGACGATTT
qP_AT3G60966rv	AT3G60966.1	ACACAACGGACACTTGGACA
qP_Cr_AT3G60966fw	Carubv10018513	AGAATGGCTGCGAAAGATCA
qP_Cr_AT3G60966rv	Carubv10018513	AAATCGTCAATCGCCTCATC
qP_Cg_AT3G60966fw	Cagra.0239s0006	TTTCCACGCTGATTGTATCG
q_PC_gAT3G60966rv	Cagra.0239s0006	AACAATAAGCGCGAGGAGAG
qP_Es_AT3G60966fw	Thhalv10006444	GATGAGGCGATTGACGAAGT
qP_Es_AT3G60966rv	Thhalv10006444	GGCGGTAAAGGAGGAATCTC
qP_At_APK4_fw	AT5G67520.1	GCCACTCCATGTTTGTGAAG
qP_At_APK4_rv	AT5G67520.1	ACAATCTCGCAATCCAAAGG
qP_Cr_APK4_fw	Carubv10026887	GCTAGAGACCCGAAGGGATT
qP_Cr_APK4_rv	Carubv10026887	ACAATCTCGCAGTCCAAAGG
qP_Es_APK4_fw	Thhalv10004693	CGGAAGGAGATTTCATCGAG
qP_Es_APK4_rv	Thhalv10004693	GCAATCCAAAGGTGGTTCAT
qP_Ch_APK4_fw	CARHR280070	TGGATGTGCCACTTCATGTT
qP_Ch_APK4_rv	CARHR280070	CAATCTCGCAATCCAAAGGT
qP_Cg_APK4_fw	Cagra.0342s0040.1	CCTTTGGACTGCGAGATTGT
qP_Cg_APK4_rv	Cagra.0342s0040.1	TGCCATTTCAGACAGAGACG
qP_Br_bZIPX_fw	AT1G02110; Carubv10008455; Cagra.1968s0147.1; CARHR000220	CAATAAAGCAGGCGGAAGAG
qP_Br_bZIPX_rv	AT1G02110; Carubv10008455; Cagra.1968s0147.1; CARHR000220	CCTATCCCAACCGTCGAGTA
qP_Es_bZIPX_fw	Thhalv10006946	AGAGTGCAGGAAAGGAGCTG
qP_Es_bZIPX_rv	Thhalv10006946	CGTCGAATACGCCTGGTAAT
qP_At_CYP77A4_fw	AT5G04660.1	CAATGGCAACCATACACGTC
qP_At_CYP77A4_rv	AT5G04660.1	ACTTCCTGGTGGATGAGCAC

Name	Locus	Sequence (5'-3')
qP_CrCg_CYP77A4_fw	Carubv10003366	GATCTGTCCAGGGCTTACGA
qP_CrCg_CYP77A4_rv	Carubv10003366	CGGCGAAATCAATCTCACTT
qP_Es_CYP77A4_fw	Thhalv10016078	GGTTCAGGAGTTCGAGTGGA
qP_Es_CYP77A4_rv	Thhalv10016078	AACGGGTTCTTCATCACCAC
qP_Ch_CYP77A4_fw	CARHR208640.1	GTGTTGGCCGTAGGATCTGT
qP_Ch_CYP77A4_rv	CARHR208640.1	ATACGCGCTCCACTCAAACT
Pto_OPRF_fw	NC_004578.1	AACTGAAAAACACCTTGGGC
Pto_OPRF_rv	NC_004578.1	CCTGGGTTGTTGAAGTGGTA

4.1.4. Genes described in this study

Table 5: Genes described in this study

Abbreviation	Full name	AGI
AGB1	*GTP BINDING PROTEIN BETA 1*	AT4G34460
AGG1	*GGAMMA-SUBUNIT 1*	AT3G63420
APK4	*ADENOSINE-5-PHOSPHOSULFATE KINASE 4*	AT5G67520
ASB1	*ANTHRANILATE SYNTHASE BETA SUBUNIT 1*	AT1G25220
BAK1	*BRI1-ASSOCIATED RECEPTOR KINASE*	AT4G33430
BIK1	*BOTRYTIS-INDUCED KINASE1*	AT2G39660
BSK1	*BRASSINOSTEROID-SIGNALING KINASE 1*	AT4G35230
CAD1	*CADMIUM SENSITIVE 1*	AT5G44070
CBP60g	*CAM-BINDING PROTEIN 60-LIKE G*	AT5G26920
CERK1	*CHITIN ELICITOR RECEPTOR KINASE 1*	AT3G21630
CPK28	*CALCIUM-DEPENDENT PROTEIN KINASE 28*	AT5G66210
CYP77A4	*CYTOCHROM P450 FAMILY PROTEIN 77A4*	AT5G04660
CYP79B2	*CYTOCHROM P450 FAMILY PROTEIN 79B2*	AT4G39950
DORN1	*DOES NOT RESPOND TO NUCLEOTIDES 1*	AT5G60300
EFR	*EF-TU RECEPTOR*	AT5G20480
FER	*FERONIA*	AT3G51550
FLS2	*FLAGELLIN-SENSITIVE 2*	AT5G46330
IGMT5	*INDOLE GLUCOSINOLATE O-METHYLTRANSFERASE 5*	AT1G76790
IOS1	*IMPAIRED OOMYCETE SUSCEPTIBILITY 1*	AT1G51800
LLG1	*LORELEI-LIKE-GPI-ANCHORED PROTEIN 1*	AT5G56170
LORE	*IPOOLIGOSACCHARIDE-SPECIFIC REDUCED ELICITATION*	AT1G61380
LYK5	*LYSM-CONTAINING RECEPTOR-LIKE KINASE 5*	AT2G33580
LYM1	*LYSM DOMAIN GPI-ANCHORED PROTEIN 1 PRECURSOR*	AT1G21880
LYM3	*LYSIN-MOTIF DOMAIN PROTEIN 3*	AT1G77630
MKKK7	*MITOGEN-ACTIVATED PROTEIN KINASE KINASE KINASE 7*	AT3G13530
MYB51	*MYB DOMAIN PROTEIN 51*	AT1G18570
NAC32	*NAC DOMAIN CONTAINING PROTEIN 32*	AT1G77450
NPR1	*NONEXPRESSER OF PR GENES 1*	AT1G64280
PBL27	*PBS1-LIKE KINASE 27*	AT5G18610
PBS3	*AVRPPHB SUSCEPTIBLE 3*	AT5G13320
PCRK1	*PTI COMPROMISED RECEPTOR-LIKE CYTOPLASMIC KINASE 1*	AT3G09830
PCRK2	*PTI COMPROMISED RECEPTOR-LIKE CYTOPLASMIC KINASE 2*	AT5G03320
PEN3	*PENETRATION 3*	AT1G59870
PEPR1	*PEP1 RECEPTOR 1*	AT1G73080

Abbreviation	Full name	AGI
PEPR2	*PEP1 RECEPTOR 2*	AT1G17750
PP2A	*SERINE/THREONINE PROTEIN PHOSPHATASE 2A*	AT1G69960
PP2C38	*PROTEIN PHOSPHATASE 2C 38*	AT3G12620
PR4	*PATHOGENESIS-RELATED 4*	AT3G04720
PUB12	*PLANT U-BOX 12*	AT2G28830
PUB13	*PLANT U-BOX 13*	AT3G46510
RAC7	*RAC-LIKE GTPASE 7*	AT4G28950
RLP23	*RECEPTOR LIKE PROTEIN 23*	AT2G32680
RLP30	*RECEPTOR LIKE PROTEIN 30*	AT3G05360
RPOPEP3	*ELICITOR PEPTIDE 3 PRECURSOR*	AT5G64905
SARD1	*SAR DEFICIENT 1*	AT1G73805
SOBIR1	*SUPPRESSOR OF BIR1*	AT2G31880
TSA1	*TRYPTOPHAN SYNTHASE ALPHA CHAIN 1*	AT3G54640
TSB1	*TRYPTOPHAN SYNTHASE BETA-SUBUNIT 1*	AT5G54810
WRKY29		AT4G23550
XLG2	*EXTRA-LARGE GTP-BINDING PROTEIN 2*	AT4G34390

ASB1, TSA1, TSB1, CYP79B2/B3, MYB51, PEN3, and IGMT5

4.1.5. Chemicals, Kits, Enzymes and Buffers

Table 6: Chemicals used in this study

Chemical	Company
Rifampicin	Duchefa (Haarlem, Netherlands)
Salicylic acid (SA)	Duchefa (Haarlem, Netherlands)
Abscisic acid (ABA)	Sigma-Aldrich (St. Louis, USA)
Tween 20	Sigma-Aldrich (St. Louis, USA)
TritonX	Sigma-Aldrich (St. Louis, USA)
NaClO	Sigma-Aldrich (St. Louis, USA)
flg22	EZBiolab Inc. (Westfield, USA)
elf18	EZBiolab Inc. (Westfield, USA)
peqGOLD TriFast™	Peqlab (Darmstadt, Germany)
L-012	Wako Chemicals (Neuss, Germany)
EvaGreen DNA Dye	Biotium (Hayward, USA)

Table 7: Kits used in this study

Kit	Company
FastDNA™ Spin Kit for Soil	MP Biomedicals (USA, Santa Ana)
Coomassie Protein assay	Biorad (Hercules, USA)

Table 8: Enzymes used in this study

Enzyme	Company
SuperScript II Reverse Transcriptase	ThermoFischer Scientific (USA, Waltham)
SuperScript IV Reverse Transcriptase	ThermoFischer Scientific (USA, Waltham)
T7 Endonuclease I	NewEnglandBiolabs (USA, Ipswich)

Enzyme	Company
RNAse OUT	Thermo Scientific (USA, Waltham)
DNaseI	Roche (Mannheim, Germany)

Table 9: Media and Buffers

Name	Components
NYGA (pH 7.0)	2% (v/v) glycerol 0.5% (w/v) Bactopeptone 0.3% (w/v) yeast extract (1% (w/v) bacto agar)
Murashige and Skoog Medium (MS) Agar	2.45 g/L M&S Medium (Duchefa, Netherlands) 1% Sucrose 0.5% Plant Agar (Duchefa, Netherlands) pH 5.8
MAPK Extraction Buffer	50 mM Tris-HCL [pH 7.5] 5 mM EDTA 5 mM EGTA 2 mM DTT 10 mM NaF 50 mM β-glycerolphosphate 10% glycerol Complete proteinase inhibitor (Roche, Germany) Phosstop phosphatase inhibitor (Roche, Germany)
PAGE Buffer	25 mM Tris 190 mM Glycin 0.1% (w/v) SDS
Blotting Buffer	3.03 g/L Tris 14.41 g/L Glycin 800 ml milipore water 200 ml methanol
TBS (10x)	23.23 g/L Tris 80.6 g/L NaCl adjusted pH to 7.6 with HCL
TBST	100 ml 10xTBS 900 ml Milipore water 1 ml Tween20
PCR Buffer (10x)	200 mM tris-HCL (pH 8.8) 100 mM KCl 100 mM $(NH4)_2SO_4$ 20 mM $MgCl_2$ 10% Triton X100

4.2. Methods

4.2.1. Plant Growth

Seeds were sterilized by vortexing in 70% ethanol for 5 min and then 6% NaClO for 10 min, washed 5 times with sterile water and stratified in sterile water for five to seven days. Sterilized seeds were grown on ½ Murashige and Skoog (MS)-Agar plates and grown in Percival growth chamber (CU-36LX5D, Percival, USA) at 22 °C, 10 h L/D for eleven days if not stated otherwise. Eleven-day-old seedlings were transferred to liquid ½ MS-Medium (same

composition as MS-Agar) one day before chemical treatments. Alternatively, 12-day-old seedlings were transferred to commercial soil (Stender, Schermbeck Germany) and grown at 23 °C/20 °C with 10 h/14 h (light/dark) and 60% relative humidity. Soil-grown-plants were transferred to another chamber at 22 °C with a 12 h photoperiod and 60% relative humidity three days before bacterial inoculation.

4.2.2. Flg22 and heat-stress treatment

Eleven-day-old seedlings were transferred from ½ MS-Agar to 24-well plates each with 1.6 ml of ½ MS-Medium 24 h prior to treatments. If not otherwise stated, five to ten seedlings per sample were transferred to each well. For the flg22 treatment, 800 µl of 3 µM flg22 solution was added to the medium containing the seedlings resulting in a final concentration of 1 µM flg22. For the heat treatment, the whole 24-well plate was transferred for one hour to another growth chamber at 22°C (control) or 38°C without light. Three wells were combined for one sample to reduce experimental variance when the seedlings were harvested in liquid nitrogen at indicated time points. The samples were stored at –80°C until use.

4.2.3. Seedling growth inhibition assay

Seven-day-old seedlings grown on ½ MS-Agar were transferred to 1.6 ml of ½-MS-Medium with and without 1 µM flg22 and grown for another 12 days in these solutions. Then, the fresh weight of 12 pooled seedlings was measured. The experiment was independently repeated three times and statistics were calculated with $\log_2$-transformed fresh weight values. This experiment was performed by Shajahan Anver.

4.2.4. Hormone quantification

Phytohormone extraction and quantification was performed in the lab of Hitoshi Sakakibara at the Riken institute Japan as previously described (Kojima and Sakakibara, 2012).

4.2.5. Bacterial Growth Assays

For preparation of bacterial inoculum, *Pseudomonas syringae* pv. *tomato* DC3000 (*Pto* DC3000) or the T3SS deficient *Pto* DC3000 mutant *Pto hrcC* was grown on NYGA agar containing 25 µg/ml rifampicin for 3 days at 28°C. Then, bacterial strains were transferred to liquid NYGA medium containing 25 µg/ml rifampicin and incubated over night at 28°C with

shaking at 200 rpm to a final OD_{600} between 0.8 and 1. The bacteria were pelleted by centrifugation at 5000 rpm and washed twice with sterile 5 mM $MgSO_4$ before diluting the bacteria to an OD_{600} of 0.0002 or 0.001 for *Pto* DC3000 and *Pto hrcC*, respectively.

Four to five-week-old plants were used. Two leaves per plant were infiltrated with 1 µM flg22 or sterile water (mock) using a needleless syringe. One day later, leaves treated with flg22 or mock solution were infiltrated at early afternoon with the bacterial suspension. Two days after bacterial infiltration, two leaf disks (0.565 cm^2) per sample from two leaves were crushed in 400 µl sterile $MgSO_4$ using a Retsch mixer mill. Dilution series were made and streaked on NYGY agar plates containing 25 µg/ml rifampicin. The plates were incubated for two days at 28°C before colony forming units (cfu) were counted.

Alternatively, bacterial growth was quantified using a qPCR based method as previously described (Ross and Somssich, 2016). In brief, DNA of *Pto* infiltrated leaves was extracted using a FastDNA^{TM} Spin Kit from (MP biomedicals). Extracted DNA was quantified and adjusted to 8.75 µg/µl to achieve a final concentration of 35 µg DNA in a qPCR reaction. Bacterial DNA was quantified using the *Pto* specific *OPRF* gene relative to plant *ACTIN2* (*ACT2*) DNA. ΔCt values were calculated subtracting the target gene expression from *ACT2* expression and statistics were calculated using these ΔCt values which correspond to log_2 expression values of a gene of interest relative to *ACTIN2*.

4.2.6. MAP kinase phosphorylation assay

MAPK3/4/6 phosphorylation assay was performed as previously described (Tsuda et al., 2009). In short, 12-day-old seedlings were treated with 1 µM flg22 or mock for 15 min, frozen in liquid nitrogen and ground with four metal beads in a Retsch MM 400 mixing mill (Retsch, Germany). Then 150 µl of MAPK extraction buffer was added to the sample and protein was extracted by centrifugation at 4°C and 12000 rpm. Protein concentrations were determined by Coomassie Protein Assay Kit with an albumin starndard curve (both ThermoFisher Scientific, USA) and 25 µg of protein was separated by SDS-PAGE for one hour at 100V. MAPK phosphorylation was detected via Immunoblotting using an antiphospho-p44/42 MAPK antibody (dilution 1:5000 in TBST, Cell Signaling Technology, USA) as first and HRP-conjugated anti-rabbit IgG (1:10000 in TBST, Sigma-Aldrich, USA) as second antibody. Luminescence was detected using supersignal west femto chemiluminescent reagent (Thermo Fisher Scientific) and a ChemiDoc MP imaging system (Biorad, USA).

4.2.7. RNA extraction, cDNA synthesis and RT-qPCR

Seedling samples were ground in 2 mL Eppendorf reaction tubes with 4 metal beads using a Retsch MM 400 mixing mill (Retsch, Germany). RNA was extracted using peqGOLD TriFast™ with an additional DNA digestion step using DNase I (Roche, Germany). Further, RNA was precipitated overnight at 4°C in 100% ethanol containing 115 mM Na-Ac (pH 5.2; Sigma Aldrich, Germany) to further clean up and increase RNA yield. RNA quality and quantity was determined using a NanoDrop photometer (Thermo Fisher Scientific). Subsequently cDNA was synthesized from 4000 ng DNAse-treated total RNA using oligo $dT_{(20)}$ primers and Superscript II or IV reverse transcriptase according to manufactures instructions. The 20 µl cDNA yielded were further diluted with RNAse free water to 200 µl. For the qPCR, 4 µl of diluted cDNA was used with the master mix described in table 8. qPCR was performed on a CFX Connect Real-Time PCR Detection System (Biorad, USA) using EvaGreen. The qPCR cycle program is depicted in table 9. The target gene was quantified relative to the expression of *ACTIN2* (*ACT2*) from Arabidopsis or other Brassicaceae. ΔCt values were calculated subtracting the Ct value for the target from that for *ACT2* expression. These ΔCt values, which correspond to $\log_2$ expression values of a gene of interest relative to *ACTIN2*, were further used for statistical analysis.

Table 10: qPCR Master Mix

Compound	Volume
10x PCR buffer	2.5 µl
10 mM dNTPs	0.5 µl
EvaGreen DNA Dye	1.25 µl
2.5 µM primer forward	2 µl
2.5 µM primer reverse	2 µl
Hommade Taq polymerase	0.5 µl

Table 11: qPCR cycling program

PCR step		Time	Temperature
Initial denaturation		3 min	95 °C
Denaturation	x40	15 sec	95 °C
Annealing		30 sec	60 °C
Elongation		30 sec	72 °C
Final elongation		1 min	55 °C
Melting curve		10 sec/step	55 – 95 °C in 0.5 °C steps

4.2.8. Statistical analysis

Statistical analysis of RT-qPCR, bacterial growth assays and seedlings growth inhibition was performed using a mixed linear model function lmer implemented in the lme4

package within the R environment. To meet assumptions of the mixed linear model, we log transformed raw data when needed. The following model was fit to the data: $measurement_{gyr} = GYgy + Rr + egyr$, where GY equals the genotype:treatment interaction, R equals independent replicate and e equals a residual factor. The p-values obtained from the mixed linear model were corrected for multiple testing calculating the false discovery rate using the qvalue (v.2.4.2) package. The obtained q-values were used to assign significant differences to the mean estimate values using the multcompLetters function of the multcompView package (v.0.1-0) with a q-value threshold <0.01 if not otherwise stated.

4.2.9. RNAseq: sequencing, read mapping and read counting

The RNA quality was checked with a capillary electrophoresis method using an Agilent 2100 Bioanalyzer or Caliper LabChip GX device. Library preparation, including polyA enrichment of total RNA samples, was performed by the Max Planck Genome Centre (Cologne, Germany). The libraries were sequenced with single 100 bp (*A. thaliana* Col-0, *C. rubella*, *C. hirsuta*, *E. salsugineum*) or 150 bp reads (A. thaliana accessions except Col-0) using Illumina HiSeq2500 or HiSeq3000 platform, respectively. After quality control, raw sequencing reads were mapped to respective reference genomes (Table 12) using TopHat2 (v2.1.1) with default parameters except from parameters described in (Table 13). The resulting .bam files were used to count the number of reads per gene using HtSeq (v 0.6.0) software with default parameters. To exclude biases caused by mapping sequence reads of different *A. thaliana* accessions to the Col-0 genome, mapping genome files for each *A. thaliana* accession were created by correcting the Col-0 reference genome with SNP data available for these accessions. The variants table for each accession was downloaded from the website of 1001 Genomes Project intersection_snp_short_indel_vcf V3.1 dataset. The pseudo-genome sequence of each accession was inferred by replacing the reference allele with the corresponding alternative allele using the getGenomeSequence function implemented in software AnnotationLiftOver (https://github.com/baoxingsong/AnnotationLiftOver). Further general feature format files (GFF) were created by projecting the coordinates of the TAIR10 gene annotations to the coordinates of each accession with the function gffCoordinateLiftOver of AnnotationLiftOver. The SNP corrected genome files and GFF files were created by Baoxing Song. With these files, a second mapping was performed. As these two mapping methods had only marginal effects on gene expression patterns (Supplemental Figure 8), the further analyses were performed using data mapped to the Col-0 reference genome for *A. thaliana* accessions.

Table 12: Reference genomes used for RNAseq analysis

Species	Reference genome	publication	Source
Arabidopsis thaliana	TAIR 10	Lamesch et al., 2012	Phytozome 10
Ath accessions	TAIR 10	Lamesch et al., 2012	Phytozome 10
Ath accessions	SNP corrected TAIR10		This study
Capsella rubella	v1.0	Slotte et al., 2013	Phytozome 10
Cardamine hirsuta	v1.0	Gan et al., 2016	Miltos Tsiantis
Eutrema salsugineum	v1.0	Yang et al., 2013	Phytozome 10

Table 13: Tophat2 parameters used for mapping RNAseq reads

TopHat2 parameter	Value
--read mismatches	10
-- read-gap-length	10
-- read-edit-dist	20
--min-anchor-length	5
--splice-mismatches	2
--min-intron-length	30
--max-intron-length	1000
--max-insertion-length	20
--max-deletion-length	20
--max-multihits	10
--segment-mismatches	3
--min-coverage-intron	30
--max-coverage-intron	10000
--library-type	fr-firstrand
--b2	very sensitive

4.2.10. Bioinformatics analysis of RNAseq data

The readcounts determined by Htseq were analysed in the R environment (v.3.3.1) using the edgeR (version 3.14.0) and limma (version 3.28.14) packages. Lowly expressed genes were excluded from analysis by filtering out genes with a mean readcount below 10 counts per sample. Then reads were normalized using TMM normalization embedded in the edge R package and the data was $\log_2$ transformed using voom function within the limma package resulting in $\log_2$-counts per million. For individual analysis of Brassicaceae species and *A. thaliana* accession data, a linear model was fit to each gene using the lmFit function of limma with the following terms: $Sgyr = GYgy + Rr + \varepsilon gyr$, where S, $\log_2$ expression value, GY, genotype:treatment interaction, and random factors; R, biological replicate; ε, residual. For the combined analysis of Brassicaceae species and *A. thaliana* accession data the replicate effect was removed from the linear model resulting in the following terms: $Sgy = GYgy + \varepsilon gy$.

For variance shrinkage of calculated p-values, eBayes function of limma was used. The resulting p-values were corrected for multiple testing by calculating the false discovery rate (or

q-value) using the qvalue (v.2.4.2) package. Genes with a q-value < 0.01 and fold change >2 compared to control samples were defined as differentially expressed genes (DEGs).

Normalization and determination of DEGs were performed separately for each Brassicaceae species and each *A. thaliana* accession. To compare expression changes mediated by flg22 between Brassicaceae species, Best Reciprocal Blast was used to determine genes having a 1to1 ortholog to a corresponding *A. thaliana* gene and genes which have a 1to1 ortholog in all Brassicaceae species were kept. This resulted in a set of 17857 1to1 ortholog genes. The analysis of *A. thaliana* accessions was restricted to the same set of 17857 genes to enable a direct comparison of results obtained from Brassicaceae species and *A. thaliana* accessions analysis (E.g. comparing numbers of overlapping genes in Venn Diagrams of Figure 2C and 5F). To directly compare Brassicaceae species with *A. thaliana* accessions, the set of 17857 ortholog genes was used to normalize and determine DEGs for all 1 h samples together.. This approach enables us as well to compare basal expression levels between Brassicaceae species and *A. thaliana* accessions.

The R-packages and software used for further analysis of the sequencing data are listed in Table 14. The expression clusters of DEGs determined for the combined RNAseq analysis of *A. thaliana* accessions together with Brassicaceae species were investigated for enrichment of GO-terms corresponding to biological processes using BinGO plugin within the Cytoscape environment. GO-term enrichment was calculated using a Hypergeometric test followed by a Benjamini and Hochberg False Discovery Rate correction implemented in the BinGO plugin. The whole annotation was used as a background.

Known TF-motifs enriched in individual expression clusters of DEGs determined for the combined RNAseq analysis of *A. thaliana* accessions together with Brassicaceae species were determined using the AME tool within the MEME suite. Therefore 5'-regulory-regions -500 bp upstream of the transcription start site were extracted for each tested Brassicaceae species. Enrichment of TF-motifs was determined in each of the 15 k-mean clusters for all tested Brassicaceae species using 500 bp 5'regulatory-regions of all expressed genes having a clear 1to1 ortholog (16100) as background. Known TF-motifs were retrieved from the Jaspar core plants (2018) database that is implemented in AME.

To compare amino acid sequence conservation with expression variation, all amino acid sequences of expressed genes with 1to1 orthologs in all species were extracted for each Brassicaceae species. The sequences were aligned using Clustal Omega and percent identity matrices were extracted. The amino acid sequence identity output of Clustal Omega was used to calculate the mean amino acid identity across *C. rubella*, *C. hirsuta* and *E. salsugineum*

compared to *A. thaliana* as a proxy of sequence conservation. The mean amino acid sequence identities were subsequently plotted against the SD/mean of flg22-expression changes across all four Brassicaceae species, which served as a proxy for expression variation among the tested Brassicaceae species. Similarly, the mean amino acid sequence identity was also plotted against the SD/mean of the normalized expression value in control samples. In addition, pairwise amino acid sequence identities between *A. thaliana* and each Brassicaceae species were plotted against the absolute difference in flg22-induced expression changes between the compared species. This analysis was performed for all expressed genes or only for DEGs.

Table 14: Software and packages used in this study

Software/Package	Version	Citation	Use
AME	4.12.0	McLeay and Bailey, 2010	TF-motif enrichment
BinGO	3.0.3	Maere et al., 2005	GO enrichment
ClueGO	2.2.5	Bindea et al., 2009	GO enrichment + grouping
Clustal Omega	1.2.4	Sievers et al., 2011	Multiple sequence alignment
Corrplot	0.77	Murdoch and Chow, 1996	Correlation plots
Cytoscape	3.3.0	Shannon et al., 2003	Run ClueGO
EdgeR	3.14.0	Robinson et al., 2009	Analysing DEGs
Genevestigator		Hruz et al., 2008	Comparison to public transcriptome data
Genesis	1.7.7	Sturn et al., 2002	Heatmaps, clustering
Htseq	0.6.0	Anders et al., 2015	Count RNSeq reads
limma	3.28.14	Ritchie et al., 2015	Analysing DEGs
MixOmics	6.0	Rohart et al., 2017	PCA
RStudio	0.99.489		
TopHat	2.1.1	Trapnell et al., 2009	Map RNAseq reads
VennDiagramm	1.6.17	Chen and Boutros, 2011	Venn Diagramms

5. References

Abramovitch, R.B., Janjusevic, R., Stebbins, C.E., and Martin, G.B. (2006). Type III effector AvrPtoB requires intrinsic E3 ubiquitin ligase activity to suppress plant cell death and immunity. Proc. Natl. Acad. Sci. **103**: 2851–2856.

Adie, B.A.T., Perez-Perez, J., Perez-Perez, M.M., Godoy, M., Sanchez-Serrano, J.-J., Schmelz, E.A., and Solano, R. (2007). ABA Is an Essential Signal for Plant Resistance to Pathogens Affecting JA Biosynthesis and the Activation of Defenses in Arabidopsis. Plant Cell **19**: 1665–1681.

Agler, M.T., Ruhe, J., Kroll, S., Morhenn, C., Kim, S.T., Weigel, D., and Kemen, E.M. (2016). Microbial Hub Taxa Link Host and Abiotic Factors to Plant Microbiome Variation. PLoS Biol. **14**: e1002352.

Albert, I. et al. (2015). An RLP23-SOBIR1-BAK1 complex mediates NLP-triggered immunity. Nat. Plants **1**: 15140.

Alvarez, M., Schrey, A.W., and Richards, C.L. (2015). Ten years of transcriptomics in wild populations: what have we learned about their ecology and evolution? Mol. Ecol. **24**: 710–725.

Amrine, K.C.H., Blanco-Ulate, B., Riaz, S., Pap, D., Jones, L., Figueroa-Balderas, R., Walker, M.A., and Cantu, D. (2015). Comparative transcriptomics of Central Asian Vitis vinifera accessions reveals distinct defense strategies against powdery mildew. Hortic. Res. **2**: 15037.

Anders, S., Pyl, P.T., and Huber, W. (2015). HTSeq-A Python framework to work with high-throughput sequencing data. Bioinformatics **31**: 166–169.

Anver, S. and Tsuda, K. (2015). Ethylene and Plant Immunity. In Ethylene in Plants (Springer Netherlands: Dordrecht), pp. 205–221.

Asai, T., Tena, G., Plotnikova, J., Willmann, M.R., Chiu, W.-L., Gomez-Gomez, L., Boller, T., Ausubel, F.M., and Sheen, J. (2002). MAP kinase signalling cascade in Arabidopsis innate immunity. Nature **415**: 977–983.

Ashfield, T. et al. (2012). Evolution of a Complex Disease Resistance Gene Cluster in Diploid Phaseolus and Tetraploid Glycine. PLANT Physiol. **159**: 336–354.

Asselbergh, B., Vleesschauwer, D. De, and Höfte, M.M. (2008). Global Switches and Fine-Tuning-ABA modulates Plant Pathogen Defense. Mol. Plant. Microbe. Interact. **21**: 709–719.

Bar, M., Sharfman, M., Ron, M., and Avni, A. (2010). BAK1 is required for the attenuation of ethylene-inducing xylanase (Eix)-induced defense responses by the decoy receptor LeEix1. Plant J. **63**: 791–800.

Baxter, L., Jironkin, A., Hickman, R., Moore, J., Barrington, C., Krusche, P., Dyer, N.P., Buchanan-Wollaston, V., Tiskin, A., Beynon, J., Denby, K., and Ott, S. (2012). Conserved Noncoding Sequences Highlight Shared Components of Regulatory Networks in Dicotyledonous Plants. Plant Cell **24**: 3949–3965.

Beckers, G.J.M., Jaskiewicz, M., Liu, Y., Underwood, W.R., He, S.Y., Zhang, S., and Conrath, U. (2009). Mitogen-Activated Protein Kinases 3 and 6 Are Required for Full Priming of Stress Responses in Arabidopsis thaliana. Plant Cell **21**: 944–953.

Bednarek, P., Piślewska-Bednarek, M., Ver Loren van Themaat, E., Maddula, R.K., Svatoš, A., and Schulze-Lefert, P. (2011). Conservation and clade-specific diversification of pathogen-inducible tryptophan and indole glucosinolate metabolism in Arabidopsis thaliana relatives. New Phytol. **192**: 713–26.

Bednarek, P., Piślewska-Bednarek, M., Svatoš, A., Schneider, B., Doubský, J., Mansurova, M., Humphry, M., Consonni, C., Panstruga, R., Sanchez-Vallet, A., Molina, A., and Schulze-Lefert, P. (2009). A glucosinolate metabolism pathway in living plant cells mediates broad-spectrum antifungal defense. Science **323**: 101–106.

Belkhadir, Y., Jaillais, Y., Epple, P., Balsemao-Pires, E., Dangl, J.L., and Chory, J. (2012). Brassinosteroids modulate the efficiency of plant immune responses to microbe-associated molecular patterns. Proc. Natl. Acad. Sci. **109**: 297–302.

Belkhadir, Y., Yang, L., Hetzel, J., Dangl, J.L., and Chory, J. (2014). The growth-defense pivot: Crisis management in plants mediated by LRR-RK surface receptors. Trends Biochem. Sci. **39**:

447–456.

Berens, M.L., Berry, H.M., Mine, A., Argueso, C.T., and Tsuda, K. (2017). Evolution of Hormone Signaling Networks in Plant Defense. Annu. Rev. Phytopathol **55**: 401–25.

Bigeard, J., Colcombet, J., and Hirt, H. (2015). Signaling mechanisms in pattern-triggered immunity (PTI). Mol. Plant **8**: 521–39.

Bindea, G., Mlecnik, B., Hackl, H., Charoentong, P., Tosolini, M., Kirilovsky, A., Fridman, W.H., Pagès, F., Trajanoski, Z., and Galon, J. (2009). ClueGO: A Cytoscape plug-in to decipher functionally grouped gene ontology and pathway annotation networks. Bioinformatics **25**: 1091–1093.

Birkenbihl, R.P., Kracher, B., and Somssich, I.E. (2017). Induced Genome-Wide Binding of Three Arabidopsis WRKY Transcription Factors during Early MAMP-Triggered Immunity. Plant Cell **29**: 20–38.

Blume, B., Nürnberger, T., Nass, N., and Scheel, D. (2000). Receptor-Mediated Increase in Cytoplasmic Free Calcium Required for Activation of Pathogen Defense in Parsley. Plant Cell **12**: 1425–1440.

Böhm, H., Albert, I., Oome, S., Raaymakers, T.M., Van den Ackerveken, G., and Nürnberger, T. (2014). A Conserved Peptide Pattern from a Widespread Microbial Virulence Factor Triggers Pattern-Induced Immunity in Arabidopsis. PLoS Pathog. **10**: e1004491.

Boller, T. and Felix, G. (2009). A Renaissance of Elicitors: Perception of Microbe-Associated Molecular Patterns and Danger Signals by Pattern-Recognition Receptors. Annu. Rev. Plant Biol. **60**: 379–406.

Boudsocq, M., Willmann, M.R., McCormack, M., Lee, H., Shan, L., He, P., Bush, J., Cheng, S.-H., and Sheen, J. (2010). Differential innate immune signalling via Ca2+ sensor protein kinases. Nature **464**: 418–422.

Brautigam, A. et al. (2011). An mRNA Blueprint for C4 Photosynthesis Derived from Comparative Transcriptomics of Closely Related C3 and C4 Species. PLANT Physiol. **155**: 142–156.

Brawand, D. et al. (2011). The evolution of gene expression levels in mammalian organs. Nature **478**: 343–348.

Breschi, A., Gingeras, T.R., and Guigó, R. (2017). Comparative transcriptomics in human and mouse. Nat. Rev. Genet. **18**: 425–440.

Briggs, A.G., Adams-Phillips, L.C., Keppler, B.D., Zebell, S.G., Arend, K.C., Apfelbaum, A.A., Smith, J.A., and Bent, A.F. (2017). A transcriptomics approach uncovers novel roles for poly(ADP-ribosyl)ation in the basal defense response in Arabidopsis thaliana. PLoS One **12**: e0190268.

Broadley, M.R., White, P.J., Hammond, J.P., Graham, N.S., Bowen, H.C., Emmerson, Z.F., Fray, R.G., Iannetta, P.P.M., McNicol, J.W., and May, S.T. (2008). Evidence of neutral transcriptome evolution in plants. New Phytol. **180**: 587–593.

Brooks, D.M., Bender, C.L., and Kunkel, B.N. (2005). The Pseudomonas syringae phytotoxin coronatine promotes virulence by overcoming salicylic acid-dependent defences in Arabidopsis thaliana. Mol. Plant Pathol. **6**: 629–39.

Buckley, B.A. (2007). Comparative environmental genomics in non-model species: using heterologous hybridization to DNA-based microarrays. J. Exp. Biol. **210**: 1602–1606.

Bulgarelli, D., Schlaeppi, K., Spaepen, S., van Themaat, E.V.L., and Schulze-Lefert, P. (2013). Structure and Functions of the Bacterial Microbiota of Plants. Annu. Rev. Plant Biol. **64**: 807–838.

Cai, R. et al. (2011). The plant pathogen pseudomonas syringae pv. tomato is genetically monomorphic and under strong selection to evade tomato immunity. PLoS Pathog. **7**: e1002130.

Campos, M.L., Kang, J.H., and Howe, G.A. (2014). Jasmonate-Triggered Plant Immunity. J. Chem. Ecol. **40**: 657–675.

Canfora, L., Bacci, G., Pinzari, F., Lo Papa, G., Dazzi, C., and Benedetti, A. (2014). Salinity and Bacterial Diversity: To What Extent Does the Concentration of Salt Affect the Bacterial Community in a Saline Soil? PLoS One **9**: e106662.

Cao, Y., Aceti, D.J., Sabat, G., Song, J., Makino, S. ichi, Fox, B.G., and Bent, A.F. (2013). Mutations in FLS2 Ser-938 Dissect Signaling Activation in FLS2-Mediated Arabidopsis Immunity. PLoS Pathog. **9**: e1003313.

Cao, Y., Liang, Y., Tanaka, K., Nguyen, C.T., Jedrzejczak, R.P., Joachimiak, A., and Stacey, G. (2014). The kinase LYK5 is a major chitin receptor in Arabidopsis and forms a chitin-induced

complex with related kinase CERK1. Elife **3**: e03766.

Carvallo, M.A., Pino, M.-T., Jeknic, Z., Zou, C., Doherty, C.J., Shiu, S.-H., Chen, T.H.H., and Thomashow, M.F. (2011). A comparison of the low temperature transcriptomes and CBF regulons of three plant species that differ in freezing tolerance: Solanum commersonii, Solanum tuberosum, and Arabidopsis thaliana. J. Exp. Bot. **62**: 3807–19.

Chen, H. et al. (2017). A Bacterial Type III Effector Targets the Master Regulator of Salicylic Acid Signaling, NPR1, to Subvert Plant Immunity. Cell Host Microbe **22**: 1–12.

Chen, H. and Boutros, P.C. (2011). VennDiagram: A package for the generation of highly-customizable Venn and Euler diagrams in R. BMC Bioinformatics **12**: 35.

Cheng, W., Munkvold, K.R., Gao, H., Mathieu, J., Schwizer, S., Wang, S., Yan, Y. Bin, Wang, J., Martin, G.B., and Chai, J. (2011). Structural analysis of pseudomonas syringae AvrPtoB bound to host BAK1 reveals two similar kinase-interacting domains in a type III effector. Cell Host Microbe **10**: 616–626.

Chinchilla, D. (2006). The Arabidopsis Receptor Kinase FLS2 Binds flg22 and Determines the Specificity of Flagellin Perception. PLANT CELL ONLINE **18**: 465–476.

Chinchilla, D., Shan, L., He, P., de Vries, S., and Kemmerling, B. (2009). One for all: the receptor-associated kinase BAK1. Trends Plant Sci. **14**: 535–541.

Chinchilla, D., Zipfel, C., Robatzek, S., Kemmerling, B., Nürnberger, T., Jones, J.D.G., Felix, G., and Boller, T. (2007). A flagellin-induced complex of the receptor FLS2 and BAK1 initiates plant defence. Nature **448**: 497–500.

Clarke, C.R., Chinchilla, D., Hind, S.R., Taguchi, F., Miki, R., Ichinose, Y., Martin, G.B., Leman, S., Felix, G., and Vinatzer, B.A. (2013). Allelic variation in two distinct *Pseudomonas syringae* flagellin epitopes modulates the strength of plant immune responses but not bacterial motility. New Phytol. **200**: 847–860.

Clauw, P., Coppens, F., De Beuf, K., Dhondt, S., Van Daele, T., Maleux, K., Storme, V., Clement, L., Gonzalez, N., and Inzé, D. (2015). Leaf Responses to Mild Drought Stress in Natural Variants of Arabidopsis. Plant Physiol. **167**: 800–816.

Clay, N.K., Adio, A.M., Denoux, C., Jander, G., and Ausubel, F.M. (2009). Glucosinolate metabolites required for an Arabidopsis innate immune response. Science **323**: 95–101.

Couto, D. et al. (2016). The Arabidopsis Protein Phosphatase PP2C38 Negatively Regulates the Central Immune Kinase BIK1. PLoS Pathog. **12**: e1005811.

Couto, D. and Zipfel, C. (2016). Regulation of pattern recognition receptor signalling in plants. Nat. Rev. Immunol. **16**: 537–552.

Cui, H., Tsuda, K., and Parker, J.E. (2015). Effector-Triggered Immunity: From Pathogen Perception to Robust Defense. Annu. Rev. Plant Biol. **66**: 487–511.

Czaban, A., Sharma, S., Byrne, S.L., Spannagl, M., Mayer, K.F.X., and Asp, T. (2015). Comparative transcriptome analysis within the Lolium/Festuca species complex reveals high sequence conservation. BMC Genomics **16**: 249.

Dassanayake, M., Oh, D.-H., Haas, J.S., Hernandez, A., Hong, H., Ali, S., Yun, D.-J., Bressan, R. a, Zhu, J.-K., Bohnert, H.J., and Cheeseman, J.M. (2011). The genome of the extremophile crucifer Thellungiella parvula. Nat. Genet. **43**: 913–8.

Davidson, R.M., Gowda, M., Moghe, G., Lin, H., Vaillancourt, B., Shiu, S.-H., Jiang, N., and Robin Buell, C. (2012). Comparative transcriptomics of three Poaceae species reveals patterns of gene expression evolution. Plant J. **71**: 492–502.

Davidsson, P., Broberg, M., Kariola, T., Sipari, N., Pirhonen, M., and Palva, E.T. (2017). Short oligogalacturonides induce pathogen resistance-associated gene expression in Arabidopsis thaliana. BMC Plant Biol. **17**: 1–19.

Davies, N.J., Krusche, P., Tauber, E., and Ott, S. (2015). Analysis of 5' gene regions reveals extraordinary conservation of novel non-coding sequences in a wide range of animals. BMC Evol. Biol. **15**: 227.

DeBiasse, M.B. and Kelly, M.W. (2016). Plastic and Evolved Responses to Global Change: What Can We Learn from Comparative Transcriptomics?: Table 1. J. Hered. **107**: 71–81.

Delport, W., Scheffler, K., and Seoighe, C. (2009). Models of coding sequence evolution. Brief. Bioinform. **10**: 97–109.

Denoux, C., Galletti, R., Mammarella, N., Gopalan, S., Werck, D., De Lorenzo, G., Ferrari, S., Ausubel, F.M., and Dewdney, J. (2008). Activation of defense response pathways by OGs and

Flg22 elicitors in Arabidopsis seedlings. Mol. Plant **1**: 423–445.

Ding, Y., Dommel, M., and Mou, Z. (2016). Abscisic acid promotes proteasome-mediated degradation of the transcription coactivator NPR1 in Arabidopsis thaliana. Plant J. **86**: 20–34.

Van der Does, D., Leon-Reyes, A., Koornneef, A., Van Verk, M.C., Rodenburg, N., Pauwels, L., Goossens, A., Körbes, A.P., Memelink, J., Ritsema, T., Van Wees, S.C.M., and Pieterse, C.M.J. (2013). Salicylic acid suppresses jasmonic acid signaling downstream of SCFCOI1-JAZ by targeting GCC promoter motifs via transcription factor ORA59. Plant Cell **25**: 744–61.

Dong, S. et al. (2014). Effector Specialization in a Lineage of the Irish Potato Famine Pathogen. Science **343**: 552–555.

Dori-Bachash, M., Shema, E., and Tirosh, I. (2011). Coupled evolution of transcription and mRNA degradation. PLoS Biol. **9**: e1001106.

Dunning, F.M., Sun, W., Jansen, K.L., Helft, L., and Bent, A.F. (2007). Identification and Mutational Analysis of Arabidopsis FLS2 Leucine-Rich Repeat Domain Residues That Contribute to Flagellin Perception. Plant Cell **19**: 3297–3313.

Edger, P.P. et al. (2015). The butterfly plant arms-race escalated by gene and genome duplications. Proc. Natl. Acad. Sci. **112**: 8362–8366.

Emms, D.M. and Kelly, S. (2015). OrthoFinder: solving fundamental biases in whole genome comparisons dramatically improves orthogroup inference accuracy. Genome Biol. **16**: 157.

Enard, W. et al. (2002). Intra- and interspecific variation in primate gene expression patterns. Science **296**: 340–343.

Evans, T.G. (2015). Considerations for the use of transcriptomics in identifying the "genes that matter" for environmental adaptation. J. Exp. Biol. **218**: 1925–1935.

Fan, J., Hill, L., Crooks, C., Doerner, P., and Lamb, C. (2009). Abscisic Acid Has a Key Role in Modulating Diverse Plant-Pathogen Interactions. PLANT Physiol. **150**: 1750–1761.

Feder, M.E. and Walser, J.-C. (2005). The biological limitations of transcriptomics in elucidating stress and stress responses. J. Evol. Biol. **18**: 901–910.

Felix, G., Duran, J.D., Volko, S., and Boller, T. (1999). Plants have a sensitive perception system for the most conserved domain of bacterial flagellin. Plant J. **18**: 265–276.

Field, Y., Fondufe-Mittendorf, Y., Moore, I.K., Mieczkowski, P., Kaplan, N., Lubling, Y., Lieb, J.D., Widom, J., and Segal, E. (2009). Gene expression divergence in yeast is coupled to evolution of DNA-encoded nucleosome organization. Nat. Genet. **41**: 438–445.

Finkelstein, R. (2013). Abscisic Acid synthesis and response. Arabidopsis Book **11**: e0166.

Franzke, A., Koch, M.A., and Mummenhoff, K. (2016). Turnip Time Travels: Age Estimates in Brassicaceae. Trends Plant Sci. **21**: 554–561.

Frei dit Frey, N. et al. (2014). Functional analysis of Arabidopsis immune-related MAPKs uncovers a role for MPK3 as negative regulator of inducible defences. Genome Biol. **15**: R87.

Frerigmann, H., Piślewska-Bednarek, M., Sánchez-Vallet, A., Molina, A., Glawischnig, E., Gigolashvili, T., and Bednarek, P. (2016). Regulation of Pathogen-Triggered Tryptophan Metabolism in Arabidopsis thaliana by MYB Transcription Factors and Indole Glucosinolate Conversion Products. Mol. Plant **9**: 682–695.

Gan, X. et al. (2016). The Cardamine hirsuta genome offers insight into the evolution of morphological diversity. Nat. Plants **2**: 16167.

Gangappa, S.N., Berriri, S., and Kumar, S.V. (2017). PIF4 Coordinates Thermosensory Growth and Immunity in Arabidopsis. Curr. Biol. **27**: 243–249.

Giaever, G. et al. (2014). The yeast deletion collection: a decade of functional genomics. Genetics **197**: 451–65.

Gigolashvili, T., Berger, B., Mock, H.P., Müller, C., Weisshaar, B., and Flügge, U.I. (2007). The transcription factor HIG1/MYB51 regulates indolic glucosinolate biosynthesis in Arabidopsis thaliana. Plant J. **50**: 886–901.

Gilad, Y. and Mizrahi-Man, O. (2015). A reanalysis of mouse ENCODE comparative gene expression data. F1000Research **4**.

Gilad, Y., Oshlack, A., and Rifkin, S.A. (2006). Natural selection on gene expression. Trends Genet. **22**: 456–461.

Gimenez-Ibanez, S., Hann, D.R., Ntoukakis, V., Petutschnig, E., Lipka, V., and Rathjen, J.P. (2009a). AvrPtoB Targets the LysM Receptor Kinase CERK1 to Promote Bacterial Virulence on Plants. Curr. Biol. **19**: 423–429.

Gimenez-Ibanez, S., Ntoukakis, V., and Rathjen, J.P. (2009b). The LysM receptor kinase CERK1 mediates bacterial perception in Arabidopsis. Plant Signal. Behav. **4**: 539–541.

Glauser, G., Grata, E., Dubugnon, L., Rudaz, S., Farmer, E.E., and Wolfender, J.L. (2008). Spatial and temporal dynamics of jasmonate synthesis and accumulation in Arabidopsis in response to wounding. J. Biol. Chem. **283**: 16400–16407.

Glazebrook, J. (2005). Contrasting Mechanisms of Defense Against Biotrophic and Necrotrophic Pathogens. Annu. Rev. Phytopathol. **43**: 205–227.

Gleason, L.U. and Burton, R.S. (2015). RNA-seq reveals regional differences in transcriptome response to heat stress in the marine snail *Chlorostoma funebralis*. Mol. Ecol. **24**: 610–627.

Göhre, V., Spallek, T., Häweker, H., Mersmann, S., Mentzel, T., Boller, T., de Torres, M., Mansfield, J.W., and Robatzek, S. (2008). Plant Pattern-Recognition Receptor FLS2 Is Directed for Degradation by the Bacterial Ubiquitin Ligase AvrPtoB. Curr. Biol. **18**: 1824–1832.

Gómez-Gómez, L. and Boller, T. (2000). FLS2: An LRR Receptor-like Kinase Involved in the Perception of the Bacterial Elicitor Flagellin in Arabidopsis. Mol. Cell **5**: 1003–1011.

Gómez-Gómez, L., Felix, G., and Boller, T. (1999). A single locus determines sensitivity to bacterial flagellin in Arabidopsis thaliana. Plant J. **18**: 277–284.

Gong, Q., Li, P., Ma, S., Indu Rupassara, S., and Bohnert, H.J. (2005). Salinity stress adaptation competence in the extremophile Thellungiella halophila in comparison with its relative Arabidopsis thaliana. Plant J. **44**: 826–39.

Gonzalez-Guzman, M., Apostolova, N., Belles, J.M., Barrero, J.M., Piqueras, P., Ponce, M.R., Micol, J.L., Serrano, R., and Rodriguez, P.L. (2002). The Short-Chain Alcohol Dehydrogenase ABA2 Catalyzes the Conversion of Xanthoxin to Abscisic Aldehyde. Plant Cell **14**: 1833–1846.

Gust, A.A., Biswas, R., Lenz, H.D., Rauhut, T., Ranf, S., Kemmerling, B., Götz, F., Glawischnig, E., Lee, J., Felix, G., and Nürnberger, T. (2007). Bacteria-derived peptidoglycans constitute pathogen-associated molecular patterns triggering innate immunity in Arabidopsis. J. Biol. Chem. **282**: 32338–32348.

Gust, A.A., Pruitt, R., and Nürnberger, T. (2017). Sensing Danger: Key to Activating Plant Immunity. Trends Plant Sci. **22**: 779–791.

Gutierrez, J.R., Balmuth, A.L., Ntoukakis, V., Mucyn, T.S., Gimenez-Ibanez, S., Jones, A.M.E., and Rathjen, J.P. (2010). Prf immune complexes of tomato are oligomeric and contain multiple Pto-like kinases that diversify effector recognition. Plant J. **61**: 507–518.

Hacquard, S., Spaepen, S., Garrido-Oter, R., and Schulze-Lefert, P. (2017). Interplay Between Innate Immunity and the Plant Microbiota. Annu. Rev. Phytopathol. **55**: 565–589.

Hammond, J.P., Bowen, H.C., White, P.J., Mills, V., Pyke, K.A., Baker, A.J.M., Whiting, S.N., May, S.T., and Broadley, M.R. (2006). A comparison of the Thlaspi caerulescens and Thlaspi arvense shoot transcriptomes. New Phytol. **170**: 239–260.

Harrison, P.W., Wright, A.E., and Mank, J.E. (2012). The evolution of gene expression and the transcriptome–phenotype relationship. Semin. Cell Dev. Biol. **23**: 222–229.

Hay, A.S. et al. (2014). Cardamine hirsuta: a versatile genetic system for comparative studies. Plant J. **78**: 1–15.

Haygood, R., Babbitt, C.C., Fedrigo, O., and Wray, G.A. (2010). Contrasts between adaptive coding and noncoding changes during human evolution. Proc. Natl. Acad. Sci. **107**: 7853–7857.

Heese, A., Hann, D.R., Gimenez-Ibanez, S., Jones, A.M.E., He, K., Li, J., Schroeder, J.I., Peck, S.C., and Rathjen, J.P. (2007). The receptor-like kinase SERK3/BAK1 is a central regulator of innate immunity in plants. Proc. Natl. Acad. Sci. **104**: 12217–22.

Herrero, E. et al. (2012). EARLY FLOWERING4 recruitment of EARLY FLOWERING3 in the nucleus sustains the Arabidopsis circadian clock. Plant Cell **24**: 428–43.

Hillmer, R.A., Tsuda, K., Rallapalli, G., Asai, S., Truman, W., Papke, M.D., Sakakibara, H., Jones, J.D.G., Myers, C.L., and Katagiri, F. (2017). The highly buffered Arabidopsis immune signaling network conceals the functions of its components. PLoS Genet. **13**: e1006639.

Hind, S.R. et al. (2016). Tomato receptor FLAGELLIN-SENSING 3 binds flgII-28 and activates the plant immune system. Nat. Plants **2**: 1–8.

Hodgins-Davis, A., Rice, D.P., Townsend, J.P., and Novembre, J. (2015). Gene expression evolves under a house-of-cards model of stabilizing selection. Mol. Biol. Evol. **32**: 2130–2140.

Hohmann, N., Wolf, E.M., Lysak, M.A., and Koch, M.A. (2015). A Time-Calibrated Road Map of Brassicaceae Species Radiation and Evolutionary History. Plant Cell **27**: 2770–84.

Holton, N., Nekrasov, V., Ronald, P.C., and Zipfel, C. (2015). The phylogenetically-related pattern recognition receptors EFR and XA21 recruit similar immune signaling components in monocots and dicots. PLoS Pathog. **11**: e1004602.

Hruz, T., Laule, O., Szabo, G., Wessendorp, F., Bleuler, S., Oertle, L., Widmayer, P., Gruissem, W., and Zimmermann, P. (2008). Genevestigator V3: A Reference Expression Database for the Meta-Analysis of Transcriptomes. Adv. Bioinformatics **2008**: 1–5.

Huang, C. et al. (2016). Resolution of Brassicaceae Phylogeny Using Nuclear Genes Uncovers Nested Radiations and Supports Convergent Morphological Evolution. Mol. Biol. Evol. **33**: 394–412.

Huffaker, A., Pearce, G., and Ryan, C.A. (2006). An endogenous peptide signal in Arabidopsis activates components of the innate immune response. Proc. Natl. Acad. Sci. **103**: 10098–10103.

Huffaker, A. and Ryan, C.A. (2007). Endogenous peptide defense signals in Arabidopsis differentially amplify signaling for the innate immune response. Proc. Natl. Acad. Sci. **104**: 10732–10736.

Hunt, B.G., Ometto, L., Keller, L., and Goodisman, M.A.D. (2013). Evolution at Two Levels in Fire Ants: The Relationship between Patterns of Gene Expression and Protein Sequence Evolution. Mol. Biol. Evol. **30**: 263–271.

Huot, B., Yao, J., Montgomery, B.L., and He, S.Y. (2014). Growth-Defense Tradeoffs in Plants: A Balancing Act to Optimize Fitness. Mol. Plant **7**: 1267–1287.

Inan, G. et al. (2004). Salt cress. A halophyte and cryophyte Arabidopsis relative model system and its applicability to molecular genetic analyses of growth and development of extremophiles. Plant Physiol. **135**: 1718–37.

Jacob, F., Kracher, B., Mine, A., Seyfferth, C., Blanvillain-Baufumé, S., Parker, J.E., Tsuda, K., Schulze-Lefert, P., and Maekawa, T. (2017). A dominant-interfering camta3 mutation compromises primary transcriptional outputs mediated by both cell surface and intracellular immune receptors in Arabidopsis thaliana. New Phytol.

Jacob, F., Vernaldi, S., and Maekawa, T. (2013). Evolution and Conservation of Plant NLR Functions. Front. Immunol. **4**: 297.

Jeworutzki, E., Roelfsema, M.R.G., Anschütz, U., Krol, E., Elzenga, J.T.M., Felix, G., Boller, T., Hedrich, R., and Becker, D. (2010). Early signaling through the arabidopsis pattern recognition receptors FLS2 and EFR involves Ca2+-associated opening of plasma membrane anion channels. Plant J. **62**: 367–378.

Jones, J.D.G. and Dangl, J.L. (2006). The plant immune system. Nature **444**: 323–9.

Kadota, Y., Sklenar, J., Derbyshire, P., Stransfeld, L., Asai, S., Ntoukakis, V., Jones, J.D., Shirasu, K., Menke, F., Jones, A., and Zipfel, C. (2014). Direct Regulation of the NADPH Oxidase RBOHD by the PRR-Associated Kinase BIK1 during Plant Immunity. Mol. Cell **54**: 43–55.

Kaku, H., Nishizawa, Y., Ishii-Minami, N., Akimoto-Tomiyama, C., Dohmae, N., Takio, K., Minami, E., and Shibuya, N. (2006). Plant cells recognize chitin fragments for defense signaling through a plasma membrane receptor. Proc. Natl. Acad. Sci. **103**: 11086–11091.

Katagiri, F. and Tsuda, K. (2010). Understanding the plant immune system. Mol. Plant. Microbe. Interact. **23**: 1531–6.

Katsir, L., Schilmiller, A.L., Staswick, P.E., He, S.Y., and Howe, G.A. (2008). COI1 is a critical component of a receptor for jasmonate and the bacterial virulence factor coronatine. Proc. Natl. Acad. Sci. U. S. A. **105**: 7100–5.

Kawakatsu, T. et al. (2016). Epigenomic Diversity in a Global Collection of Arabidopsis thaliana Accessions. Cell **166**: 492–505.

Kei Hiruma, A., Gerlach, N., Sacristá, S., Bucher, M., O, R.J., and Schulze-Lefert Correspondence, P. (2016). Root Endophyte Colletotrichum tofieldiae Confers Plant Fitness Benefits that Are Phosphate Status Dependent. Cell **165**: 464–474.

Khaitovich, P., Pääbo, S., and Weiss, G. (2005). Toward a neutral evolutionary model of gene expression. Genetics **170**: 929–939.

Khaitovich, P., Weiss, G., Lachmann, M., Hellmann, I., Enard, W., Muetzel, B., Wirkner, U., Ansorge, W., and Pääbo, S. (2004). A neutral model of transcriptome evolution. PLoS Biol. **2**: e132.

Khaled, S. Ben, Postma, J., and Robatzek, S. (2015). A Moving View: Subcellular Trafficking Processes in Pattern Recognition Receptor– Triggered Plant Immunity. Annu. Rev. Phytopathol **53**: 379–402.

Kim, T.-W. and Wang, Z.-Y. (2010). Brassinosteroid Signal Transduction from Receptor Kinases to

Transcription Factors. Annu. Rev. Plant Biol. **61**: 681–704.

Kimura, M. (1983). The Neutral Theory of Molecular Evolution (Cambridge University Press).

Koch, M.A. and German, D.A. (2013). Taxonomy and systematics are key to biological information: Arabidopsis, Eutrema (Thellungiella), Noccaea and Schrenkiella (Brassicaceae) as examples. Front. Plant Sci. **4**: 267.

Koenig, D. et al. (2013). Comparative transcriptomics reveals patterns of selection in domesticated and wild tomato. Proc. Natl. Acad. Sci. **110**: E2655-62.

Koenig, D. and Weigel, D. (2015). Beyond the thale: comparative genomics and genetics of Arabidopsis relatives. Nat. Rev. Genet. **16**: 285–298.

Kohler, A., Schwindling, S., and Conrath, U. (2002). Benzothiadiazole-induced priming for potentiated responses to pathogen infection, wounding, and infiltration of water into leaves requires the NPR1/NIM1 gene in Arabidopsis. Plant Physiol. **128**: 1046–1056.

Kojima, M. and Sakakibara, H. (2012). Highly sensitive high-throughput profiling of six phytohormones using MS-probe modification and liquid chromatography-tandem mass spectrometry. Methods Mol. Biol. **918**: 151–164.

Kong, Q., Sun, T., Qu, N., Ma, J., Li, M., Cheng, Y., Zhang, Q., Wu, D., Zhang, Z., and Zhang, Y. (2016). Two redundant receptor-like cytoplasmic kinases function downstream of pattern recognition receptors to regulate activation of SA biosynthesis in Arabidopsis. Plant Physiol. **171**: 1344–1354.

Koo, A.J.K., Gao, X., Daniel Jones, A., and Howe, G.A. (2009). A rapid wound signal activates the systemic synthesis of bioactive jasmonates in Arabidopsis. Plant J. **59**: 974–986.

Koornneef, M., Léon-Kloosterziel, K.M., Schwartz, S.H., and Zeevaart, J.A.D. (1998). The genetic and molecular dissection of abscisic acid biosynthesis and signal transduction in Arabidopsis. Plant Physiol. Biochem. **36**: 83–89.

Koornneef, M. and Meinke, D. (2010). The development of Arabidopsis as a model plant. Plant J. **61**: 909–921.

Korkuc, P., Schippers, J.H.M., and Walther, D. (2014). Characterization and Identification of cis-Regulatory Elements in Arabidopsis Based on Single-Nucleotide Polymorphism Information. PLANT Physiol. **164**: 181–200.

Kunze, G., Zipfel, C., Robatzek, S., Niehaus, K., Boller, T., and Felix, G. (2004). The N Terminus of Bacterial Elongation Factor Tu Elicits Innate Immunity in Arabidopsis Plants. Plant Cell **16**: 3496–3507.

Lacombe, S., Rougon-Cardoso, A., Sherwood, E., Peeters, N., Dahlbeck, D., van Esse, H.P., Smoker, M., Rallapalli, G., Thomma, B.P.H.J., Staskawicz, B., Jones, J.D.G., and Zipfel, C. (2010). Interfamily transfer of a plant pattern-recognition receptor confers broad-spectrum bacterial resistance. Nat. Biotechnol. **28**: 365–369.

Lai, Z., Schluttenhofer, C.M., Bhide, K., Shreve, J., Thimmapuram, J., Lee, S.Y., Yun, D.J., and Mengiste, T. (2014). MED18 interaction with distinct transcription factors regulates multiple plant functions. Nat. Commun. **5**: 3064.

Lamesch, P. et al. (2012). The Arabidopsis Information Resource (TAIR): Improved gene annotation and new tools. Nucleic Acids Res. **40**: D1202–D1210.

Le Roux, C. et al. (2015). A Receptor Pair with an Integrated Decoy Converts Pathogen Disabling of Transcription Factors to Immunity. Cell **161**: 1074–1088.

Lee, S., I. Sergeeva, L., and Vreugdenhil, D. (2018). Natural variation of hormone levels in Arabidopsis roots and correlations with complex root architecture. J. Integr. Plant Biol.

Lemos, B., Meiklejohn, C.D., Cáceres, M., and Hartl, D.L. (2005). Rates of divergence in gene expression profiles of primates, mice, and flies: stabilizing selection and variability among functional categories. Evolution (N. Y). **59**: 126–37.

Lenka, S.K., Katiyar, A., Chinnusamy, V., and Bansal, K.C. (2011). Comparative analysis of drought-responsive transcriptome in Indica rice genotypes with contrasting drought tolerance. Plant Biotechnol. J. **9**: 315–327.

Lewis, L.A. et al. (2015). Transcriptional Dynamics Driving MAMP-Triggered Immunity and Pathogen Effector-Mediated Immunosuppression in Arabidopsis Leaves Following Infection with Pseudomonas syringae pv tomato DC3000. Plant Cell **27**: 3038–3064.

Li, B., Meng, X., Shan, L., and He, P. (2016). Transcriptional Regulation of Pattern-Triggered Immunity in Plants. Cell Host Microbe **19**: 641–650.

Li, F. et al. (2014a). Modulation of RNA Polymerase II Phosphorylation Downstream of Pathogen Perception Orchestrates Plant Immunity. Cell Host Microbe **16**: 748–758.

Li, J., Wen, J., Lease, K.A., Doke, J.T., Tax, F.E., and Walker, J.C. (2002). BAK1, an Arabidopsis LRR receptor-like protein kinase, interacts with BRI1 and modulates brassinosteroid signaling. Cell **110**: 213–222.

Li, L., Li, M., Yu, L., Zhou, Z., Liang, X., Liu, Z., Cai, G., Gao, L., Zhang, X., Wang, Y., Chen, S., and Zhou, J.M. (2014b). The FLS2-associated kinase BIK1 directly phosphorylates the NADPH oxidase RbohD to control plant immunity. Cell Host Microbe **15**: 329–338.

Li, L., Stoeckert, C.J., and Roos, D.S. (2003). OrthoMCL: identification of ortholog groups for eukaryotic genomes. Genome Res. **13**: 2178–89.

Liang, X., Ding, P., Lian, K., Wang, J., Ma, M., Li, L., Li, L., Li, M., Zhang, X., Chen, S., Zhang, Y., and Zhou, J.M. (2016). Arabidopsis heterotrimeric G proteins regulate immunity by directly coupling to the FLS2 receptor. Elife **5**: e13568.

Liebrand, T.W.H., van den Burg, H.A., and Joosten, M.H.A.J. (2014). Two for all: receptor-associated kinases SOBIR1 and BAK1. Trends Plant Sci. **19**: 123–32.

Lindlöf, A. et al. (2015). Comparative Transcriptomics of Sijung and Jumli Marshi Rice during Early Chilling Stress Imply Multiple Protective Mechanisms. PLoS One **10**: e0125385.

Liu, L., Sonbol, F.-M., Huot, B., Gu, Y., Withers, J., Mwimba, M., Yao, J., He, S.Y., and Dong, X. (2016). Salicylic acid receptors activate jasmonic acid signalling through a non-canonical pathway to promote effector-triggered immunity. Nat. Commun. **7**: 13099.

Liu, S., Kracher, B., Ziegler, J., Birkenbihl, R.P., and Somssich, I.E. (2015). Negative regulation of ABA Signaling By WRKY33 is critical for Arabidopsis immunity towards Botrytis cinerea 2100. Elife **4**: e07295.

López-maury, L., Marguerat, S., and Bähler, J. (2008). Tuning gene expression to changing to evolutionary adaptation. Nat. Rev. Genet. **9**: 583–593.

Lou, Y., Xu, X.F., Zhu, J., Gu, J.N., Blackmore, S., and Yang, Z.N. (2014). The tapetal AHL family protein TEK determines nexine formation in the pollen wall. Nat. Commun. **5**: 3855.

Lozano-Durán, R. and Zipfel, C. (2015). Trade-off between growth and immunity: role of brassinosteroids. Trends Plant Sci. **20**: 12–9.

Lu, D., Lin, W., Gao, X., Wu, S., Cheng, C., Avila, J., Heese, A., Devarenne, T.P., He, P., and Shan, L. (2011). Direct Ubiquitination of Pattern Recognition Receptor FLS2 Attenuates Plant Innate Immunity. Science **332**: 1439–1442.

Lu, D., Wu, S., Gao, X., Zhang, Y., Shan, L., and He, P. (2010a). A receptor-like cytoplasmic kinase, BIK1, associates with a flagellin receptor complex to initiate plant innate immunity. Proc. Natl. Acad. Sci. **107**: 496–501.

Lu, H., Zou, Y., and Feng, N. (2010b). Overexpression of AHL20 negatively regulates defenses in arabidopsis. J. Integr. Plant Biol. **52**: 801–808.

Lu, X., Tintor, N., Mentzel, T., Kombrink, E., Boller, T., Robatzek, S., Schulze-Lefert, P., and Saijo, Y. (2009). Uncoupling of sustained MAMP receptor signaling from early outputs in an Arabidopsis endoplasmic reticulum glucosidase II allele. Proc. Natl. Acad. Sci. **106**: 22522–22527.

Macho, A.P. and Zipfel, C. (2014). Plant PRRs and the Activation of Innate Immune Signaling. Mol. Cell **54**: 263–272.

MacKay, T.F.C., Stone, E.A., and Ayroles, J.F. (2009). The genetics of quantitative traits: Challenges and prospects. Nat. Rev. Genet. **10**: 565–577.

Maere, S., Heymans, K., and Kuiper, M. (2005). BiNGO: A Cytoscape plugin to assess overrepresentation of Gene Ontology categories in Biological Networks. Bioinformatics **21**: 3448–3449.

Manceau, M., Domingues, V.S., Mallarino, R., and Hoekstra, H.E. (2011). The Developmental Role of Agouti in Color Pattern Evolution. Science **331**: 1062–1065.

Mangelsen, E., Kilian, J., Harter, K., Jansson, C., Wanke, D., and Sundberg, E. (2011). Transcriptome analysis of high-temperature stress in developing barley caryopses: Early stress responses and effects on storage compound biosynthesis. Mol. Plant **4**: 97–115.

Mao, G., Meng, X., Liu, Y., Zheng, Z., Chen, Z., and Zhang, S. (2011). Phosphorylation of a WRKY Transcription Factor by Two Pathogen-Responsive MAPKs Drives Phytoalexin Biosynthesis in Arabidopsis. Plant Cell **23**: 1639–1653.

Martin, F. and Kamoun, S. (2012). Effectors in plant-microbe interactions (Wiley-Blackwell).

Mbengue, M., Bourdais, G., Gervasi, F., Beck, M., Zhou, J., Spallek, T., Bartels, S., Boller, T., Ueda, T., Kuhn, H., and Robatzek, S. (2016). Clathrin-dependent endocytosis is required for immunity mediated by pattern recognition receptor kinases. Proc. Natl. Acad. Sci. **113**: 11034–11039.

McLeay, R.C. and Bailey, T.L. (2010). Motif Enrichment Analysis: A unified framework and an evaluation on ChIP data. BMC Bioinformatics **11**: 165.

Meldau, S., Erb, M., and Baldwin, I.T. (2012). Defence on demand: mechanisms behind optimal defence patterns. Ann. Bot. **110**: 1503–1514.

Mengiste, T. (2012). Plant Immunity to Necrotrophs. Annu. Rev. Phytopathol. **50**: 267–294.

Mine, A., Nobori, T., Salazar-Rondon, M.C., Winkelmüller, T.M., Anver, S., Becker, D., and Tsuda, K. (2017). An incoherent feed-forward loop mediates robustness and tunability in a plant immune network. EMBO Rep. **18**: 464–476.

Miyata, T. and Yasunaga, T. (1980). Molecular evolution of mRNA: A method for estimating evolutionary rates of synonymous and amino acid substitutions from homologous nucleotide sequences and its application. J. Mol. Evol. **16**: 23–36.

Monaghan, J., Matschi, S., Shorinola, O., Rovenich, H., Matei, A., Segonzac, C., Malinovsky, F.G., Rathjen, J.P., MacLean, D., Romeis, T., and Zipfel, C. (2014). The Calcium-Dependent Protein Kinase CPK28 Buffers Plant Immunity and Regulates BIK1 Turnover. Cell Host Microbe **16**: 605–615.

Mondragón-Palomino, M., John-Arputharaj, A., Pallmann, M., and Dresselhaus, T. (2017). Similarities between Reproductive and Immune Pistil Transcriptomes of Arabidopsis Species. Plant Physiol. **174**: 1559–1575.

Mondragón-Palomino, M., Meyers, B.C., Michelmore, R.W., and Gaut, B.S. (2002). Patterns of positive selection in the complete NBS-LRR gene family of Arabidopsis thaliana. Genome Res. **12**: 1305–15.

Morandin, C., Tin, M.M.Y., Abril, S., Gómez, C., Pontieri, L., Schiøtt, M., Sundström, L., Tsuji, K., Pedersen, J.S., Helanterä, H., and Mikheyev, A.S. (2016). Comparative transcriptomics reveals the conserved building blocks involved in parallel evolution of diverse phenotypic traits in ants. Genome Biol. **17**: 43.

Mukhtar, M.S. et al. (2011). Independently evolved virulence effectors converge onto hubs in a plant immune system network. Science **333**: 596–601.

Murdoch, D.J. and Chow, E.D. (1996). A Graphical Display of Large Correlation Matrices. Am. Stat. **50**: 178–180.

Mustroph, A., Lee, S.C., Oosumi, T., Zanetti, M.E., Yang, H., Ma, K., Yaghoubi-Masihi, A., Fukao, T., and Bailey-Serres, J. (2010). Cross-kingdom comparison of transcriptomic adjustments to low-oxygen stress highlights conserved and plant-specific responses. Plant Physiol. **152**: 1484–500.

De Nadal, E., Ammerer, G., and Posas, F. (2011). Controlling gene expression in response to stress. Nat. Rev. Genet. **12**: 833–845.

Nam, K.H. and Li, J. (2002). BRI1/BAK1, a receptor kinase pair mediating brassinosteroid signaling. Cell **110**: 203–212.

Nam, Y.-J. et al. (2017). Natural Variation of Molecular and Morphological Gibberellin Responses. Plant Physiol. **173**: 703–714.

Navarro, L., Zipfel, C., Rowland, O., Keller, I., Robatzek, S., Boller, T., and Jones, J.D.G. (2004). The Transcriptional Innate Immune Response to flg22. Interplay and Overlap with Avr Gene-Dependent Defense Responses and Bacterial Pathogenesis. PLANT Physiol. **135**: 1113–1128.

Necsulea, A. and Kaessmann, H. (2014). Evolutionary dynamics of coding and non-coding transcriptomes. Nat. Rev. Genet. **15**: 734–748.

Nichio, B.T.L., Marchaukoski, J.N., and Raittz, R.T. (2017). New tools in orthology analysis: A brief review of promising perspectives. Front. Genet. **8**: 165.

Nühse, T.S., Bottrill, A.R., Jones, A.M.E., and Peck, S.C. (2007). Quantitative phosphoproteomic analysis of plasma membrane proteins reveals regulatory mechanisms of plant innate immune responses. Plant J. **51**: 931–940.

Oleksiak, M.F., Churchill, G.A., and Crawford, D.L. (2002). Variation in gene expression within and among natural populations. Nat. Genet. **32**: 261–266.

Pandey, S.P. and Somssich, I.E. (2009). The role of WRKY transcription factors in plant immunity.

Plant Physiol. **150**: 1648–1655.

Pedras, M.S.C. and Adio, A.M. (2008). Phytoalexins and phytoanticipins from the wild crucifers Thellungiella halophila and Arabidopsis thaliana: Rapalexin A, wasalexins and camalexin. Phytochemistry **69**: 889–893.

Pedras, M.S.C., Yaya, E.E., and Hossain, S. (2010). Unveiling the phytoalexin biosynthetic puzzle in salt cress: unprecedented incorporation of glucobrassicin into wasalexins A and B. Org. Biomol. Chem. **8**: 5150–5158.

Pedras, M.S.C. and Zheng, Q.-A. (2010). Metabolic responses of Thellungiella halophila/salsuginea to biotic and abiotic stresses: metabolite profiles and quantitative analyses. Phytochemistry **71**: 581–9.

Peele, H.M., Guan, N., Fogelqvist, J., and Dixelius, C. (2014). Loss and retention of resistance genes in five species of the Brassicaceae family. BMC Plant Biol. **14**: 298.

Perry, G.H., Melsted, P., Marioni, J.C., Wang, Y., Bainer, R., Pickrell, J.K., Michelini, K., Zehr, S., Yoder, A.D., Stephens, M., Pritchard, J.K., and Gilad, Y. (2012). Comparative RNA sequencing reveals substantial genetic variation in endangered primates. Genome Res. **22**: 602–610.

Piasecka, A., Jedrzejczak-Rey, N., and Bednarek, P. (2015). Secondary metabolites in plant innate immunity: Conserved function of divergent chemicals. New Phytol. **206**: 948–964.

Pieterse, C.M.J., Van der Does, D., Zamioudis, C., Leon-Reyes, A., and Van Wees, S.C.M. (2012). Hormonal modulation of plant immunity. Annu. Rev. Cell Dev. Biol. **28**: 489–521.

Pieterse, C.M.J., Leon-Reyes, A., Van der Ent, S., and Van Wees, S.C.M. (2009). Networking by small-molecule hormones in plant immunity. Nat. Chem. Biol. **5**: 308–16.

Pruitt, R.N. et al. (2015). The rice immune receptor XA21 recognizes a tyrosine-sulfated protein from a Gram-negative bacterium. Sci. Adv. **1**: e1500245.

Pye, M.F., Hakuno, F., MacDonald, J.D., and Bostock, R.M. (2013). Induced resistance in tomato by SAR activators during predisposing salinity stress. Front. Plant Sci. **4**: 1431–1434.

Qin, F., Shinozaki, K., and Yamaguchi-Shinozaki, K. (2011). Achievements and challenges in understanding plant abiotic stress responses and tolerance. Plant Cell Physiol. **52**: 1569–1582.

Qin, Y., Druzhinina, I.S., Pan, X., and Yuan, Z. (2016). Microbially Mediated Plant Salt Tolerance and Microbiome-based Solutions for Saline Agriculture. Biotechnol. Adv. **34**: 1245–1259.

Rajniak, J., Barco, B., Clay, N.K., and Sattely, E.S. (2015). A new cyanogenic metabolite in Arabidopsis required for inducible pathogen defence. Nature **525**: 376–379.

Ranf, S. (2017). Sensing of molecular patterns through cell surface immune receptors. Curr. Opin. Plant Biol. **38**: 68–77.

Ranf, S., Gisch, N., Schäffer, M., Illig, T., Westphal, L., Knirel, Y.A., Sánchez-Carballo, P.M., Zähringer, U., Hückelhoven, R., Lee, J., and Scheel, D. (2015). A lectin S-domain receptor kinase mediates lipopolysaccharide sensing in Arabidopsis thaliana. Nat. Immunol. **16**: 426–433.

Rebeiz, M., Pool, J.E., Kassner, V.A., Aquadro, C.F., and Carroll, S.B. (2009). Stepwise modification of a modular enhancer underlies adaptation in a Drosophila population. Science **326**: 1663–1667.

Renaut, S., Maillet, N., Normandeau, E., Sauvage, C., Derome, N., Rogers, S.M., and Bernatchez, L. (2012). Genome-wide patterns of divergence during speciation: the lake whitefish case study. Philos. Trans. R. Soc. B Biol. Sci. **367**: 354–363.

Rifkin, S.A., Kim, J., and White, K.P. (2003). Evolution of gene expression in the Drosophila melanogaster subgroup. Nat. Genet. **33**: 138–144.

Ritchie, M.E., Phipson, B., Wu, D., Hu, Y., Law, C.W., Shi, W., and Smyth, G.K. (2015). limma powers differential expression analyses for RNA-sequencing and microarray studies. Nucleic Acids Res. **43**: e47.

Robatzek, S., Bittel, P., Chinchilla, D., Köchner, P., Felix, G., Shiu, S.H., and Boller, T. (2007). Molecular identification and characterization of the tomato flagellin receptor LeFLS2, an orthologue of Arabidopsis FLS2 exhibiting characteristically different perception specificities. Plant Mol. Biol. **64**: 539–547.

Robatzek, S., Chinchilla, D., and Boller, T. (2006). Ligand-induced endocytosis of the pattern recognition receptor FLS2 in Arabidopsis. Genes Dev. **20**: 537–42.

Robert-Seilaniantz, A., Grant, M., and Jones, J.D.G. (2011). Hormone crosstalk in plant disease and defense: more than just jasmonate-salicylate antagonism. Annu. Rev. Phytopathol. **49**: 317–43.

Robinson, M.D., McCarthy, D.J., and Smyth, G.K. (2009). edgeR: A Bioconductor package for differential expression analysis of digital gene expression data. Bioinformatics **26**: 139–140.

Rohart, F., Gautier, B., Singh, A., and Lê Cao, K.-A. (2017). mixOmics: An R package for 'omics feature selection and multiple data integration. PLOS Comput. Biol. **13**: e1005752.

Romero, I.G., Ruvinsky, I., and Gilad, Y. (2012). Comparative studies of gene expression and the evolution of gene regulation. Nat. Rev. Genet. **13**: 505–516.

Ron, M. and Adi, A. (2004). The Receptor for the Fungal Elicitor Ethylene-Inducing Xylanase Is a Member of a Resistance-Like Gene Family in Tomato. Plant Cell **16**: 1604–1615.

Rosli, H.G., Zheng, Y., Pombo, M.A., Zhong, S., Bombarely, A., Fei, Z., Collmer, A., and Martin, G.B. (2013). Transcriptomics-based screen for genes induced by flagellin and repressed by pathogen effectors identifies a cell wall-associated kinase involved in plant immunity. Genome Biol. **14**: R139.

Ross, A. and Somssich, I.E. (2016). A DNA-based real-time PCR assay for robust growth quantification of the bacterial pathogen Pseudomonas syringae on Arabidopsis thaliana. Plant Methods **12**: 48.

Ross, A., Yamada, K., Hiruma, K., Yamashita-Yamada, M., Lu, X., Takano, Y., Tsuda, K., and Saijo, Y. (2014). The Arabidopsis PEPR pathway couples local and systemic plant immunity. EMBO J. **33**: 62–75.

Roux, M., Schwessinger, B., Albrecht, C., Chinchilla, D., Jones, A., Holton, N., Malinovsky, F.G., Tör, M., de Vries, S., and Zipfel, C. (2011). The Arabidopsis leucine-rich repeat receptor-like kinases BAK1/SERK3 and BKK1/SERK4 are required for innate immunity to hemibiotrophic and biotrophic pathogens. Plant Cell **23**: 2440–55.

Ruppel, S., Franken, P., and Witzel, K. (2013). Properties of the halophyte microbiome and their implications for plant salt tolerance. In Functional Plant Biology (CSIRO PUBLISHING), pp. 940–951.

Sagi, M., Fluhr, R., and Dangl, J.L. (2006). Superoxide Production by Plant Homologues of the gp91phox NADPH Oxidase. Modulation of Activity by Calcium and by Tobacco Mosaic Virus Infection. PLANT Physiol. **141**: 373–378.

Salmeron, J.M., Oldroyd, G.E., Rommens, C.M., Scofield, S.R., Kim, H.S., Lavelle, D.T., Dahlbeck, D., and Staskawicz, B.J. (1996). Tomato Prf is a member of the leucine-rich repeat class of plant disease resistance genes and lies embedded within the Pto kinase gene cluster. Cell **86**: 123–33.

Sanchez, D.H., Pieckenstain, F.L., Szymanski, J., Erban, A., Bromke, M., Hannah, M.A., Kraemer, U., Kopka, J., and Udvardi, M.K. (2011). Comparative Functional Genomics of Salt Stress in Related Model and Cultivated Plants Identifies and Overcomes Limitations to Translational Genomics. PLoS One **6**: e17094.

Sarris, P.F. et al. (2015). A Plant Immune Receptor Detects Pathogen Effectors that Target WRKY Transcription Factors. Cell **161**: 1089–1100.

Saur, I.M.L., Kadota, Y., Sklenar, J., Holton, N.J., Smakowska, E., Belkhadir, Y., Zipfel, C., and Rathjen, J.P. (2016). NbCSPR underlies age-dependent immune responses to bacterial cold shock protein in Nicotiana benthamiana. Proc. Natl. Acad. Sci. **113**: 3389–3394.

Schranz, M.E., Song, B.-H., Windsor, A.J., and Mitchell-Olds, T. (2007). Comparative genomics in the Brassicaceae: a family-wide perspective. Curr. Opin. Plant Biol. **10**: 168–75.

Schroder, K. et al. (2012). Conservation and divergence in Toll-like receptor 4-regulated gene expression in primary human versus mouse macrophages. Proc. Natl. Acad. Sci. **109**: E944–E953.

Schulze-Lefert, P. and Panstruga, R. (2011). A molecular evolutionary concept connecting nonhost resistance, pathogen host range, and pathogen speciation. Trends Plant Sci. **16**: 117–125.

Schulze, B., Mentzel, T., Jehle, A.K., Mueller, K., Beeler, S., Boller, T., Felix, G., and Chinchilla, D. (2010). Rapid heteromerization and phosphorylation of ligand-activated plant transmembrane receptors and their associated kinase BAK1. J. Biol. Chem. **285**: 9444–9451.

Schwessinger, B., Roux, M., Kadota, Y., Ntoukakis, V., Sklenar, J., Jones, A., and Zipfel, C. (2011). Phosphorylation-dependent differential regulation of plant growth, cell death, and innate immunity by the regulatory receptor-like kinase BAK1. PLoS Genet. **7**: e1002046.

Segonzac, C., Macho, A.P., Sanmartin, M., Ntoukakis, V., Sanchez-Serrano, J.J., and Zipfel, C. (2014). Negative control of BAK1 by protein phosphatase 2A during plant innate immunity. EMBO J. **33**: 2069–2079.

Shannon, P., Markiel, A., Ozier, O., Baliga, N.S., Wang, J.T., Ramage, D., Amin, N., Schwikowski, B., and Ideker, T. (2003). Cytoscape: A software Environment for integrated models of biomolecular interaction networks. Genome Res. **13**: 2498–2504.

Shapiro, M.D., Marks, M.E., Peichel, C.L., Blackman, B.K., Nereng, K.S., Jónsson, B., Schluter, D., and Kingsley, D.M. (2004). Genetic and developmental basis of evolutionary pelvic reduction in threespine sticklebacks. Nature **428**: 717–723.

Shen, Q., Bourdais, G., Pan, H., Robatzek, S., and Tang, D. (2017). Arabidopsis glycosylphosphatidylinositol-anchored protein LLG1 associates with and modulates FLS2 to regulate innate immunity. Proc. Natl. Acad. Sci. **114**: 5749–5754.

Shi, H., Shen, Q., Qi, Y., Yan, H., Nie, H., Chen, Y., Zhao, T., Katagiri, F., and Tang, D. (2013). BR-SIGNALING KINASE1 Physically Associates with FLAGELLIN SENSING2 and Regulates Plant Innate Immunity in Arabidopsis. Plant Cell **25**: 1143–1157.

Shi, X., Ng, D.W.K., Zhang, C., Comai, L., Ye, W., and Jeffrey Chen, Z. (2012). Cis- and trans-regulatory divergence between progenitor species determines gene-expression novelty in Arabidopsis allopolyploids. Nat. Commun. **3**: 950.

Shinya, T. et al. (2014). Selective regulation of the chitin-induced defense response by the Arabidopsis receptor-like cytoplasmic kinase PBL27. Plant J. **79**: 56–66.

Sievers, F., Wilm, A., Dineen, D., Gibson, T.J., Karplus, K., Li, W., Lopez, R., McWilliam, H., Remmert, M., Söding, J., Thompson, J.D., and Higgins, D.G. (2011). Fast, scalable generation of high-quality protein multiple sequence alignments using Clustal Omega. Mol. Syst. Biol. **7**: 539.

Slotte, T. et al. (2013). The Capsella rubella genome and the genomic consequences of rapid mating system evolution. Nat. Genet. **45**: 831–5.

Somerville, C. and Koornneef, M. (2002). A fortunate choice: the history of Arabidopsis as a model plant. Nat. Rev. Genet. **3**: 883–889.

Song, W.-Y., Wang, G.-L., Chen, L.-L., Kim, H.-S., Pi, L.-Y., Holsten, T., Gardner, J., Wang, B., Zhai, W.-X., Zhu, L.-H., Fauquet, C., and Ronald, P. (1995). A Receptor Kinase-Like Protein Encoded by the Rice Disease Resistance Gene, Xa21. Science (80-.). **270**: 1804–1806.

Spoel, S.H. and Dong, X. (2012). How do plants achieve immunity? Defence without specialized immune cells. Nat. Rev. Immunol. **12**: 89–100.

Sreekanta, S., Bethke, G., Hatsugai, N., Tsuda, K., Thao, A., Wang, L., Katagiri, F., and Glazebrook, J. (2015). The receptor-like cytoplasmic kinase PCRK1 contributes to pattern-triggered immunity against Pseudomonas syringae in Arabidopsis thaliana. New Phytol. **207**: 78–90.

Staiger, D., Korneli, C., Lummer, M., and Navarro, L. (2013). Emerging role for RNA-based regulation in plant immunity. New Phytol. **197**: 394–404.

Stegmann, M., Monaghan, J., Smakowska-Luzan, E., Rovenich, H., Lehner, A., Holton, N., Belkhadir, Y., and Zipfel, C. (2017). The receptor kinase FER is a RALF-regulated scaffold controlling plant immune signaling. Science **355**: 287–289.

Sturn, A., Quackenbush, J., and Trajanoski, Z. (2002). Genesis: cluster analysis of microarray data. Bioinformatics **18**: 207–8.

Sun, W., Xu, X., Zhu, H., Liu, A., Liu, L., Li, J., and Hua, X. (2010). Comparative transcriptomic profiling of a salt-tolerant wild tomato species and a salt-sensitive tomato cultivar. Plant Cell Physiol. **51**: 997–1006.

Sun, Y., Li, L., Macho, A.P., Han, Z., Hu, Z., Zipfel, C., Zhou, J.-M., and Chai, J. (2013). Structural Basis for flg22-Induced Activation of the Arabidopsis FLS-BAK1 Immune Complex. Science **342**: 624–628.

Taji, T., Seki, M., Satou, M., Sakurai, T., Kobayashi, M., Ishiyama, K., Narusaka, Y., Narusaka, M., Zhu, J.-K., and Shinozaki, K. (2004). Comparative genomics in salt tolerance between Arabidopsis and aRabidopsis-related halophyte salt cress using Arabidopsis microarray. Plant Physiol. **135**: 1697–709.

Takai, R., Isogai, A., Takayama, S., and Che, F.-S. (2008). Analysis of Flagellin Perception Mediated by flg22 Receptor OsFLS2 in Rice. Mol. Plant-Microbe Interact. **21**: 1635–1642.

Tang, D., Wang, G., and Zhou, J.-M. (2017). Receptor Kinases in Plant-Pathogen Interactions: More Than Pattern Recognition. Plant Cell **29**: 618–637.

Tang, X., Frederick, R.D., Zhou, J., Halterman, D.A., Jia, Y., and Martin, G.B. (1996). Initiation of Plant Disease Resistance by Physical Interaction of AvrPto and Pto Kinase. Science **274**: 2060–

2063.

Tekaia, F. (2016). Inferring orthologs: Open questions and perspectives. Genomics Insights **9**: 17–28.

Thaler, J.S., Humphrey, P.T., and Whiteman, N.K. (2012). Evolution of jasmonate and salicylate signal crosstalk. Trends Plant Sci. **17**: 260–270.

Thatcher, J.W., Shaw, J.M., and Dickinson, W.J. (1998). Marginal fitness contributions of nonessential genes in yeast. Proc. Natl. Acad. Sci. **95**: 253–7.

Thomma, B.P.H.J., Nelissen, I., Eggermont, K., and Broekaert, W.F. (1999). Deficiency in phytoalexin production causes enhanced susceptibility of Arabidopsis thaliana to the fungus Alternaria brassicicola. Plant J. **19**: 163–171.

Tirosh, I., Reikhav, S., Levy, A.A., and Barkai, N. (2009). A Yeast Hybrid Provides Insight into the Evolution of Gene Expression Regulation. Science **324**: 659–662.

Todesco, M. et al. (2010). Natural allelic variation underlying a major fitness trade-off in Arabidopsis thaliana. Nature **465**: 632–636.

De Torres Zabala, M., Bennett, M.H., Truman, W.H., and Grant, M.R. (2009). Antagonism between salicylic and abscisic acid reflects early host-pathogen conflict and moulds plant defence responses. Plant J. **59**: 375–386.

Toruño, T.Y., Stergiopoulos, I., and Coaker, G. (2016). Plant-Pathogen Effectors: Cellular Probes Interfering with Plant Defenses in Spatial and Temporal Manners. Annu. Rev. Phytopathol. **54**: 419–441.

Touchman, J. (2010). Comparative Genomics. Nat. Educ. Knowl. **3**: 13.

Trapnell, C., Pachter, L., and Salzberg, S.L. (2009). TopHat: Discovering splice junctions with RNA-Seq. Bioinformatics **25**: 1105–1111.

Tsankov, A.M., Thompson, D.A., Socha, A., Regev, A., and Rando, O.J. (2010). The Role of Nucleosome Positioning in the Evolution of Gene Regulation. PLoS Biol. **8**: e1000414.

Tsuda, K., Sato, M., Glazebrook, J., Cohen, J.D., and Katagiri, F. (2008). Interplay between MAMP-triggered and SA-mediated defense responses. Plant J. **53**: 763–75.

Tsuda, K., Sato, M., Stoddard, T., Glazebrook, J., and Katagiri, F. (2009). Network properties of robust immunity in plants. PLoS Genet. **5**: e1000772.

Tsuda, K. and Somssich, I.E. (2015). Transcriptional networks in plant immunity. New Phytol. **206**: 932–947.

Uebbing, S. et al. (2016). Divergence in gene expression within and between two closely related flycatcher species. Mol. Ecol. **25**: 2015–2028.

Ueno, Y., Yoshida, R., Kishi-Kaboshi, M., Matsushita, A., Jiang, C.-J., Goto, S., Takahashi, A., Hirochika, H., and Takatsuji, H. (2015). Abiotic Stresses Antagonize the Rice Defence Pathway through the Tyrosine-Dephosphorylation of OsMPK6. PLoS Pathog. **11**: e1005231.

Varden, F.A., De la Concepcion, J.C., Maidment, J.H., and Banfield, M.J. (2017). Taking the stage: effectors in the spotlight. Curr. Opin. Plant Biol. **38**: 25–33.

Van Veen, H. et al. (2016). Transcriptomes of eight Arabidopsis thaliana accessions reveal core conserved, genotype- and organ-specific responses to flooding stress. Plant Physiol. **172**: pp.00472.2016.

Van de Velde, J., Van Bel, M., Van Eechoutte, D., and Vandepoele, K. (2016). A Collection of Conserved Non-Coding Sequences to Study Gene Regulation in Flowering Plants. Plant Physiol. **171**: pp.00821.2016.

Vetter, M., Karasov, T.L., and Bergelson, J. (2016). Differentiation between MAMP Triggered Defenses in Arabidopsis thaliana. PLOS Genet. **12**: e1006068.

Vetter, M.M., Kronholm, I., He, F., Häweker, H., Reymond, M., Bergelson, J., Robatzek, S., and de Meaux, J. (2012). Flagellin perception varies quantitatively in Arabidopsis thaliana and its relatives. Mol. Biol. Evol. **29**: 1655–67.

Vlad, D. et al. (2014). Leaf Shape Evolution Through Duplication, Regulatory Diversification, and Loss of a Homeobox Gene. Science **343**: 780–783.

Voelckel, C., Gruenheit, N., and Lockhart, P. (2017). Evolutionary Transcriptomics and Proteomics: Insight into Plant Adaptation. Trends Plant Sci. **22**: 462–471.

Vos, I.A., Moritz, L., Pieterse, C.M.J., and Van Wees, S.C.M. (2015). Impact of hormonal crosstalk on plant resistance and fitness under multi-attacker conditions. Front. Plant Sci. **6**: 639.

Vos, I.A., Pieterse, C.M.J., and Van Wees, S.C.M. (2013). Costs and benefits of hormone-regulated plant defences. Plant Pathol. **62**: 43–55.

De Vos, M., Van Oosten, V.R., Van Poecke, R.M.P., Van Pelt, J.A., Pozo, M.J., Mueller, M.J., Buchala, A.J., Métraux, J.-P., Van Loon, L.C., Dicke, M., and Pieterse, C.M.J. (2005). Signal Signature and Transcriptome Changes of Arabidopsis During Pathogen and Insect Attack. Mol. Plant-Microbe Interact. **18**: 923–937.

Voss, T.C. and Hager, G.L. (2014). Dynamic regulation of transcriptional states by chromatin and transcription factors. Nat. Rev. Genet. **15**: 69–81.

Wan, J., Zhang, X.-C., Neece, D., Ramonell, K.M., Clough, S., Kim, S. -y., Stacey, M.G., and Stacey, G. (2008). A LysM Receptor-Like Kinase Plays a Critical Role in Chitin Signaling and Fungal Resistance in Arabidopsis. Plant Cell **20**: 471–481.

Wang, G. et al. (2008). A Genome-Wide Functional Investigation into the Roles of Receptor-Like Proteins in Arabidopsis. PLANT Physiol. **147**: 503–517.

Wang, L., Albert, M., Einig, E., Fürst, U., Krust, D., and Felix, G. (2016). The pattern-recognition receptor CORE of Solanaceae detects bacterial cold-shock protein. Nat. Plants **2**: 16185.

Wang, Z.-Y. (2012). Brassinosteroids modulate plant immunity at multiple levels. Proc. Natl. Acad. Sci. **109**: 7–8.

Weber, M., Harada, E., Vess, C., Roepenack-Lahaye, E. v., and Clemens, S. (2004). Comparative microarray analysis of Arabidopsis thaliana and Arabidopsis halleri roots identifies nicotianamine synthase, a ZIP transporter and other genes as potential metal hyperaccumulation factors. Plant J. **37**: 269–281.

Whitehead, A. (2012). Comparative genomics in ecological physiology: toward a more nuanced understanding of acclimation and adaptation. J. Exp. Biol. **215**: 884–891.

Whitehead, A. and Crawford, D.L. (2006). Neutral and adaptive variation in gene expression. Proc. Natl. Acad. Sci. **103**: 5425–5430.

Whittle, C.A., Sun, Y., and Johannesson, H. (2014). Dynamics of transcriptome evolution in the model eukaryote Neurospora. J. Evol. Biol. **27**: 1125–1135.

Wildermuth, M.C., Dewdney, J., Wu, G., and Ausubel, F.M. (2001). Isochorismate synthase is required to synthesize salicylic acid for plant defence. Nature **414**: 562–5.

Willmann, R. et al. (2011). Arabidopsis lysin-motif proteins LYM1 LYM3 CERK1 mediate bacterial peptidoglycan sensing and immunity to bacterial infection. Proc. Natl. Acad. Sci. **108**: 19824–9.

Wu, H.-J. et al. (2012). Insights into salt tolerance from the genome of Thellungiella salsuginea. Proc. Natl. Acad. Sci. **109**: 12219–24.

Xin, X.-F., Nomura, K., Aung, K., Velásquez, A.C., Yao, J., Boutrot, F., Chang, J.H., Zipfel, C., and He, S.Y. (2016). Bacteria establish an aqueous living space in plants crucial for virulence. Nature **539**: 524–529.

Yaish, M.W., Al-Lawati, A., Jana, G.A., Patankar, H.V., and Glick, B.R. (2016). Impact of soil salinity on the structure of the bacterial endophytic community identified from the roots of caliph medic (Medicago truncatula). PLoS One **11**: e0159007.

Yamada, K. et al. (2016). The Arabidopsis CERK1-associated kinase PBL27 connects chitin perception to MAPK activation. EMBO J. **35**: 2468–2483.

Yamaguchi, Y., Huffaker, A., Bryan, A.C., Tax, F.E., and Ryan, C.A. (2010). PEPR2 is a second receptor for the Pep1 and Pep2 peptides and contributes to defense responses in Arabidopsis. Plant Cell **22**: 508–22.

Yamaguchi, Y., Pearce, G., and Ryan, C.A. (2006). The cell surface leucine-rich repeat receptor for AtPep1, an endogenous peptide elicitor in Arabidopsis, is functional in transgenic tobacco cells. Proc. Natl. Acad. Sci. **103**: 10104–10109.

Yanai, I., Graur, D., and Ophir, R. (2004). Incongruent Expression Profiles between Human and Mouse Orthologous Genes Suggest Widespread Neutral Evolution of Transcription Control. Omi. A J. Integr. Biol. **8**.

Yang, D.-L. et al. (2012). Plant hormone jasmonate prioritizes defense over growth by interfering with gibberellin signaling cascade. Proc. Natl. Acad. Sci. **109**: E1192–E1200.

Yang, H., Hu, J., Long, X., Liu, Z., and Rengel, Z. (2016). Salinity altered root distribution and increased diversity of bacterial communities in the rhizosphere soil of Jerusalem artichoke. Sci. Rep. **6**: 20687.

Yang, Q.S., Gao, J., He, W. Di, Dou, T.X., Ding, L.J., Wu, J.H., Li, C.Y., Peng, X.X., Zhang, S., and Yi, G.J. (2015). Comparative transcriptomics analysis reveals difference of key gene expression between banana and plantain in response to cold stress. BMC Genomics **16**: 446.

Yang, R. et al. (2013). The Reference Genome of the Halophytic Plant Eutrema salsugineum. Front. Plant Sci. **4**: 46.

Yang, Z. (2007). PAML 4: Phylogenetic analysis by maximum likelihood. Mol. Biol. Evol. **24**: 1586–1591.

Yang, Z. and Bielawski, J.R. (2000). Statistical methods for detecting molecular adaptation. Trends Ecol. Evol. **15**: 496–503.

Yasuda, M., Ishikawa, A., Jikumaru, Y., Seki, M., Umezawa, T., Asami, T., Maruyama-Nakashita, A., Kudo, T., Shinozaki, K., Yoshida, S., and Nakashita, H. (2008). Antagonistic interaction between systemic acquired resistance and the abscisic acid-mediated abiotic stress response in Arabidopsis. Plant Cell **20**: 1678–92.

Yasuda, S., Okada, K., and Saijo, Y. (2017). A look at plant immunity through the window of the multitasking coreceptor BAK1. Curr. Opin. Plant Biol. **38**: 10–18.

Yeh, Y.-H., Panzeri, D., Kadota, Y., Huang, Y.-C., Huang, P.-Y., Tao, C.-N., Roux, M., Chien, H.-C., Chin, T.-C., Chu, P.-W., Zipfel, C., and Zimmerli, L. (2016). The Arabidopsis Malectin-Like/LRR-RLK IOS1 is Critical for BAK1-Dependent and BAK1-Independent Pattern-Triggered Immunity. Plant Cell **28**: 1701–1721.

Yeo, M.T.S., Carella, P., Fletcher, J., Champigny, M.J., Weretilnyk, E.A., and Cameron, R.K. (2015). Development of a Pseudomonas syringae-Eutrema salsugineum pathosystem to investigate disease resistance in a stress tolerant extremophile model plant. Plant Pathol. **64**: 297–306.

Yu, C.-P., Lin, J.-J., and Li, W.-H. (2016). Positional distribution of transcription factor binding sites in Arabidopsis thaliana. Sci. Rep. **6**: 25164.

Yu, X., Feng, B., He, P., and Shan, L. (2017). From Chaos to Harmony: Responses and Signaling Upon Microbial Pattern Recognition. Annu. Rev. Phytopathol **55**: 1–529.

Zhang, J. et al. (2010). Receptor-like cytoplasmic kinases integrate signaling from multiple plant immune receptors and are targeted by a Pseudomonas syringae effector. Cell Host Microbe **7**: 290–301.

Zhang, J., Feng, J., Lu, J., Yang, Y., Zhang, X., Wan, D., and Liu, J. (2014). Transcriptome differences between two sister desert poplar species under salt stress. BMC Genomics **15**: 337.

Zhang, J. and Zhou, J.-M. (2010). Plant Immunity Triggered by Microbial Molecular Signatures. Mol. Plant **3**: 783–793.

Zhang, W., Fraiture, M., Kolb, D., Löffelhardt, B., Desaki, Y., Boutrot, F.F.G., Tör, M., Zipfel, C., Gust, A.A., and Brunner, F. (2013a). Arabidopsis receptor-like protein30 and receptor-like kinase suppressor of BIR1-1/EVERSHED mediate innate immunity to necrotrophic fungi. Plant Cell **25**: 4227–41.

Zhang, X., Yao, J., Zhang, Y., Sun, Y., and Mou, Z. (2013b). The Arabidopsis Mediator complex subunits MED14/SWP and MED16/SFR6/IEN1 differentially regulate defense gene expression in plant immune responses. Plant J. **75**: 484–497.

Zhang, Z.F., Li, Y.Y., and Xiao, B.Z. (2016). Comparative transcriptome analysis highlights the crucial roles of photosynthetic system in drought stress adaptation in upland rice. Sci. Rep. **6**: 19349.

Zhao, J., Favero, D.S., Peng, H., and Neff, M.M. (2013). Arabidopsis thaliana AHL family modulates hypocotyl growth redundantly by interacting with each other via the PPC/DUF296 domain. Proc. Natl. Acad. Sci. **110**: E4688–E4697.

Zhao, J., Favero, D.S., Qiu, J., Roalson, E.H., and Neff, M.M. (2014). Insights into the evolution and diversification of the AT-hook Motif Nuclear Localized gene family in land plants. BMC Plant Biol. **14**: 266.

Zheng, X.-Y., Spivey, N.W., Zeng, W., Liu, P.-P., Fu, Z.Q., Klessig, D.F., He, S.Y., and Dong, X. (2012). Coronatine promotes Pseudomonas syringae virulence in plants by activating a signaling cascade that inhibits salicylic acid accumulation. Cell Host Microbe **11**: 587–96.

Zhu, J.-K. (2001). Plant salt tolerance. Trends Plant Sci. **6**: 66–71.

Zipfel, C., Kunze, G., Chinchilla, D., Caniard, A., Jones, J.D.G., Boller, T., and Felix, G. (2006). Perception of the bacterial PAMP EF-Tu by the receptor EFR restricts Agrobacterium-mediated transformation. Cell **125**: 749–60.

Zipfel, C., Robatzek, S., Navarro, L., Oakeley, E.J., Jones, J.D.G., Felix, G., and Boller, T. (2004). Bacterial disease resistance in Arabidopsis through flagellin perception. Nature **428**: 764–767.

6. Supplement

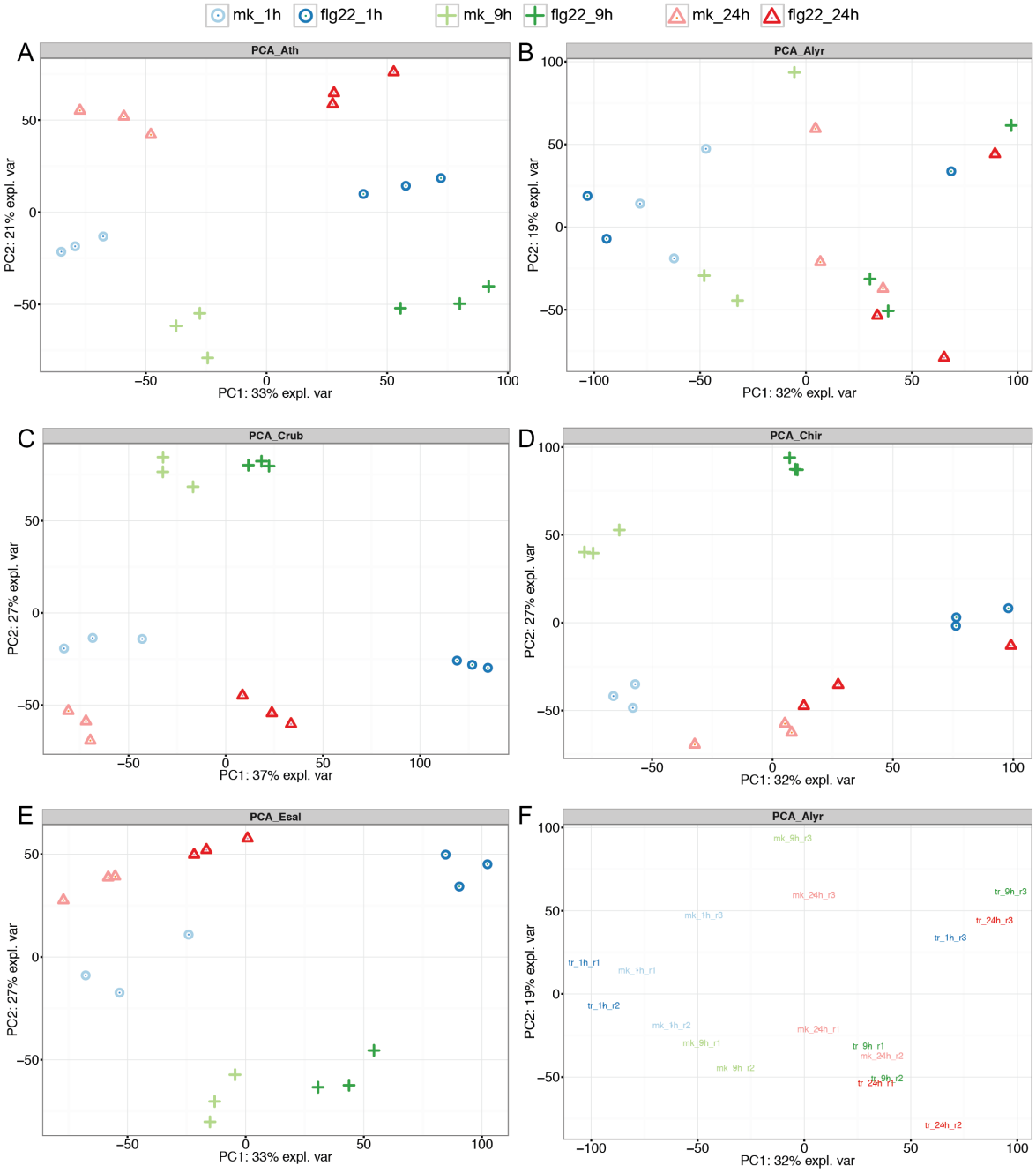

Supplement Figure 1: Principal component analysis of normalized RNAseq data. PCA was performed with normalized expression values (log_2-transformed counts per million) using MixOmics R package. Time points are indicated by different colours and mock and flg22 treatment are indicated by pale and deep colour, respectively. Time-points are indicated by circles (1 h), crosses (9 h) and triangles (24 h) **A-E** show the PCA from *A. thaliana*, *A. lyrata*, *C. rubella*, *C. hirsuta* and *E. salsugineum*, respectively. **F:** *A. lyrata* PCA is further plotted with individual replicates indicated by r1-r3.

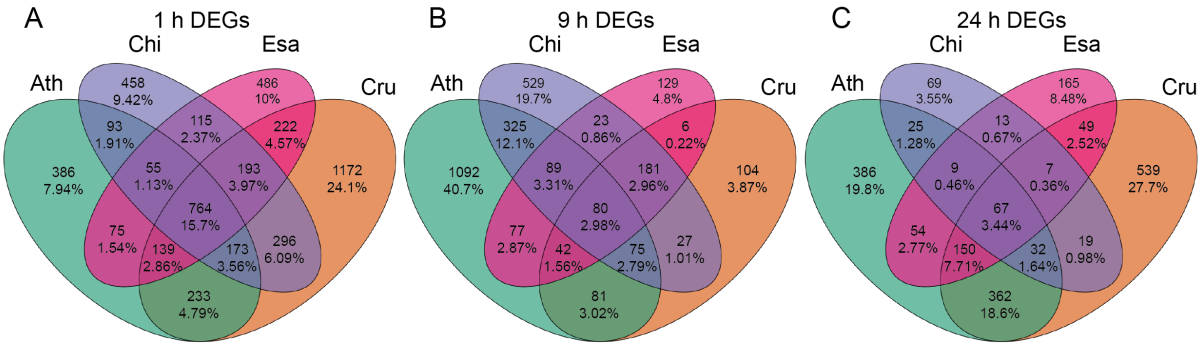

Supplement Figure 2: Overlap of DEGs at different time-points. Venn diagrams showing shared DEGs between species at 1 h (**A**), 9 h (**B**), and 24 h (**C**) after flg22-treatment. All DEGs which are differentially expressed in at least 1 species at the respective time points were used.

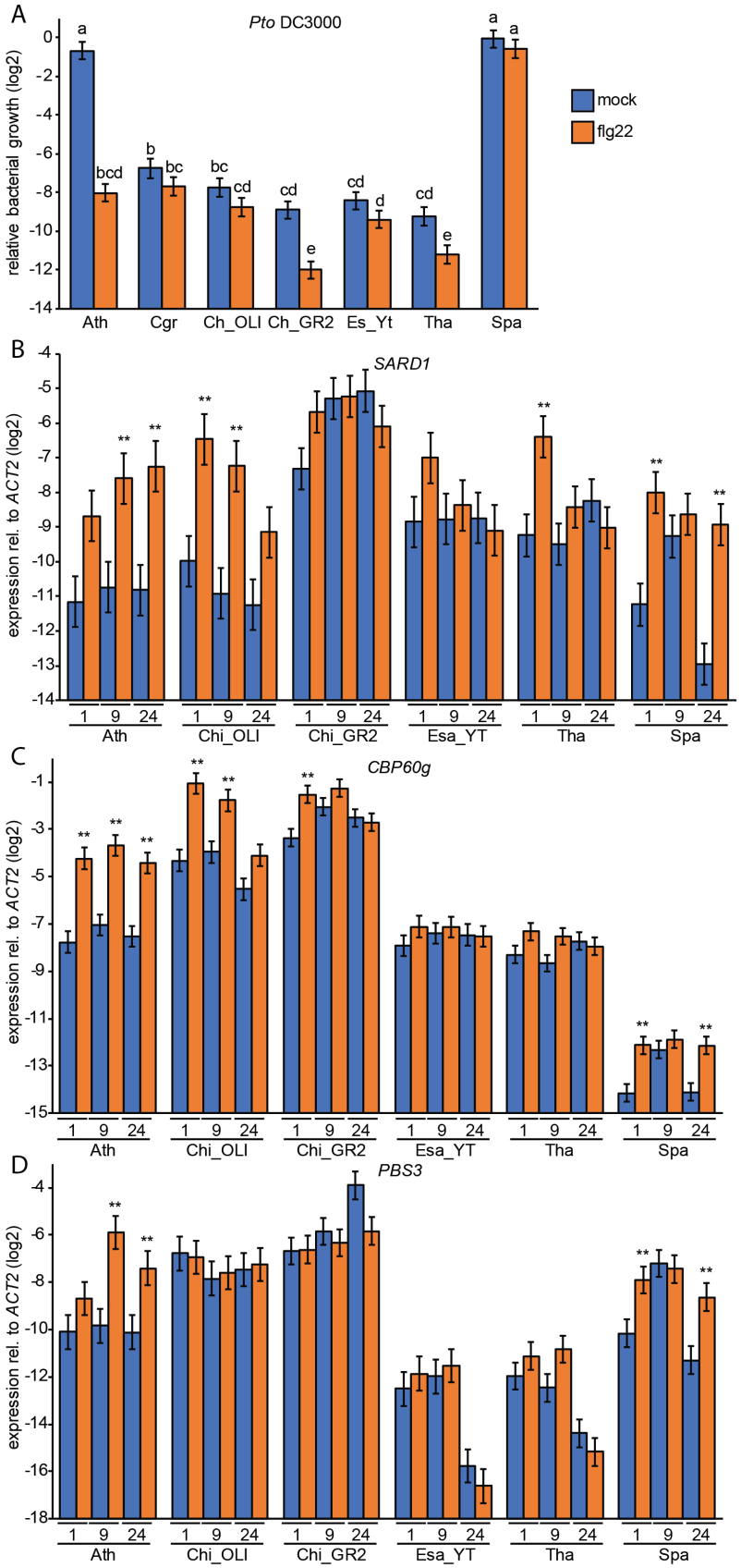

Supplement Figure 3: flg22-triggered bacterial suppression does not correlate with marker gene induction 24 h after flg22 treatment. A: 5-week-old Brassicaceae plants were syringe-infiltrated with 1 µM flg22 or mock 24 h prior to infiltration with *Pto* DC3000 (OD_{600} = 0.0002). The bacterial titer was determined 48 h after bacterial infiltration by measuring the DNA amount of the *Pseudomonas syringae* specific *OprF* gene relative to the plant *ACT2* gene by qPCR. Bars represent the means ±SE from 2 independent experiments with each 3 biological replicates (n = 6). Different letters indicate statistically significant differences (mixed linear model followed by

Student´s t-test; adjusted $p < 0.01$). **B, C, D:** 12-day-old Brassicaceae seedlings grown on 1⁄2 MS-medium were treated with 1⁄2 MS media (mock) or 1 µM flg22 for 1, 9 or 24 h. Expression of three marker-genes extracted from the heatmap in Figure 7C namely *SARD1* **C**, *CBP60g* **C** and *PBS3* **D** was quantified via RT-qPCR. Bars represent the means ±SE from 2 independent experiments and asterisks indicate significant differences between flg22 and mock samples (mixed linear model followed by Student´s t-test; **, $p < 0.01$) Ath, *Arabidopsis thaliana* Col-0; Cru, *Capsella rubella*; Cgr, *Capsella grandiflora*; Chi_Ox, Chi_GR, Chi_Ol, different *Cardamina hirsuta* accessions; Esa_Sh, *Eutrema salsugineum* Shandong; Esa_YT, Esa Yukon; Tha, *Thellungiella halophila.*

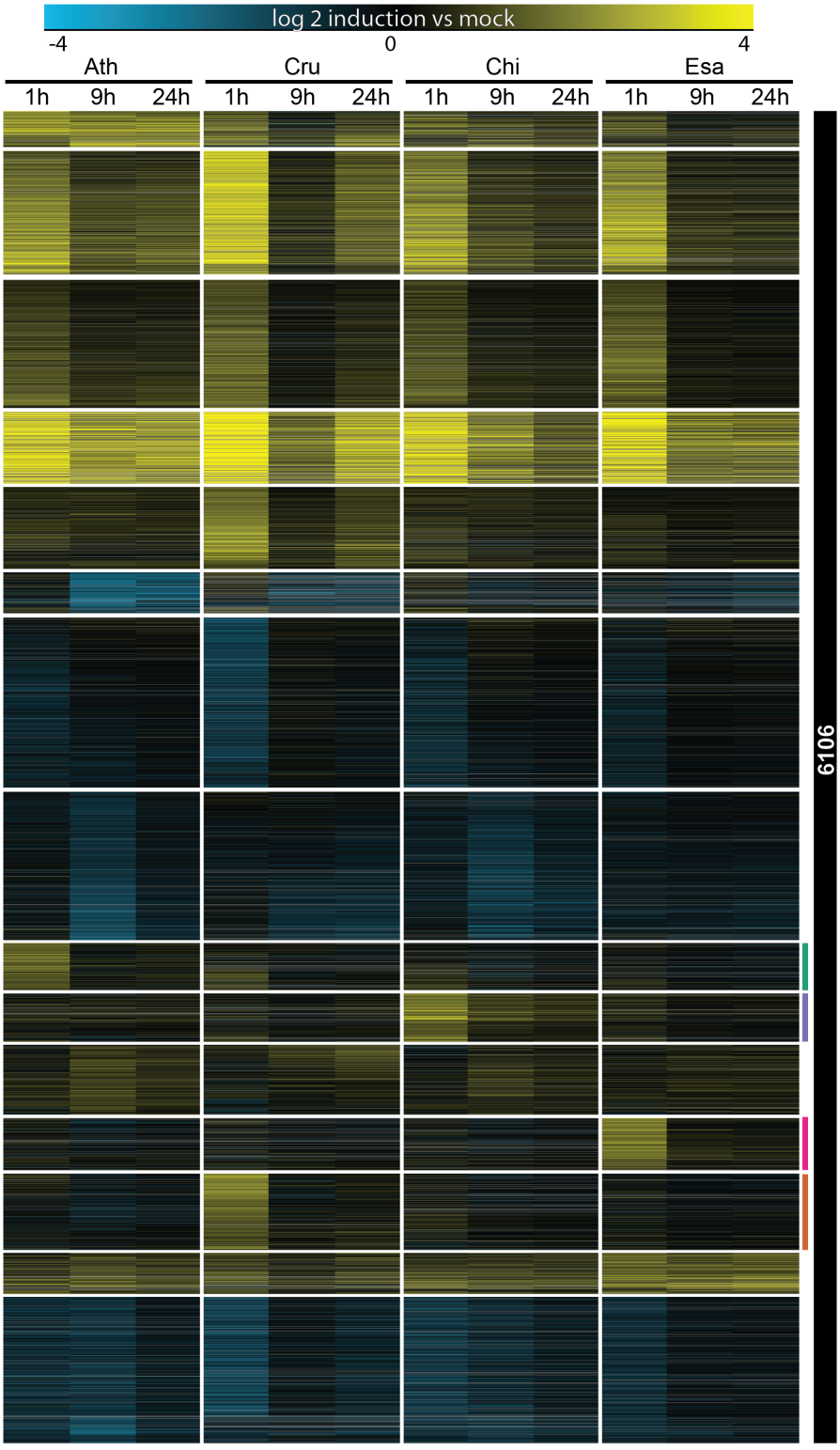

Supplement Figure 4: Heatmap for all DEGs in Brassicaceae species after flg22 treatment. Heatmap of all 6106 DEGs in all Brassicaceae species generated using k-means clustering. All DEGs which are at least differentially expressed at 1 time point in 1 species were used. Expression changes are shown. Species-specific expression signatures shown in Figure 9A are indicated by coloured bars on the right side.

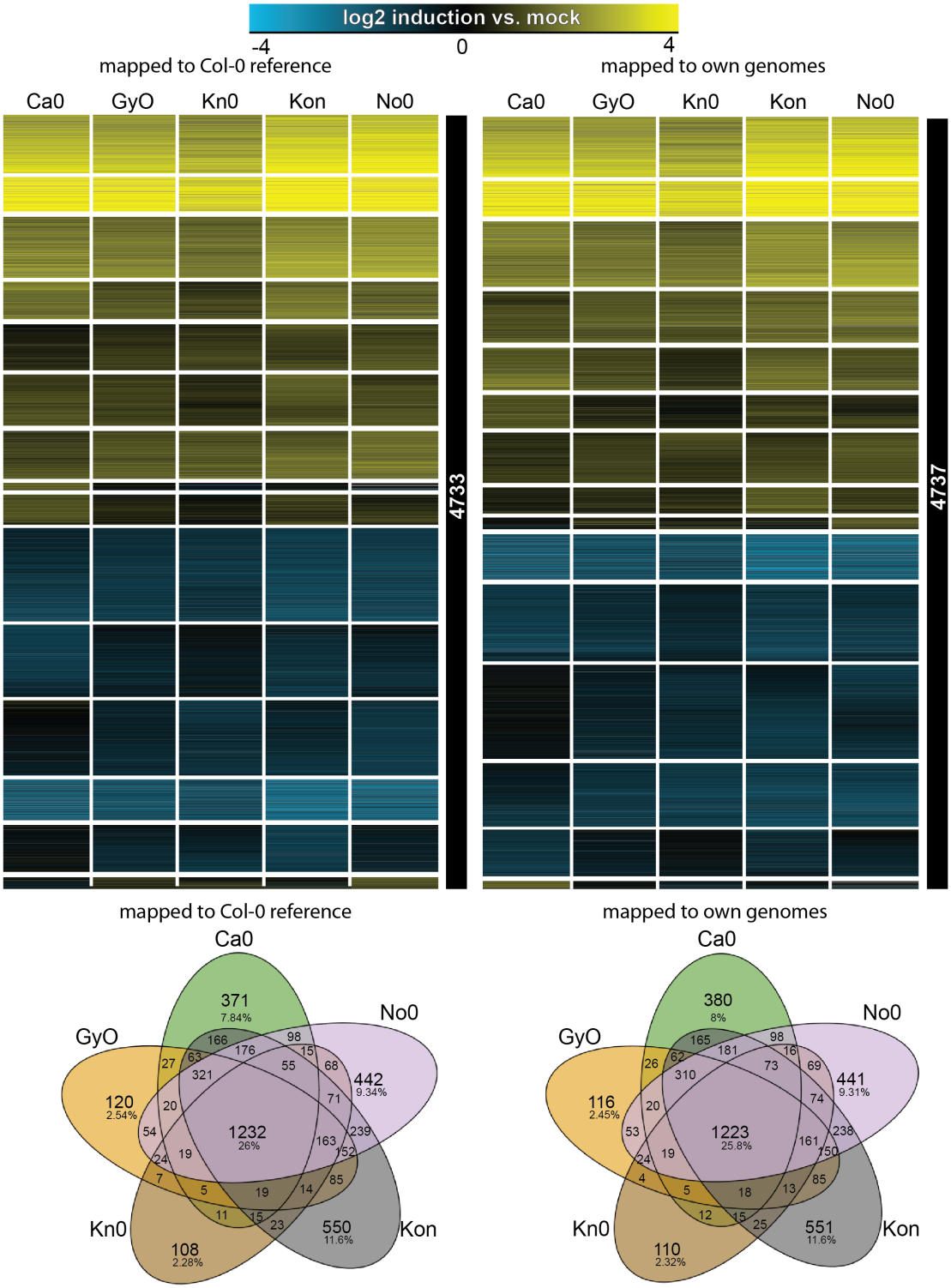

Supplement Figure 5: Comparison of two different mapping approaches for *A. thaliana* accessions RNAseq reads. RNAseq reads were mapped to the Col-0 (TAIR10) reference genome (left) or to individual *A. thaliana* accession genomes generated in this study using SNP data (right). This comparison was made to test whether highly similar transcriptome responses were caused by mapping RNAseq reads of different accessions onto the single Col-0 genome. Since both mapping methods yielded similar results, the data mapped to the Col-0 reference genome was used throughout this study.

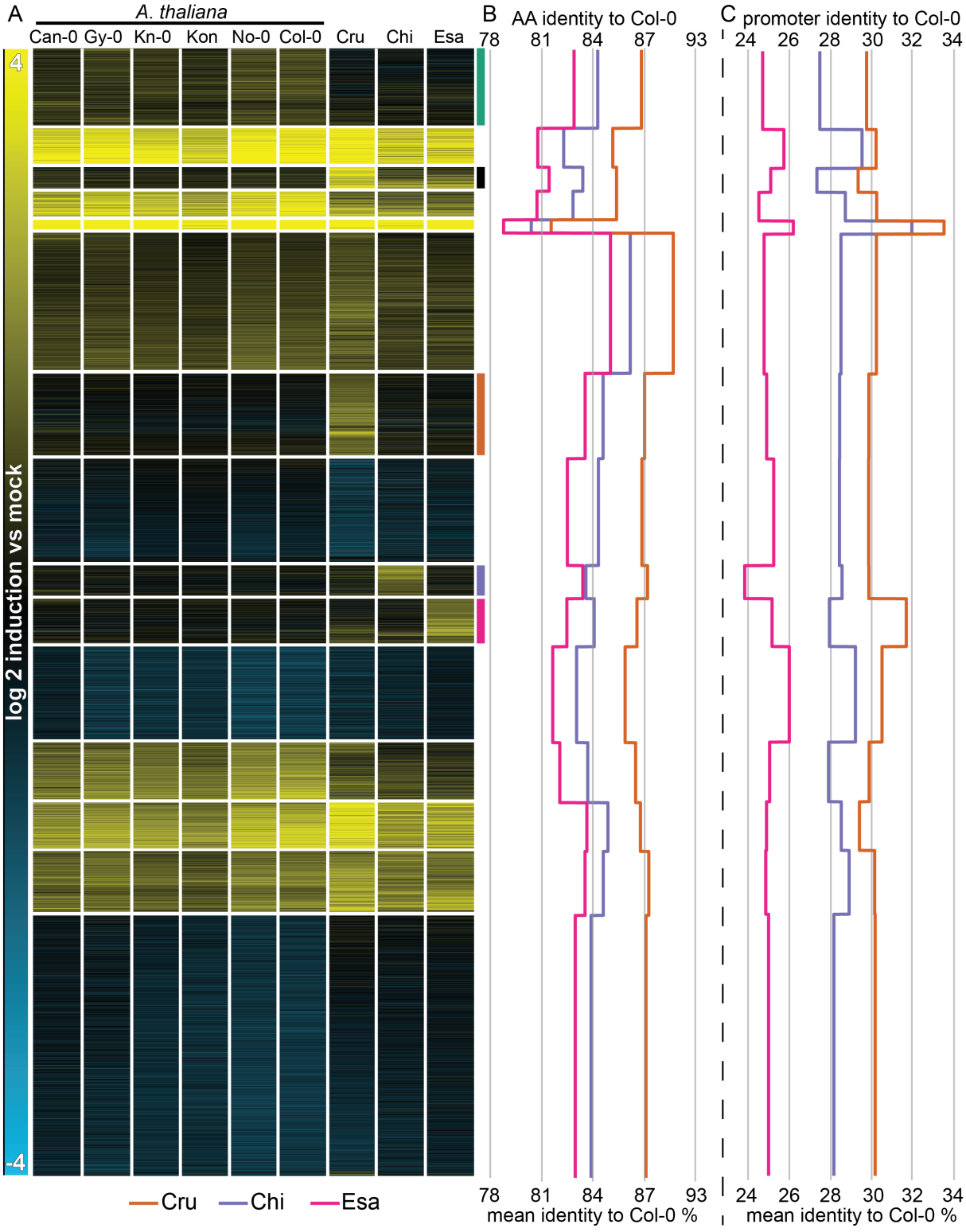

Supplement Figure 6: Variation in coding and upstream sequences does not explain lineage –specific expression signatures in response to flg22. A: Brassicaceae and *A. thaliana* accession expression changes 1 h after flg22 treatment were normalized and analysed together. All 5961 DEGs were clustered using k-mean clustering and lineage-specific expression signatures are highlighted by coloured bars on the right side of the heatmap as shown in Figure 6A. **B, C:** Coloured lines represent the mean % identity of amino acid sequences (B) and 500 bp sequences upstream of the transcription start site (C) for each cluster in each species compared to *A. thaliana* Col-0.

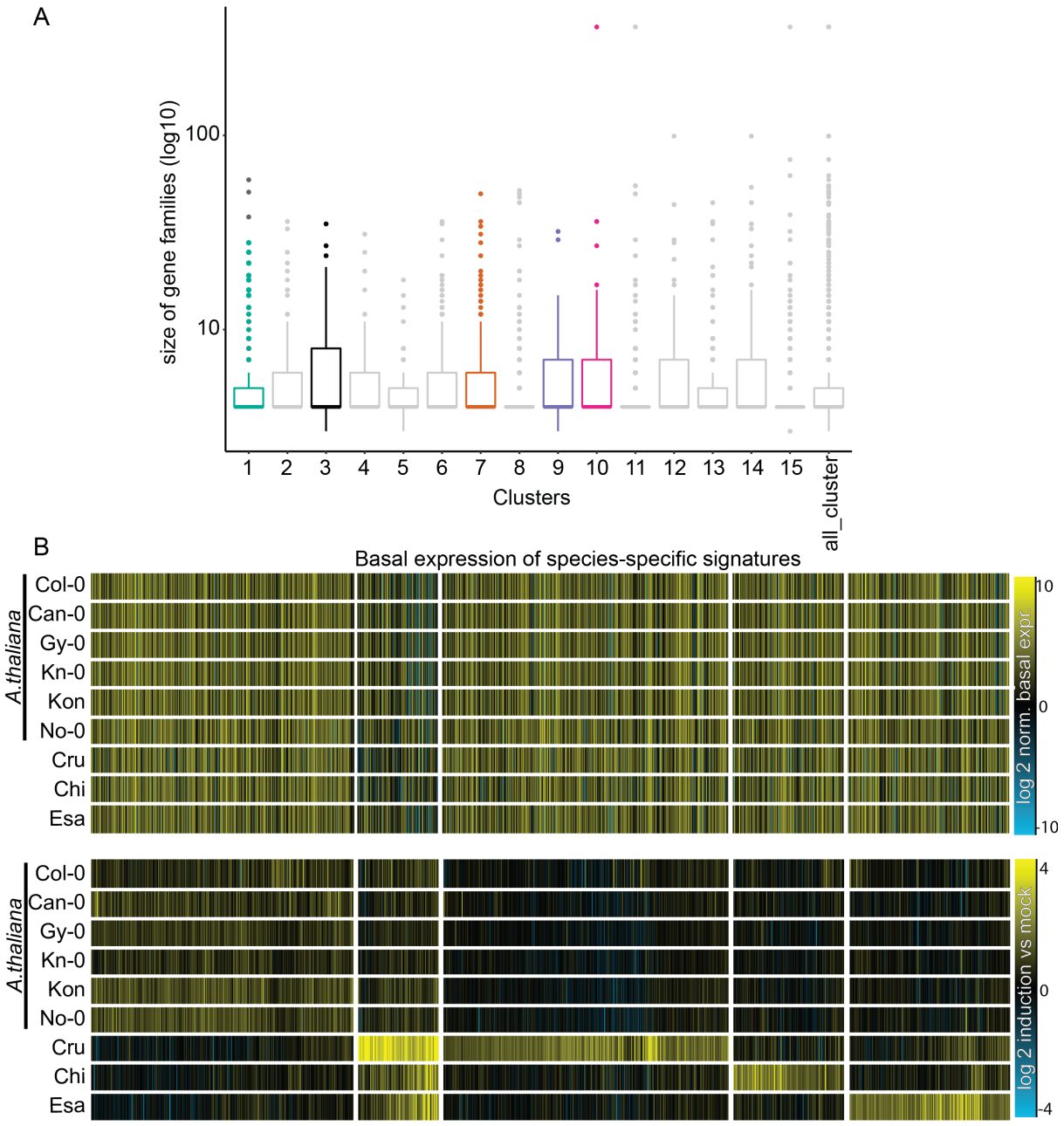

Supplement Figure 7: The size of gene family and basal gene expression levels do not explain species-specific expression signatures. A: The sizes of gene families among the 4 tested Brassicaceae species are plotted for each of the 15 clusters (See Figure 7). Species specific clusters are highlighted by colours (Ath = green, non-Ath = black, Cru = orange, Chi = purple, Esa = magenta). **B:** Basal (mock condition) expression levels (normalized and $\log_2$-transformed counts per million) of genes showing species-specific expression signatures are shown in the upper heatmap. Expression changes after flg22 treatment are shown in the bottom heatmap.

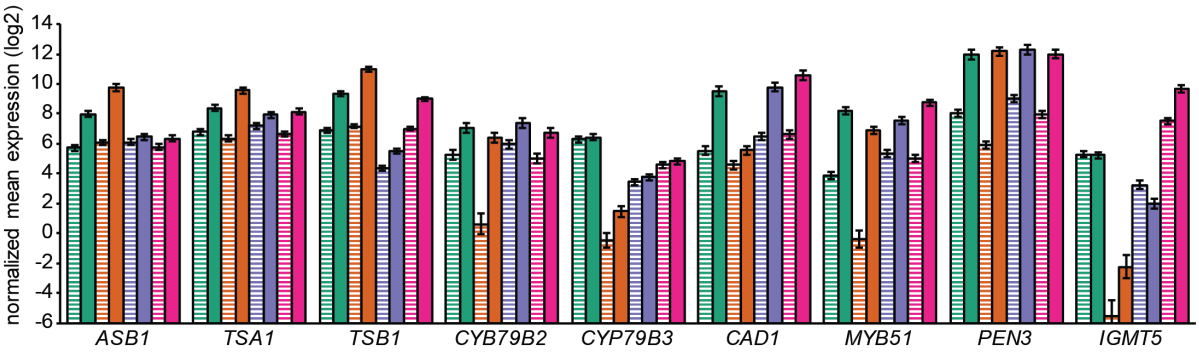

Supplement Figure 8: Some of key secondary metabolism genes are lowly expressed in *C. rubella* compared to other Brassicaceae species. Mean expression values ± SE (log_2-transformed counts per million) of mock and flg22-treated samples in RNAseq for genes exhibiting significantly different flg22-triggered expression changes in *C. rubella* compared to other Brassicaceae species were plotted.

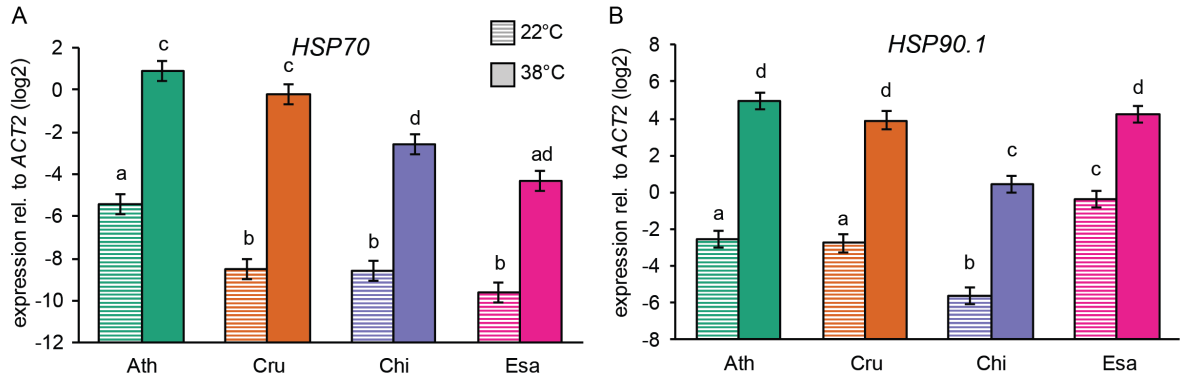

Supplement Figure 9: Conserved heat-stress responses in tested Brassicaceae species. 12-day-old Brassicaceae seedlings were transferred for 1 h to 22°C (control) or 38°C (heat-stress) and expression of heat-responsive marker genes *HSP70* and *HSP90.1* was quantified using RT-qPCR. Bars represent the means ±SE from 3 independent experiments (n = 3). Different letters indicate significant differences (mixed linear model followed by Student´s t-test; adjusted $p < 0.01$).

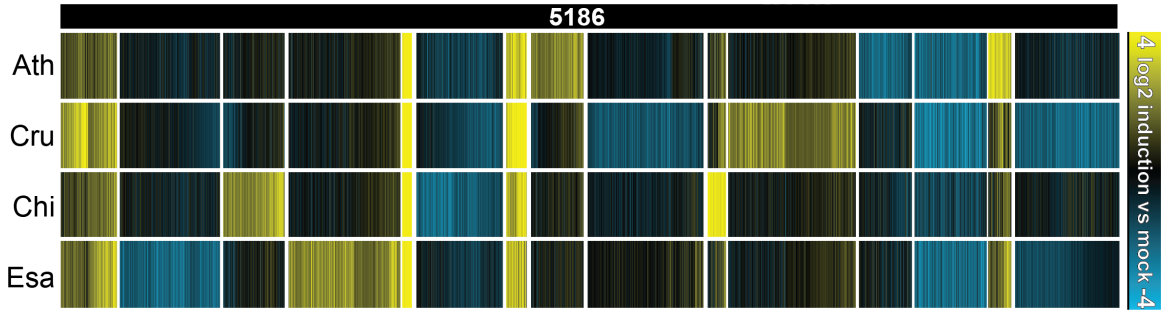

Supplement Figure 10: Heatmap for all DEGs in Brassicaceae species after heat stress treatment. Heatmap visualizing expression changes of all 5186 DEGs after 1 h heat stress in all tested Brassicaceae species generated using k-means clustering. In contrast to Figure 16, the RNAseq data depicted here was normalized and analyzed together for all four Brassicaceae, excluding genes with low expression in specific species.

Supplement Table 1: Mapping statistics of RNAseq reads from flg22 RNAseq dataset

Species	reference genome	mean No reads [Mio]	% mapped reads	% counted
Ath (Col-0)	Col-0 (TAIR10)	33.63	98.27	85.07
Cru	v1.0	33.53	94.72	87.44
Chi	v1.0	33.76	98.09	83.42
Esa	v1.0	32.23	96.88	87.87
Can-0	Col-0 (TAIR10)	20.40	97.66	92.02
Gy-0	Col-0 (TAIR10)	23.59	98.03	92.59
Kn-0	Col-0 (TAIR10)	21.43	98.08	92.30
Kondora	Col-0 (TAIR10)	21.27	97.94	92.37
No-0	Col-0 (TAIR10)	20.85	97.94	92.12
Can-0	Ca0	20.40	96.78	92.01
Gy-0	Gy0	23.59	96.90	91.13
Kn-0	Kn0	21.43	97.18	92.26
Kondora	Kon	21.27	97.16	92.35
No-0	No0	20.85	96.77	91.98

Supplement Table 2: Mapping statistics of RNAseq reads from heat-stress RNAseq dataset

Species	reference genome	mean No reads [Mio]	% mapped reads	% counted
Ath (Col-0)	Col-0 (TAIR10)	21.86	98.67	91.25
Cru	v1.0	20.78	95.96	83.46
Chi	v1.0	19.71	90.96	73.08
Esa	v1.0	21.37	92.63	83.35

Supplement Table 3: Overrepresented GO-terms for DEGs expression clusters 1h after flg22 treatment. The top 30 most significantly enriched biological processes were determined for each expression cluster depicted in Supplemental Figure 4. Grey terms have a adjusted p-value over 0.05 and are not considered significantly enriched.

Cluster	adj. p-value	GO_ID	No. Genes	Description
1	7.70E-02	50896	73	response to stimulus
1	2.33E-01	6790	9	sulfur metabolic process
1	2.33E-01	9733	12	response to auxin stimulus
1	2.33E-01	9719	24	response to endogenous stimulus
1	2.33E-01	44272	6	sulfur compound biosynthetic process
1	2.33E-01	44281	32	small molecule metabolic process
1	2.33E-01	44283	19	small molecule biosynthetic process
1	2.33E-01	9611	7	response to wounding
1	2.33E-01	6950	42	response to stress
1	2.33E-01	9725	21	response to hormone stimulus
1	2.33E-01	42221	38	response to chemical stimulus
1	2.33E-01	44242	4	cellular lipid catabolic process
1	2.33E-01	16559	2	peroxisome fission
1	2.33E-01	42762	2	regulation of sulfur metabolic process
1	2.33E-01	19758	3	glycosinolate biosynthetic process
1	2.33E-01	19761	3	glucosinolate biosynthetic process
1	2.33E-01	16144	3	S-glycoside biosynthetic process
1	2.33E-01	19748	11	secondary metabolic process
1	2.33E-01	96	4	sulfur amino acid metabolic process
1	2.33E-01	44282	7	small molecule catabolic process
1	2.33E-01	43289	2	apocarotenoid biosynthetic process
1	2.33E-01	9688	2	abscisic acid biosynthetic process
1	2.33E-01	50794	50	regulation of cellular process
1	2.33E-01	10033	25	response to organic substance
1	2.33E-01	16042	4	lipid catabolic process
1	2.33E-01	31668	6	cellular response to extracellular stimulus
1	2.33E-01	42545	6	cell wall modification
1	2.33E-01	71496	6	cellular response to external stimulus
1	2.33E-01	724	2	double-strand break repair via homologous recombination
1	2.33E-01	725	2	recombinational repair
2	3.56E-18	10200	19	response to chitin
2	3.15E-15	9743	20	response to carbohydrate stimulus
2	5.78E-13	42221	48	response to chemical stimulus
2	5.30E-12	10033	36	response to organic substance
2	2.95E-10	50896	62	response to stimulus

Cluster	adj. p-value	GO_ID	No. Genes	Description
2	7.93E-10	50832	13	defense response to fungus
2	1.96E-09	9620	14	response to fungus
2	2.56E-09	6952	25	defense response
2	7.54E-08	51707	21	response to other organism
2	1.40E-07	9607	21	response to biotic stimulus
2	3.09E-07	51704	23	multi-organism process
2	4.79E-06	6950	37	response to stress
2	1.74E-05	2376	13	immune system process
2	1.79E-05	43687	26	post-translational protein modification
2	2.54E-05	16998	5	cell wall macromolecule catabolic process
2	2.68E-05	31347	7	regulation of defense response
2	2.68E-05	6468	22	protein amino acid phosphorylation
2	4.57E-05	6464	27	protein modification process
2	4.92E-05	6955	12	immune response
2	4.92E-05	2679	3	respiratory burst involved in defense response
2	4.92E-05	51865	3	protein autoubiquitination
2	4.92E-05	10185	3	regulation of cellular defense response
2	6.68E-05	80134	7	regulation of response to stress
2	6.77E-05	16310	22	phosphorylation
2	7.10E-05	42742	10	defense response to bacterium
2	7.60E-05	60548	4	negative regulation of cell death
2	9.96E-05	45730	3	respiratory burst
2	1.33E-04	10941	5	regulation of cell death
2	1.76E-04	6796	22	phosphate metabolic process
2	1.76E-04	6793	22	phosphorus metabolic process
3	7.36E-02	6468	12	protein amino acid phosphorylation
3	7.36E-02	16310	12	phosphorylation
3	7.36E-02	9901	2	anther dehiscence
3	7.36E-02	6796	12	phosphate metabolic process
3	7.36E-02	6793	12	phosphorus metabolic process
3	8.33E-02	9900	2	dehiscence
3	8.33E-02	8219	5	cell death
3	8.33E-02	16265	5	death
3	8.33E-02	6950	17	response to stress
3	8.33E-02	43687	12	post-translational protein modification
3	8.33E-02	6464	13	protein modification process
3	1.11E-01	1561	1	fatty acid alpha-oxidation
3	1.26E-01	50896	24	response to stimulus
3	1.28E-01	70882	3	cellular cell wall organization or biogenesis
3	1.28E-01	6952	8	defense response
3	1.28E-01	43412	13	macromolecule modification
3	1.28E-01	5975	9	carbohydrate metabolic process
3	1.28E-01	12501	4	programmed cell death
3	1.40E-01	45490	1	pectin catabolic process
3	1.47E-01	48653	2	anther development
3	1.47E-01	44262	6	cellular carbohydrate metabolic process
3	1.47E-01	9830	1	cell wall modification involved in abscission
3	1.47E-01	43650	1	dicarboxylic acid biosynthetic process
3	1.47E-01	9423	1	chorismate biosynthetic process
3	1.47E-01	44277	1	cell wall disassembly
3	1.47E-01	15700	1	arsenite transport
3	1.47E-01	60871	1	cellular cell wall disassembly
3	1.76E-01	6915	3	apoptosis
3	1.76E-01	46713	1	boron transport
3	1.76E-01	6094	1	gluconeogenesis
4	3.89E-07	10033	24	response to organic substance
4	4.69E-07	50896	43	response to stimulus
4	5.78E-07	10200	9	response to chitin
4	5.78E-07	9607	17	response to biotic stimulus
4	1.79E-06	51707	16	response to other organism
4	2.73E-06	9743	10	response to carbohydrate stimulus
4	2.84E-06	6952	17	defense response
4	1.21E-05	42221	27	response to chemical stimulus
4	1.50E-05	6950	28	response to stress
4	3.63E-05	51704	16	multi-organism process
4	2.03E-03	9867	4	jasmonic acid mediated signaling pathway
4	2.03E-03	71395	4	cellular response to jasmonic acid stimulus
4	3.58E-03	6955	8	immune response
4	3.64E-03	31348	3	negative regulation of defense response
4	3.95E-03	2376	8	immune system process
4	3.95E-03	9753	6	response to jasmonic acid stimulus
4	6.50E-03	9814	5	defense response, incompatible interaction
4	6.99E-03	2238	2	response to molecule of fungal origin
4	7.24E-03	9617	7	response to bacterium
4	7.53E-03	23052	15	signaling

Cluster	adj. p-value	GO_ID	No. Genes	Description
4	8.55E-03	31347	4	regulation of defense response
4	8.55E-03	9697	2	salicylic acid biosynthetic process
4	8.80E-03	45087	7	innate immune response
4	9.06E-03	23033	11	signaling pathway
4	1.03E-02	42742	6	defense response to bacterium
4	1.03E-02	23046	10	signaling process
4	1.03E-02	23060	10	signal transmission
4	1.28E-02	80134	4	regulation of response to stress
4	1.88E-02	42762	2	regulation of sulfur metabolic process
4	1.88E-02	35556	4	intracellular signal transduction
5	1.46E-06	10200	7	response to chitin
5	2.85E-05	9743	7	response to carbohydrate stimulus
5	2.37E-03	45449	13	regulation of transcription
5	2.37E-03	10556	13	regulation of macromolecule biosynthetic process
5	2.37E-03	19219	13	regulation of nucleobase, nucleoside, nucleotide and nucleic acid metabolic process
5	2.37E-03	31326	13	regulation of cellular biosynthetic process
5	2.37E-03	9889	13	regulation of biosynthetic process
5	2.37E-03	51171	13	regulation of nitrogen compound metabolic process
5	3.07E-03	80090	13	regulation of primary metabolic process
5	3.48E-03	10468	13	regulation of gene expression
5	3.50E-03	31323	13	regulation of cellular metabolic process
5	3.50E-03	60255	13	regulation of macromolecule metabolic process
5	3.50E-03	10033	10	response to organic substance
5	3.71E-03	42221	13	response to chemical stimulus
5	6.47E-03	19222	13	regulation of metabolic process
5	2.22E-02	50896	17	response to stimulus
5	2.43E-02	46864	1	isoprenoid transport
5	2.43E-02	46865	1	terpenoid transport
5	3.63E-02	9723	3	response to ethylene stimulus
5	3.68E-02	6355	7	regulation of transcription, DNA-dependent
5	3.68E-02	51252	7	regulation of RNA metabolic process
5	6.02E-02	50794	13	regulation of cellular process
5	7.57E-02	15692	1	lead ion transport
5	1.52E-01	50789	13	regulation of biological process
5	1.73E-01	6979	3	response to oxidative stress
5	2.04E-01	65007	14	biological regulation
5	2.23E-01	6536	1	glutamate metabolic process
5	2.57E-01	43562	1	cellular response to nitrogen levels
5	2.57E-01	9725	5	response to hormone stimulus
5	2.57E-01	9751	2	response to salicylic acid stimulus
6	7.27E-07	42221	87	response to chemical stimulus
6	1.06E-05	10033	58	response to organic substance
6	1.06E-05	50896	131	response to stimulus
6	2.71E-05	35466	14	regulation of signaling pathway
6	2.71E-05	9607	37	response to biotic stimulus
6	2.00E-04	51707	34	response to other organism
6	2.22E-04	10646	13	regulation of cell communication
6	2.80E-04	51704	40	multi-organism process
6	3.38E-04	70887	26	cellular response to chemical stimulus
6	3.53E-04	48583	16	regulation of response to stimulus
6	4.40E-04	65007	123	biological regulation
6	9.70E-04	6950	78	response to stress
6	9.70E-04	70297	5	regulation of two-component signal transduction system (phosphorelay)
6	9.70E-04	10104	5	regulation of ethylene mediated signaling pathway
6	1.21E-03	6464	57	protein modification process
6	1.21E-03	9787	7	regulation of abscisic acid mediated signaling pathway
6	1.55E-03	9651	24	response to salt stress
6	1.69E-03	6970	25	response to osmotic stress
6	1.69E-03	50794	95	regulation of cellular process
6	1.71E-03	9719	42	response to endogenous stimulus
6	1.92E-03	23033	34	signaling pathway
6	1.95E-03	35467	7	negative regulation of signaling pathway
6	2.17E-03	10648	7	negative regulation of cell communication
6	2.17E-03	9725	39	response to hormone stimulus
6	3.67E-03	43067	6	regulation of programmed cell death
6	4.32E-03	22622	17	root system development
6	4.32E-03	48364	17	root development
6	4.67E-03	70298	4	negative regulation of two-component signal transduction system (phosphorelay)
6	4.67E-03	42631	4	cellular response to water deprivation
6	4.67E-03	10105	4	negative regulation of ethylene mediated signaling pathway
7	2.00E-01	42219	4	cellular amino acid derivative catabolic process
7	2.00E-01	9861	3	jasmonic acid and ethylene-dependent systemic resistance

Cluster	adj. p-value	GO_ID	No. Genes	Description
7	2.00E-01	15893	4	drug transport
7	2.00E-01	42493	4	response to drug
7	2.50E-01	48468	9	cell development
7	2.50E-01	9888	11	tissue development
7	2.50E-01	19439	3	aromatic compound catabolic process
7	2.50E-01	22622	10	root system development
7	2.50E-01	48364	10	root development
7	2.50E-01	6575	10	cellular amino acid derivative metabolic process
7	2.50E-01	38	3	very long-chain fatty acid metabolic process
7	2.50E-01	44281	32	small molecule metabolic process
7	2.50E-01	9698	7	phenylpropanoid metabolic process
7	2.50E-01	16126	3	sterol biosynthetic process
7	2.50E-01	9719	23	response to endogenous stimulus
7	2.50E-01	6725	11	cellular aromatic compound metabolic process
7	2.50E-01	272	3	polysaccharide catabolic process
7	2.50E-01	6855	3	drug transmembrane transport
7	2.50E-01	9653	16	anatomical structure morphogenesis
7	2.50E-01	6810	36	transport
7	2.50E-01	44262	14	cellular carbohydrate metabolic process
7	2.50E-01	32989	10	cellular component morphogenesis
7	2.50E-01	16125	3	sterol metabolic process
7	2.50E-01	50896	67	response to stimulus
7	2.50E-01	51179	37	localization
7	2.50E-01	51234	36	establishment of localization
7	2.50E-01	904	6	cell morphogenesis involved in differentiation
7	2.50E-01	6913	4	nucleocytoplasmic transport
7	2.50E-01	51169	4	nuclear transport
7	2.50E-01	9734	3	auxin mediated signaling pathway
8	2.89E-04	65007	105	biological regulation
8	2.02E-03	50794	81	regulation of cellular process
8	2.91E-03	50789	88	regulation of biological process
8	6.79E-03	19219	54	regulation of nucleobase, nucleoside, nucleotide and nucleic acid metabolic process
8	6.79E-03	10556	53	regulation of macromolecule biosynthetic process
8	6.79E-03	45449	52	regulation of transcription
8	6.79E-03	51171	54	regulation of nitrogen compound metabolic process
8	8.56E-03	31326	53	regulation of cellular biosynthetic process
8	8.56E-03	9889	53	regulation of biosynthetic process
8	8.56E-03	7389	10	pattern specification process
8	8.56E-03	31323	56	regulation of cellular metabolic process
8	1.00E-02	80090	54	regulation of primary metabolic process
8	1.00E-02	60255	56	regulation of macromolecule metabolic process
8	1.22E-02	9719	33	response to endogenous stimulus
8	1.49E-02	10468	54	regulation of gene expression
8	1.96E-02	19222	58	regulation of metabolic process
8	2.19E-02	9938	3	negative regulation of gibberellic acid mediated signaling pathway
8	2.29E-02	6869	10	lipid transport
8	2.50E-02	48878	9	chemical homeostasis
8	2.56E-02	3002	8	regionalization
8	3.27E-02	42592	12	homeostatic process
8	3.36E-02	6833	3	water transport
8	3.36E-02	42044	3	fluid transport
8	3.46E-02	9725	29	response to hormone stimulus
8	3.89E-02	10876	10	lipid localization
8	4.07E-02	51457	2	maintenance of protein location in nucleus
8	6.33E-02	9937	3	regulation of gibberellic acid mediated signaling pathway
8	6.33E-02	50896	87	response to stimulus
8	6.33E-02	10033	35	response to organic substance
8	9.77E-02	45165	4	cell fate commitment
9	5.12E-02	9926	4	auxin polar transport
9	5.12E-02	60918	4	auxin transport
9	5.12E-02	9914	4	hormone transport
9	8.70E-02	10540	2	basipetal auxin transport
9	8.70E-02	6820	4	anion transport
9	1.85E-01	6817	2	phosphate transport
9	1.85E-01	15698	3	inorganic anion transport
9	1.85E-01	65008	10	regulation of biological quality
9	1.85E-01	43086	3	negative regulation of catalytic activity
9	1.85E-01	51346	1	negative regulation of hydrolase activity
9	1.85E-01	43666	1	regulation of phosphoprotein phosphatase activity
9	1.85E-01	10921	1	regulation of phosphatase activity
9	1.85E-01	10923	1	negative regulation of phosphatase activity
9	1.85E-01	32515	1	negative regulation of phosphoprotein phosphatase activity
9	1.85E-01	60191	1	regulation of lipase activity

Cluster	adj. p-value	GO_ID	No. Genes	Description
9	1.85E-01	51004	1	regulation of lipoprotein lipase activity
9	1.99E-01	44092	3	negative regulation of molecular function
9	1.99E-01	10817	4	regulation of hormone levels
9	1.99E-01	10315	1	auxin efflux
9	1.99E-01	80055	1	low affinity nitrate transport
9	1.99E-01	10119	2	regulation of stomatal movement
9	1.99E-01	6464	15	protein modification process
9	1.99E-01	9734	2	auxin mediated signaling pathway
9	1.99E-01	6810	17	transport
9	1.99E-01	51234	17	establishment of localization
9	1.99E-01	10289	1	homogalacturonan biosynthetic process
9	1.99E-01	46477	1	glycosylceramide catabolic process
9	1.99E-01	46479	1	glycosphingolipid catabolic process
9	1.99E-01	46514	1	ceramide catabolic process
9	1.99E-01	46521	1	sphingoid catabolic process
10	2.22E-01	10345	2	suberin biosynthetic process
10	2.22E-01	9312	3	oligosaccharide biosynthetic process
10	2.22E-01	16051	7	carbohydrate biosynthetic process
10	2.22E-01	42546	4	cell wall biogenesis
10	2.22E-01	80090	24	regulation of primary metabolic process
10	2.22E-01	70882	4	cellular cell wall organization or biogenesis
10	2.22E-01	50794	33	regulation of cellular process
10	2.22E-01	19219	23	regulation of nucleobase, nucleoside, nucleotide and nucleic acid metabolic process
10	2.22E-01	31326	23	regulation of cellular biosynthetic process
10	2.22E-01	9889	23	regulation of biosynthetic process
10	2.22E-01	51171	23	regulation of nitrogen compound metabolic process
10	2.22E-01	7131	2	reciprocal meiotic recombination
10	2.22E-01	10273	1	detoxification of copper ion
10	2.22E-01	6216	1	cytidine catabolic process
10	2.22E-01	6279	1	premeiotic DNA synthesis
10	2.22E-01	80142	1	regulation of salicylic acid biosynthetic process
10	2.22E-01	30397	1	membrane disassembly
10	2.22E-01	9972	1	cytidine deamination
10	2.22E-01	10184	1	cytokinin transport
10	2.22E-01	45449	22	regulation of transcription
10	2.22E-01	31323	24	regulation of cellular metabolic process
10	2.22E-01	6310	3	DNA recombination
10	2.22E-01	10556	22	regulation of macromolecule biosynthetic process
10	2.22E-01	9311	3	oligosaccharide metabolic process
10	2.22E-01	46688	2	response to copper ion
10	2.22E-01	9699	4	phenylpropanoid biosynthetic process
10	2.22E-01	6725	7	cellular aromatic compound metabolic process
10	2.22E-01	9832	3	plant-type cell wall biogenesis
10	2.22E-01	16138	3	glycoside biosynthetic process
10	2.22E-01	50789	35	regulation of biological process
11	5.49E-08	9416	33	response to light stimulus
11	6.77E-08	9314	33	response to radiation
11	2.30E-05	31326	60	regulation of cellular biosynthetic process
11	2.30E-05	9889	60	regulation of biosynthetic process
11	3.91E-05	10556	58	regulation of macromolecule biosynthetic process
11	3.91E-05	51171	59	regulation of nitrogen compound metabolic process
11	4.60E-05	19219	58	regulation of nucleobase, nucleoside, nucleotide and nucleic acid metabolic process
11	4.60E-05	80090	60	regulation of primary metabolic process
11	4.89E-05	65007	100	biological regulation
11	5.07E-05	45449	56	regulation of transcription
11	5.86E-05	9725	36	response to hormone stimulus
11	1.02E-04	31323	60	regulation of cellular metabolic process
11	1.16E-04	9638	5	phototropism
11	1.23E-04	9719	37	response to endogenous stimulus
11	1.23E-04	60255	60	regulation of macromolecule metabolic process
11	1.72E-04	19222	63	regulation of metabolic process
11	2.09E-04	10468	58	regulation of gene expression
11	3.09E-04	9739	11	response to gibberellin stimulus
11	9.57E-04	10033	40	response to organic substance
11	1.34E-03	9628	43	response to abiotic stimulus
11	2.34E-03	9639	12	response to red or far red light
11	2.62E-03	16556	3	mRNA modification
11	2.83E-03	50794	73	regulation of cellular process
11	5.05E-03	10374	5	stomatal complex development
11	7.98E-03	48367	16	shoot development
11	8.69E-03	22621	16	shoot system development
11	8.69E-03	65008	24	regulation of biological quality
11	8.92E-03	9606	6	tropism

Cluster	adj. p-value	GO_ID	No. Genes	Description
11	9.02E-03	50789	78	regulation of biological process
11	1.04E-02	48827	13	phyllome development
12	7.22E-05	2376	16	immune system process
12	7.22E-05	45087	15	innate immune response
12	7.22E-05	10200	10	response to chitin
12	1.02E-04	6955	15	immune response
12	1.05E-04	9617	14	response to bacterium
12	4.06E-04	48584	7	positive regulation of response to stimulus
12	4.06E-04	6952	22	defense response
12	4.06E-04	8219	12	cell death
12	4.06E-04	16265	12	death
12	4.06E-04	12501	11	programmed cell death
12	4.31E-04	50896	63	response to stimulus
12	4.31E-04	2218	5	activation of innate immune response
12	4.31E-04	2253	5	activation of immune response
12	4.64E-04	42221	40	response to chemical stimulus
12	4.64E-04	51707	19	response to other organism
12	4.64E-04	45089	5	positive regulation of innate immune response
12	4.64E-04	45089	5	positive regulation of immune response
12	4.64E-04	45089	5	positive regulation of immune system process
12	4.82E-04	45089	42	response to stress
12	6.76E-04	45089	19	response to biotic stimulus
12	8.07E-04	45089	5	positive regulation of defense response
12	8.93E-04	45089	3	detection of biotic stimulus
12	1.12E-03	45089	10	response to carbohydrate stimulus
12	1.65E-03	45089	27	response to organic substance
12	1.88E-03	45089	5	regulation of innate immune response
12	2.06E-03	45089	10	defense response to bacterium
12	2.35E-03	45089	6	regulation of defense response
12	2.35E-03	45089	5	regulation of immune response
12	2.35E-03	45089	5	regulation of immune system process
12	2.39E-03	45089	19	signaling pathway
13	6.36E-11	6468	35	protein amino acid phosphorylation
13	7.11E-11	6796	37	phosphate metabolic process
13	7.11E-11	6793	37	phosphorus metabolic process
13	9.93E-11	9743	17	response to carbohydrate stimulus
13	9.93E-11	10200	14	response to chitin
13	9.93E-11	16310	35	phosphorylation
13	1.72E-10	43687	38	post-translational protein modification
13	1.59E-09	6464	39	protein modification process
13	2.74E-08	50896	65	response to stimulus
13	2.74E-08	43412	39	macromolecule modification
13	2.39E-07	9611	12	response to wounding
13	5.05E-07	10033	31	response to organic substance
13	8.74E-07	42221	41	response to chemical stimulus
13	2.57E-06	6950	42	response to stress
13	1.25E-03	6952	18	defense response
13	1.34E-03	9719	21	response to endogenous stimulus
13	1.34E-03	51707	16	response to other organism
13	1.69E-03	9737	11	response to abscisic acid stimulus
13	1.94E-03	9607	16	response to biotic stimulus
13	8.52E-03	51704	17	multi-organism process
13	9.51E-03	31347	5	regulation of defense response
13	1.90E-02	23033	15	signaling pathway
13	1.90E-02	80134	5	regulation of response to stress
13	1.90E-02	15695	2	organic cation transport
13	1.90E-02	15696	2	ammonium transport
13	2.01E-02	9725	17	response to hormone stimulus
13	2.62E-02	10555	2	response to mannitol stimulus
13	3.11E-02	23052	20	signaling
13	3.59E-02	44267	41	cellular protein metabolic process
13	3.63E-02	6904	3	vesicle docking involved in exocytosis
14	1.56E-13	43687	50	post-translational protein modification
14	3.80E-13	6796	46	phosphate metabolic process
14	3.80E-13	6793	46	phosphorus metabolic process
14	4.44E-13	16310	44	phosphorylation
14	5.69E-13	6468	42	protein amino acid phosphorylation
14	9.30E-13	6464	51	protein modification process
14	4.62E-11	43412	51	macromolecule modification
14	3.98E-04	9611	10	response to wounding
14	1.21E-03	45860	4	positive regulation of protein kinase activity
14	1.21E-03	33674	4	positive regulation of kinase activity
14	2.53E-03	51347	4	positive regulation of transferase activity
14	1.22E-02	43549	4	regulation of kinase activity
14	1.22E-02	45859	4	regulation of protein kinase activity

Cluster	adj. p-value	GO_ID	No. Genes	Description
14	1.22E-02	50896	60	response to stimulus
14	1.55E-02	44267	53	cellular protein metabolic process
14	1.55E-02	51338	4	regulation of transferase activity
14	1.55E-02	6950	39	response to stress
14	1.55E-02	48317	2	seed morphogenesis
14	1.61E-02	43085	4	positive regulation of catalytic activity
14	1.61E-02	42325	4	regulation of phosphorylation
14	1.74E-02	44093	4	positive regulation of molecular function
14	1.82E-02	9620	8	response to fungus
14	1.86E-02	19220	4	regulation of phosphate metabolic process
14	1.86E-02	51174	4	regulation of phosphorus metabolic process
14	1.86E-02	42221	36	response to chemical stimulus
14	1.86E-02	6952	18	defense response
14	2.59E-02	9607	16	response to biotic stimulus
14	3.23E-02	9743	8	response to carbohydrate stimulus
14	3.30E-02	19538	56	protein metabolic process
14	3.50E-02	10200	6	response to chitin
15	1.11E-10	90304	97	nucleic acid metabolic process
15	5.45E-09	6139	109	nucleobase, nucleoside, nucleotide and nucleic acid metabolic process
15	6.21E-09	6259	47	DNA metabolic process
15	8.61E-08	34641	130	cellular nitrogen compound metabolic process
15	1.49E-07	6807	133	nitrogen compound metabolic process
15	2.26E-06	32501	140	multicellular organismal process
15	8.59E-06	6974	27	response to DNA damage stimulus
15	8.95E-06	6281	26	DNA repair
15	9.22E-06	7275	132	multicellular organismal development
15	1.36E-05	48608	71	reproductive structure development
15	1.49E-05	9791	81	post-embryonic development
15	2.06E-05	6260	19	DNA replication
15	2.10E-05	32502	140	developmental process
15	2.15E-05	9314	51	response to radiation
15	4.01E-05	9416	49	response to light stimulus
15	4.01E-05	7167	19	enzyme linked receptor protein signaling pathway
15	4.01E-05	7169	19	transmembrane receptor protein tyrosine kinase signaling pathway
15	5.82E-05	48856	111	anatomical structure development
15	1.10E-04	7018	12	microtubule-based movement
15	1.37E-04	48316	46	seed development
15	1.46E-04	3006	73	reproductive developmental process
15	1.56E-04	7166	20	cell surface receptor linked signaling pathway
15	1.79E-04	8033	11	tRNA processing
15	1.92E-04	9658	14	chloroplast organization
15	2.00E-04	6298	7	mismatch repair
15	2.75E-04	9793	40	embryonic development ending in seed dormancy
15	3.11E-04	9790	44	embryonic development
15	3.42E-04	10154	46	fruit development
15	5.16E-04	7017	17	microtubule-based process
15	5.32E-04	3	77	reproduction

Supplement Table 4: Known TF-motifs enriched in *A. thaliana* 5´regulatory regions of DEGs. Known TF-motifs were determined using AME for the -500 bp region upstream of the transcriptional start site. The motifs were determined separately for each expression clusters depicted in Supplemental Figure 4.

Cluster	Motif ID	Binding TF	Motif	p-val	adj. p-val
1	MA1079.1	WRKY21	(NNRGTCAACG)	2.59E-05	0.01256
1	MA1386.1	AT1G25550	(RGAATMTTCND)	6.21E-05	0.02992
1	MA1164.1	AT4G37180	(HARAAGATTCY)	6.45E-05	0.03103
1	MA1089.1	WRKY57	(DWRGTCAAMN)	9.86E-05	0.04706
2	MA1094.1	WRKY8	(NRGTCAAMN)	3.99E-11	1.95E-08
2	MA1089.1	WRKY57	(DWRGTCAAMN)	6.77E-11	3.31E-08
2	MA1088.1	WRKY48	(NNRGTCAAMN)	8.45E-11	4.13E-08
2	MA1317.1	WRKY50	(YKTTGACTTTTTH)	5.57E-10	2.72E-07
2	MA1079.1	WRKY21	(NNRGTCAACG)	1.91E-09	9.33E-07
2	MA1086.1	WRKY43	(HRGTCAAMVN)	2.37E-09	1.16E-06
2	MA1076.1	WRKY15	(NRGTCAACSN)	2.41E-09	1.18E-06
2	MA1085.2	WRKY40	(HWAGTCAANN)	3.91E-09	1.91E-06
2	MA1311.1	WRKY28	(DDCGTTGACTTTT)	9.95E-09	4.87E-06
2	MA1077.1	WRKY18	(NHRGTCAAVV)	1.42E-08	6.95E-06
2	MA1316.1	WRKY71	(AAAAGTCAACG)	2.51E-08	1.23E-05
2	MA1304.1	WRKY59	(HAAAAGTCAAMN)	3.14E-08	1.54E-05
2	MA1315.1	WRKY24	(NCGTTGACTTTTTW)	6.31E-08	3.09E-05
2	MA1295.1	WRKY20	(DNCGTTGACYWDD)	7.89E-08	3.86E-05
2	MA1298.1	WRKY29	(AAAAGTCAACK)	8.81E-08	4.31E-05
2	MA1302.1	WRKY65	(AAAAGTCAACG)	9.02E-08	4.41E-05
2	MA1313.1	WRKY7	(DNCGTTGACTTTTT)	1.88E-07	9.19E-05
2	MA1310.1	WRKY42	(BWTDMHHHNNCGTTGACTWWD)	1.99E-07	9.74E-05
2	MA1305.1	WRKY55	(DNCGTTGACTTT)	2.49E-07	0.0001215
2	MA1303.1	WRKY22	(AAAAGTCAACKNH)	2.55E-07	0.0001244
2	MA1314.1	WRKY14	(AAAAGTCAACGNH)	2.66E-07	0.0001298
2	MA1306.1	WRKY11	(DNCGTTGACTTTTD)	3.70E-07	0.0001808
2	MA1083.1	WRKY30	(RGTCAACGNN)	3.70E-07	0.000181
2	MA1309.1	WRKY3	(AAAAGTCAACG)	5.85E-07	0.0002859
2	MA1301.1	WRKY33	(AAAAGTCAACG)	6.49E-07	0.0003174
2	MA1093.1	WRKY75	(HRGTCAAC)	7.69E-07	0.0003758
2	MA1078.1	WRKY2	(BGGTCAAM)	8.59E-07	0.00042
2	MA1308.1	WRKY70	(DNCGTTGACTTTT)	1.17E-06	0.0005722
2	MA1090.1	WRKY60	(NYGGTCAACSN)	2.33E-06	0.001137
2	MA1081.1	WRKY25	(YGGTCAAC)	2.93E-06	0.001434
2	MA1300.1	WRKY6	(CGTTGACTWWDDYWDWNHH)	4.33E-06	0.002113
2	MA1092.1	WRKY63	(HGGTCAAC)	5.03E-06	0.002458
2	MA1318.1	WRKY27	(ANCGTTGACTTTT)	5.25E-06	0.002562
2	MA1299.1	WRKY17	(AAAAAGTCAACGNH)	6.76E-06	0.003298
2	MA1091.1	WRKY62	(TGGTCAAC)	9.18E-06	0.004479
2	MA1080.1	WRKY23	(AGTCAACG)	9.57E-06	0.004668
2	MA1084.1	WRKY38	(CGTTGACC)	1.05E-05	0.005098
2	MA1087.1	WRKY45	(CGTTGACY)	1.77E-05	0.008601
2	MA1297.1	WRKY26	(AAAAGTCAACGNY)	1.95E-05	0.009502
2	MA1307.1	WRKY31	(DDNNHWRHHAAAGTCAACG)	2.52E-05	0.01226
2	MA1075.1	WRKY12	(CGTTGACC)	2.67E-05	0.01297
2	MA1162.1	TCX2	(WTTYAAAATTYAAAW)	3.17E-05	0.0154
4	MA1089.1	WRKY57	(DWRGTCAAMN)	7.95E-08	3.89E-05
4	MA1088.1	WRKY48	(NNRGTCAAMN)	8.06E-08	3.94E-05
4	MA1077.1	WRKY18	(NHRGTCAAVV)	9.98E-08	4.88E-05
4	MA1094.1	WRKY8	(NRGTCAAMN)	1.39E-07	6.78E-05
4	MA1315.1	WRKY24	(NCGTTGACTTTTTW)	2.50E-07	0.0001224
4	MA1079.1	WRKY21	(NNRGTCAACG)	3.32E-07	0.0001625
4	MA1318.1	WRKY27	(ANCGTTGACTTTT)	3.87E-07	0.0001894
4	MA1083.1	WRKY30	(RGTCAACGNN)	4.37E-07	0.0002138
4	MA1305.1	WRKY55	(DNCGTTGACTTT)	4.96E-07	0.0002425
4	MA1076.1	WRKY15	(NRGTCAACSN)	5.72E-07	0.0002797
4	MA1317.1	WRKY50	(YKTTGACTTTTTH)	7.91E-07	0.0003869
4	MA1295.1	WRKY20	(DNCGTTGACYWDD)	8.22E-07	0.0004018
4	MA1086.1	WRKY43	(HRGTCAAMVN)	9.17E-07	0.0004481
4	MA1087.1	WRKY45	(CGTTGACY)	1.08E-06	0.0005285
4	MA1080.1	WRKY23	(AGTCAACG)	1.21E-06	0.0005895
4	MA1309.1	WRKY3	(AAAAGTCAACG)	1.34E-06	0.0006524
4	MA1085.2	WRKY40	(HWAGTCAANN)	1.46E-06	0.0007128
4	MA1316.1	WRKY71	(AAAAGTCAACG)	1.73E-06	0.0008437
4	MA1308.1	WRKY70	(DNCGTTGACTTTT)	1.78E-06	0.0008701
4	MA1311.1	WRKY28	(DDCGTTGACTTTT)	1.97E-06	0.0009624
4	MA1093.1	WRKY75	(HRGTCAAC)	2.23E-06	0.00109
4	MA1306.1	WRKY11	(DNCGTTGACTTTTD)	2.69E-06	0.001314
4	MA1304.1	WRKY59	(HAAAAGTCAAMN)	2.89E-06	0.001414
4	MA1091.1	WRKY62	(TGGTCAAC)	3.23E-06	0.001576
4	MA1084.1	WRKY38	(CGTTGACC)	3.28E-06	0.001601

Cluster	Motif ID	Binding TF	Motif	p-val	adj. p-val
4	MA1303.1	WRKY22	(AAAAGTCAACKNH)	3.30E-06	0.001613
4	MA1300.1	WRKY6	(CGTTGACTWWDDYWDWNHH)	3.49E-06	0.001707
4	MA1301.1	WRKY33	(AAAAGTCAACG)	3.95E-06	0.001932
4	MA1314.1	WRKY14	(AAAAGTCAACGNH)	3.97E-06	0.00194
4	MA1092.1	WRKY63	(HGGTCAAC)	4.05E-06	0.001979
4	MA1081.1	WRKY25	(YGGTCAAC)	5.62E-06	0.002745
4	MA1313.1	WRKY7	(DNCGTTGACTTTTT)	7.10E-06	0.003465
4	MA1299.1	WRKY17	(AAAAAGTCAACGNH)	7.43E-06	0.003625
4	MA1090.1	WRKY60	(NYGGTCAACSN)	7.52E-06	0.00367
4	MA1075.1	WRKY12	(CGTTGACC)	9.60E-06	0.004681
4	MA1298.1	WRKY29	(AAAAGTCAACK)	1.43E-05	0.00695
4	MA1302.1	WRKY65	(AAAAGTCAACG)	1.74E-05	0.008489
4	MA1078.1	WRKY2	(BGGTCAAM)	2.20E-05	0.01068
4	MA1307.1	WRKY31	(DDNNHWRHHAAAGTCAACG)	3.63E-05	0.01758
4	MA1312.1	WRKY47	(MYYKNCGTTGACYW)	6.11E-05	0.02943
4	MA1297.1	WRKY26	(AAAAGTCAACGNY)	6.77E-05	0.03256
4	MA1036.1	MYB111	(GKTAGGTR)	7.75E-05	0.03718
4	MA1040.1	MYB46	(GKTAGGTR)	9.06E-05	0.04335
4	MA1310.1	WRKY42	(BWTDMHHHNNCGTTGACTWWD)	0.0001007	0.04806
5	MA1081.1	WRKY25	(YGGTCAAC)	2.10E-12	1.03E-09
5	MA1078.1	WRKY2	(BGGTCAAM)	3.37E-11	1.65E-08
5	MA1092.1	WRKY63	(HGGTCAAC)	3.96E-11	1.94E-08
5	MA1088.1	WRKY48	(NNRGTCAAMN)	1.22E-10	5.94E-08
5	MA1090.1	WRKY60	(NYGGTCAACSN)	3.06E-09	1.50E-06
5	MA1077.1	WRKY18	(NHRGTCAAVV)	3.44E-09	1.68E-06
5	MA1094.1	WRKY8	(NRGTCAAMN)	3.56E-09	1.74E-06
5	MA1295.1	WRKY20	(DNCGTTGACYWDD)	1.40E-08	6.83E-06
5	MA1076.1	WRKY15	(NRGTCAACSN)	1.43E-08	7.00E-06
5	MA1091.1	WRKY62	(TGGTCAAC)	2.25E-08	1.10E-05
5	MA1093.1	WRKY75	(HRGTCAAC)	5.42E-08	2.65E-05
5	MA1086.1	WRKY43	(HRGTCAAMVN)	6.21E-08	3.04E-05
5	MA1084.1	WRKY38	(CGTTGACC)	1.07E-07	5.21E-05
5	MA1089.1	WRKY57	(DWRGTCAAMN)	1.30E-07	6.37E-05
5	MA1079.1	WRKY21	(NNRGTCAACG)	3.39E-07	0.0001659
5	MA1310.1	WRKY42	(BWTDMHHHNNCGTTGACTWWD)	7.01E-07	0.0003428
5	MA1075.1	WRKY12	(CGTTGACC)	7.95E-07	0.0003886
5	MA1300.1	WRKY6	(CGTTGACTWWDDYWDWNHH)	8.20E-07	0.0004008
5	MA1309.1	WRKY3	(AAAAGTCAACG)	1.09E-06	0.0005348
5	MA1301.1	WRKY33	(AAAAGTCAACG)	1.32E-06	0.0006439
5	MA1304.1	WRKY59	(HAAAAGTCAAMN)	1.53E-06	0.0007458
5	MA1083.1	WRKY30	(RGTCAACGNN)	1.59E-06	0.0007766
5	MA1087.1	WRKY45	(CGTTGACY)	2.72E-06	0.001327
5	MA1307.1	WRKY31	(DDNNHWRHHAAAGTCAACG)	2.83E-06	0.001382
5	MA1305.1	WRKY55	(DNCGTTGACTTT)	3.38E-06	0.001652
5	MA1311.1	WRKY28	(DDCGTTGACTTTT)	4.84E-06	0.002363
5	MA0589.1	ZAP1	(TTGACCGAGYY)	7.44E-06	0.003633
5	MA1080.1	WRKY23	(AGTCAACG)	1.02E-05	0.004985
5	MA1315.1	WRKY24	(NCGTTGACTTTTTW)	1.11E-05	0.005413
5	MA1302.1	WRKY65	(AAAAGTCAACG)	1.12E-05	0.005449
5	MA1314.1	WRKY14	(AAAAGTCAACGNH)	1.49E-05	0.007257
5	MA1298.1	WRKY29	(AAAAGTCAACK)	1.80E-05	0.008759
5	MA1317.1	WRKY50	(YKTTGACTTTTTH)	1.92E-05	0.009337
5	MA1297.1	WRKY26	(AAAAGTCAACGNY)	3.71E-05	0.01798
5	MA1303.1	WRKY22	(AAAAGTCAACKNH)	5.98E-05	0.02884
5	MA1316.1	WRKY71	(AAAAGTCAACG)	6.14E-05	0.0296
5	MA1306.1	WRKY11	(DNCGTTGACTTTTD)	7.93E-05	0.03805
5	MA0930.1	ABF3	(ACACGTGT)	9.59E-05	0.04581
6	MA1089.1	WRKY57	(DWRGTCAAMN)	9.53E-10	4.66E-07
6	MA1094.1	WRKY8	(NRGTCAAMN)	1.67E-09	8.14E-07
6	MA1090.1	WRKY60	(NYGGTCAACSN)	1.05E-08	5.15E-06
6	MA1086.1	WRKY43	(HRGTCAAMVN)	1.34E-08	6.53E-06
6	MA1079.1	WRKY21	(NNRGTCAACG)	1.93E-08	9.44E-06
6	MA1304.1	WRKY59	(HAAAAGTCAAMN)	2.65E-08	1.30E-05
6	MA1076.1	WRKY15	(NRGTCAACSN)	2.69E-08	1.32E-05
6	MA1077.1	WRKY18	(NHRGTCAAVV)	3.14E-08	1.54E-05
6	MA1311.1	WRKY28	(DDCGTTGACTTTT)	4.69E-08	2.30E-05
6	MA1302.1	WRKY65	(AAAAGTCAACG)	5.61E-08	2.75E-05
6	MA1088.1	WRKY48	(NNRGTCAAMN)	7.53E-08	3.68E-05
6	MA1316.1	WRKY71	(AAAAGTCAACG)	7.80E-08	3.82E-05
6	MA1091.1	WRKY62	(TGGTCAAC)	7.88E-08	3.85E-05
6	MA1314.1	WRKY14	(AAAAGTCAACGNH)	7.93E-08	3.88E-05
6	MA1087.1	WRKY45	(CGTTGACY)	9.30E-08	4.55E-05
6	MA1295.1	WRKY20	(DNCGTTGACYWDD)	1.15E-07	5.65E-05
6	MA1310.1	WRKY42	(BWTDMHHHNNCGTTGACTWWD)	1.92E-07	9.40E-05
6	MA1305.1	WRKY55	(DNCGTTGACTTT)	1.97E-07	9.64E-05
6	MA1298.1	WRKY29	(AAAAGTCAACK)	2.04E-07	9.96E-05

Cluster	Motif ID	Binding TF	Motif	p-val	adj. p-val
6	MA1301.1	WRKY33	(AAAAGTCAACG)	2.80E-07	0.0001371
6	MA1303.1	WRKY22	(AAAAGTCAACKNH)	3.06E-07	0.0001497
6	MA1309.1	WRKY3	(AAAAGTCAACG)	5.84E-07	0.0002857
6	MA1315.1	WRKY24	(NCGTTGACTTTTTW)	8.02E-07	0.0003919
6	MA1081.1	WRKY25	(YGGTCAAC)	8.60E-07	0.0004203
6	MA1306.1	WRKY11	(DNCGTTGACTTTTD)	1.08E-06	0.0005298
6	MA1093.1	WRKY75	(HRGTCAAC)	1.09E-06	0.0005322
6	MA1083.1	WRKY30	(RGTCAACGNN)	1.91E-06	0.0009341
6	MA1080.1	WRKY23	(AGTCAACG)	2.47E-06	0.001208
6	MA1308.1	WRKY70	(DNCGTTGACTTTT)	3.05E-06	0.001488
6	MA1092.1	WRKY63	(HGGTCAAC)	3.49E-06	0.001706
6	MA1075.1	WRKY12	(CGTTGACC)	3.50E-06	0.001708
6	MA1084.1	WRKY38	(CGTTGACC)	5.90E-06	0.00288
6	MA1312.1	WRKY47	(MYYKNCGTTGACYW)	6.42E-06	0.003135
6	MA1078.1	WRKY2	(BGGTCAAM)	8.40E-06	0.004097
6	MA1300.1	WRKY6	(CGTTGACTWWDDYWDWNHH)	1.29E-05	0.006281
6	MA1318.1	WRKY27	(ANCGTTGACTTTT)	3.14E-05	0.01524
6	MA1297.1	WRKY26	(AAAAGTCAACGNY)	3.40E-05	0.01648
6	MA1317.1	WRKY50	(YKTTGACTTTTTH)	5.00E-05	0.02414
8	MA1329.1	ATHB25	(THAYTAATTAHNHWW)	2.27E-05	0.01102
8	MA1330.1	ATHB24	(AAWHRTAATTAAKDW)	2.87E-05	0.01395
8	MA1326.1	ATHB33	(NHGTRATTARB)	4.06E-05	0.01968
8	MA0933.1	AHL20	(AATTAAWT)	4.91E-05	0.0237
8	MA0934.1	AHL25	(AWTTAAWT)	4.98E-05	0.02404
11	MA1272.1	AT2G28810	(TTYTTTTTTTTTWACTTTTTB)	6.81E-05	0.03276
12	MA1094.1	WRKY8	(NRGTCAAMN)	1.59E-13	7.75E-11
12	MA1076.1	WRKY15	(NRGTCAACSN)	9.01E-13	4.40E-10
12	MA1079.1	WRKY21	(NNRGTCAACG)	9.19E-13	4.50E-10
12	MA1080.1	WRKY23	(AGTCAACG)	1.09E-12	5.34E-10
12	MA1088.1	WRKY48	(NNRGTCAAMN)	1.25E-12	6.13E-10
12	MA1086.1	WRKY43	(HRGTCAAMVN)	1.84E-12	9.02E-10
12	MA1077.1	WRKY18	(NHRGTCAAVV)	2.61E-12	1.28E-09
12	MA1093.1	WRKY75	(HRGTCAAC)	2.88E-12	1.41E-09
12	MA1295.1	WRKY20	(DNCGTTGACYWDD)	2.96E-12	1.45E-09
12	MA1087.1	WRKY45	(CGTTGACY)	4.56E-12	2.23E-09
12	MA1089.1	WRKY57	(DWRGTCAAMN)	1.18E-11	5.76E-09
12	MA1091.1	WRKY62	(TGGTCAAC)	5.48E-11	2.68E-08
12	MA1305.1	WRKY55	(DNCGTTGACTTT)	8.87E-11	4.34E-08
12	MA1301.1	WRKY33	(AAAAGTCAACG)	9.00E-11	4.40E-08
12	MA1300.1	WRKY6	(CGTTGACTWWDDYWDWNHH)	9.05E-11	4.43E-08
12	MA1084.1	WRKY38	(CGTTGACC)	1.71E-10	8.37E-08
12	MA1081.1	WRKY25	(YGGTCAAC)	2.03E-10	9.94E-08
12	MA1083.1	WRKY30	(RGTCAACGNN)	2.16E-10	1.05E-07
12	MA1078.1	WRKY2	(BGGTCAAM)	2.34E-10	1.15E-07
12	MA1298.1	WRKY29	(AAAAGTCAACK)	3.73E-10	1.83E-07
12	MA1090.1	WRKY60	(NYGGTCAACSN)	4.68E-10	2.29E-07
12	MA1314.1	WRKY14	(AAAAGTCAACGNH)	5.66E-10	2.77E-07
12	MA1307.1	WRKY31	(DDNNHWRHHAAAGTCAACG)	6.45E-10	3.15E-07
12	MA1315.1	WRKY24	(NCGTTGACTTTTTW)	6.47E-10	3.16E-07
12	MA1309.1	WRKY3	(AAAAGTCAACG)	1.20E-09	5.85E-07
12	MA1311.1	WRKY28	(DDCGTTGACTTTT)	1.43E-09	7.01E-07
12	MA1075.1	WRKY12	(CGTTGACC)	2.24E-09	1.09E-06
12	MA1302.1	WRKY65	(AAAAGTCAACG)	3.08E-09	1.51E-06
12	MA1308.1	WRKY70	(DNCGTTGACTTTT)	4.02E-09	1.97E-06
12	MA1303.1	WRKY22	(AAAAGTCAACKNH)	8.02E-09	3.92E-06
12	MA1306.1	WRKY11	(DNCGTTGACTTTTD)	9.53E-09	4.66E-06
12	MA1310.1	WRKY42	(BWTDMHHHNNCGTTGACTWWD)	1.18E-08	5.75E-06
12	MA1316.1	WRKY71	(AAAAGTCAACG)	1.82E-08	8.90E-06
12	MA1092.1	WRKY63	(HGGTCAAC)	2.29E-08	1.12E-05
12	MA1297.1	WRKY26	(AAAAGTCAACGNY)	4.50E-08	2.20E-05
12	MA1304.1	WRKY59	(HAAAAGTCAAMN)	4.77E-08	2.33E-05
12	MA1085.2	WRKY40	(HWAGTCAANN)	2.85E-07	0.0001394
12	MA1312.1	WRKY47	(MYYKNCGTTGACYW)	4.88E-07	0.0002386
12	MA1299.1	WRKY17	(AAAAAGTCAACGNH)	4.98E-06	0.002432
12	MA1318.1	WRKY27	(ANCGTTGACTTTT)	9.37E-06	0.004573
12	MA0589.1	ZAP1	(TTGACCGAGYY)	1.35E-05	0.00656
12	MA1317.1	WRKY50	(YKTTGACTTTTTH)	3.24E-05	0.01572
13	MA1088.1	WRKY48	(NNRGTCAAMN)	1.30E-13	6.36E-11
13	MA1094.1	WRKY8	(NRGTCAAMN)	1.44E-13	7.03E-11
13	MA1076.1	WRKY15	(NRGTCAACSN)	2.14E-12	1.05E-09
13	MA1086.1	WRKY43	(HRGTCAAMVN)	1.63E-11	7.96E-09
13	MA1089.1	WRKY57	(DWRGTCAAMN)	1.93E-11	9.46E-09
13	MA1093.1	WRKY75	(HRGTCAAC)	1.13E-10	5.53E-08
13	MA1079.1	WRKY21	(NNRGTCAACG)	1.44E-10	7.04E-08
13	MA1077.1	WRKY18	(NHRGTCAAVV)	1.46E-10	7.11E-08
13	MA1090.1	WRKY60	(NYGGTCAACSN)	1.82E-10	8.89E-08

Cluster	Motif ID	Binding TF	Motif	p-val	adj. p-val
13	MA1083.1	WRKY30	(RGTCAACGNN)	3.01E-10	1.47E-07
13	MA1075.1	WRKY12	(CGTTGACC)	4.88E-10	2.39E-07
13	MA1078.1	WRKY2	(BGGTCAAM)	9.69E-10	4.74E-07
13	MA1311.1	WRKY28	(DDCGTTGACTTTT)	2.02E-09	9.85E-07
13	MA1084.1	WRKY38	(CGTTGACC)	2.03E-09	9.90E-07
13	MA1305.1	WRKY55	(DNCGTTGACTTT)	2.60E-09	1.27E-06
13	MA1092.1	WRKY63	(HGGTCAAC)	5.89E-09	2.88E-06
13	MA1315.1	WRKY24	(NCGTTGACTTTTTW)	1.18E-08	5.75E-06
13	MA1300.1	WRKY6	(CGTTGACTWWDDYWDWNHH)	1.37E-08	6.71E-06
13	MA1091.1	WRKY62	(TGGTCAAC)	1.65E-08	8.06E-06
13	MA1309.1	WRKY3	(AAAAGTCAACG)	3.11E-08	1.52E-05
13	MA1295.1	WRKY20	(DNCGTTGACYWDD)	3.22E-08	1.58E-05
13	MA1299.1	WRKY17	(AAAAAGTCAACGNH)	4.05E-08	1.98E-05
13	MA1314.1	WRKY14	(AAAAGTCAACGNH)	4.27E-08	2.09E-05
13	MA1081.1	WRKY25	(YGGTCAAC)	4.52E-08	2.21E-05
13	MA1313.1	WRKY7	(DNCGTTGACTTTTT)	5.56E-08	2.72E-05
13	MA1087.1	WRKY45	(CGTTGACY)	5.79E-08	2.83E-05
13	MA1308.1	WRKY70	(DNCGTTGACTTTT)	7.20E-08	3.52E-05
13	MA1302.1	WRKY65	(AAAAGTCAACG)	7.83E-08	3.83E-05
13	MA1301.1	WRKY33	(AAAAGTCAACG)	8.65E-08	4.23E-05
13	MA1303.1	WRKY22	(AAAAGTCAACKNH)	9.26E-08	4.53E-05
13	MA1316.1	WRKY71	(AAAAGTCAACG)	9.98E-08	4.88E-05
13	MA0589.1	ZAP1	(TTGACCGAGYY)	1.18E-07	5.79E-05
13	MA1310.1	WRKY42	(BWTDMHHHNNCGTTGACTWWD)	1.77E-07	8.68E-05
13	MA1298.1	WRKY29	(AAAAGTCAACK)	1.82E-07	8.87E-05
13	MA1312.1	WRKY47	(MYYKNCGTTGACYW)	2.04E-07	9.97E-05
13	MA1085.2	WRKY40	(HWAGTCAANN)	2.32E-07	0.0001136
13	MA1318.1	WRKY27	(ANCGTTGACTTTT)	2.35E-07	0.0001151
13	MA1317.1	WRKY50	(YKTTGACTTTTTH)	2.58E-07	0.0001261
13	MA1304.1	WRKY59	(HAAAAGTCAAMN)	4.10E-07	0.0002002
13	MA1307.1	WRKY31	(DDNNHWRHHAAAGTCAACG)	5.98E-07	0.0002921
13	MA1306.1	WRKY11	(DNCGTTGACTTTTD)	7.23E-07	0.0003537
13	MA1297.1	WRKY26	(AAAAGTCAACGNY)	8.58E-07	0.0004196
13	MA1197.1	CAMTA1	(AAARCGCGTGDD)	1.47E-06	0.0007161
13	MA0970.1	CMTA3	(CCGCGTNNN)	2.05E-06	0.001002
13	MA1080.1	WRKY23	(AGTCAACG)	3.19E-06	0.001557
13	MA0969.1	CMTA2	(NNDVCGCGT)	4.04E-06	0.001972
13	MA1296.1	WRKY46	(CGTTGACTTTK)	3.40E-05	0.01647
14	MA1316.1	WRKY71	(AAAAGTCAACG)	2.81E-10	1.37E-07
14	MA1306.1	WRKY11	(DNCGTTGACTTTTD)	5.16E-10	2.52E-07
14	MA1089.1	WRKY57	(DWRGTCAAMN)	8.13E-10	3.98E-07
14	MA1298.1	WRKY29	(AAAAGTCAACK)	8.89E-10	4.35E-07
14	MA1311.1	WRKY28	(DDCGTTGACTTTT)	1.19E-09	5.82E-07
14	MA1317.1	WRKY50	(YKTTGACTTTTTH)	2.62E-09	1.28E-06
14	MA1094.1	WRKY8	(NRGTCAAMN)	2.73E-09	1.33E-06
14	MA1303.1	WRKY22	(AAAAGTCAACKNH)	2.85E-09	1.40E-06
14	MA1299.1	WRKY17	(AAAAAGTCAACGNH)	5.70E-09	2.79E-06
14	MA1088.1	WRKY48	(NNRGTCAAMN)	6.12E-09	2.99E-06
14	MA1304.1	WRKY59	(HAAAAGTCAAMN)	6.16E-09	3.01E-06
14	MA1314.1	WRKY14	(AAAAGTCAACGNH)	1.59E-08	7.78E-06
14	MA1301.1	WRKY33	(AAAAGTCAACG)	1.94E-08	9.47E-06
14	MA1076.1	WRKY15	(NRGTCAACSN)	2.00E-08	9.77E-06
14	MA1318.1	WRKY27	(ANCGTTGACTTTT)	3.36E-08	1.64E-05
14	MA1309.1	WRKY3	(AAAAGTCAACG)	3.75E-08	1.84E-05
14	MA1315.1	WRKY24	(NCGTTGACTTTTTW)	4.57E-08	2.23E-05
14	MA1310.1	WRKY42	(BWTDMHHHNNCGTTGACTWWD)	1.60E-07	7.81E-05
14	MA1297.1	WRKY26	(AAAAGTCAACGNY)	1.68E-07	8.19E-05
14	MA1086.1	WRKY43	(HRGTCAAMVN)	1.81E-07	8.84E-05
14	MA1093.1	WRKY75	(HRGTCAAC)	1.88E-07	9.20E-05
14	MA1079.1	WRKY21	(NNRGTCAACG)	1.90E-07	9.31E-05
14	MA1302.1	WRKY65	(AAAAGTCAACG)	2.14E-07	0.0001047
14	MA1313.1	WRKY7	(DNCGTTGACTTTTT)	2.89E-07	0.0001414
14	MA1300.1	WRKY6	(CGTTGACTWWDDYWDWNHH)	7.11E-07	0.0003477
14	MA1077.1	WRKY18	(NHRGTCAAVV)	9.78E-07	0.000478
14	MA1307.1	WRKY31	(DDNNHWRHHAAAGTCAACG)	1.07E-06	0.0005205
14	MA1295.1	WRKY20	(DNCGTTGACYWDD)	1.32E-06	0.0006472
14	MA1083.1	WRKY30	(RGTCAACGNN)	3.25E-06	0.00159
14	MA1305.1	WRKY55	(DNCGTTGACTTT)	4.95E-06	0.002418
14	MA1091.1	WRKY62	(TGGTCAAC)	9.88E-06	0.004819
14	MA1308.1	WRKY70	(DNCGTTGACTTTT)	1.10E-05	0.00538
14	MA0937.1	NAC055	(ACACGTAA)	1.16E-05	0.005662
14	MA1078.1	WRKY2	(BGGTCAAM)	1.18E-05	0.00577
14	MA1085.2	WRKY40	(HWAGTCAANN)	1.31E-05	0.006386
14	MA1296.1	WRKY46	(CGTTGACTTTK)	1.45E-05	0.007077
14	MA1090.1	WRKY60	(NYGGTCAACSN)	1.58E-05	0.007689
14	MA1087.1	WRKY45	(CGTTGACY)	1.71E-05	0.008343

Cluster	Motif ID	Binding TF	Motif	p-val	adj. p-val
14	MA1383.1	KAN2	(HTHRGAATATTCTTT)	4.82E-05	0.02328
14	MA0982.1	DOF2.4	(DWAAAGB)	6.16E-05	0.02965
14	MA1075.1	WRKY12	(CGTTGACC)	8.89E-05	0.04253

Supplement Table 5: Known TF-motifs enriched in *C.rubella* 5´regulatory regions of DEGs. Known TF-motifs were determined using AME for the -500 bp region upstream of the transcriptional start site. The motifs were determined separately for each expression clusters depicted in Supplemental Figure 4.

Cluster	Motif ID	Binding TF	Motif	p-val	adj. p-val
2	MA1089.1	WRKY57	(DWRGTCAAMN)	1.23E-16	5.99E-14
2	MA1298.1	WRKY29	(AAAAGTCAACK)	1.50E-16	7.36E-14
2	MA1302.1	WRKY65	(AAAAGTCAACG)	3.61E-16	1.76E-13
2	MA1303.1	WRKY22	(AAAAGTCAACKNH)	5.38E-16	2.63E-13
2	MA1314.1	WRKY14	(AAAAGTCAACGNH)	6.21E-16	3.04E-13
2	MA1308.1	WRKY70	(DNCGTTGACTTTT)	1.02E-15	4.98E-13
2	MA1311.1	WRKY28	(DDCGTTGACTTTT)	1.08E-15	5.29E-13
2	MA1306.1	WRKY11	(DNCGTTGACTTTTD)	2.01E-15	9.80E-13
2	MA1094.1	WRKY8	(NRGTCAAMN)	3.01E-15	1.47E-12
2	MA1318.1	WRKY27	(ANCGTTGACTTTT)	5.53E-15	2.70E-12
2	MA1310.1	WRKY42	(BWTDMHHHNNCGTTGACTWWD)	1.50E-14	7.35E-12
2	MA1316.1	WRKY71	(AAAAGTCAACG)	1.63E-14	7.97E-12
2	MA1086.1	WRKY43	(HRGTCAAMVN)	1.82E-14	8.90E-12
2	MA1305.1	WRKY55	(DNCGTTGACTTT)	2.33E-14	1.14E-11
2	MA1079.1	WRKY21	(NNRGTCAACG)	3.47E-14	1.70E-11
2	MA1304.1	WRKY59	(HAAAAGTCAAMN)	7.32E-14	3.58E-11
2	MA1301.1	WRKY33	(AAAAGTCAACG)	8.30E-14	4.06E-11
2	MA1088.1	WRKY48	(NNRGTCAAMN)	1.01E-13	4.92E-11
2	MA1076.1	WRKY15	(NRGTCAACSN)	2.25E-13	1.10E-10
2	MA1077.1	WRKY18	(NHRGTCAAVV)	2.34E-13	1.14E-10
2	MA1317.1	WRKY50	(YKTTGACTTTTTH)	2.38E-13	1.16E-10
2	MA1093.1	WRKY75	(HRGTCAAC)	3.17E-13	1.55E-10
2	MA1309.1	WRKY3	(AAAAGTCAACG)	4.38E-13	2.14E-10
2	MA1085.2	WRKY40	(HWAGTCAANN)	4.47E-13	2.18E-10
2	MA1295.1	WRKY20	(DNCGTTGACYWDD)	5.17E-13	2.53E-10
2	MA1300.1	WRKY6	(CGTTGACTWWDDYWDWNHH)	6.02E-13	2.94E-10
2	MA1297.1	WRKY26	(AAAAGTCAACGNY)	7.27E-13	3.56E-10
2	MA1315.1	WRKY24	(NCGTTGACTTTTTW)	7.37E-13	3.60E-10
2	MA1313.1	WRKY7	(DNCGTTGACTTTTT)	2.06E-12	1.01E-09
2	MA1083.1	WRKY30	(RGTCAACGNN)	5.33E-12	2.61E-09
2	MA1307.1	WRKY31	(DDNNHWRHHAAAGTCAACG)	5.44E-12	2.66E-09
2	MA1087.1	WRKY45	(CGTTGACY)	1.25E-11	6.09E-09
2	MA1299.1	WRKY17	(AAAAAGTCAACGNH)	3.17E-11	1.55E-08
2	MA1090.1	WRKY60	(NYGGTCAACSN)	2.32E-10	1.14E-07
2	MA1078.1	WRKY2	(BGGTCAAM)	2.45E-10	1.20E-07
2	MA1091.1	WRKY62	(TGGTCAAC)	2.74E-10	1.34E-07
2	MA1092.1	WRKY63	(HGGTCAAC)	5.76E-10	2.82E-07
2	MA1296.1	WRKY46	(CGTTGACTTTK)	1.25E-09	6.12E-07
2	MA1081.1	WRKY25	(YGGTCAAC)	1.44E-09	7.02E-07
2	MA1080.1	WRKY23	(AGTCAACG)	2.21E-09	1.08E-06
2	MA1075.1	WRKY12	(CGTTGACC)	3.06E-09	1.49E-06
2	MA1084.1	WRKY38	(CGTTGACC)	5.81E-09	2.84E-06
2	MA1312.1	WRKY47	(MYYKNCGTTGACYW)	9.30E-09	4.55E-06
2	MA1027.1	KAN1	(RNWTATTC)	1.53E-08	7.50E-06
2	MA0982.1	DOF2.4	(DWAAAGB)	1.52E-06	0.0007441
2	MA1385.1	AT2G40260	(TWWWAAHATTCTYTT)	8.20E-06	0.004001
2	MA0082.1	squamosa	(MCAWAWATRGWAAN)	1.51E-05	0.007333
2	MA1167.1	AT2G03500	(RGAATATTCND)	1.78E-05	0.00867
2	MA0932.1	AHL12	(AAWWWWTT)	1.82E-05	0.008853
2	MA1383.1	KAN2	(HTHRGAATATTCTTT)	2.11E-05	0.01025
2	MA0934.1	AHL25	(AWTTAAWT)	3.75E-05	0.01819
2	MA0933.1	AHL20	(AATTAAWT)	3.85E-05	0.01865
2	MA0981.1	DOF1.8	(NNWAAAGBNN)	4.05E-05	0.01959
2	MA1071.1	DOF5.3	(NNWAAMG)	4.47E-05	0.02162
2	MA1389.1	AT5G29000	(AARGAATATTCBNWW)	5.56E-05	0.02684
2	MA1166.1	AT3G12730	(AAARRGAATATTCY)	9.77E-05	0.04667
2	MA0953.1	ATHB-6	(NCAATHATD)	9.94E-05	0.04744
3	MA1309.1	WRKY3	(AAAAGTCAACG)	8.46E-05	0.04054
3	MA1301.1	WRKY33	(AAAAGTCAACG)	8.61E-05	0.04122
4	MA1303.1	WRKY22	(AAAAGTCAACKNH)	3.40E-05	0.01646
4	MA1308.1	WRKY70	(DNCGTTGACTTTT)	3.54E-05	0.01716
4	MA1298.1	WRKY29	(AAAAGTCAACK)	6.83E-05	0.03284
4	MA1306.1	WRKY11	(DNCGTTGACTTTTD)	7.88E-05	0.0378
4	MA1302.1	WRKY65	(AAAAGTCAACG)	7.96E-05	0.03817
4	MA1314.1	WRKY14	(AAAAGTCAACGNH)	9.70E-05	0.04633
5	MA1091.1	WRKY62	(TGGTCAAC)	1.53E-08	7.48E-06
5	MA1295.1	WRKY20	(DNCGTTGACYWDD)	3.60E-08	1.76E-05
5	MA1077.1	WRKY18	(NHRGTCAAVV)	7.31E-08	3.57E-05
5	MA1088.1	WRKY48	(NNRGTCAAMN)	7.79E-08	3.81E-05
5	MA1094.1	WRKY8	(NRGTCAAMN)	1.23E-07	6.00E-05
5	MA1090.1	WRKY60	(NYGGTCAACSN)	1.39E-07	6.78E-05

Cluster	Motif ID	Binding TF	Motif	p-val	adj. p-val
5	MA1081.1	WRKY25	(YGGTCAAC)	1.54E-07	7.54E-05
5	MA1093.1	WRKY75	(HRGTCAAC)	2.20E-07	0.0001077
5	MA1078.1	WRKY2	(BGGTCAAM)	2.52E-07	0.0001232
5	MA1076.1	WRKY15	(NRGTCAACSN)	3.67E-07	0.0001796
5	MA1086.1	WRKY43	(HRGTCAAMVN)	6.30E-07	0.000308
5	MA1089.1	WRKY57	(DWRGTCAAMN)	1.87E-06	0.0009134
5	MA1092.1	WRKY63	(HGGTCAAC)	2.11E-06	0.00103
5	MA0589.1	ZAP1	(TTGACCGAGYY)	5.00E-06	0.002443
5	MA1309.1	WRKY3	(AAAAGTCAACG)	5.18E-06	0.002532
5	MA1300.1	WRKY6	(CGTTGACTWWDDYWDWNHH)	6.30E-06	0.003074
5	MA1311.1	WRKY28	(DDCGTTGACTTTT)	6.41E-06	0.003129
5	MA1079.1	WRKY21	(NNRGTCAACG)	9.32E-06	0.004545
5	MA1304.1	WRKY59	(HAAAAGTCAAMN)	1.15E-05	0.005615
5	MA1301.1	WRKY33	(AAAAGTCAACG)	1.19E-05	0.005805
5	MA1315.1	WRKY24	(NCGTTGACTTTTTW)	1.30E-05	0.006359
5	MA1087.1	WRKY45	(CGTTGACY)	2.27E-05	0.01103
5	MA1305.1	WRKY55	(DNCGTTGACTTT)	2.52E-05	0.01224
5	MA1080.1	WRKY23	(AGTCAACG)	3.11E-05	0.01511
5	MA1314.1	WRKY14	(AAAAGTCAACGNH)	4.27E-05	0.02064
5	MA1083.1	WRKY30	(RGTCAACGNN)	4.45E-05	0.02154
5	MA1084.1	WRKY38	(CGTTGACC)	4.76E-05	0.023
5	MA1310.1	WRKY42	(BWTDMHHHNNCGTTGACTWWD)	4.80E-05	0.0232
5	MA1075.1	WRKY12	(CGTTGACC)	6.12E-05	0.02947
5	MA1302.1	WRKY65	(AAAAGTCAACG)	8.91E-05	0.04263
5	MA1316.1	WRKY71	(AAAAGTCAACG)	9.49E-05	0.04533
6	MA1090.1	WRKY60	(NYGGTCAACSN)	1.40E-08	6.86E-06
6	MA1087.1	WRKY45	(CGTTGACY)	3.60E-08	1.76E-05
6	MA1094.1	WRKY8	(NRGTCAAMN)	4.26E-08	2.08E-05
6	MA1086.1	WRKY43	(HRGTCAAMVN)	5.25E-08	2.57E-05
6	MA1080.1	WRKY23	(AGTCAACG)	5.42E-08	2.65E-05
6	MA1076.1	WRKY15	(NRGTCAACSN)	5.56E-08	2.72E-05
6	MA1083.1	WRKY30	(RGTCAACGNN)	7.25E-08	3.54E-05
6	MA1078.1	WRKY2	(BGGTCAAM)	7.48E-08	3.66E-05
6	MA1077.1	WRKY18	(NHRGTCAAVV)	7.51E-08	3.67E-05
6	MA1305.1	WRKY55	(DNCGTTGACTTT)	9.70E-08	4.74E-05
6	MA1084.1	WRKY38	(CGTTGACC)	1.36E-07	6.64E-05
6	MA1295.1	WRKY20	(DNCGTTGACYWDD)	1.52E-07	7.44E-05
6	MA1088.1	WRKY48	(NNRGTCAAMN)	1.54E-07	7.53E-05
6	MA1092.1	WRKY63	(HGGTCAAC)	2.24E-07	0.0001097
6	MA1081.1	WRKY25	(YGGTCAAC)	2.33E-07	0.0001139
6	MA1075.1	WRKY12	(CGTTGACC)	2.39E-07	0.0001166
6	MA1302.1	WRKY65	(AAAAGTCAACG)	3.35E-07	0.0001636
6	MA1079.1	WRKY21	(NNRGTCAACG)	3.40E-07	0.000166
6	MA1316.1	WRKY71	(AAAAGTCAACG)	4.76E-07	0.0002325
6	MA1093.1	WRKY75	(HRGTCAAC)	6.22E-07	0.0003043
6	MA1089.1	WRKY57	(DWRGTCAAMN)	6.65E-07	0.000325
6	MA1315.1	WRKY24	(NCGTTGACTTTTTW)	7.19E-07	0.0003517
6	MA0589.1	ZAP1	(TTGACCGAGYY)	7.52E-07	0.0003674
6	MA1310.1	WRKY42	(BWTDMHHHNNCGTTGACTWWD)	1.34E-06	0.0006568
6	MA1311.1	WRKY28	(DDCGTTGACTTTT)	1.36E-06	0.0006621
6	MA1314.1	WRKY14	(AAAAGTCAACGNH)	1.37E-06	0.0006718
6	MA1301.1	WRKY33	(AAAAGTCAACG)	1.40E-06	0.000683
6	MA1309.1	WRKY3	(AAAAGTCAACG)	3.13E-06	0.001529
6	MA1304.1	WRKY59	(HAAAAGTCAAMN)	3.76E-06	0.001836
6	MA1297.1	WRKY26	(AAAAGTCAACGNY)	7.94E-06	0.003873
6	MA1303.1	WRKY22	(AAAAGTCAACKNH)	8.93E-06	0.004356
6	MA1312.1	WRKY47	(MYYKNCGTTGACYW)	9.34E-06	0.004555
6	MA1298.1	WRKY29	(AAAAGTCAACK)	1.06E-05	0.005163
6	MA1091.1	WRKY62	(TGGTCAAC)	1.08E-05	0.005258
6	MA1317.1	WRKY50	(YKTTGACTTTTTH)	1.15E-05	0.0056
6	MA1197.1	CAMTA1	(AAARCGCGTGDD)	1.70E-05	0.008297
6	MA1306.1	WRKY11	(DNCGTTGACTTTTD)	1.84E-05	0.008952
6	MA1300.1	WRKY6	(CGTTGACTWWDDYWDWNHH)	1.85E-05	0.009001
6	MA1308.1	WRKY70	(DNCGTTGACTTTT)	2.31E-05	0.01121
6	MA0969.1	CMTA2	(NNDVCGCGT)	3.36E-05	0.01631
6	MA0045.1	HMG-I/Y	(VWAVAAAHRVMRAMAY)	4.47E-05	0.02163
6	MA1307.1	WRKY31	(DDNNHWRHHAAAGTCAACG)	6.43E-05	0.03093
6	MA1299.1	WRKY17	(AAAAAGTCAACGNH)	7.82E-05	0.03752
6	MA0984.1	DOF5.7	(DAAARRKB)	7.87E-05	0.03773
6	MA0970.1	CMTA3	(CCGCGTNNN)	8.73E-05	0.04181
6	MA0559.1	PI	(CCAAAARWRGAAAR)	0.0001001	0.04777
7	MA0932.1	AHL12	(AAWWWWTT)	1.98E-05	0.00962
7	MA0934.1	AHL25	(AWTTAAWT)	4.93E-05	0.0238
8	MA0953.1	ATHB-6	(NCAATHATD)	3.06E-07	0.0001497
8	MA0990.1	EDT1	(HAWTWAATGC)	2.59E-06	0.001265
8	MA1214.1	ATHB40	(DHACCAATAATTGDDNHHWWW)	5.65E-06	0.002757

Cluster	Motif ID	Binding TF	Motif	p-val	adj. p-val
8	MA0578.1	SPL8	(WWDWHYGTACHHYWWW)	1.15E-05	0.005624
8	MA1213.1	ATHB21	(NCAMCAATWATTGD)	1.90E-05	0.009255
8	MA1375.1	ANL2	(GCATTAATTRY)	2.06E-05	0.01004
8	MA1046.1	NTL9	(TTAAGTAAT)	2.39E-05	0.0116
8	MA1369.1	HDG1	(RYAATTAATGM)	3.28E-05	0.01592
8	MA0932.1	AHL12	(AAWWWWTT)	4.87E-05	0.02352
8	MA0934.1	AHL25	(AWTTAAWT)	6.35E-05	0.03059
8	MA1211.1	ATHB18	(NYAATYATTDD)	6.55E-05	0.0315
8	MA1330.1	ATHB24	(AAWHRTAATTAAKDW)	0.0001038	0.04949
8	MA0952.1	ATHB-51	(AATWATTG)	0.000104	0.04958
13	MA1086.1	WRKY43	(HRGTCAAMVN)	3.75E-10	1.84E-07
13	MA1295.1	WRKY20	(DNCGTTGACYWDD)	4.11E-10	2.01E-07
13	MA1089.1	WRKY57	(DWRGTCAAMN)	6.24E-10	3.05E-07
13	MA1094.1	WRKY8	(NRGTCAAMN)	9.96E-10	4.87E-07
13	MA1093.1	WRKY75	(HRGTCAAC)	2.49E-09	1.22E-06
13	MA1315.1	WRKY24	(NCGTTGACTTTTTW)	2.87E-09	1.41E-06
13	MA1298.1	WRKY29	(AAAAGTCAACK)	4.09E-09	2.00E-06
13	MA1079.1	WRKY21	(NNRGTCAACG)	4.76E-09	2.33E-06
13	MA1088.1	WRKY48	(NNRGTCAAMN)	6.52E-09	3.19E-06
13	MA1076.1	WRKY15	(NRGTCAACSN)	7.04E-09	3.44E-06
13	MA1301.1	WRKY33	(AAAAGTCAACG)	1.09E-08	5.31E-06
13	MA1078.1	WRKY2	(BGGTCAAM)	1.24E-08	6.07E-06
13	MA1309.1	WRKY3	(AAAAGTCAACG)	2.70E-08	1.32E-05
13	MA1305.1	WRKY55	(DNCGTTGACTTT)	3.01E-08	1.47E-05
13	MA1311.1	WRKY28	(DDCGTTGACTTTT)	5.19E-08	2.54E-05
13	MA1300.1	WRKY6	(CGTTGACTWWDDYWDWNHH)	5.45E-08	2.67E-05
13	MA1080.1	WRKY23	(AGTCAACG)	5.76E-08	2.82E-05
13	MA1302.1	WRKY65	(AAAAGTCAACG)	6.52E-08	3.19E-05
13	MA1304.1	WRKY59	(HAAAAGTCAAMN)	7.57E-08	3.70E-05
13	MA1091.1	WRKY62	(TGGTCAAC)	7.59E-08	3.71E-05
13	MA1306.1	WRKY11	(DNCGTTGACTTTTD)	8.70E-08	4.25E-05
13	MA1312.1	WRKY47	(MYYKNCGTTGACYW)	8.86E-08	4.33E-05
13	MA1084.1	WRKY38	(CGTTGACC)	1.17E-07	5.72E-05
13	MA1087.1	WRKY45	(CGTTGACY)	1.26E-07	6.15E-05
13	MA1077.1	WRKY18	(NHRGTCAAVV)	1.61E-07	7.88E-05
13	MA1081.1	WRKY25	(YGGTCAAC)	2.23E-07	0.0001088
13	MA1314.1	WRKY14	(AAAAGTCAACGNH)	2.43E-07	0.0001187
13	MA1297.1	WRKY26	(AAAAGTCAACGNY)	4.24E-07	0.0002073
13	MA1308.1	WRKY70	(DNCGTTGACTTTT)	4.65E-07	0.0002275
13	MA1303.1	WRKY22	(AAAAGTCAACKNH)	5.30E-07	0.000259
13	MA1310.1	WRKY42	(BWTDMHHHNNCGTTGACTWWD)	5.55E-07	0.0002713
13	MA1083.1	WRKY30	(RGTCAACGNN)	7.61E-07	0.0003719
13	MA1316.1	WRKY71	(AAAAGTCAACG)	8.28E-07	0.0004048
13	MA1307.1	WRKY31	(DDNNHWRHHAAAGTCAACG)	9.69E-07	0.0004738
13	MA1317.1	WRKY50	(YKTTGACTTTTTH)	2.25E-06	0.0011
13	MA1085.2	WRKY40	(HWAGTCAANN)	2.51E-06	0.001228
13	MA1090.1	WRKY60	(NYGGTCAACSN)	3.83E-06	0.001869
13	MA1313.1	WRKY7	(DNCGTTGACTTTTT)	5.88E-06	0.002872
13	MA1092.1	WRKY63	(HGGTCAAC)	1.01E-05	0.004931
13	MA1075.1	WRKY12	(CGTTGACC)	2.89E-05	0.01401
13	MA1299.1	WRKY17	(AAAAAGTCAACGNH)	4.91E-05	0.02374
13	MA1318.1	WRKY27	(ANCGTTGACTTTT)	5.34E-05	0.02578
13	MA1027.1	KAN1	(RNWTATTC)	5.44E-05	0.02624
13	MA0982.1	DOF2.4	(DWAAAGB)	7.71E-05	0.03698
14	MA1317.1	WRKY50	(YKTTGACTTTTTH)	2.31E-09	1.13E-06
14	MA1316.1	WRKY71	(AAAAGTCAACG)	1.49E-08	7.29E-06
14	MA1308.1	WRKY70	(DNCGTTGACTTTT)	1.53E-08	7.48E-06
14	MA1318.1	WRKY27	(ANCGTTGACTTTT)	1.60E-08	7.83E-06
14	MA1314.1	WRKY14	(AAAAGTCAACGNH)	3.19E-08	1.56E-05
14	MA1089.1	WRKY57	(DWRGTCAAMN)	3.61E-08	1.77E-05
14	MA1311.1	WRKY28	(DDCGTTGACTTTT)	4.26E-08	2.08E-05
14	MA1086.1	WRKY43	(HRGTCAAMVN)	7.89E-08	3.86E-05
14	MA1094.1	WRKY8	(NRGTCAAMN)	8.41E-08	4.11E-05
14	MA1302.1	WRKY65	(AAAAGTCAACG)	9.83E-08	4.81E-05
14	MA1299.1	WRKY17	(AAAAAGTCAACGNH)	9.89E-08	4.84E-05
14	MA1306.1	WRKY11	(DNCGTTGACTTTTD)	1.05E-07	5.15E-05
14	MA1303.1	WRKY22	(AAAAGTCAACKNH)	1.10E-07	5.35E-05
14	MA1088.1	WRKY48	(NNRGTCAAMN)	1.61E-07	7.86E-05
14	MA1305.1	WRKY55	(DNCGTTGACTTT)	2.65E-07	0.0001295
14	MA1298.1	WRKY29	(AAAAGTCAACK)	2.71E-07	0.0001327
14	MA1304.1	WRKY59	(HAAAAGTCAAMN)	2.83E-07	0.0001384
14	MA1315.1	WRKY24	(NCGTTGACTTTTTW)	3.38E-07	0.0001651
14	MA1310.1	WRKY42	(BWTDMHHHNNCGTTGACTWWD)	5.53E-07	0.0002705
14	MA1083.1	WRKY30	(RGTCAACGNN)	6.12E-07	0.0002991
14	MA1309.1	WRKY3	(AAAAGTCAACG)	6.94E-07	0.0003393
14	MA1090.1	WRKY60	(NYGGTCAACSN)	9.20E-07	0.0004496

Cluster	Motif ID	Binding TF	Motif	p-val	adj. p-val
14	MA1079.1	WRKY21	(NNRGTCAACG)	9.40E-07	0.0004596
14	MA1076.1	WRKY15	(NRGTCAACSN)	1.04E-06	0.0005086
14	MA1301.1	WRKY33	(AAAAGTCAACG)	1.13E-06	0.0005516
14	MA1077.1	WRKY18	(NHRGTCAAVV)	1.71E-06	0.0008361
14	MA1297.1	WRKY26	(AAAAGTCAACGNY)	1.98E-06	0.0009663
14	MA1085.2	WRKY40	(HWAGTCAANN)	2.76E-06	0.001347
14	MA1300.1	WRKY6	(CGTTGACTWWDDYWDWNHH)	5.66E-06	0.002763
14	MA1296.1	WRKY46	(CGTTGACTTTK)	6.59E-06	0.003215
14	MA1313.1	WRKY7	(DNCGTTGACTTTTT)	7.13E-06	0.003478
14	MA1084.1	WRKY38	(CGTTGACC)	1.78E-05	0.008663
14	MA1093.1	WRKY75	(HRGTCAAC)	1.91E-05	0.009277
14	MA1295.1	WRKY20	(DNCGTTGACYWDD)	3.93E-05	0.01905
14	MA1075.1	WRKY12	(CGTTGACC)	4.38E-05	0.02118
14	MA1307.1	WRKY31	(DDNNHWRHHAAAGTCAACG)	7.37E-05	0.03542
14	MA1087.1	WRKY45	(CGTTGACY)	8.32E-05	0.03987
14	MA1092.1	WRKY63	(HGGTCAAC)	9.26E-05	0.04425
14	MA0951.1	ATHB-16	(TAATMATT)	9.93E-05	0.04739

Supplement Table 6 Known TF-motifs enriched in *C. hirsuta* 5´regulatory regions of DEGs. Known TF-motifs were determined using AME for the -500 bp region upstream of the transcriptional start site. The motifs were determined separately for each expression clusters depicted in Supplemental Figure 4.

Cluster	Motif ID	Binding TF	Motif	p-val	adj. p-val
1	MA0930.1	ABF3	(ACACGTGT)	4.90E-06	2.39E-03
1	MA1041.1	MYB55	(ACCTACCG)	9.10E-05	4.35E-02
2	MA1088.1	WRKY48	(NNRGTCAAMN)	1.25E-08	6.13E-06
2	MA1094.1	WRKY8	(NRGTCAAMN)	2.32E-08	1.14E-05
2	MA1077.1	WRKY18	(NHRGTCAAVV)	4.31E-08	2.11E-05
2	MA1086.1	WRKY43	(HRGTCAAMVN)	6.89E-08	3.37E-05
2	MA1076.1	WRKY15	(NRGTCAACSN)	1.09E-07	5.32E-05
2	MA1089.1	WRKY57	(DWRGTCAAMN)	2.28E-07	1.12E-04
2	MA1083.1	WRKY30	(RGTCAACGNN)	2.31E-07	1.13E-04
2	MA1079.1	WRKY21	(NNRGTCAACG)	2.35E-07	1.15E-04
2	MA1090.1	WRKY60	(NYGGTCAACSN)	3.13E-07	1.53E-04
2	MA1311.1	WRKY28	(DDCGTTGACTTTT)	3.17E-07	1.55E-04
2	MA1300.1	WRKY6	(CGTTGACTWWDDYWDWNHH)	5.28E-07	2.58E-04
2	MA1078.1	WRKY2	(BGGTCAAM)	7.81E-07	3.82E-04
2	MA1093.1	WRKY75	(HRGTCAAC)	7.82E-07	3.82E-04
2	MA1091.1	WRKY62	(TGGTCAAC)	7.97E-07	3.90E-04
2	MA1305.1	WRKY55	(DNCGTTGACTTT)	1.28E-06	6.24E-04
2	MA1317.1	WRKY50	(YKTTGACTTTTTH)	1.53E-06	7.49E-04
2	MA1081.1	WRKY25	(YGGTCAAC)	1.76E-06	8.60E-04
2	MA1084.1	WRKY38	(CGTTGACC)	1.98E-06	9.70E-04
2	MA1092.1	WRKY63	(HGGTCAAC)	2.04E-06	9.98E-04
2	MA1304.1	WRKY59	(HAAAAGTCAAMN)	2.60E-06	1.27E-03
2	MA1309.1	WRKY3	(AAAAGTCAACG)	2.63E-06	1.29E-03
2	MA1295.1	WRKY20	(DNCGTTGACYWDD)	2.68E-06	1.31E-03
2	MA1085.2	WRKY40	(HWAGTCAANN)	2.69E-06	1.31E-03
2	MA1316.1	WRKY71	(AAAAGTCAACG)	2.93E-06	1.43E-03
2	MA1303.1	WRKY22	(AAAAGTCAACKNH)	4.02E-06	1.97E-03
2	MA1310.1	WRKY42	(BWTDMHHHNNCGTTGACTWWD)	4.11E-06	2.01E-03
2	MA1301.1	WRKY33	(AAAAGTCAACG)	4.19E-06	2.05E-03
2	MA1314.1	WRKY14	(AAAAGTCAACGNH)	4.70E-06	2.30E-03
2	MA1302.1	WRKY65	(AAAAGTCAACG)	5.19E-06	2.54E-03
2	MA0589.1	ZAP1	(TTGACCGAGYY)	6.75E-06	3.30E-03
2	MA1298.1	WRKY29	(AAAAGTCAACK)	6.83E-06	3.33E-03
2	MA0932.1	AHL12	(AAWWWWTT)	6.97E-06	3.40E-03
2	MA1308.1	WRKY70	(DNCGTTGACTTTT)	8.20E-06	4.00E-03
2	MA1315.1	WRKY24	(NCGTTGACTTTTTW)	8.74E-06	4.27E-03
2	MA1087.1	WRKY45	(CGTTGACY)	1.12E-05	5.48E-03
2	MA1307.1	WRKY31	(DDNNHWRHHAAAGTCAACG)	1.55E-05	7.53E-03
2	MA1306.1	WRKY11	(DNCGTTGACTTTTD)	1.75E-05	8.52E-03
2	MA1075.1	WRKY12	(CGTTGACC)	1.90E-05	9.24E-03
2	MA1379.1	SOL1	(WTTWAAAATTTAAAW)	2.87E-05	1.39E-02
2	MA1380.1	AT2G20110	(WTTTAAATTTTTWAA)	3.01E-05	1.46E-02
2	MA1161.1	TSO1	(WWTTWAAAATTTAAA)	3.34E-05	1.62E-02
2	MA1080.1	WRKY23	(AGTCAACG)	4.08E-05	0.01975
2	MA1318.1	WRKY27	(ANCGTTGACTTTT)	4.54E-05	0.02195
2	MA0934.1	AHL25	(AWTTAAWT)	5.68E-05	0.0274
4	MA1302.1	WRKY65	(AAAAGTCAACG)	2.23E-07	0.000109
4	MA1305.1	WRKY55	(DNCGTTGACTTT)	2.94E-07	0.0001438
4	MA1300.1	WRKY6	(CGTTGACTWWDDYWDWNHH)	3.49E-07	0.0001705
4	MA1308.1	WRKY70	(DNCGTTGACTTTT)	6.01E-07	0.000294
4	MA1315.1	WRKY24	(NCGTTGACTTTTTW)	6.57E-07	0.000321
4	MA1295.1	WRKY20	(DNCGTTGACYWDD)	6.89E-07	0.0003366
4	MA1314.1	WRKY14	(AAAAGTCAACGNH)	6.90E-07	0.0003373
4	MA1092.1	WRKY63	(HGGTCAAC)	8.02E-07	0.0003922
4	MA1309.1	WRKY3	(AAAAGTCAACG)	9.34E-07	0.0004566
4	MA1084.1	WRKY38	(CGTTGACC)	1.05E-06	0.0005139
4	MA1081.1	WRKY25	(YGGTCAAC)	1.53E-06	0.0007494
4	MA1301.1	WRKY33	(AAAAGTCAACG)	1.65E-06	0.0008055
4	MA1317.1	WRKY50	(YKTTGACTTTTTH)	1.75E-06	0.0008538
4	MA1303.1	WRKY22	(AAAAGTCAACKNH)	1.89E-06	0.0009214
4	MA1083.1	WRKY30	(RGTCAACGNN)	2.39E-06	0.001166
4	MA1078.1	WRKY2	(BGGTCAAM)	2.41E-06	0.001175
4	MA1310.1	WRKY42	(BWTDMHHHNNCGTTGACTWWD)	2.93E-06	0.001431
4	MA1093.1	WRKY75	(HRGTCAAC)	3.12E-06	0.001526
4	MA1306.1	WRKY11	(DNCGTTGACTTTTD)	4.46E-06	0.00218
4	MA1316.1	WRKY71	(AAAAGTCAACG)	4.51E-06	0.002202
4	MA1311.1	WRKY28	(DDCGTTGACTTTT)	4.92E-06	2.40E-03
4	MA1304.1	WRKY59	(HAAAAGTCAAMN)	5.39E-06	2.63E-03
4	MA1075.1	WRKY12	(CGTTGACC)	5.55E-06	2.71E-03
4	MA1298.1	WRKY29	(AAAAGTCAACK)	6.31E-06	3.08E-03
4	MA1089.1	WRKY57	(DWRGTCAAMN)	8.00E-06	3.90E-03

Cluster	Motif ID	Binding TF	Motif	p-val	adj. p-val
4	MA1077.1	WRKY18	(NHRGTCAAVV)	8.89E-06	4.34E-03
4	MA1318.1	WRKY27	(ANCGTTGACTTTT)	9.53E-06	4.65E-03
4	MA1087.1	WRKY45	(CGTTGACY)	1.02E-05	0.004997
4	MA1313.1	WRKY7	(DNCGTTGACTTTTT)	2.06E-05	0.01004
4	MA1299.1	WRKY17	(AAAAAGTCAACGNH)	2.14E-05	0.01042
4	MA1307.1	WRKY31	(DDNNHWRHHAAAGTCAACG)	2.18E-05	0.01062
4	MA1079.1	WRKY21	(NNRGTCAACG)	2.67E-05	0.01299
4	MA1086.1	WRKY43	(HRGTCAAMVN)	2.99E-05	0.01449
4	MA1076.1	WRKY15	(NRGTCAACSN)	5.60E-05	0.02703
4	MA1090.1	WRKY60	(NYGGTCAACSN)	5.77E-05	0.02781
4	MA1094.1	WRKY8	(NRGTCAAMN)	7.14E-05	0.03432
4	MA1297.1	WRKY26	(AAAAGTCAACGNY)	9.34E-05	0.04466
5	MA1092.1	WRKY63	(HGGTCAAC)	5.98E-05	0.02881
5	MA1088.1	WRKY48	(NNRGTCAAMN)	9.01E-05	0.04309
6	MA1086.1	WRKY43	(HRGTCAAMVN)	3.25E-06	0.001586
6	MA1079.1	WRKY21	(NNRGTCAACG)	3.44E-06	0.001678
6	MA1094.1	WRKY8	(NRGTCAAMN)	3.69E-06	0.001801
6	MA1093.1	WRKY75	(HRGTCAAC)	4.02E-06	0.001963
6	MA1089.1	WRKY57	(DWRGTCAAMN)	6.23E-06	0.00304
6	MA1088.1	WRKY48	(NNRGTCAAMN)	7.45E-06	0.003634
6	MA1087.1	WRKY45	(CGTTGACY)	1.72E-05	0.008387
6	MA1076.1	WRKY15	(NRGTCAACSN)	2.29E-05	0.01111
6	MA1091.1	WRKY62	(TGGTCAAC)	3.43E-05	0.01662
6	MA1310.1	WRKY42	(BWTDMHHHNNCGTTGACTWWD)	3.89E-05	0.01886
6	MA1302.1	WRKY65	(AAAAGTCAACG)	5.79E-05	0.02793
6	MA1080.1	WRKY23	(AGTCAACG)	7.94E-05	3.81E-02
6	MA1314.1	WRKY14	(AAAAGTCAACGNH)	8.12E-05	3.89E-02
8	MA0934.1	AHL25	(AWTTAAWT)	1.01E-06	4.95E-04
8	MA0953.1	ATHB-6	(NCAATHATD)	1.21E-06	5.92E-04
8	MA0933.1	AHL20	(AATTAAWT)	1.72E-06	8.38E-04
8	MA0578.1	SPL8	(WWDWHYGTACHHYWWW)	2.97E-06	1.45E-03
8	MA0952.1	ATHB-51	(AATWATTG)	9.53E-06	4.65E-03
8	MA0990.1	EDT1	(HAWTWAATGC)	1.17E-05	5.70E-03
8	MA1215.1	ATHB53	(HCAATAATTGD)	1.40E-05	6.82E-03
8	MA1212.1	ATHB13	(HYAATAATTDW)	1.71E-05	8.30E-03
8	MA1209.1	ATHB20	(HYAATAATTRA)	4.88E-05	2.36E-02
8	MA1274.1	OBP3	(TTTWCTTTTTHHYTTTTTTTT)	5.83E-05	2.81E-02
8	MA0932.1	AHL12	(AAWWWWTT)	7.12E-05	0.03422
8	MA1211.1	ATHB18	(NYAATYATTDD)	7.66E-05	0.03675
8	MA1268.1	AT1G69570	(TTTTYACTTTTTYTTTTTTTTTTTTTW)	8.10E-05	0.03885
8	MA1213.1	ATHB21	(NCAMCAATWATTGD)	9.18E-05	0.04391
11	MA1026.2	ATHB15	(RAWDRTAATGATKAY)	9.41E-07	0.0004599
11	MA1372.1	STZ	(CACTNHCACTN)	6.18E-06	0.00302
11	MA1326.1	ATHB33	(NHGTRATTARB)	3.02E-05	0.01466
11	MA1329.1	ATHB25	(THAYTAATTAHNHWW)	3.40E-05	0.0165
11	MA1369.1	HDG1	(RYAATTAATGM)	5.89E-05	0.0284
11	MA1405.1	SIZF2	(BACTGACAGT)	7.56E-05	0.03627
11	MA1375.1	ANL2	(GCATTAATTRY)	8.19E-05	0.03924
11	MA0990.1	EDT1	(HAWTWAATGC)	8.69E-05	0.0416
12	MA1079.1	WRKY21	(NNRGTCAACG)	1.11E-05	0.005421
12	MA1094.1	WRKY8	(NRGTCAAMN)	1.49E-05	0.007279
12	MA1089.1	WRKY57	(DWRGTCAAMN)	1.51E-05	0.007378
12	MA1370.1	IDD5	(TTTTTGTCGTTTWSTG)	1.97E-05	0.009564
12	MA1086.1	WRKY43	(HRGTCAAMVN)	2.48E-05	0.01207
12	MA1088.1	WRKY48	(NNRGTCAAMN)	2.84E-05	0.01377
12	MA1160.1	AT1G14580	(WWWWTTTTTGTCGTTTTSTK)	5.30E-05	0.02557
12	MA1371.1	IDD4	(MASAAAAMGACAAAAAW)	6.25E-05	0.03012
13	MA1086.1	WRKY43	(HRGTCAAMVN)	4.33E-12	2.12E-09
13	MA1094.1	WRKY8	(NRGTCAAMN)	1.15E-11	5.62E-09
13	MA1077.1	WRKY18	(NHRGTCAAVV)	2.55E-11	1.25E-08
13	MA1089.1	WRKY57	(DWRGTCAAMN)	7.35E-11	3.60E-08
13	MA1088.1	WRKY48	(NNRGTCAAMN)	1.33E-10	6.52E-08
13	MA1079.1	WRKY21	(NNRGTCAACG)	1.49E-10	7.29E-08
13	MA1076.1	WRKY15	(NRGTCAACSN)	1.82E-10	8.89E-08
13	MA1300.1	WRKY6	(CGTTGACTWWDDYWDWNHH)	7.38E-10	3.61E-07
13	MA1301.1	WRKY33	(AAAAGTCAACG)	8.09E-10	3.96E-07
13	MA1315.1	WRKY24	(NCGTTGACTTTTTW)	9.34E-10	4.57E-07
13	MA1295.1	WRKY20	(DNCGTTGACYWDD)	1.08E-09	5.30E-07
13	MA1093.1	WRKY75	(HRGTCAAC)	2.53E-09	1.24E-06
13	MA1309.1	WRKY3	(AAAAGTCAACG)	2.74E-09	1.34E-06
13	MA1078.1	WRKY2	(BGGTCAAM)	2.78E-09	1.36E-06
13	MA1305.1	WRKY55	(DNCGTTGACTTT)	3.82E-09	1.87E-06
13	MA1092.1	WRKY63	(HGGTCAAC)	6.04E-09	2.95E-06
13	MA1081.1	WRKY25	(YGGTCAAC)	8.97E-09	4.39E-06
13	MA1090.1	WRKY60	(NYGGTCAACSN)	1.93E-08	9.45E-06

Cluster	Motif ID	Binding TF	Motif	p-val	adj. p-val
13	MA1307.1	WRKY31	(DDNNHWRHHAAAGTCAACG)	2.88E-08	1.41E-05
13	MA1311.1	WRKY28	(DDCGTTGACTTTT)	3.01E-08	1.47E-05
13	MA1304.1	WRKY59	(HAAAAGTCAAMN)	4.78E-08	2.34E-05
13	MA1087.1	WRKY45	(CGTTGACY)	5.44E-08	2.66E-05
13	MA1298.1	WRKY29	(AAAAGTCAACK)	6.98E-08	3.42E-05
13	MA1080.1	WRKY23	(AGTCAACG)	7.08E-08	3.46E-05
13	MA1302.1	WRKY65	(AAAAGTCAACG)	7.16E-08	3.50E-05
13	MA1084.1	WRKY38	(CGTTGACC)	1.11E-07	5.43E-05
13	MA1316.1	WRKY71	(AAAAGTCAACG)	1.26E-07	6.14E-05
13	MA1314.1	WRKY14	(AAAAGTCAACGNH)	1.50E-07	7.32E-05
13	MA1091.1	WRKY62	(TGGTCAAC)	1.79E-07	8.77E-05
13	MA1303.1	WRKY22	(AAAAGTCAACKNH)	5.80E-07	2.84E-04
13	MA1310.1	WRKY42	(BWTDMHHHNNCGTTGACTWWD)	7.75E-07	3.79E-04
13	MA1083.1	WRKY30	(RGTCAACGNN)	8.11E-07	3.96E-04
13	MA1306.1	WRKY11	(DNCGTTGACTTTTD)	8.85E-07	4.33E-04
13	MA1075.1	WRKY12	(CGTTGACC)	1.22E-06	5.94E-04
13	MA1317.1	WRKY50	(YKTTGACTTTTTH)	2.38E-06	1.16E-03
13	MA1312.1	WRKY47	(MYYKNCGTTGACYW)	2.60E-06	1.27E-03
13	MA1085.2	WRKY40	(HWAGTCAANN)	4.17E-06	2.04E-03
13	MA1308.1	WRKY70	(DNCGTTGACTTTT)	4.29E-06	2.10E-03
13	MA1297.1	WRKY26	(AAAAGTCAACGNY)	5.81E-06	2.84E-03
13	MA1318.1	WRKY27	(ANCGTTGACTTTT)	6.55E-06	3.20E-03
13	MA0982.1	DOF2.4	(DWAAAGB)	7.83E-06	3.82E-03
13	MA1299.1	WRKY17	(AAAAAGTCAACGNH)	9.76E-06	4.76E-03
13	MA1071.1	DOF5.3	(NNWAAMG)	1.97E-05	9.60E-03
13	MA1313.1	WRKY7	(DNCGTTGACTTTTT)	6.24E-05	3.00E-02
14	MA1089.1	WRKY57	(DWRGTCAAMN)	1.18E-12	5.79E-10
14	MA1306.1	WRKY11	(DNCGTTGACTTTTD)	8.42E-12	4.12E-09
14	MA1308.1	WRKY70	(DNCGTTGACTTTT)	1.01E-11	4.92E-09
14	MA1303.1	WRKY22	(AAAAGTCAACKNH)	1.93E-11	9.44E-09
14	MA1316.1	WRKY71	(AAAAGTCAACG)	3.70E-11	1.81E-08
14	MA1086.1	WRKY43	(HRGTCAAMVN)	4.17E-11	2.04E-08
14	MA1094.1	WRKY8	(NRGTCAAMN)	4.83E-11	2.36E-08
14	MA1302.1	WRKY65	(AAAAGTCAACG)	4.89E-11	2.39E-08
14	MA1314.1	WRKY14	(AAAAGTCAACGNH)	6.58E-11	3.22E-08
14	MA1315.1	WRKY24	(NCGTTGACTTTTTW)	8.52E-11	4.16E-08
14	MA1305.1	WRKY55	(DNCGTTGACTTT)	1.14E-10	5.60E-08
14	MA1311.1	WRKY28	(DDCGTTGACTTTT)	1.46E-10	7.15E-08
14	MA1299.1	WRKY17	(AAAAAGTCAACGNH)	2.51E-10	1.23E-07
14	MA1304.1	WRKY59	(HAAAAGTCAAMN)	2.66E-10	1.30E-07
14	MA1077.1	WRKY18	(NHRGTCAAVV)	3.11E-10	1.52E-07
14	MA1088.1	WRKY48	(NNRGTCAAMN)	3.95E-10	1.93E-07
14	MA1298.1	WRKY29	(AAAAGTCAACK)	4.43E-10	2.17E-07
14	MA1313.1	WRKY7	(DNCGTTGACTTTTT)	5.73E-10	2.80E-07
14	MA1079.1	WRKY21	(NNRGTCAACG)	1.21E-09	5.93E-07
14	MA1317.1	WRKY50	(YKTTGACTTTTTH)	1.55E-09	7.57E-07
14	MA1295.1	WRKY20	(DNCGTTGACYWDD)	2.24E-09	1.10E-06
14	MA1076.1	WRKY15	(NRGTCAACSN)	2.30E-09	1.13E-06
14	MA1318.1	WRKY27	(ANCGTTGACTTTT)	2.35E-09	1.15E-06
14	MA1301.1	WRKY33	(AAAAGTCAACG)	3.26E-09	1.60E-06
14	MA1083.1	WRKY30	(RGTCAACGNN)	3.42E-09	1.67E-06
14	MA1310.1	WRKY42	(BWTDMHHHNNCGTTGACTWWD)	3.88E-09	1.90E-06
14	MA1309.1	WRKY3	(AAAAGTCAACG)	4.88E-09	2.39E-06
14	MA1093.1	WRKY75	(HRGTCAAC)	1.16E-08	5.66E-06
14	MA1085.2	WRKY40	(HWAGTCAANN)	1.36E-08	6.66E-06
14	MA1090.1	WRKY60	(NYGGTCAACSN)	2.21E-08	1.08E-05
14	MA1300.1	WRKY6	(CGTTGACTWWDDYWDWNHH)	5.57E-08	2.72E-05
14	MA1084.1	WRKY38	(CGTTGACC)	7.08E-08	3.46E-05
14	MA1297.1	WRKY26	(AAAAGTCAACGNY)	7.65E-08	3.74E-05
14	MA1092.1	WRKY63	(HGGTCAAC)	8.55E-08	4.18E-05
14	MA1312.1	WRKY47	(MYYKNCGTTGACYW)	2.01E-07	9.84E-05
14	MA1087.1	WRKY45	(CGTTGACY)	5.16E-07	2.52E-04
14	MA1091.1	WRKY62	(TGGTCAAC)	6.43E-07	3.14E-04
14	MA1080.1	WRKY23	(AGTCAACG)	7.03E-07	3.44E-04
14	MA1307.1	WRKY31	(DDNNHWRHHAAAGTCAACG)	2.65E-06	1.29E-03
14	MA1075.1	WRKY12	(CGTTGACC)	3.04E-06	1.49E-03
14	MA1078.1	WRKY2	(BGGTCAAM)	8.25E-06	4.02E-03
14	MA1081.1	WRKY25	(YGGTCAAC)	1.43E-05	6.97E-03
14	MA0990.1	EDT1	(HAWTWAATGC)	4.45E-05	0.02152
14	MA0969.1	CMTA2	(NNDVCGCGT)	5.94E-05	0.02863
14	MA1296.1	WRKY46	(CGTTGACTTTK)	7.77E-05	0.0373

Supplement Table 7: Known TF-motifs enriched in *E. salsugineum* 5´regulatory regions of DEGs. Known TF-motifs were determined using AME for the -500 bp region upstream of the transcriptional start site. The motifs were determined separately for each expression clusters depicted in Supplemental Figure 4.

Cluster	Motif ID	Binding TF	Motif	p-val	adj. p-val
2	MA1089.1	WRKY57	(DWRGTCAAMN)	1.76E-13	8.58E-11
2	MA1094.1	WRKY8	(NRGTCAAMN)	3.27E-13	1.60E-10
2	MA1088.1	WRKY48	(NNRGTCAAMN)	5.93E-12	2.90E-09
2	MA1079.1	WRKY21	(NNRGTCAACG)	7.82E-12	3.82E-09
2	MA1308.1	WRKY70	(DNCGTTGACTTTT)	1.45E-11	7.10E-09
2	MA1083.1	WRKY30	(RGTCAACGNN)	2.64E-11	1.29E-08
2	MA1076.1	WRKY15	(NRGTCAACSN)	3.48E-11	1.70E-08
2	MA1086.1	WRKY43	(HRGTCAAMVN)	4.57E-11	2.24E-08
2	MA1306.1	WRKY11	(DNCGTTGACTTTTD)	4.86E-11	2.38E-08
2	MA1297.1	WRKY26	(AAAAGTCAACGNY)	6.76E-11	3.31E-08
2	MA1314.1	WRKY14	(AAAAGTCAACGNH)	7.45E-11	3.64E-08
2	MA1302.1	WRKY65	(AAAAGTCAACG)	8.14E-11	3.98E-08
2	MA1313.1	WRKY7	(DNCGTTGACTTTTT)	1.53E-10	7.46E-08
2	MA1318.1	WRKY27	(ANCGTTGACTTTT)	1.88E-10	9.21E-08
2	MA1305.1	WRKY55	(DNCGTTGACTTT)	2.31E-10	1.13E-07
2	MA1075.1	WRKY12	(CGTTGACC)	2.56E-10	1.25E-07
2	MA1315.1	WRKY24	(NCGTTGACTTTTTW)	3.21E-10	1.57E-07
2	MA1310.1	WRKY42	(BWTDMHHHNNCGTTGACTWWD)	5.42E-10	2.65E-07
2	MA1317.1	WRKY50	(YKTTGACTTTTTH)	5.54E-10	2.71E-07
2	MA1303.1	WRKY22	(AAAAGTCAACKNH)	6.27E-10	3.07E-07
2	MA1295.1	WRKY20	(DNCGTTGACYWDD)	6.64E-10	3.25E-07
2	MA1077.1	WRKY18	(NHRGTCAAVV)	7.21E-10	3.53E-07
2	MA1311.1	WRKY28	(DDCGTTGACTTTT)	7.33E-10	3.58E-07
2	MA1298.1	WRKY29	(AAAAGTCAACK)	8.83E-10	4.32E-07
2	MA1087.1	WRKY45	(CGTTGACY)	1.22E-09	5.95E-07
2	MA1085.2	WRKY40	(HWAGTCAANN)	1.26E-09	6.18E-07
2	MA1304.1	WRKY59	(HAAAAGTCAAMN)	1.50E-09	7.32E-07
2	MA1084.1	WRKY38	(CGTTGACC)	1.54E-09	7.52E-07
2	MA1316.1	WRKY71	(AAAAGTCAACG)	1.82E-09	8.91E-07
2	MA1300.1	WRKY6	(CGTTGACTWWDDYWDWNHH)	1.85E-09	9.07E-07
2	MA1307.1	WRKY31	(DDNNHWRHHAAAGTCAACG)	1.94E-09	9.50E-07
2	MA1093.1	WRKY75	(HRGTCAAC)	2.37E-09	1.16E-06
2	MA1312.1	WRKY47	(MYYKNCGTTGACYW)	4.35E-09	2.13E-06
2	MA1301.1	WRKY33	(AAAAGTCAACG)	5.25E-09	2.57E-06
2	MA1299.1	WRKY17	(AAAAAGTCAACGNH)	6.60E-09	3.23E-06
2	MA1080.1	WRKY23	(AGTCAACG)	9.06E-09	4.43E-06
2	MA1309.1	WRKY3	(AAAAGTCAACG)	2.03E-08	9.93E-06
2	MA1090.1	WRKY60	(NYGGTCAACSN)	3.64E-08	1.78E-05
2	MA1091.1	WRKY62	(TGGTCAAC)	1.92E-06	0.0009393
2	MA1383.1	KAN2	(HTHRGAATATTCTTT)	2.57E-06	0.001254
2	MA1078.1	WRKY2	(BGGTCAAM)	3.73E-06	0.001822
2	MA1092.1	WRKY63	(HGGTCAAC)	7.83E-06	0.003821
2	MA0933.1	AHL20	(AATTAAWT)	1.14E-05	0.005559
2	MA1296.1	WRKY46	(CGTTGACTTTK)	1.20E-05	0.005838
2	MA1081.1	WRKY25	(YGGTCAAC)	1.65E-05	0.008037
2	MA0934.1	AHL25	(AWTTAAWT)	2.39E-05	0.0116
2	MA1027.1	KAN1	(RNWTATTC)	3.20E-05	0.01552
2	MA0953.1	ATHB-6	(NCAATHATD)	3.52E-05	0.01708
2	MA0127.1	PEND	(AYTTCTTATK)	4.38E-05	0.02117
2	MA0932.1	AHL12	(AAWWWWTT)	4.38E-05	0.02121
2	MA1162.1	TCX2	(WTTYAAAATTYAAAW)	4.99E-05	0.0241
2	MA0990.1	EDT1	(HAWTWAATGC)	5.52E-05	0.02662
2	MA1214.1	ATHB40	(DHACCAATAATTGDDNHHWWW)	9.58E-05	0.04576
4	MA1093.1	WRKY75	(HRGTCAAC)	5.60E-05	0.02703
5	MA1307.1	WRKY31	(DDNNHWRHHAAAGTCAACG)	1.02E-06	0.0004962
5	MA1309.1	WRKY3	(AAAAGTCAACG)	1.58E-06	0.0007709
5	MA1310.1	WRKY42	(BWTDMHHHNNCGTTGACTWWD)	2.00E-06	0.000977
5	MA1300.1	WRKY6	(CGTTGACTWWDDYWDWNHH)	2.20E-06	0.001077
5	MA1302.1	WRKY65	(AAAAGTCAACG)	2.21E-06	0.001078
5	MA1305.1	WRKY55	(DNCGTTGACTTT)	2.54E-06	0.001239
5	MA1077.1	WRKY18	(NHRGTCAAVV)	3.85E-06	0.00188
5	MA1301.1	WRKY33	(AAAAGTCAACG)	5.06E-06	0.002472
5	MA1085.2	WRKY40	(HWAGTCAANN)	5.25E-06	0.002565
5	MA1297.1	WRKY26	(AAAAGTCAACGNY)	5.36E-06	0.002618
5	MA1089.1	WRKY57	(DWRGTCAAMN)	5.85E-06	0.002857
5	MA1314.1	WRKY14	(AAAAGTCAACGNH)	6.53E-06	0.003187
5	MA1094.1	WRKY8	(NRGTCAAMN)	6.85E-06	0.003343
5	MA1315.1	WRKY24	(NCGTTGACTTTTTW)	9.15E-06	0.004463
5	MA1308.1	WRKY70	(DNCGTTGACTTTT)	1.02E-05	0.004956
5	MA1316.1	WRKY71	(AAAAGTCAACG)	1.09E-05	0.00529
5	MA1295.1	WRKY20	(DNCGTTGACYWDD)	1.30E-05	0.006328

Cluster	Motif ID	Binding TF	Motif	p-val	adj. p-val
5	MA1076.1	WRKY15	(NRGTCAACSN)	1.95E-05	0.009473
5	MA1093.1	WRKY75	(HRGTCAAC)	2.11E-05	0.01028
5	MA1087.1	WRKY45	(CGTTGACY)	3.49E-05	0.0169
5	MA1086.1	WRKY43	(HRGTCAAMVN)	3.61E-05	0.01748
5	MA1083.1	WRKY30	(RGTCAACGNN)	3.78E-05	0.01832
5	MA1080.1	WRKY23	(AGTCAACG)	4.04E-05	0.01956
5	MA1088.1	WRKY48	(NNRGTCAAMN)	5.54E-05	0.02675
5	MA1311.1	WRKY28	(DDCGTTGACTTTT)	5.69E-05	0.02745
5	MA1318.1	WRKY27	(ANCGTTGACTTTT)	6.37E-05	0.03067
5	MA1303.1	WRKY22	(AAAAGTCAACKNH)	6.64E-05	0.03196
5	MA1296.1	WRKY46	(CGTTGACTTTK)	7.82E-05	0.0375
5	MA1079.1	WRKY21	(NNRGTCAACG)	9.13E-05	0.04365
5	MA1091.1	WRKY62	(TGGTCAAC)	0.0001023	0.0488
6	MA0932.1	AHL12	(AAWWWWTT)	3.50E-05	0.01694
8	MA0953.1	ATHB-6	(NCAATHATD)	2.29E-05	0.01112
8	MA0982.1	DOF2.4	(DWAAAGB)	0.0001044	0.04976
10	MA1079.1	WRKY21	(NNRGTCAACG)	8.14E-07	0.0003981
10	MA1088.1	WRKY48	(NNRGTCAAMN)	1.05E-06	0.0005108
10	MA1309.1	WRKY3	(AAAAGTCAACG)	1.66E-06	0.0008112
10	MA1086.1	WRKY43	(HRGTCAAMVN)	1.83E-06	0.0008953
10	MA1076.1	WRKY15	(NRGTCAACSN)	1.97E-06	0.0009648
10	MA1301.1	WRKY33	(AAAAGTCAACG)	3.18E-06	0.001555
10	MA1310.1	WRKY42	(BWTDMHHHNNCGTTGACTWWD)	3.44E-06	0.001683
10	MA1094.1	WRKY8	(NRGTCAAMN)	3.47E-06	0.001696
10	MA1300.1	WRKY6	(CGTTGACTWWDDYWDWNHH)	3.59E-06	0.001756
10	MA1316.1	WRKY71	(AAAAGTCAACG)	3.70E-06	0.001809
10	MA1089.1	WRKY57	(DWRGTCAAMN)	3.95E-06	0.00193
10	MA1087.1	WRKY45	(CGTTGACY)	4.99E-06	0.002438
10	MA1093.1	WRKY75	(HRGTCAAC)	6.61E-06	0.003229
10	MA1080.1	WRKY23	(AGTCAACG)	7.19E-06	0.00351
10	MA1083.1	WRKY30	(RGTCAACGNN)	7.21E-06	0.003519
10	MA1091.1	WRKY62	(TGGTCAAC)	9.75E-06	0.004756
10	MA1078.1	WRKY2	(BGGTCAAM)	1.12E-05	0.005439
10	MA1314.1	WRKY14	(AAAAGTCAACGNH)	1.15E-05	0.005584
10	MA1295.1	WRKY20	(DNCGTTGACYWDD)	1.21E-05	0.005899
10	MA1311.1	WRKY28	(DDCGTTGACTTTT)	1.41E-05	0.006872
10	MA1305.1	WRKY55	(DNCGTTGACTTT)	1.65E-05	0.008013
10	MA1081.1	WRKY25	(YGGTCAAC)	1.79E-05	0.008727
10	MA1307.1	WRKY31	(DDNNHWRHHAAAGTCAACG)	2.37E-05	0.01152
10	MA1303.1	WRKY22	(AAAAGTCAACKNH)	3.16E-05	0.01531
10	MA1297.1	WRKY26	(AAAAGTCAACGNY)	3.92E-05	0.01898
10	MA1298.1	WRKY29	(AAAAGTCAACK)	4.74E-05	0.02293
10	MA1302.1	WRKY65	(AAAAGTCAACG)	4.99E-05	0.02409
10	MA1304.1	WRKY59	(HAAAAGTCAAMN)	5.16E-05	0.02494
10	MA1308.1	WRKY70	(DNCGTTGACTTTT)	6.12E-05	0.02947
10	MA1317.1	WRKY50	(YKTTGACTTTTTH)	6.66E-05	0.03202
10	MA1090.1	WRKY60	(NYGGTCAACSN)	6.77E-05	0.03255
11	MA1192.1	At5g58900	(WDWRGATAAGRTTWD)	2.07E-05	0.01007
12	MA1311.1	WRKY28	(DDCGTTGACTTTT)	1.13E-06	0.0005509
12	MA1327.1	ATHB23	(AWWNWTAATTAATDAWWWAWTW)	2.82E-06	0.001378
12	MA1314.1	WRKY14	(AAAAGTCAACGNH)	4.25E-06	0.002076
12	MA1089.1	WRKY57	(DWRGTCAAMN)	4.67E-06	0.002279
12	MA1316.1	WRKY71	(AAAAGTCAACG)	8.90E-06	0.004341
12	MA1305.1	WRKY55	(DNCGTTGACTTT)	1.13E-05	0.00549
12	MA1302.1	WRKY65	(AAAAGTCAACG)	1.33E-05	0.006499
12	MA1306.1	WRKY11	(DNCGTTGACTTTTD)	1.85E-05	0.009018
12	MA1301.1	WRKY33	(AAAAGTCAACG)	2.37E-05	0.01153
12	MA1298.1	WRKY29	(AAAAGTCAACK)	2.83E-05	0.01374
12	MA1317.1	WRKY50	(YKTTGACTTTTTH)	3.30E-05	0.016
12	MA1093.1	WRKY75	(HRGTCAAC)	3.35E-05	0.01624
12	MA1080.1	WRKY23	(AGTCAACG)	3.71E-05	0.01798
12	MA1076.1	WRKY15	(NRGTCAACSN)	3.85E-05	0.01865
12	MA1308.1	WRKY70	(DNCGTTGACTTTT)	3.98E-05	0.01926
12	MA1094.1	WRKY8	(NRGTCAAMN)	4.10E-05	0.01983
12	MA1297.1	WRKY26	(AAAAGTCAACGNY)	4.35E-05	0.02106
12	MA1309.1	WRKY3	(AAAAGTCAACG)	4.39E-05	0.02122
12	MA1079.1	WRKY21	(NNRGTCAACG)	4.82E-05	0.02331
12	MA1303.1	WRKY22	(AAAAGTCAACKNH)	5.55E-05	0.02678
12	MA1304.1	WRKY59	(HAAAAGTCAAMN)	6.02E-05	0.02899
12	MA1315.1	WRKY24	(NCGTTGACTTTTTW)	6.21E-05	0.02991
12	MA1086.1	WRKY43	(HRGTCAAMVN)	6.95E-05	0.03343
12	MA0953.1	ATHB-6	(NCAATHATD)	7.10E-05	0.0341
12	MA1077.1	WRKY18	(NHRGTCAAVV)	8.24E-05	0.03951
12	MA1300.1	WRKY6	(CGTTGACTWWDDYWDWNHH)	8.75E-05	0.04189
12	MA1083.1	WRKY30	(RGTCAACGNN)	9.95E-05	0.04749

Cluster	Motif ID	Binding TF	Motif	p-val	adj. p-val
12	MA1295.1	WRKY20	(DNCGTTGACYWDD)	0.0001033	0.04925
13	MA1089.1	WRKY57	(DWRGTCAAMN)	5.49E-12	2.69E-09
13	MA1086.1	WRKY43	(HRGTCAAMVN)	2.09E-11	1.02E-08
13	MA1094.1	WRKY8	(NRGTCAAMN)	7.27E-11	3.55E-08
13	MA1088.1	WRKY48	(NNRGTCAAMN)	7.34E-11	3.59E-08
13	MA1079.1	WRKY21	(NNRGTCAACG)	4.45E-10	2.18E-07
13	MA1093.1	WRKY75	(HRGTCAAC)	6.07E-10	2.97E-07
13	MA1301.1	WRKY33	(AAAAGTCAACG)	1.29E-09	6.29E-07
13	MA1309.1	WRKY3	(AAAAGTCAACG)	1.59E-09	7.79E-07
13	MA1076.1	WRKY15	(NRGTCAACSN)	1.64E-09	8.04E-07
13	MA1077.1	WRKY18	(NHRGTCAAVV)	2.08E-09	1.02E-06
13	MA1317.1	WRKY50	(YKTTGACTTTTTH)	2.17E-09	1.06E-06
13	MA1315.1	WRKY24	(NCGTTGACTTTTTW)	2.42E-09	1.18E-06
13	MA1300.1	WRKY6	(CGTTGACTWWDDYWDWNHH)	5.57E-09	2.72E-06
13	MA1316.1	WRKY71	(AAAAGTCAACG)	6.62E-09	3.24E-06
13	MA1314.1	WRKY14	(AAAAGTCAACGNH)	1.01E-08	4.96E-06
13	MA1302.1	WRKY65	(AAAAGTCAACG)	1.03E-08	5.04E-06
13	MA1305.1	WRKY55	(DNCGTTGACTTT)	1.36E-08	6.65E-06
13	MA1303.1	WRKY22	(AAAAGTCAACKNH)	1.49E-08	7.29E-06
13	MA1308.1	WRKY70	(DNCGTTGACTTTT)	1.87E-08	9.13E-06
13	MA1091.1	WRKY62	(TGGTCAAC)	3.27E-08	1.60E-05
13	MA1311.1	WRKY28	(DDCGTTGACTTTT)	3.53E-08	1.72E-05
13	MA1084.1	WRKY38	(CGTTGACC)	3.73E-08	1.82E-05
13	MA1092.1	WRKY63	(HGGTCAAC)	4.70E-08	2.30E-05
13	MA1075.1	WRKY12	(CGTTGACC)	5.95E-08	2.91E-05
13	MA1087.1	WRKY45	(CGTTGACY)	6.26E-08	3.06E-05
13	MA1306.1	WRKY11	(DNCGTTGACTTTTD)	7.13E-08	3.48E-05
13	MA1295.1	WRKY20	(DNCGTTGACYWDD)	8.22E-08	4.02E-05
13	MA1298.1	WRKY29	(AAAAGTCAACK)	8.52E-08	4.17E-05
13	MA1304.1	WRKY59	(HAAAAGTCAAMN)	8.54E-08	4.17E-05
13	MA1297.1	WRKY26	(AAAAGTCAACGNY)	9.84E-08	4.81E-05
13	MA1083.1	WRKY30	(RGTCAACGNN)	1.09E-07	5.34E-05
13	MA1299.1	WRKY17	(AAAAAGTCAACGNH)	1.28E-07	6.26E-05
13	MA1318.1	WRKY27	(ANCGTTGACTTTT)	1.41E-07	6.88E-05
13	MA1080.1	WRKY23	(AGTCAACG)	2.70E-07	0.0001322
13	MA1307.1	WRKY31	(DDNNHWRHHAAAGTCAACG)	3.68E-07	0.0001798
13	MA1085.2	WRKY40	(HWAGTCAANN)	5.71E-07	0.0002793
13	MA1310.1	WRKY42	(BWTDMHHHNNCGTTGACTWWD)	7.39E-07	0.0003613
13	MA1090.1	WRKY60	(NYGGTCAACSN)	7.69E-07	0.0003758
13	MA1081.1	WRKY25	(YGGTCAAC)	9.26E-07	0.0004525
13	MA1313.1	WRKY7	(DNCGTTGACTTTTT)	9.37E-07	0.000458
13	MA1078.1	WRKY2	(BGGTCAAM)	1.12E-06	0.0005471
13	MA0982.1	DOF2.4	(DWAAAGB)	9.70E-05	0.04633
14	MA1088.1	WRKY48	(NNRGTCAAMN)	6.33E-12	3.10E-09
14	MA1094.1	WRKY8	(NRGTCAAMN)	7.79E-12	3.81E-09
14	MA1076.1	WRKY15	(NRGTCAACSN)	4.85E-11	2.37E-08
14	MA1090.1	WRKY60	(NYGGTCAACSN)	1.49E-10	7.27E-08
14	MA1089.1	WRKY57	(DWRGTCAAMN)	1.57E-10	7.67E-08
14	MA1079.1	WRKY21	(NNRGTCAACG)	1.74E-10	8.50E-08
14	MA1083.1	WRKY30	(RGTCAACGNN)	2.82E-10	1.38E-07
14	MA1298.1	WRKY29	(AAAAGTCAACK)	2.91E-10	1.42E-07
14	MA1077.1	WRKY18	(NHRGTCAAVV)	3.18E-10	1.56E-07
14	MA1300.1	WRKY6	(CGTTGACTWWDDYWDWNHH)	4.04E-10	1.98E-07
14	MA1302.1	WRKY65	(AAAAGTCAACG)	1.45E-09	7.09E-07
14	MA1078.1	WRKY2	(BGGTCAAM)	1.83E-09	8.95E-07
14	MA1314.1	WRKY14	(AAAAGTCAACGNH)	1.83E-09	8.95E-07
14	MA1092.1	WRKY63	(HGGTCAAC)	2.19E-09	1.07E-06
14	MA1093.1	WRKY75	(HRGTCAAC)	2.90E-09	1.42E-06
14	MA1081.1	WRKY25	(YGGTCAAC)	3.08E-09	1.51E-06
14	MA1303.1	WRKY22	(AAAAGTCAACKNH)	3.55E-09	1.74E-06
14	MA1307.1	WRKY31	(DDNNHWRHHAAAGTCAACG)	3.62E-09	1.77E-06
14	MA1316.1	WRKY71	(AAAAGTCAACG)	4.59E-09	2.24E-06
14	MA1311.1	WRKY28	(DDCGTTGACTTTT)	4.84E-09	2.37E-06
14	MA1309.1	WRKY3	(AAAAGTCAACG)	5.83E-09	2.85E-06
14	MA1086.1	WRKY43	(HRGTCAAMVN)	5.91E-09	2.89E-06
14	MA1306.1	WRKY11	(DNCGTTGACTTTTD)	7.31E-09	3.57E-06
14	MA1301.1	WRKY33	(AAAAGTCAACG)	8.81E-09	4.31E-06
14	MA1305.1	WRKY55	(DNCGTTGACTTT)	1.00E-08	4.90E-06
14	MA1295.1	WRKY20	(DNCGTTGACYWDD)	1.12E-08	5.47E-06
14	MA1304.1	WRKY59	(HAAAAGTCAAMN)	1.15E-08	5.64E-06
14	MA1075.1	WRKY12	(CGTTGACC)	1.31E-08	6.41E-06
14	MA1087.1	WRKY45	(CGTTGACY)	1.84E-08	9.01E-06
14	MA1308.1	WRKY70	(DNCGTTGACTTTT)	2.11E-08	1.03E-05
14	MA1084.1	WRKY38	(CGTTGACC)	3.12E-08	1.52E-05
14	MA1310.1	WRKY42	(BWTDMHHHNNCGTTGACTWWD)	3.72E-08	1.82E-05
14	MA1318.1	WRKY27	(ANCGTTGACTTTT)	4.03E-08	1.97E-05

Cluster	Motif ID	Binding TF	Motif	p-val	adj. p-val
14	MA1315.1	WRKY24	(NCGTTGACTTTTTW)	6.03E-08	2.95E-05
14	MA1313.1	WRKY7	(DNCGTTGACTTTTT)	3.49E-07	0.0001707
14	MA1296.1	WRKY46	(CGTTGACTTTK)	4.22E-07	0.0002065
14	MA1091.1	WRKY62	(TGGTCAAC)	5.19E-07	0.0002536
14	MA1299.1	WRKY17	(AAAAAGTCAACGNH)	5.87E-07	0.0002868
14	MA1317.1	WRKY50	(YKTTGACTTTTTH)	7.17E-07	0.0003505
14	MA1297.1	WRKY26	(AAAAGTCAACGNY)	1.12E-06	0.0005466
14	MA1080.1	WRKY23	(AGTCAACG)	1.69E-06	0.0008239
14	MA1312.1	WRKY47	(MYYKNCGTTGACYW)	2.58E-06	0.001259
14	MA0589.1	ZAP1	(TTGACCGAGYY)	2.56E-05	0.01243
14	MA1085.2	WRKY40	(HWAGTCAANN)	7.08E-05	0.03404

Acknowledgments

First of all, I want to thank Ken for the great supervision and encouragement throughout the last years. I highly appreciate that your office door was always open and that you always took time for discussions and any potential problems. I am thankful for your patience and for the tremendous constructive input that helped me to successfully finish my PhD and develop myself.

I also want to thank Prof. Dr. Paul Schulze-Lefert for many fruitful discussions during my TAC meetings and for taking over the position as first examiner of my thesis. It was very helpful that you tried to be the devil's advocate and thereby advanced my critical thinking. Many thanks also to Dr. Eric Kemen for his constructive inputs during my TAC meetings.

Moreover, I want to thank Prof. Dr. Stanislav Kopriva for joining my thesis committee as a second examiner. Special thanks to Prof. Dr. Gunther Döhlemann for chairing my thesis committee and to Dr. Imre Somssich for taking over the "Beisitz" during my PhD defence.

The last years at the MPIPZ were so enjoyable because of the great colleagues and friends I met along my way. A great thanks to all Tsuda lab members: Matthias, Caro, Maria, Sayan, Tatsi, Kaori, Kasia, Dieter, Ping, Yiming and Akira for your great support and especially Shajahan for the practical supervision in the beginning of my project. A special thanks to Besen aka Harry for your awesome support throughout the last years, I especially enjoyed our stimulating coffee breaks. Maria, I want to thank you for our awesome dance sessions in the lab! You are by far the best lab mate I could have hoped for and a great friend. Moreover, it was a great pleasure to spend time with Alfredo and the awesome pals angels Sam, Paul and Jonny. I had a great time with all of you in and outside of the institute and you made my PhD a truly unforgettable time!

Der größte Dank gilt meinen Eltern und Larissa. Eure Unterstützung gibt mir stets den nötigen Rückhalt und ihr habt immer an mich geglaubt. Ich kann mich jederzeit auf euch verlassen und ihr schafft es stets mich wieder aufzumuntern, wenn es mal nicht so läuft. Dafür möchte ich euch von Herzen danken!

Erklärung

Ich versichere, dass ich die von mir vorgelegte Dissertation selbständig angefertigt, die benutzten Quellen und Hilfsmittel vollständig angegeben und die Stellen der Arbeit − einschließlich Tabellen, Karten und Abbildungen − , die anderen Werken im Wortlaut oder dem Sinn nach entnommen sind, in jedem Einzelfall als Entlehnung kenntlich gemacht habe; dass diese Dissertation noch keiner anderen Fakultät oder Universität zur Prüfung vorgelegen hat; dass sie − abgesehen von unten angegebenen Teilpublikationen − noch nicht veröffentlicht worden ist, sowie, dass ich eine solche Veröffentlichung vor Abschluss des Promotionsverfahrens nicht vornehmen werde.

Die Bestimmungen der Promotionsordnung sind mir bekannt. Die von mir vorgelegte Dissertation ist von Prof. Dr. Paul Schulze-Lefert betreut worden.

Ich versichere, dass ich alle Angaben wahrheitsgemäß nach bestem Wissen und Gewissen gemacht habe und verpflichte mich, jedmögliche, die obigen Angaben betreffenden Veränderungen, dem Dekanat unverzüglich mitzuteilen

Köln, 19.02.2018

Thomas Winkelmüller